PhD

95/KAZ

SCC

Ref.

PNEUMATIC FLOCCULATION IN WATER TREATMENT

Noor Mohammed Kazi

M Sc (Civil Engg.)

A thesis submitted in partial fulfilment of the requirements of The Nottingham Trent University for the degree of Doctor of Philosophy

September 1995

To

My parents

ABSTRACT

The removal of turbidity by flocculation is based on the amount of the temporal mean velocity gradient. Many means are available to produce the velocity gradients and one of these is pneumatic flocculation.

This thesis describes an investigation of the development of a technique of air diffusion that generates a specific temporal mean velocity gradient to enhance the flocculation of suspended materials. Three types of synthetic turbidity namely kaolin, lycopodium and polyvinyl chloride (PVC) were coagulated with aluminium sulphate and ferric sulphate. Each material was flocculated under constant and step-down agitation using a diffused air model treatment process. Four air diffusion pads with different sizes of orifice 1.0, 1.5, 2.0 and 3.0 mm in diameter were used in order to investigate the optimum orifice size and the optimum air flow rates.

The best turbidity removal was obtained with an orifice diameter of either 1.5 mm (78.00% to 94.81% removal) or 2.0 mm (83.18% to 96.00% removal). The optimum range of air flow rate per unit area of the flocculator was found to be 0.077 to 0.618 and 0.077 to 0.463 cc/sq.cm-min. for the diffusion pads of orifice sizes of 1.5 and 2.0 mm respectively.

Removal of soluble iron, aluminium and nitrogenous matter in the process of coagulation followed by pneumatic flocculation through forming the hydroxide which is a non soluble matter and other physicochemical processes which might occur during the flocculation and settling processes.

A mathematical relationship has been established to describe the kinetics of the pneumatic flocculation in terms of the process variables.

The pneumatic flocculator required 1/16 of the power required for the mechanical flocculator in order to obtain the same degree of treatment.

ACKNOWLEDGMENTS

The author is deeply indebted to Dr. Ihsan H. Sholji, First Supervisor, Department of Civil and Structural Engineering, the Nottingham Trent University, for his suggestions on the research and equipment for this work, continuous supervision, invaluable advice and constant encouragement in this work. The candidate is grateful to Professor R. K. Hawkins, Head of the Department of Civil and Structural Engineering, for the opportunity to carry out the research in his department.

Sincere gratitude and thanks are due to Professor K. J. Ives, Second Supervisor, Emeritus Professor of Public Health Engineering, University College, London, who advised on this work and Mr. M. J. Shapley, Third Supervisor, Department of Civil and Structural Engineering, the Nottingham Trent University for his technical suggestions and contributions.

Sincere thanks are also due to all the technical staff, Department of Civil and Structural Engineering, the Nottingham Trent University, for their assistance, particularly Mr. R. C. Gregory for his great contribution during manufacturing and installing of the experimental set up and Mr. C. Chamber for his assistance during the course of experimental work. Thanks are also due to all the author's research colleagues in the department for their help in all aspects during this work. Many thanks are expressed to Mrs Patricia Bradbury who helped in reviewing the language of this thesis. Credit is due to author's family, particularly to Evu, for her encouragement, patience and continuous assistance during this work.

The study was made possible by the joint scholarship scheme of the Nottingham Trent University, Nottingham with the Association of Commonwealth Universities (ACU), 36 Gordon Square, London SW1. The financial support from the ACU and the Nottingham Trent University as the host institution is gratefully acknowledged.

DECLARATION

This thesis is composed by myself. The work and the results reported herein are my own except where otherwise stated.

No paper has yet been published on elements of the work described in this thesis. However, three papers as titled below, are under preparation for publication; based on the results of this research:

1. Pneumatic Flocculation in Water Treatment Industries.

2. Taper Pneumatic Flocculation in Water Treatment Industries.

3. Settling Behaviour of Lighter Particles under Pneumatic Coagulation-Flocculation and Settling Process.

LIST OF CONTENTS

Page

Page

Page

Page

LIST OF TABLES

LIST OF FIGURES

NOTATION

Symbol	Meaning
A	plan area, m^2
a	ratio of collision to physical radius of a floc
C	volume concentration of the particles
C_0	initial concentration of the particles, mg/l
C_t	concentration of the particles at time, t, mg/l
C_D	drag coefficient
C_d	coefficient of discharge
D_{ij}	diffusion coefficient of particles i and j
d	diameter of colloidal particles, m
d_b	diameter of air bubble, m
d_i	depth, m
d_s	diameter of solid particle, m
E	removal efficiency, per cent
G	velocity gradient, s^{-1}
g	gravitional acceleration (9.81), m/s^2
H,h	depth of the diffuser below the water surface, m
h_i	depth, m
i	label for particle of the ith kind
J_{ij}	number of contacts per unit time per unit volume between particles of radius R_i and R_j
J_{ok}	orthokinetic flocculation
J_{pk}	perikinetic flocculation
j	label for particle of the jth kind
k	label for particle formed by aggregation of i and j - particles
k'	constant of proportionality
K	slope of the line, $(cc/min.)^{-1/2}$
K_1	interception of the line

Symbol	Meaning
K_s	proportionality coefficient
L	length of the stirrer blade, m
N	number of contacts per unit time per unit volume
N_0	initial number of particles per unit volume
N_t	number of particles per unit volume at time, t
n	variable power function (chapter 2)
	number of revolutions per minute (chapter 3)
n_i	number of i-fold particles per unit volume
n_j	number of j-fold particles per unit volume
P	power dissipated in fluid motion, watt
p	absolute pressure intensity, N/m^2
p_a	pressure of air at free state, N/m^2
p_{ah}	atmospheric pressure in water column at MSL, m
p_c	pressure of air at compressed state, N/m^2
Q_a	volumetric flow rate of air, m^3/s
R	Reynolds number
R_i	radius of an i-particle, m
R_j	radius of a j-particle, m
R_{ij}	radius of interaction of two particles, m
R_F	radius of floc, m
r	radius, m
r_{max}	radius of maximum floc size, m
T	Kelvin temperature, K
t	time, s
u	mean square velocity fluctuation, m/s
u_r	relative velocity of the jar tester blade, m/s
V	volume of the fluid, m^3
v_r	rising velocity of bubble, m/s
v_s	rising velocity of solid particle, m/s
v_z	rising velocity of bubble at height z, m/s

Symbol	Meaning
W	width of the stirrer blade, m
α	numerical coefficient (chapter 2)
η	collision efficiency factor
κ	Boltzmann's constant, J/K
μ_L	dynamic viscosity of liquid, N.s/m^2
μ_w	dynamic viscosity of water, N.s/m^2
ρ_L	density of liquid, kg/m^3
ρ_s	density of solid particles, kg/m^3
ρ_w	density of water, kg/m^3
ρ_a	density of air, kg/m^3
γ_w	specific weight of water, kN/m^3
σ	surface tension, N/m
ϕ	floc volume fraction
δ	particle size distribution function

CHAPTER 1

INTRODUCTION

1.1 IMPURITIES IN WATER

Water from natural sources may contain different types of impurities which can be physical, chemical or biological in nature as shown in Figure 1.1 (Barnes *et al.*, 1981). The impurities which are present in physical form may exist either in a suspended or a dissolved state. Suspended particles can be classified as coarse, fine and colloidal according to their sizes in microns as shown in Figure 1.2 (Tebbutt, 1983). Colloids are classified as those suspended particles whose size range is generally 10^{-3} to 1 μm (Peavy *et al.*, 1985). Fine suspended particles are of size of 1 to 50 μm and those above 50 μm are all defined as coarse suspended particles. The aim of this investigation is to remove the fine suspended and colloidal particles from raw water by the process of pneumatic flocculation.

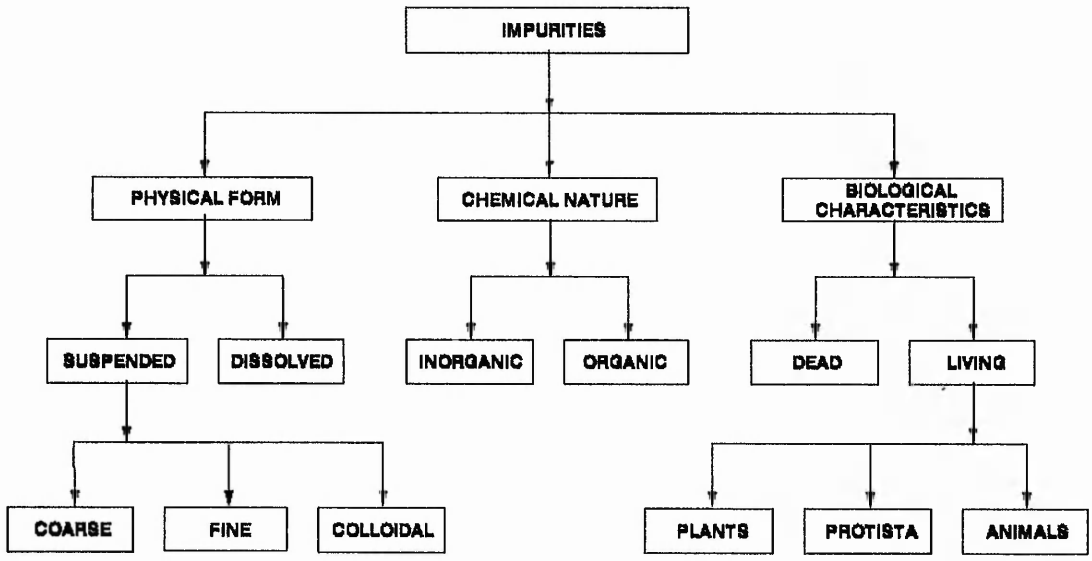

Figure 1.1 Nature of impurities in water.

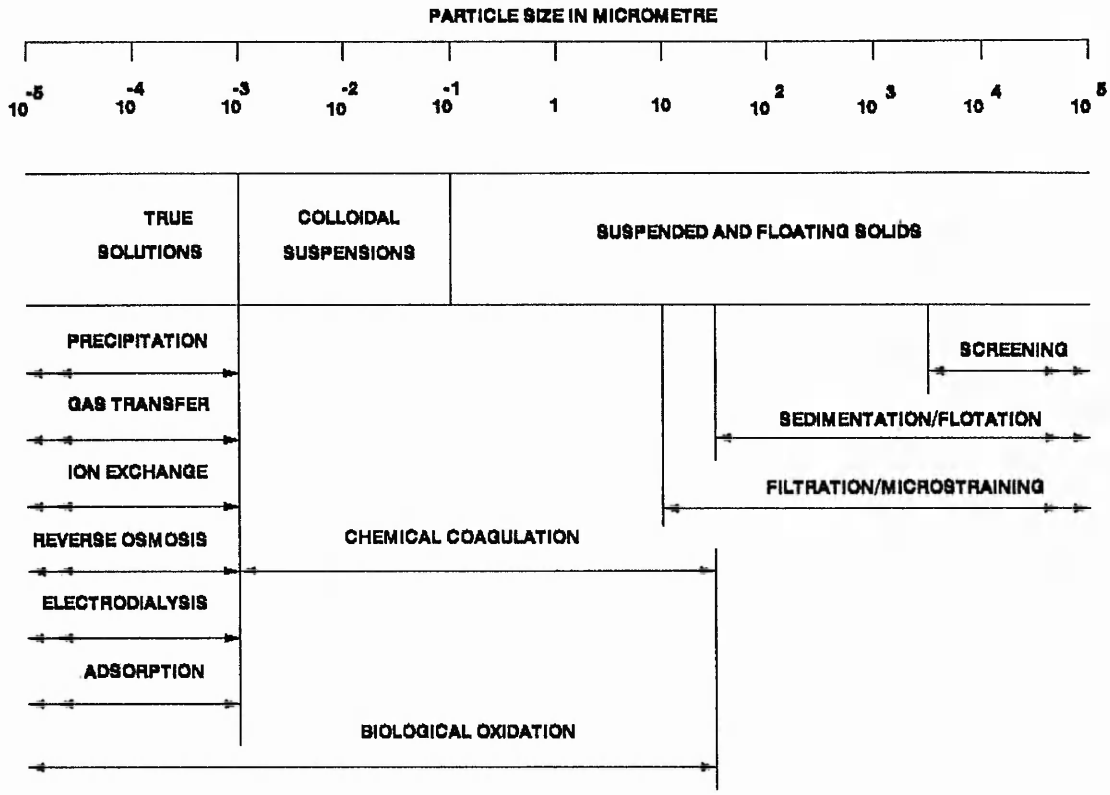

Figure 1.2 Classification of impurities in water.

1.2 COLLOIDS AND COLLOIDAL DISPERSION

Colloidal dispersions in water consist of discrete particles held in suspension due to their extremely small sizes, state of hydration i. e. chemical combination with water and surface electrical charges (Clark *et al.*, 1977). Colloids have a large surface area per unit volume, called the specific surface area, as they are very small in size and thus surface effects predominate over the mass effect. Two surface effects are very important - adsorption of substances and accumulation of electrical charges on the surface (Barnes *et al.*, 1981). Most of the colloidal particles carry a residual charge on their surface, usually this is a negative charge (Steel and McGhee, 1979). There are three mechanisms which can cause this charge: (i) imperfections in the crystalline structure, (ii) ionisation of peripheral chemical groups and (iii) adsorption of specific ions from the surrounding environment.

In most natural waters, the colloidal surfaces are negatively charged (AWWA, 1971). There is a natural tendency of the colloids to combine and precipitate, however, this tendency is countered either by mutual repulsion of the same charged particles (called hydrophobic colloids) or by the strong combination of the particles and water (called hydrophilic colloids). When these effects are strong and natural aggregation of the particles does not occur, the suspension is said to be stable. Colloidal particles which are stable require a long time to settle under the influence of gravity alone, as shown in Table 1.1 (Degre'mont, 1991).

Table 1.1 Time needed for the particles and organisms to settle vertically through 1 metre of water at 20^0C, under the influence of gravity alone.

Particle size (μm)	Type of particle	Settling time through 1 m water	Specific area ($m^2 . m^{-3}$)
10^4	Gravel	1 second	$6 . 10^2$
10^3	Sand	10 seconds	$6 . 10^3$
10^2	Fine sand	2 minutes	$6 . 10^4$
10	Clay	2 hours	$6 . 10^5$
1	Bacteria	8 days	$6 . 10^6$
10^{-1}	Colloid	2 years	$6 . 10^7$
10^{-2}	Colloid	20 years	$6 . 10^8$
10^{-3}	Colloid	200 years	$6 . 10^9$

1.3 COLLOIDAL STABILITY

Colloidal particles carry an electric charge which is counterbalanced in the aqueous phase. As a result, an electric double layer exists at every interface between a solid and water. This double layer consists of the charged-particle surface and a surrounding sheath of ions of opposite charge which accumulate in the water near the surface of the particle. These counter-ions are attracted electrostatically to this

interfacial region and formed a bound layer of water, called the Stern layer, in which ions of opposite charge drawn from the bulk solution produce a rapid drop in potential. This drop within the bound water layer is called the Stern potential. The Stern layer is surrounded by movable, diffuse layers of counter-ions. The concentration of these counter-ions in the diffuse zone decreases as it extends into the surrounding bulk of electroneutral solution. The boundary surface between the Stern layer and the solution serves as a shear plane when the particle undergoes movement relative to the solution. A more gradual drop occurs between the shear surface of the bound water layer and the point of electroneutrality in the solution, called the zeta potential. The zeta potential magnitude can be estimated from electrophoretic measurement of the particle mobility in an electric field. The repulsive force of the charged double layer disperses particles and prevents aggregation, thus particles with a high zeta potential produce a stable suspension.

A schematic representation of the colloidal state is presented in Figure 1.3.

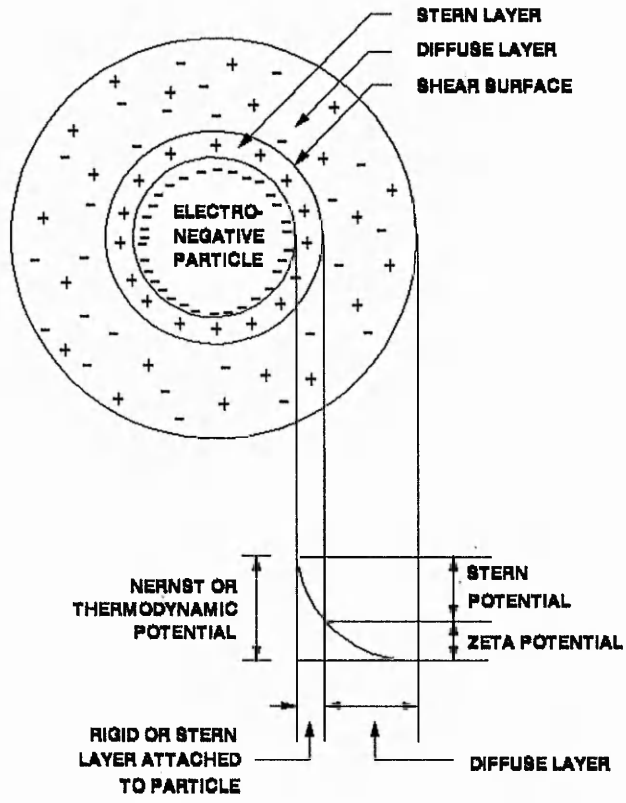

Figure 1.3 Structure of a double layer and the corresponding potentials.

The net effect of the existence of electrical double layers around particles is to inhibit the close approach of particles to each other, and hence the double layers confer stability on the suspension. Both the thickness of the double layer and the surface-charge density are sensitive to concentration and valence of the ions in solution, and hence stability of the suspension can be markedly affected by adding suitable ions to the solution.

Due to Brownian motion and van der Waals force of attraction, the colloidal particles have the opportunity to be more close to each other, impairing the mutual repulsive force and the strong combination of particles and the fluid media. This state of suspension is said to be unstable. In this research work the stable colloidal particles are destabilised by dispersing coagulant chemicals in the aqueous solution to force the particles to aggregate and promote their cluster size. They are then physically separated. The applied technique used in this investigation is called pneumatic flocculation followed by sedimentation in a standing column of water.

1.4 DESTABILISATION

Destabilisation of hydrophobic colloids can be accomplished by compressing the electrical double layers which contribute to the stability of the suspension. Factors tending to destabilise a suspension are van der Waals force of attraction and Brownian movement. van der Waals forces are the molecular cohesive forces of attraction that increase in intensity as particles approach each other. These forces are negligible when the particles are slightly separated but become dominant at particles contact. Brownian movement is the random motion of colloids caused by their bombardment by molecules of the dispersion medium. This movement has a destabilising effect on a suspension due to a possible aggregation.

The forces between charged colloidal particles can be represented by the graph shown in Figure 1.4. When two colloids of the same charge come into close proximity there are two forces acting on them. The electrostatic potential reacts to

repel the particles, thus preventing contact and the van der Waals force of attraction supports the contact. As noted in Figure 1.4, the net force is repulsive at greater distances and decreases after passing through a maximum net repulsive force, called the energy barrier, and when the net force becomes zero the attractive force becomes dominant. Once the force becomes attractive, contact between particles takes place. The hatched area represents the energy required to bring two particles close enough so that the net attraction between them may be expected to draw them together. The source of this energy may be either impacts from Brownian motion or relative movement in the fluids.

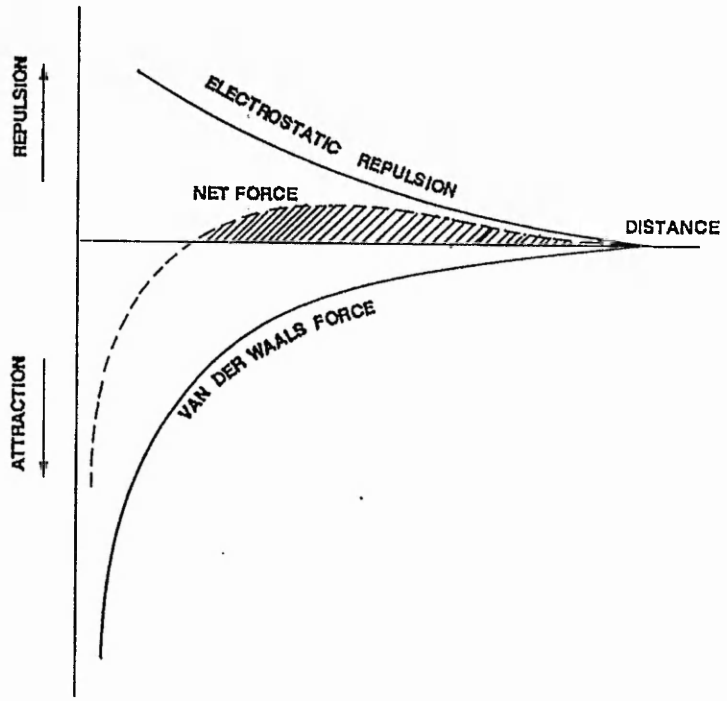

Figure 1.4 Forces between charged colloidal particles.

If the electrical forces of repulsion between particles are sufficiently reduced to permit particle-to-particle contact, then the van der Waals force will cause particles to stick to each other, leading to progressive agglomeration of particles. For larger particles, Brownian movement becomes a negligible factor. A far more effective way of promoting particle collisions is to establish hydraulic velocity gradients by creating areas of turbulence.

Diffused air bubbles were used to generate a power input and produce the relative movement in the tested water column, thus overcoming the energy barrier discussed above, promoting agglomeration.

1.5 COAGULATION

Coagulation is a process for destabilising dissolved and colloid impurities and producing larger floc aggregates (Jiang *et al.*, 1995). This process describes the effect produced by the addition of a chemical to a colloidal dispersion resulting in particle destabilisation by a reduction of the forces tending to keep the particles apart.

Operationally, coagulation is achieved by adding the appropriate chemical, associated with the availability of sufficient alkalinity, which causes particles to stick together when contact is made. Rapid mixing is important at this stage to ensure a uniform dispersion of the chemical and to increase the opportunity of particle to particle contact. The entire process of formation of submicroscopic floc particles, occurs in a very short time, probably less than a second (AWWA, 1971).

1.5.1 Mechanism of Coagulation: Coagulation of colloids is accomplished in different ways. These include (i) ionic layer compression, (ii) adsorption and charge neutralisation, (iii) enmeshment in a precipitate and (iv) interparticle bridging. These mechanisms are described briefly as follows:

1.5.1(a) Ionic layer compression: The electric potential of a colloid is a function of the ionic concentration of the surrounding water. When an electrolyte is added to the suspension, the concentration of the counter-ions will increase, which will compress the diffuse layer. If this layer is sufficiently compressed, the net force will be negative, as the van der Waals force will be predominant, and there will be no energy barrier in this state.

1.5.1(b) Adsorption and charge neutralisation: Some hydrolysis species, of

opposite charge to those carried by the colloid, tend to be adsorbed on the colloid surface, causing it to neutralise, thus removing the energy barrier and destabilising the colloids.

1.5.1(c) Enmeshment in a precipitate: When metal salts like aluminium sulphate, $Al_2(SO_4)_3$ or ferric chloride, $FeCl_3$ are used as a coagulant, hydroxide precipitates are formed in the presence of sufficient alkalinity. These are amorphous, gelatinous flocs, which enhance the separation of formed floc particles by gravity. Colloids may become entrapped or enmeshed by the sticky surface of separated flocs.

1.5.1(d) Interparticle bridging: When polyelectrolytes are used, their highly surface reactive chains or branches are extended into the solution. Colloids will stick on to active parts of the chain. One colloid attaches to another by means of a chain or bridging mechanism, thus the several colloids may become attached to one polyelectrolyte and several of the polyelectrolyte-colloid groups may become enmeshed resulting in a settleable mass.

It is thought that one of the first three mechanisms or more than one mechanism may occur during the coagulation in the experimental processes of this investigation.

1.5.2 Factors affecting Coagulation: The following parameters are considered as factors affecting the process of coagulation:

(i) pH
(ii) coagulant dosage
(iii) colloidal concentration
(iv) valency of the coagulant
(v) mixing intensity
(vi) mixing time
(vii) temperature
(viii) sufficient alkalinity

The effect of these parameters will be described in chapter 2.

1.5.3 Coagulant Dosage: The optimum dose of coagulant is determined experimentally by the widely used Jar Test (Ives, 1978). This test apparatus and the procedure has been described in section 3.6.

1.6 FLOCCULATION

Flocculation is the process of producing relative velocities, characterised by the velocity gradient, by gently stirring the water. By this means the size distribution of colloidal particles and their unstable state accelerate the aggregation and agglomeration of coagulated particles. The agglomerated particles are of adequate size to settle with a velocity acceptable for separation. This investigation puts emphasis on both coagulation and flocculation and concentrates on the latter.

1.6.1 Principle of Flocculation

The principle of flocculation describes the mechanism of achieving the contact between the colloidal particles. The mechanism of interparticle contacts needed differential fluid motion, either spatial, temporal or both. The motion of the fluid can be produced either automatically due to Brownian motion (perikinetic flocculation) or artificially by introducing some means of power input (orthokinetic flocculation). Interparticle contacts can be accomplished in different ways, three separate mechanisms (Ernest *et al.*, 1995) of which are of concern in the field of water treatment. These are: (i) contacts by molecular thermal motion (perikinetic flocculation), (ii) contacts by fluid motion generated by power input (orthokinetic flocculation) and (iii) contacts resulting from differential settling of the particle (differential settling).

1.6.1(a) Perikinetic Flocculation: The fluid molecules are always in rapid and random movement, called Brownian motion, which causes the rapid and random

bombardment of the colloidal particles. The colloidal particles stick together as they move randomly under the influence of Brownian motion. The collisions promote the formation of microflocs in a very short time, less than a minute (Barnes *et al.*, 1981). This stage of transport process is called perikinetic flocculation. The rate of reduction in the total concentration of particles with time due to perikinetic flocculation, J_{pk}, may be represented as follows (Swift and Friedlander, 1964):

$$J_{pk} = \frac{d}{dt}(N_0) = -\frac{4}{3}\frac{\eta\kappa T}{\mu}(N_0)^2 \qquad (1.1)$$

where N_0 is the total concentration of the particles (number of the particles) at time t, η is the collision efficiency factor (representing the fraction of the total number of collisions which are successful in producing aggregates), κ is Boltzmann's constant, T is absolute temperature and μ is the fluid dynamic viscosity.

1.6.1(b) Orthokinetic Flocculation: By introducing a power input to achieve the gentle stirring, interparticles contacts can be accomplished through the relative fluid motion. This process is termed orthokinetic flocculation. For a colloidal suspension of particles having a uniform particle size, the rate of reduction in the total concentration of the particles with time due to orthokinetic flocculation, J_{ok}, may be describe by the following equation:

$$J_{ok} = \frac{d}{dt}(N_0) = -\frac{2\eta G d^3 (N_0)^2}{3} \qquad (1.2)$$

where d is the uniform diameter of the colloidal particles and G is the temporal mean velocity gradient.

1.6.1(c) Differential Settling Flocculation: Due to the varying sizes of the particles, a third type of settling flocculation may occur as the larger particles settle faster than smaller particles and collide with them to form a larger mass. The settling flocculation rate is also increased by the concentration of the particles.

Orthokinetic flocculation processes have been employed by introducing compressed

air into the water during the course of the experimental work of this research. Orthokinetic flocculation was noticed during this investigation and differential settling flocculation was also observed during the settling period of orthokinetically flocculated water.

1.6.2 Types of Flocculation

Depending on the sequence of the agitation employed, two types of flocculation process can be considered. One type is with a constant degree of agitation throughout the detention time and is designated as "Normal flocculation" in this research work. The other one is step-down flocculation, applying a progressively decreasing degree of agitation, and preventing the floc rupture either by internal tension, by surface shear stress erosion or both. This type of flocculation is generally called taper or step-down flocculation and and will be called "Taper flocculation" in this research work. The effects of both the normal and taper agitation on the process efficiency associated with pneumatic flocculation have been studied in this investigation.

1.6.3 Flocculation Equipments

Many means are available to produce the agitation required for inducing the flocculation. These are as follows:

(i) Hydraulic: a. Jets
b. Baffled channels
c. Carrying raw water pipes

(ii) Mechanical: a. Paddles and reels
b. Turbine
c. Propeller

(iii) Pneumatic: Air injection - rising bubbles

The former two are conventionally used all over the world and the latter is not fully investigated on either its practicability or its scientific applicability in the field of water treatment. The major objective of this research work is to investigate and monitor the process of air diffusion or pneumatic flocculation under various initial conditions. Prior to discussing the pneumatic flocculation process, it is imperative to mention and discuss the significance of the velocity gradient, which is universally used to define the rate of flocculation.

1.7 THE VELOCITY GRADIENT

1.7.1 Physical Conception: The velocity gradient is a measure of the relative velocity of two particles of fluid and the distance between them. As for example, two water particles, moving 500 mm/s relative to each other at a distance of 10 mm apart, would have a velocity gradient of 500/10 = 50 s^{-1}. The velocity gradient is strictly defined at a point, for the whole system the mean velocity gradient is considered and denoted as the temporal mean velocity gradient.

1.7.2 Application: The velocity gradient determines the power input required to give a particular degree of flocculation. The intensity of the velocity gradient controls the degree of flocculation, i. e. the degree of flocculation is directly proportional (within limitations) to the velocity gradients established in the water being treated. The stirring action derived from the flocculating mechanism is responsible for establishing these gradients and is therefore fundamental to the process.

1.7.3 Estimation: The expression for the temporal mean velocity gradient, denoted by G can be derived either by using the principle of fluid mechanics i. e. shearing force on the element of the fluid (Tebbutt, 1983; Barnes *et al.*, 1981) or by the Dimensional Analysis (Sholji, 1994).

1.7.3(a) Principle of fluid mechanics: Figure 1.5 shows an element of fluid of height h, and of plan area A. The upper surface of the fluid is moving at a velocity

$\frac{dv}{dy}h$. From the fundamental of fluid mechanics, the horizontal viscous stress, $\tau=\mu\frac{dv}{dy}$

Therefore, the viscous shear force is equal to $A\,\mu\,\frac{dv}{dy}$

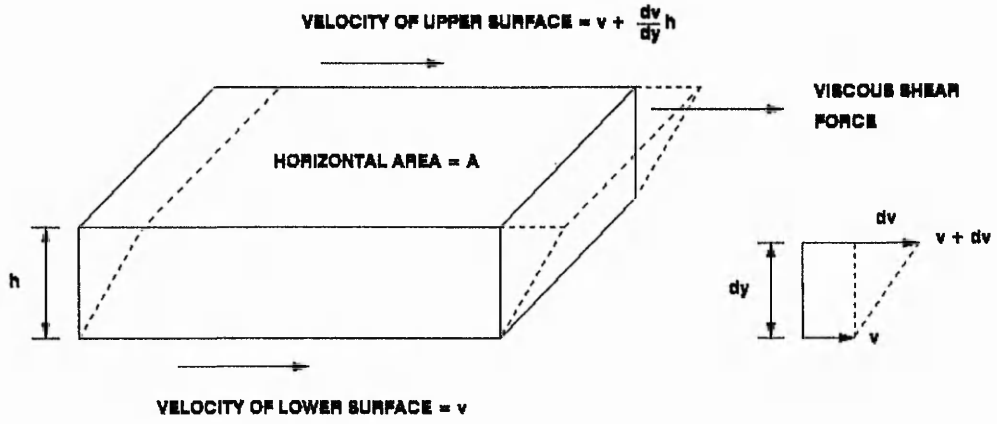

Figure 1.5 Fluid element under relative movement.

The external work per second i. e. power = force × velocity = $A\,\mu\,\frac{dv}{dy}\times\frac{dv}{dy}h$ = $A\,\mu\,G^2\,h$. The external work per second must be equal to the internal dissipation of energy within the same time.

Hence, the dissipated energy i.e. power consumed, $P = A\,\mu\,G^2\,h$

The volume of fluid, $V = A \times h$

Therefore, dissipated power, $P = \mu G^2 \times (A \times h) = \mu G^2 V$

And thus, the temporal mean velocity gradient, $G = (P/\mu\,V)^{1/2}$ (1.3)

In non-uniform, unsteady and turbulent flow conditions, the root-mean-square value of G, calculated from power input is considered.

1.7.3(b) Dimensional analysis: The velocity gradient, G is a function of total power input P, viscosity, μ and total volume of fluid in the chamber V, *i. e.*

$$G = f(P^x \mu^y V^z) \tag{1.4.1}$$

Now, the dissipated power, P = Force × Velocity = $F.L/T = FLT^{-1}$

Viscosity, μ = (Force × Time)/Area = $F.T/L^2 = FTL^{-2}$

Volume of fluid, $V = L^3$

Velocity gradient, $G = T^{-1}$

Now, $G = T^{-1} = (FLT^{-1})^x, (FTL^{-2})^y, (L^3)^z$

Solving for L, $0 = x - 2y + 3z$ (1.4.2)

T, $-1 = -x + y$ (1.4.3)

F, $0 = x + y$ (1.4.4)

From Equation (1.4.4), $y = -x$ (1.4.5)

Substituting the value of y in Equation (1.4.3), $-1 = -x -x = -2x$

Therefore, $x = 1/2$ (1.4.6)

Substituting the value of x from Equation (1.4.6) into Equation (1.4.3)

$-1 = -1/2 + y$, *i. e.* $y = -1/2$ (1.4.7)

Substituting the value of x from Equation (1.4.6) and y from Equation (1.4.7) in Equation (1.4.2), $0 = 1/2 + 1 + 3z$, *i. e.* $z = -1/2$ (1.4.8)

Now, substituting the value of x, y, and z in Equation (1.4.1) and solving for G,

$$G = P^{1/2} \mu^{-1/2} V^{-1/2} = (P/\mu V)^{1/2} \tag{1.3}$$

1.8 PNEUMATIC FLOCCULATION

Flocculation may be achieved by diffusing compressed air into water that will produce sufficient velocity gradients required for the achievement of submicrofloc agglomeration. Pneumatic flocculation is the process in which low pressurised air is used to induce the required size of air bubbles through a diffusion pad in order to agglomerate the destabilised colloidal suspended matters in water. The air bubbles rising through water are increased in volume while the associated pressure decreases, thus producing a relative velocity (the velocity gradient) in water and ultimately flocculating the coagulated suspended particles contained in the tested water column.

The process of producing agitation by using compressed air to generate the velocity gradient in the coagulation-flocculation process of water treatment has long been known (Camp, 1955; Ives, 1981; McConnachie, 1984; Al-Hiary, 1988). However, no detailed and complete description of the method has yet been recorded. Consequently, the practical application of this process is very rarely seen in the water treatment industries. It has been felt since 1955 (Camp, 1955) that much research and development would be required in order to obtain a satisfactory output from the process of pneumatic flocculation. The theoretical background of pneumatic flocculation will be described in the subsequent sections for the better understanding of the process.

1.8.1 Advantages of Pneumatic Flocculation: This process offers some additional merits over its rivals as follows:

i) there will be an increase in the amount of dissolved oxygen (DO) which will enhance the quality of water, thus inhibiting anaerobic conditions.

ii) it will transform soluble iron and manganese to an insoluble product promoting their ultimate goal of separation by pneumatic flocculation, with a beneficial impact on the treatment of underground water.

iii) it is possibly less mechanically troublesome and requires less maintenance compared with mechanical flocculation.

iv) it aids the removal of nitrogen due to the settling of the floc.

v) it uses less power consumption on the basis of power value calculation and there is ultimately less operational cost.

vi) there is an expected lower initial cost, as it is very simple and flexible in operation and affords better control over the system as states in item (v) above.

1.8.2 Computation of Dissipated Power: Two approaches are available to compute the dissipated power in order to evaluate the degree of flocculation in terms of the temporal mean velocity gradient (Camp, 1955).

Approach 1 is based on the work done by the expansion of the air bubbles. The expansion can be assumed to take place either adiabatically or isothermally. Both will give approximately the same results.

Approach 2 is based on the drag force between the air bubbles and the water. Both the approaches give approximately the same results. In this work, a difference of 0.4% in the calculated G values have been noted by using both the approaches separately. The derivation of the expression for dissipated power will be described in the next section.

1.8.2(a) Approach 1 - Work done by the expansion of air bubbles: When air is diffused into water from a compressed state, it normally expands isothermally (Fair *et al.*, 1968). Based on the isothermal condition during the process, the work done by the expansion of the air bubbles from the compressed state to a free state in water is given by

$$\int p \, dV \tag{1.5}$$

where p is the absolute pressure intensity in N/m^2 and V is the volume of air in m^3.

From Boyle's law, $pV = p_aV_a = p_cV_c$ = constant i. e. $p = p_aV_a / V$, where V_a is the volume of air at free state in m^3, V_c is the volume of air at compressed state in m^3, p_a is the pressure of air at free state in N/m^2 and p_c is the pressure of air at compressed state in N/m^2.

Therefore, the work done, $W = p_aV_a \int_{V_c}^{V_a} (1 / V\, dV) = p_aV_a\, ln[V]_{V_c}^{V_a} = p_aV_a\, ln \frac{V_a}{V_c}$

Thus, work done, $W = p_aV_a\, ln \frac{p_c}{p_a}$. Power is equal to the rate of work done and hence it is the time rate for releasing V_a. Now, power, $P = p_aV_a/t\, .\, ln \frac{p_c}{p_a}$, *i.e.*

$$P = p_aQ_a\, ln \frac{p_{ah}+h}{p_{ah}} \tag{1.6}$$

where p_{ah} the pressure of air at free state in water column in meter.

Considering that the air is induced at a depth h below the water surface and substituting p_a = 101.3 x 10^3 N/m^2 at MSL(Mean Sea Level) at 20^{0}C, then the dissipated power will be

$$P = 101.3\times10^3\, Q_a\, ln \frac{10.3 + h}{10.3} \tag{1.7}$$

1.8.2(b) Approach 2 - The drag force between the air bubbles and the liquid: The work done by the drag forces on an air bubble in water is equal to the drag force times the distance travelled by the bubble, which is the depth of the diffusers below the water surface. The drag force is nearly equal to the weight of water displaced by the volume of air bubbles at a depth h/2 (Camp, 1955).

Thus, work done = drag force × depth of the diffuser

= weight of the water displaced by the volume of air bubble (at a depth of h/2) × h.

= unit specific weight of water × volume of the bubble (at a depth h/2) × h

$$= \gamma_w \left(V_a \frac{p_{ah}}{p_{ah} + h/2}\right) h$$

where, V_a is the volume of the bubbles at atmospheric pressure in water column in meter at MSL, p_{ah} , which is equal to $Q_a \times t$.

Now the rate of work done i. e. the power dissipated, P = Work done / time or,

$$P = \gamma_w Q_a \left(\frac{p_{ah}}{p_{ah} + \frac{h}{2}}\right) h \tag{1.8}$$

At atmospheric pressure and at MSL at 20^0C, the dissipated power will be

$$P = \gamma_w Q_a \left(\frac{10.3}{10.3 + \frac{h}{2}}\right) h \tag{1.9}$$

Equations (1.6) and (1.8) can be used to compute the dissipated power both of which yield approximately the same results.

1.8.3 Computation of Air Flow Rate: The quantity of diffused air required to generate a temporal mean velocity gradient, G, into the water of volume, V, can be computed from equation (1.6) and (1.8) which will be as follows:

(a) Based on the concept of work done by the expansion of air bubble, the quantity of air flow is

$$Q_a = \frac{P}{p_a ln \frac{p_{ah} + h}{p_{ah}}} \tag{1.10}$$

(b) Based on the concept of the drag force between the air bubbles and the water, the quantity of air flow is

$$Q_a = \frac{P}{\gamma_w \left(\frac{p_{ah}}{p_{ah} + \frac{h}{2}}\right) h} \tag{1.11}$$

Using equation (1.3) and (1.11),

$$Q_a = \frac{G^2 \mu V}{\gamma_w \left(\frac{P_{ah}}{P_{ah} + \frac{h}{2}} \right) h} \tag{1.12}$$

Using equation (1.3) and (1.10),

$$Q_a = \frac{G^2 \mu V}{P_a ln \frac{P_{ah}+h}{P_{ah}}} \tag{1.13}$$

Equation (1.12) and (1.13) can also be used to compute the temporal mean velocity gradient, G, produced by the given amount of air flow rate, Q_a , and the given volume of water.

For better understanding of the pneumatic flocculation process, knowledge of hydrodynamic behaviour of the rising air bubbles is very important and will be discussed in the following section.

1.9 HYDRODYNAMICS OF RISING BUBBLES

The hydrodynamic behaviour of rising bubbles through liquids is of prime importance in the study of pneumatic flocculation. The size, shape, rising velocity and the path of air bubbles and the physical properties of both the liquid and air play significant roles in the generation of velocity gradients throughout the process of coagulation and flocculation. As bubbles are of principal importance in pneumatic flocculation process, it is essential to understand the behaviour of a rising bubble through liquid. This will now be described in the following sections:

1.9.1 Mechanism of Bubble Formation: The mechanism of bubble formation is accomplished in two stages (Tsuge and Hibino, 1981). The first stage is the bubble

formation and it is called attachment stage (the expansion) of the static bubble; the second stage is the detachment stage. When air is supplied through the orifice, the surrounding liquid is displaced by the air emerged from the opening due to the drag forces acting on the top surface of the air bubble. If the air inlet chamber pressure is constant, the growth of the bubble is increased. The growth of the static air bubble ends when the inertia force, the buoyancy, the surface tension and the viscous drag acting upon the static air bubble, reach equilibrium. Due to the inward circulation of water surrounding the static air bubble at the level of the orifice opening, the bubble is necked in and detached by the combined effect of buoyant forces and the motion of the liquid toward the orifice. The detached bubble rises and the portion of its volume remaining at the orifice becomes the nucleus of the next bubble to be formed (Leibson *et al.*, 1956).

1.9.2 Rising Velocity: The rising velocity of the bubble in liquid varies with the height. Bubbles are accelerated up to a maximum rise velocity and then the rise velocity decreases asymptotically (Tapucu, 1974). This phenomenon is related to surface active impurities in liquid which adhere to the bubble's surface. The effect of these impurities is great on the small bubbles. For large bubbles, surface tension forces become very small and the surface active impurities have a vanishing effect on the rising velocity after reaching its maximum value before steadying up as shown by Tapucu (1974).

The regime of liquid motion near the surface of the small bubble is viscous and thus the motion corresponds to low Reynolds number. When Reynolds number, **R**<1.0, where $\mathbf{R} = v_s d_s \rho_L / \mu_L$, Stokes' law for a solid-liquid interface is given by

$$v_s = \frac{g}{18} \frac{(\rho_s - \rho_L)}{\mu_L} d_s^2 \qquad (1.14)$$

where, v_s is the settling velocity of solid spherical particle, g is the acceleration of gravity, ρ_s is the mass density of the solid, ρ_L is the mass density of the liquid, and d_s is the diameter of the solid particle. This law can be applied to compute the velocity of the individual bubble rising in still water under the laminar flow

condition. For a single bubble rising in water, the gas-liquid interface theoretical velocity is considered and the rising velocity v_r, is given by Levich (1962).

$$v_r = \frac{g}{12} \frac{(\rho_a - \rho_w)}{\mu_w} d_b^2 \tag{1.15}$$

where, ρ_a and ρ_w are the mass density of the air and the water respectively and d_b is the equivalent diameter of the spherical bubble. The velocity pattern is somewhat different for larger bubbles depending on the liquid properties and also the other parameters like bubble diameter, gas flow rate, volume of the gas chamber etc., which create a different state and conditions of flow and Stokes' law is no longer applicable. Different aspects of bubble rising velocity will be discussed in details in chapter 2.

1.9.3 Shape of the Bubbles: The shape of the rising bubbles in liquids may be spherical, ellipsoidal (with or without surface oscillation), spherical cap (with open or closed wake) and disk-like bubbles (Tapucu, 1974; Bhaga and Weber, 1981). The transition points from one shape to another are determined as the function of Liquid Property Number, M which is defined as follows:

$$M = \frac{g\mu_L^4}{\rho_L \sigma^3} \tag{1.16}$$

where σ is the surface tension.

1.9.4 Bubble Path: The motion of bubbles rising in liquids may be rectilinear, helical (first sinusoidal and then helical), sinusoidal and rectilinear with rocking depending on the bubble's and liquid's physical properties (Tapucu, 1974).

1.9.5 Size of Bubbles: Bubble size increases with the increase of the orifice diameter when the other related parameters are kept constant. The size is many times larger say, 10 to 100 times (Verschoor, 1950), than the orifice from which the bubbles escape, depending on the gas flow rates, volume and pressure of the gas chamber and also the liquid physical properties. The feature of the size of bubbles will also

be elaborated on in chapter 2.

The bubbles are relatively uniform in size at low Reynolds numbers when air flow rate is small. At high rates of air flow, the bubbles formed are not uniform in size (Leibson, 1956).

The hydrodynamic behaviour of the rising bubbles observed during the course of the experimental work of present investigation will be discussed in detail in chapter 4.

CHAPTER 2

LITERATURE REVIEW

2.1 GENERAL

Extensive literature has been surveyed and reviewed in order to identify the current level of information regarding coagulation and flocculation by using the compressed air in the field of water treatment. The main factors that influence the coagulation-flocculation process and the specific conditions to obtain the efficient flocculation have been identified.

Coagulation and flocculation have long been recognised and recommended as the important process for the removal of colloidal turbidity from raw water. In the past, considerable research has been devoted to the coagulation-flocculation process operated either hydraulically or mechanically. By contrast, little information is known about the process operated pneumatically or using compressed air. However, it has been felt since 1955 that much research and development would be required in order to obtain a satisfactory output from pneumatic flocculation (Camp, 1955).

The hydrodynamic behaviour of gas bubbles rising in liquids has been studied both theoretically and experimentally by a large number of investigators. Most of their work is related to the behaviour of bubbles rising through liquids in the field of hydrodynamics, mineral engineering or chemical processing. However, very little information is available concerning bubble characteristics that influence the coagulation-flocculation process in the field of water treatment. Although bubbles play a key role in many physical and chemical processes and they have received substantial attention in the literature, nevertheless, a systematic framework of bubble characteristics has so far been lacking.

Based on the discussion highlighted above, the reviewed literature has been classified into three groups for the convenience of description: (i) Previous works on diffused air flocculation, (ii) General theory and practice of coagulation and flocculation and (iii) The hydrodynamics of rising gas bubbles through liquids. The contribution of the previous investigators in all aspects of these fields will be reviewed and discussed in the following sections.

2.2 DIFFUSED AIR FLOCCULATION

The fact of using compressed air to generate velocity gradients in the coagulation-flocculation process of water treatment has been reported in the past by many investigators (Camp, 1955; Patwardhan, 1975; McConnachie, 1984; Al-Hiary, 1988). However, the method was not fully investigated in either the practicability or the scientific applicability in aspects of coagulation and flocculation in the field of water treatment. Although it has been felt since 1955 (Camp, 1955) that much research and development would be required for satisfactory output, the method was in the experimental stage until 1981 (Ives, 1981). After that, further research and development have been achieved by some investigators (McConnachie, 1984; Al-Hiary, 1988) and there were more indications that this process might be applicable in practice. However, its practical application for coagulation and flocculation is not seen in the water treatment industries until recently. The findings of the previous workers are reviewed and discussed below:

Camp, T. R. (1955): Camp has mentioned two approaches of computing the dissipated power required to produce the velocity gradient by diffused air agitation. The first approach was based on the concept of work done by the expansion of air bubbles under suitable isothermal or adiabatic condition. The results were approximately the same whether the expansion of air bubbles was assumed to be adiabatic or isothermal. Considering the isothermal expansion, Camp (1955) stated the following equations for computing the dissipated power and the quantity of air required to generate any mean velocity gradient:

$$P = 4890\ Q_a\ log\frac{H + 34}{34} \tag{2.1}$$

where P is the dissipated power in foot-pounds per second, Q_a is the flow of free air in cubic feet per second and H is the depth of the diffuser in feet, and

$$Q_a = \frac{G^2 \mu V}{4890\ log\frac{H+34}{34}} \tag{2.2}$$

where G is the velocity gradient in s^{-1}, μ is the absolute viscosity of the fluid in pound second per square foot and V is the volume of the liquid in the tank in cubic feet.

The second approach of computing the dissipated power and the required quantity of air was based on the concept of work done by the drag force on air bubbles and the corresponding equations are as follows:

$$P = 62.4\ Q_a \frac{34\ H}{\frac{H}{2} + 34} \tag{2.3}$$

$$Q_a = \frac{G^2 \mu V}{2120 \frac{H}{\frac{H}{2} + 34}} \tag{2.4}$$

Both approaches yielded approximately the same results. It can be seen from Equation (2.2) and (2.4) that the quantity of air required to produce a given velocity gradient is independent of the bubble size.

The rising velocity of the individual bubble in still water is given by the Stokes' law under the laminar flow conditions:

$$v_r = \frac{1}{18} \frac{g}{\mu} (\rho_a - \rho_w)\ d_b^2 \tag{2.5}$$

where v_r is the rising velocity; g, the gravity constant; ρ_a , the mass density of air

bubble; ρ_w , the mass density of water; and d_b, the equivalent diameter of the spherical air bubble. It was stated that an individual bubble rising in still water would conform to the Stokes' law for a bubble diameter less than 1.4 mm.

Camp (1955) also stated that in the Stokes' law region, the maximum value of the velocity gradient G_{max} occurs at the air-water interface and he suggested the following equation for maximum velocity gradient.

$$G_{max} = \frac{1}{6}\frac{g}{\mu}(\rho_a - \rho_w)\ d_b \qquad (2.6)$$

Camp (1955) estimated the quantity of air required, for a typical case with diffusers at a depth of 14 ft (4270 mm), and water temperature of 50^0F (10^0C) for a G value equal to 10 s^{-1} (required for the final compartment of flocculation basin) and found to be 0.00315 cu ft per min per sq ft (0.095 cc/sq.cm-min.) of tank area. However, the devices were not available at that time to produce such a small flow of air to implement the process of diffused air flocculation.

Camp (1955) also concluded the following:

(i) For good flocculation, air bubbles should be distributed uniformly throughout the volume of water.

(ii) Air bubbles should be small enough in size so that the velocity gradients close to the bubbles are not great enough to disrupt the floc.

(iii) Floc particles might be carried upward by the air bubbles to form a scum at the surface of the water and that would reduce the concentration of flocculable particles and thus increase the time of flocculation.

(iv) Diffused air flocculation offered an opportunity for a saving in the initial cost of the plant.

(v) Much research and development would be required in order to obtain satisfactory diffusers so that flocculation by aeration might be controlled within optimum limits.

McConnachie, G. L. (1984): McConnachie published the results of his work in which the flocculation efficiency with the intensity of bubble agitation was examined and the pattern of fluid velocity and the velocity fluctuations throughout the volume resulting from the bubble stream was monitored using laser-Doppler anemometry. The efficiency of flocculation was shown to be affected by bubble size and air flow rate. Correlation was made between flocculation efficiency and the intensity of agitation imparted to the liquid from the bubbles.

Kaolinite suspension was made by adding kaolin and alkalinity to distilled water and coagulated with alum. Kaolin was chosen as it produced results from treatment that were similar to those using river water. A perspex tube of 92 mm internal diameter with an operational water height of 315 mm was used in McConnachie's (1984) work. Three different bubble sizes were used, 0.2 - 0.5 mm (very small), 0.5 - 1.5 mm (small) and 1.5 - 4.0 mm (large) effective diameter. Size measurement was made from photographs. Air was diffused through a sintered glass filter funnel of maximum pore diameter 5 - 10 μm in the case of the small and very small bubbles and through a 0.9 mm diameter hypodermic needle for the large bubbles.

It was mentioned that the size of the bubble formed was affected not only by the size of the opening but also by the surface tension that has to be overcome at the mouth of the opening and the air flow rate. However, the bubbles were not uniform in size, different size ranges were applied in the investigation. It was also reported that there was no flotation of solids in the test and there was no difficulty of coalescing the bubbles up to the maximum air flow used in his work. At the end of his investigation he drew the following conclusions:

(i) The use of bubbles as a source of mixing for flocculation was confirmed, with tapered agitation intensity giving significant improvement in efficiency over fixed

agitation.

(ii) Minimum residual turbidity occured at relatively low air-flows. This, and the improvement from compartmentalised tanks and subsequent filtration might make bubble agitation more economical than paddle mixers in conventional systems.

(iii) The efficiency of flocculation was affected by the size of the bubbles. Of the three size ranges used, 0.5 - 1.5 mm gave the lowest residual turbidity.

(iv) The flocculation efficiency was found to be related to the degree of turbulence induced and appeared to be influenced by the distribution of turbulence within the reactor. An even distribution of many bubble streams in a tank would be beneficial in promoting flocculation.

A cost comparison was also made and it was shown that the power required in diffused air flocculation to treat a volume of water of 2160 m^3 per day was 125 Nm/s. This compared with 160 Nm/s for mechanical paddle stirrers (Smethurst, 1979) for the same flow rate.

An optimum air loading of 0.16 cc/sq.cm-min. was reported for a water depth of 315 mm.

Al-Hiary, S.M. (1988): Al-Hiary conducted the experimental work to study the validity of using optimal introduced air flow rates and orifice diameter in the process of diffused air flocculation. A 400 × 400 mm chamber with an operational water height of 2000 mm and made of perspex plastic sheet was used in his work. Perforated metal pipes were used as the diffusers. Four different sizes of the orifice, 1.0, 2.0, 3.0 and 4.0 mm in diameter and different air flow rates ranging from 200 to 10,000 cc/min. were applied in this investigation. Silica (mass density = 2.6 g/cc) and kaolinite (mass density = 2.45 g/cc) suspensions were treated with aluminium sulphate as the coagulant in the model flocculator by using diffused air. The optimum air flow rates were found in the range of 1,000 - 2,000 cc/min for silica

turbidity and 400 - 1,000 cc/min for kaolin turbidity.

From the experimental work and analysed results, Al-Hiary concluded the following:

(i) The process of pneumatic flocculation was valid to coagulate and flocculate the turbid water according to the procedure used in his work.

(ii) The working range of air flow rate per unit area of the chamber was 0.625 to 1.250 cc/sq.cm-min. for silica and 0.250 to 0.625 cc/sq.cm-min. for kaolin turbidity. That was for a chamber of water depth of 2000 mm.

(iii) Contrasting behaviour of silica and kaolin turbidities had been observed due to differences in the physico-chemical characteristics of the turbidity materials. Flocs made up of silica were more settleable and less sensitive for power variations than those made up of kaolin due to the differences in shape, size, density and electrical properties.

(iv) The best removal of silica turbidity (95% efficiency) was achieved after 2 hours at an air flow rate of 2000 cc/min (1.25 cc/sq.cm-min.) and 1.0 mm orifice diameter. And the best removal of kaolin turbidity (94.3% efficiency) was achieved at an air flow rate of 600 cc/min. (0.375 cc/sq.cm-min.) and 3.0 mm orifice diameter.

(v) The rate of producing flocs followed an oscillatory shape of curve with respect to the orifice diameters.

(vi) The rate of settling for silica flocs was faster than that of kaolin flocs at the same air flow rate.

(vii) Dissolved oxygen content increased by aerating the water.

(viii) The method appeared to be flexible, simple and economical and recommended to apply in water treatment plants, with minimum mechanical maintenance.

2.3 THEORY AND PRACTICE OF COAGULATION-FLOCCULATION AND SEDIMENTATION

The medical erudition of Sanskrit and the Egyptian inscriptions provide the information on water treatment by using a variety of mineral and vegetable substances (AWWA, 1971). The earliest use of coagulation for the treatment of municipal water supplies occurred in Bolton, England in 1881. From 1885 onward coagulation was widely used for water treatment. Thus, coagulation and flocculation each used in a small way through the ages, were finally wedded. Until today, coagulation, generally followed by flocculation has been used most widely as the process to remove substances producing turbidity in water.

Historically, the term "coagulation" and "flocculation" have been used indiscriminately to describe the process of the removal of turbidity from water. In the literature on the subject a number of definitions have been variously used in describing these two terms. However, there is a clear distinction between the two terms widely accepted in the field of water treatment.

Coagulation refers to the destabilisation of colloidal particles in the suspension, whereas flocculation refers to the inducement of the destabilised particles to come together, make contact and thereby form larger agglomerates.

Historically, two broad theories have been proposed to explain the mechanisms of coagulation and flocculation. The chemical theory (older) assumes that colloids acquire electrical charges on their surfaces by the ionisation of chemical groups present at the surface and that coagulation or destabilisation is accomplished by chemical reactions between the colloid particles and the coagulant. The physical theory concentrates on the physical factors of electrical double layer and counterion adsorption where destabilisation occurs through reduction of zeta potential. Several studies have been undertaken to describe the concept of the electrical double layer. The theory was first proposed by Helmholtz in 1879 and subsequently modified by a number of workers. The contribution of Gouy , Chapman and Stern are

mentionable, with the latter's theory being more generally accepted (AWWA, 1971). These theories are very complex and can be found elsewhere (Weber, 1972; Clark *et al.*, 1977; Bratby, 1980). However, the theories are described briefly in their simplest form in chapter 1, section 1.3 to section 1.5.

The process of coagulation and flocculation is sensitive to many variables such as pH, coagulant dose and concentration, intensity and duration of mixing, physico-chemical properties of the suspended materials etc. Extensive literature has been surveyed and the main factors that influence the process of coagulation and flocculation have also been identified. The summary of the literature surveyed on this aspect will be discussed in the following sections.

2.3.1 Classical Theory of Coagulation: During the 1800s, the colloid chemists working with monodisperse colloidal suspension at high concentration observed that coagulation could be obtained by the addition of electrolytes (AWWA, 1971). Schultze in 1882 and Hardy in 1900 studied the reactions of electrolytes in suspension quantitatively and their results led to the Schultze-Hardy rules. Essentially, they stated that coagulation is caused by ions having a charge opposite to that of the colloidal particles and that the coagulating power of an ion is markedly dependent on its valency. They further showed that the stability of a colloidal suspension was due to the electrical repulsion existing between particles and that the introduction of ions of opposite charge results in charge neutralisation with consequent zeta potential reduction to zero under which condition, the coagulation occurred.

The quantitative theory of colloid stability was proposed by Deryagin and Landau (1941) and Verwey and Overbeek (1948) and confirmed the Schultze-Hardy rule of valency dependence. They showed that stability was not due to electrical repulsion but the interaction between two particles, each of which is surrounded by an electrical double layer. This double layer prevented the close approach of the particles within the distance in which van der Waals forces could operate to cause coagulation. By addition of electrolytes the thickness of the electrical double layer

was reduced and coagulation would occur due to the reduction of the barrier to close approach of particles.

It is to be noted from their work that zeta potential is not a determining measure of this reduction of double-layer interaction and consequent increase in extent of coagulation. More important than zeta potential is the reduction in double-layer thickness. While zeta potential tends to approach zero, coagulation is possible well before electrical neutrality is achieved (AWWA, 1971).

The removal of colloid particles from water by the process of coagulation and flocculation can be crucially dependent on the manipulation of colloid interactions. There are several types of colloid interaction and the most important of them, as discussed by Gregory (1993), are van der Waals forces, electrical interaction, hydration forces, hydrophobic interaction and effects associated with adsorbed polymers and polymer bridging. The classical theory of colloid stability proposed independently by Deryagin and Landau (1941) and Verwey and Overbeek (1948), as discussed above, is based on the concept of van der Waals attraction and electrical interaction. This is the earliest, and still the only truly quantitative theory of colloidal stability and widely known simply as DLVO theory (Gregory, 1993). Essentially van der Waals attraction and electrical double layer repulsion are assumed to be additive between the particles as a function of separation distance. Conventional coagulation is still by and large the treatment technology of choice in water treatment industries (Dempsey, 1995).

2.3.2 Theory of Flocculation

Flocculation is the term that is used to describe the growth of destabilised tiny colloidal particles, formed in the coagulation stage, into large visible agglomerates through particle transportation and bond formation.

The transportation of particles can be attained either automatically due to Brownian motion, called perikinetic flocculation (Overbeek, 1952) or artificially by introducing

some means of power input, generating velocity gradient, called orthokinetic flocculation. Thus there are two stages in the flocculation process. Perikinetic flocculation involved with the formation of minute particles, often called "unit flocs", which are smaller than 1 μm and usually formed very rapidly, in less than a minute, whereas orthokinetic flocculation brings the "unit flocs" into intimate contact to form bulky separable floc with particle size > 1 μm and formed more slowly as the particles grow (Weber, 1972; Clark *et al.*, 1977).

Perikinetic flocculation is beyond the control of designer or operator (Ives and Bhole, 1973). Root *et al.* (1940) showed that this stage of flocculation is completed in a few seconds and is therefore of negligible importance in fixing tank dimension as compared to the turbulent-mixing phase (Camp, 1955). Orthokinetic flocculation can be under the control of the designer or operator of a treatment works. The theoretical development and practical applications of perikinetic and orthokinetic flocculation will be dealt with in the following paragraphs.

Perikinetic Flocculation: The knowledge of particle transport in the flocculation process is based on the work of Von Smoluchowski (1917). He developed a theory for perikinetic flocculation to explain the effect of particle movement due to Brownian motion that promotes flocculation of minute particles. According to this theory the rate of contacts per unit time between two sizes of particles is proportional to the product of particle concentrations, to the mutual diffusion coefficient of the particles and the radius of interaction of the two particles i. e.

$$J_{ij} = 4\pi D_{ij} R_{ij} n_i n_j \qquad (2.7)$$

where, J_{ij} is the number of contacts per unit time between particles of radius R_i and R_j , D_{ij} is the mutual diffusion coefficient of particles i and j , R_{ij} is the radius of interaction of the two particles i.e. $R_{ij} = R_i + R_j$ and n_i , n_j are the number of i-fold and j-fold particles.

Diffusion coefficient for this system is defined by the Stokes-Einstein equation as

follows:

$$D_{ij} = \frac{2\kappa T}{3\pi\mu R_{ij}} \tag{2.8}$$

where, κ is the Boltzmann's constant (1.38×10^{-23} J/K), T is the absolute temperature (deg K) and μ is the absolute viscosity.

Perikinetic transport resulting from Brownian motion is represented by the diffusion coefficient D_{ij} in Equation (2.7). This is the basic equation describing the perikinetic flocculation. It has been verified (Manley and Mason, 1952; Swift and Friedlander, 1964) experimentally for monodispersed system. This equation is also derived theoretically by Ives (1978). Swift and Friedlander (1964) expressed the equation for initial rate of flocculation in modified form also for monodispersed system which is presented by equation (1.1) as follows:

$$J_{pk} = \frac{d}{dt}(N_0) = -\frac{4}{3}\frac{\eta\kappa T}{\mu}(N_0)^2 \tag{1.1}$$

If the velocity gradients exist in the liquid of a magnitude greater than 5 s^{-1} and if particle sizes are larger than 1 μm the effect of perikinetic flocculation is negligible and orthokinetic flocculation need only be considered under such conditions (Bratby, 1980).

Orthokinetic Flocculation: Von Smoluchowski (1917) developed a theory for orthokinetic flocculation of colloidal particles under laminar flow condition. According to this theory the rate of contact of two sizes of particles is proportional to the product of the particle concentrations, to the velocity gradient, and to the cube of the radius of interaction of the two particles and thus,

$$J_{ij} = \frac{4}{3}n_i n_j (R_{ij})^3 \frac{du}{dz} \tag{2.9}$$

where $\frac{du}{dz}$ is the velocity gradient in laminar flow. This equation is considered to be the basic equation describing the orthokinetic flocculation (Ives and Bhole, 1973).

The equation has been verified experimentally by Manley and Mason (1952) and also by Swift and Friedlander (1964) for monodispersed system.

This equation is applicable for the system of particles of uniform size or for the particles of two sizes. Use of the equation for a general system consisting of many sizes of particles has not been feasible (except to a very limited extent, using a digital computer) (Ives and Bhole, 1973). Furthermore, as the theoretical treatment is based on laminar flow conditions, the application of the equation to the design of flocculation tanks is also limited (Bratby, 1980). Such flow condition is difficult to achieve in practice (Ives, 1978). The more usual condition existing for the practicable velocity gradients applied during flocculation is a turbulent regime (Camp, 1969).

The velocity gradient term $\frac{du}{dz}$ was replaced by G, the average velocity gradient by Camp and Stein (1943) in order to avoid the unknown local velocity gradients in turbulent mixing. The average velocity gradient term G designated the root mean square velocity gradient which was defined by Camp (1955) as

$$G = (W/\mu)^{1/2} = (P/\mu V)^{1/2} \tag{1.3}$$

where, W is the dissipation function, i.e. total power dissipated divided by the volume of the fluid.

Substituting $\frac{du}{dz}$ in Equation (2.9) by G, Camp and Stein's (1943) equation for orthokinetic flocculation is given by

$$J_{ij} = \frac{4}{3} n_i n_j R_{ij}^3 G \simeq \frac{1}{6} n_i n_j (d_i + d_j)^3 G \tag{2.10}$$

The disadvantage of using the average velocity gradient, G is that it does not describe the length scale over which local velocity gradients extend. That is, velocity gradients which extend for a given mixing length do not influence the flocculation

of particles which are larger than this distance (Bratby, 1980).

Smoluchowski's (1917) Equation(2.9) has been extended (Fair and Gemmell, 1964) to describe the rate of change in number concentration of flocs of a given size R_k :

$$\frac{dn_k}{dt} = \frac{2}{3}\left[\sum_{\substack{i=1\\ j=k-1}}^{k-1} n_i n_j R_{ij}^3 - 2n_k \sum_{i=1}^{\infty} n_i R_{ik}^3\right]\frac{dv}{dz} \qquad (2.11)$$

in which the first term in the parenthesis describes the formation of particles of radius R_k from a range of particles. The second term in the parentheses depicts the elimination of *k*-fold particles due to their collisions with all other particles.

In all the equations above floc break up was not considered and all collisions were assumed to result in lasting contact. Harris and Kaufman (1966) and Harris *et al.* (1966) modified Equation (2.11) to include floc break up and the possibility of non-lasting collisions. They considered the case of $k = 1$, which describes the rate at which primary (1 - fold) particles are removed from the system. Their expression for the rate of change in primary particle concentration is as

$$\frac{dn_1}{dt} = -\frac{\alpha\delta a^3}{\pi}\phi n_i \qquad (2.12)$$

where, α is the fraction of collisions which result in aggregation, a is the ratio of collision radius of a floc to its physical radius, ϕ is the floc volume fraction and δ is the size distribution function which is given by

$$\delta = \frac{\sum_{i=0}^{p-1} n_i \left(i^{1/3} + 1\right)^3}{\sum_{i=0}^{p} i\, n_i} \qquad (3.13)$$

The maximum floc size permitted is p - fold. Hudson (1965) considered a simplified bimodal floc size distribution in a continous flow system. The removal of primary

particles, in a system composed of only primary particles and large flocs and assuming the size variations within each group are small in comparison to the difference between the groups, is hypothesised to occur primarily by their collisions with flocs. Based on this consideration Equation (2.11) is simplified as

$$\frac{dn_1}{dt} = \frac{4}{3} n_1 n_F R_F^3 \frac{dv}{dz} \tag{2.14}$$

where, R_F is the radius of flocs and n_F is the floc number concentration.

This type of flocculation probably occurs whenever applied velocity gradients are linear over a distance of a particle diameter (Bratby, 1980). It is also applied to floc blanket clarification (Ives, 1995).

Based on the hypothesis that particles suspended in a turbulent regime experience a random motion resembling gas molecules, Argaman and Kaufman (1968, 1970) proposed a diffusion model for orthokinetic flocculation. An assumption of simplified bimodal floc size distribution comprising primary particles and large flocs was made in their analysis. This assumption was also made by Hudson (1965) in his work. Argaman and Kaufman (1968, 1970) experimentally verified the validity of the bimodal distribution by analysing floc size measurements. Their model for orthokinetic flocculation is analogous to that of Von Smoluchowski (1917) for perikinetic flocculation and is given by:

$$H_{1F} = 4\pi K_s R_F^3 n_1 n_F u^2 \tag{2.15}$$

where, K_s is the proportionality coefficient expressing the effect of the turbulence energy spectrum on the effective diffusion coefficient, R_F is the radius of floc, n_1, n_F are the number concentration of primary particles and the flocs respectively, u^2 is the mean square velocity fluctuation, which is related to the root mean square velocity gradient, G, and is a measure of the intensity of turbulence.

It is interesting to note that although Equation (2.15) was derived for orthokinetic flocculation using the concept of turbulent diffusion, it is equivalent in form to the

orthokinetic flocculation equation of Von Smoluchowski (1917) using the concept of laminar flow velocity gradients. In fact all the equations derived for particle aggregation kinetics during orthokinetic flocculation are similar in form to Equation (2.9). The differences lie in the constant terms and the definitions of velocity gradient (Bratby, 1980).

Ratio of Perikinetic and Orthokinetic Rates: The relative significance of perikinetic and orthokinetic flocculation may be examined by considering the initial aggregation rates for a monodisperse system of spherical particles of radius *R*. The ratio of these rates is useful and can be obtained by dividing Equation (2.9) by Equation (2.7):

$$\frac{J_{ik(ok)}}{J_{ij(pk)}} = \frac{\frac{4}{3} n_i n_j (R_{ij})^3 \frac{du}{dz}}{4\pi D_{ij} R_{ij} n_i n_j} \qquad \text{so that,}$$

$$\frac{J_{ok}}{J_{pk}} = \frac{\mu G d^3}{2\kappa T} \qquad (2.16)$$

In water at 25^{0}C containing colloidal particles having a diameter of 1 μm, this ratio is unity when the velocity gradient is 10 s^{-1}. For colloidal particles having a diameter of 0.1 μm, it is apparent that a velocity gradient of 10,000 s^{-1} is necessary for orthokinetic flocculation to be as rapid as perikinetic flocculation. Similarly, for the particles which are 10 μm in diameter, a velocity gradient of 0.01 s^{-1} will provide sufficient orthokinetic flocculation to equal the contacts resulting from diffusion.

This indicates that stirring will not enhance the aggregation rate of small particles until they grow to a size of about 1 μm. Orthokinetic transport predominates in the aggregation of larger particles. Particle growth to a size larger than 1 μm requires velocity gradients by agitation to construct large aggregates. However, at all times the two rates are assumed to be additive, therefore, in some orthokinetic flocculation experiments, the perikinetic flocculation has first to be measured to establish a baseline for observing orthokinetic flocculation (Bratby, 1980).

2.3.3 Rapid Mixing in Coagulation

In the overall coagulation-flocculation process of water treatment, rapid mixing or flash mixing refers to that stage where coagulant chemicals are added and the water is then vigorously agitated to ensure the uniform mixing of coagulant chemicals in a very short period of time. This stage is probably the most significant operation in the process as destabilisation reaction occurred and primary floc particles are formed, the characteristics of which markedly influence the subsequent flocculation kinetics (Bratby, 1980).

Objectives: The main objective of rapid mixing is to disperse the coagulants uniformly and intimately throughout the volume of water in order to allow adequate contact between the coagulant and the suspended particles prior to completion of hydrolysis. Rapid mixing of the coagulant with raw water is necessary as the first step in good flocculation (Tolman, 1942). As the coagulant dosage is proportional to the total flow of water into the plant and the concentration of colloidal matters in raw water (Kawamura, 1973), the necessity of uniform dispersion is quite clear. In the absence of sufficient mixing, some portions of the water may receive concentrations of coagulant high enough to restabilise the particles whereas other portions may have concentrations too low to initiate coagulation (Hudson and Wolfner, 1967). Consequently, poor plant performance or wastage of chemicals or both would result.

Hudson (1965) observed that rapid mixing during coagulant addition prior to slow mixing was important for effective flocculation when a low degree of agitations were used during the slow-mix operation. Measurements reported by Hudson (1965) show that flocs formed following rapid mixing contained appreciably more solids than those formed without a rapid mix period.

Thus it appears that rapid mixing of the suspension during coagulant addition is essential to disperse, quickly and evenly, the chemicals added (Tekippe and Ham, 1971).

Rapid Mixing Device: Several types of device are available for rapid mixing in water treatment industries. Mechanical agitation by a propeller is possibly the most common (Tekippe and Ham, 1971) since it is reliable, very effective and extremely flexible in operation (Reynolds, 1982). The most common rapid-mix device is a single back-mix type chamber with a single turbine or propeller impeller (Letterman *et al.*, 1973). A description of this device is given in *Water Treatment Plant Design* (AWWA, 1969). The in-line mixer is the most compact method and is increasing in popularity (Reynolds, 1982). Most water treatment facilities in the U.S.A. use either turbine or static mixers during coagulant addition (Dempsey, 1995).

Numerous configurations of the tanks and the impellers are used, with the most popular units being square tanks with back-mix impellers (Howard *et al.*, 1987). A more effective unit might be a square tank with baffles and blade impellers (Amirtharajah, 1988).

Design Parameters: The mixing time of coagulants, t and the intensity i.e. velocity gradients, G, are considered as the design parameters in rapid mix operation. The reaction occurred in the destabilisation of colloidal particles control the design of the rapid mix unit. The reactions are very rapid, it is believed they occur in less than a second (Weber, 1972). The time required for complete hydrolysis was estimated by Hudson and Wolffer (1967) and found to be of the order of a fraction of a second after addition of the coagulant. In an article on water-treatment chemistry Moffett (1968) stated, ".... it is indicated that coagulation has taken place and that flocculation, due to Brownian motion, is essentially completed in 0.1 second".

In the study by Griffith and William (1972), the time of rapid mix in the several tests varied from 5 to 60 seconds and it was found, without exception, that turbidity removal was not improved by rapid-mix detention periods greater than 5 seconds. All tests demonstrated that very rapid and uniform coagulant dispersion is required for maximum turbidity removal.

In fact, beyond a certain rapid mix time, a detrimental effect on flocculation

efficiency may result. Letterman *et al.* (1973), studied the optimum rapid mix period for minimum residual turbidity and concluded that the existence of an optimum rapid-mix period suggested that the early conditions of floc formation were important and the function of the rapid-mix operation was more than simply to disperse the coagulant. For a particular water and type of coagulant applied, the optimum rapid mixing time is dependent on the velocity gradient and the coagulant dosage applied.

Rapid mix detention times of 30 - 60 seconds are traditional, with a minimum of 30 seconds required by many water authorities. According to a survey of 15 water treatment plants reported by Hubbell (1969), the nominal detention time of the rapid mix chamber ranged from 48 seconds to 5 minutes with an average value of 1.9 minutes.

Letterman *et al.* (1973) found, in their studies, the optimum rapid mix time as 9 seconds to 2.5 minutes for a turbidity range of 10 to 100 mg/l with a G value of 1000 s^{-1}.

The optimum rapid mix detention time and the intensity suggested by various authors and researchers are summarised in Table 2.1.

Table 2.1 Suggested rapid mixing time and intensity

Authors/Researchers	Mixing Time	Mixing Intensity, s^{-1}
AWWA (1969)	20 - 40 seconds	700 - 1000
Hubbell (1969)	48 seconds - 5 minutes	-
Letterman *et al.* (1973)	9 seconds - 2.5 minutes	1000
Steel and McGhee (1979)	1 - 2 minutes	500 - 1000
Reynolds (1982)	20 - 60 seconds	700 - 1000
Twort (1985)	20 - 30 seconds	500 - 600
Degre'mont (1991)	1 - 3 minutes	250 - 1000

It is understood from the theory and literature that the chemical reactions occurred in the destabilisation of colloidal particles in a very short time, in a fraction of a second. The theoretical detention time is much less than that adopted in treatment

plants for many reasons such as the quality of raw water, intensity of mixing, prevention of short-circuiting flow, type, dose and concentration of coagulants etc.

Based on the theory and practice of rapid mixing, throughout the experimental work of the present investigation, it was decided to work with a rapid mix detention time of 120 seconds both in mechanical stirring (Jar Test) and diffused air agitation (pneumatic coagulation-flocculation). The corresponding G values of 690 s^{-1} and 300 s^{-1} were applied for the mechanical (Jar test) and the pneumatic agitation respectively.

An air flow rate of 38,000 cc/min. was applied during the operation of rapid mixing in pneumatic coagulation-flocculation. The corresponding mixing intensity, at a G value of 300 s^{-1}, was hoped to be enough to disperse the coagulant thoroughly and homogeneously throughout the chamber to produce appreciated settleable flocs after slow-mixing under initial standardised conditions.

2.3.4 Slow Mixing in Flocculation

The theory of orthokinetic flocculation indicates that the velocity gradient in the water is an important parameter. In practice, it is measured indirectly in terms of power transmitted to the water to provide the fluid motion.

Practical experience and the laboratory investigations have proved that the maximum limiting floc size changes inversely with respect to velocity gradient (Ives and Bhole, 1973) i.e.

$$r_{max} = k/G \tag{2.17}$$

where r_{max} is the radius of the maximum floc size and k is the constant of proportionality and thus

$$(\text{Volume})_{max} = (k'/G)^3 \tag{2.18}$$

where k' is another constant of proportionality.

Camp (1968) stated that there is a limiting size of floc corresponding to each value of the velocity gradient and floc sizes are smaller for greater velocity gradient. Langelier (1921), Ritchie (1956), Michaels and Bolger (1962), Lagvankar (1968) and Argaman and Kaufman (1968) also observed the same fact.

The intensity of velocity gradient controls the degree of flocculation. Hudson (1965) has noted that previous publications have indicated the existence of a maximum velocity gradient. Mixing at intensities beyond this maximum appeared to be detrimental to floc formation (Villegas and Letterman, 1976). Several publications (Camp, 1955; Griffith and William, 1972; Letterman *et al.*, 1973) have noted the observation of an optimum velocity gradient.

The optimum G value in the flocculation process is defined as the G value which, when other conditions such as the alum concentration, flocculation period length and physico-chemical characteristics of the water are held constant, maximises turbidity removal by the flocculation and sedimentation process, i.e. minimises residual turbidity (Villegas and Letterman, 1976). The optimum value of G and flocculation time t, depend on the chemical composition of the water and the nature and amount of colloids present. The optimum G tends to decrease with increasing turbidity (Barnes *et al.*, 1981).

For any water, there is an optimum combination of G and t, and a range of G and t values near the optimum which will give adequate performance (Barnes *et al.*, 1981). Figure 2.1 shows the typical zones in the G-t plane. Combination of G and t falling in the hatched area give satisfactory performance. Excessive velocity gradients cause floc rupture and excessive flocculation time allows floc erosion to occur. The zones of satisfactory performance are different for waters from different sources. In extreme cases, the zones for two different waters may not overlap (Barnes *et al.*, 1981).

Kawamura (1973) investigated the effect of the mixing intensity on residual turbidity, when water of varying quality and alum concentrations were used. An optimum

mixing intensity was observed for each alum concentration studied. In general, this optimum decreased as the alum concentration was increased.

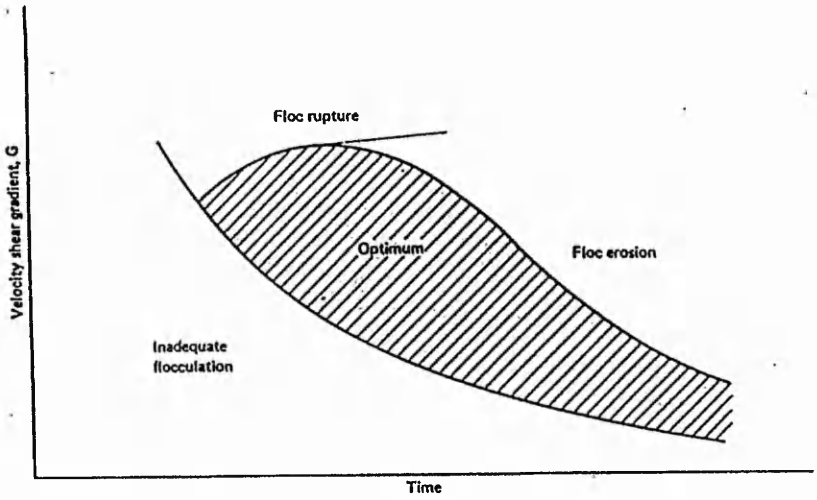

Figure 2.1 Typical zones in *G-t* plane

Griffith and William (1972) observed that the optimum *G* value was a function of the chemical characteristics of the water being treated. They also determined that the optimum *G* value was not a function of the sedimentation period used.

Mean *G* values of between 20 and 100 s^{-1} and flocculation time of 20 to 40 minutes are commonly used (Barnes *et al.*, 1981). The recommended values of flocculation time are 20 to 60 minutes and that of *G* are 5 to 100 s^{-1} (AWWA, 1969). Camp (1955) has reported *G* values and flocculation tank detention time for 20 operating water treatment plants in USA. The *G* value ranged from 20 to 74 s^{-1} and detention time ranged from 10 to 100 minutes. Kawamura (1973) noted that, in general a maximum *G* value of 100 s^{-1} and an optimum *G* value of 50 s^{-1} appears to apply to a wide range of flocculation process. Kawamura (1976) also noted that values of *G* from 25 to 100 s^{-1} are accepted by many researchers, based on the data from laboratory scale studies and actual operation data in many treatment plants. In the study by Argaman and Kaufman (1968), the optimum *G* values observed were 30

s^{-1} for a detention time of 48 minutes to 100 s^{-1} for a detention time of 4 minutes.

Many authors and researchers used the dimensionless product of *G* and *t*, sometimes called "Camp Number", to indicate the intensity of turbulence and the degree of flocculation. It is more convenient to use the *Gt* value in the sense that just a number can be used. Based on the observational data from twenty water works in the USA, the optimum value of *Gt* was set between the limits of 2×10^4 and 2×10^5 (Camp, 1955) to achieve a satisfactory flocculation (Camp, 1955).

However, the Camp number *Gt*, is not a sufficient criterion to cover all cases of flocculation, particularly those of the floc blanket clarification (Ives, 1981). To overcome this shortcoming other workers have suggested that the effect of particle or floc concentration should be included in any assessment of flocculation adequacy (Barnes *et al.*, 1981). The number *GtC*, where *C* is the particle or floc volume concentration, has been suggested as a useful parameter in such a case of flocculation (Barnes *et al.*, 1981). The very low *G* values (typically < 5 s^{-1}) in the floc blanket clarifiers, are compensated by much higher *C* values (Ives, 1981).

2.3.5 Factors Influencing Coagulation-Flocculation

The attainment of optimum coagulation-flocculation treatment of raw water indicates a very complex equilibrium which depends on many interrelated variables such as pH, alkalinity, turbidity, chemical composition of water, type of coagulant and physical factors as temperature and mixing conditions. These interrelations are so complex that it is impossible to predict from theoretical bases the optimum coagulant dose for any particular water (AWWA, 1971). The optimum dose and other conditions for coagulation are determined empirically for each water which will be discussed later. In spite of these difficulties, a knowledge of the effects on coagulation of several variables would be advantageous for practical purposes. The factors that influence the process of coagulation and flocculation have been identified and will be discussed in the following sections:

2.3.5 (a) Effect of pH: Early investigators of the coagulation process in water treatment clearly established that there is at least one pH range for any given water within which good coagulation-flocculation occurs in the shortest time with a given coagulant dose. This range is affected by the type of coagulant used, the chemical composition of water and the concentration of coagulant. Coagulation should be carried out within the optimum range of pH, failure of which produces either waste of chemical or poor plant performance (AWWA, 1971).

The charge on colloidal surfaces is usually a function of the type of material and the pH. Colloids tend to be negatively charged at a high value of pH, while at low values they tend to be positively charged. This may be related to exchange of H^+ and OH^- ions to establish equilibrium with the water at different pH values (Barnes *et al.*, 1981).

At a certain pH value, the colloidal charge is zero. This pH value is known as the iso-electric point for that particular colloid. Thus, the adjustment of pH can be considered as a method of destabilisation. However, for common colloids in raw water, it would require large amounts of acid and then, later, large amounts of alkali for pH adjustment which involve more costs (Barnes *et al.*, 1981).

There have been many papers showing that pH is one of the most important variables of those that have to be considered for effective coagulation-flocculation (Kawamura, 1976). The metal coagulants (salts of aluminium and iron) have been shown to precipitate and coagulate most rapidly and with minimum solubility in a certain pH range, depending upon the coagulant used (AWWA, 1971). Typical solubility curves for alum floc and iron floc have been shown by Sawyer (1960), Weber (1972), AWWA (1971) and Camp (1952).

In practice, in the presence of ions and turbidity normally present in natural waters, the optimum pH range is generally 6.0 - 7.8 for alum flocculation and 4.0 - 8.0 for iron hydroxide flocculation (Kawamura, 1976).

Black and Chen (1965) stated, "The adjustment of pH to a range where the most effective hydrolysis species of the coagulant is formed is shown to be very essential in producing optimum coagulation". Kawamura (1959) showed that the water which received pH adjustment before alum application, produced a much lower supernatant turbidity than the unadjusted water with the same amount of alum dosage.

pH can be adjusted by adding a proper amount of sulphuric acid or carbon dioxide gas to water. From the viewpoint of water quality, carbon dioxide is the better pH control agent, but sulphuric acid has advantages from the viewpoint of storage capacity and feeding problems (Kawamura, 1976). In some treatment plants, addition of excess coagulant might be a more practical way to reduce pH to the favourable range than separate acid addition (AWWA, 1971).

A study by Kawamura (1967) on organic colour removal by alum flocculation indicated that the best removal was achieved at the optimum pH range of 5.0 - 6.0. Black *et al.* (1961, 1963) conducted similar studies and the optimum pH was reported about 5.0 by alum flocculation and about 4.0 by ferric sulphate flocculation.

Relationship between pH and Alkalinity: For optimum removal of turbidity by alum flocculation, only optimum pH or optimum alkalinity is generally considered as the factor to be adjusted. Experiments were conducted by Kawamura (1976) who found that the most efficient turbidity removal using alum as a coagulant was related to optimum values of pH and alkalinity for each water. The result of the experiments has led to the conclusion that both pH and alkalinity must be considered for optimal flocculation.

2.3.5(b) Effect of Coagulant: The selection of a coagulant is one of the important factors that influence the process of coagulation. A wide variety of coagulants, polymers and polyelectrolytes are available for coagulation. Aluminium sulphate is still one of the most effective, economical and foolproof coagulants and is extensively used in the field of water treatment. Alum is popular because it is relatively inexpensive and the water treatment industry has experience and

confidence in the use of alum (Dempsey, 1995). Alum coagulation and flocculation can, however, be affected by many factors such as pH, temperature, nature of colloids, size of the turbidity particles, mixing intensity and duration and alum concentration (Kawamura, 1976). Aluminium compounds, in particular alum, have been known to be used in water treatment for 4000 years. Its use in the U.K. started in the 13th century, being imported from Spanish sources before U.K. production started in the 17th century (Simpson, 1995).

A significant advantage of iron salts over aluminium is the broader pH range for good flocculation. Packham (1963) showed that the considerable differences in pH zones of good flocculation between aluminium and iron salts as shown in Figure 2.2. For alum the pH zone for optimum coagulation is quite narrow, ranging from about 6.8 to 7.5; the comparable range for ferric sulphate is considerably broadened, to a pH range of about 5.5 to 8.8 (AWWA, 1971). Ferric salts would normally be used at pH 4.0 to 5.0 when good colour removal is required (Simpson, 1995).

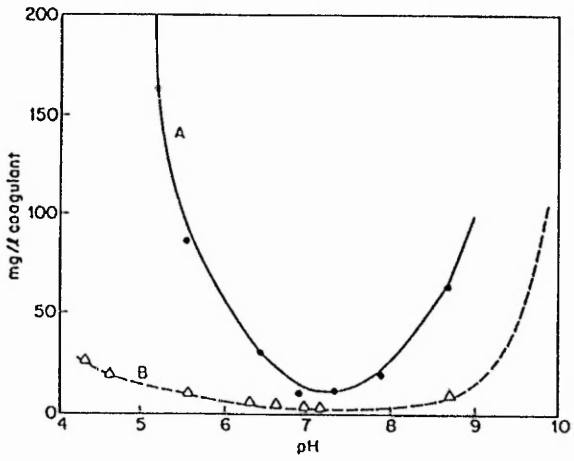

Coagulation of 50 mg/l kaolin with aluminium sulfate and ferric sulfate Comparison of pH zones of coagulation of clay turbidity by aluminium sulfate, curve A, and ferric sulfate, curve B. Points on the curves represents the coagulant dosage required to reduce clay turbidity to one-half its original value. [Adapted from R.F. Packham, Proc. Soc. Water Treat. Exam. 12:15 (1963).]

Figure 2.2 pH zones for alum and iron salts

Ferric sulphate has been used in UK specifically as a coagulant for water and

industrial effluent treatment since 1966 when, as a result of experiments performed by the CEGB (Central Electricity Generation Board), U.K., it was found that the material proved to be particularly effective for the removal of humic and fulvic acids from upland waters, prior to use for boiler make-up water. Before the advent of ferric sulphate the traditional chemicals used for water and effluent treatment had been aluminium sulphate, chlorinated ferrous sulphate and sodium aluminate (Water Services, 1975).

Although iron salts such as ferric chloride, chlorinated copperas, and ferric sulphate have been used in some treatment plants, iron salts as coagulants are not as popular as other substances because of their aggressive corrosiveness, higher chemical costs, and other adverse aspects as compared to alum and polymers (Kawamura, 1976). The selection of coagulant will depend on cost, availability, consumer confidence, compatibility with goals for reduction of residuals, flashiness of the water supply and adequacy of automatic dosing, etc. (Dempsey, 1995). The choice of the coagulant to be used for any particular water should be based on an experimental comparison of performance, with the final choice being influenced by economics (AWWA, 1971).

2.3.5(c) Dosage of Coagulant: The most important factor for coagulation is a proper dosage of coagulation (Kawamura, 1976). Coagulation is not yet an exact science, although recent advances have been made in understanding the mechanics of the process. Therefore, selection and optimum dosage of coagulants are determined experimentally by the jar test instead of quantitatively by formula. Jar-testing is supposed to duplicate conditions that might be imposed at full-scale (Dempsey, 1995).

The single most widely used test to determine dosage and other parameters such as the effectiveness of various coagulants, optimum pH for coagulation, concentration of coagulation and most effective order in which to add various chemicals is the jar test (AWWA, 1971; Clark *et al.*, 1977). The jar test attempts to simulate the chemical conditions and dosages of the full- scale coagulation-flocculation process and has remained the most common control test in the laboratory since its

introduction in 1918 (AWWA, 1971).

Neither the jar test equipment nor the procedure nor the method of reporting the results has been standardised (Barnes *et al.*, 1981). Since the intent is to simulate an individual plant's conditions, it is not surprising that there has been no standardisation of the test. Recently, ASTM has published a method for the jar test (ASTM D2035 - 80), which describes the basic logic and apparatus (Dempsey, 1995). The equipment for this test and the directions for proper performance are available (AWWA, 1971). Several aspects of jar testing were reviewed in an AWWA seminar (1988). A typical design of paddle and beaker and the operating conditions are described by Ives (1978). Detailed description of the apparatus, procedure and method of reporting are available that similar to methods used by some authorities (Charles, 1969; Barnes *et al.*, 1981).

2.3.5(d) Concentration of Coagulant: Alum solution concentration is a significant factor in coagulation-flocculation. Some works revealed that there is a relationship between alum concentration and residual turbidity following flocculation (Kitano and Kawamura, 1954; Kawamura, 1973; Letterman *et al.*, 1973; Kawamura, 1976). It is generally agreed that the concentration of alum solution to be fed to raw water should be low (<0.5 per cent solution). The alum solution concentration exerts an important effect on alum coagulation and this should not be overlooked (Kawamura, 1976).

The result of Kawamura's (1973) work indicated that the optimum economical alum dosage should be selected on the basis of most efficient alum concentrations for turbidity removal rather than in accordance with the simple correlation of alum dosage versus turbidity removal. The results indicated a turbidity hump that peaks between 1 - 3 per cent alum concentration and ends at about 7.5 per cent. Further it was suggested that the optimum dosage and concentration of feed be considered in the design of alum-feeding equipment in order to ensure operation at maximum efficiency.

The effect of ferric sulphate and ferric chloride concentration on flocculation were also tested, however, no significant difference was found within the limited number of tests performed (Kawamura, 1973).

The work of Griffith and William (1972) indicated that reasonable dilution might offer some mixing advantages that promote rapid and uniform coagulant dispersion. They showed that dilution of alum down to 1.5 per cent solution did not impair its effectiveness as a coagulant.

Extensive testing by Walker (1971) demonstrated the practicability of diluting to about a 0.6 per cent alum solution. Below a dilution of about 0.3 per cent Walker (1971) found a "decisive fall-off in coagulation effect".

Point of Application of Coagulant: Moffett (1968) stressed the importance of the location of the point of alum feed. In his experimental work it was found that 27 per cent more alum was required to obtain zero zeta potential when the coagulant was introduced on the surface of the water rather than at the agitator blade level of a Phipps-Bird Jar Tester.

2.3.5(e) Effect of Type of Turbidity Material: The nature of the turbidity materials must also be considered in coagulation (AWWA, 1971). The adsorption or ion exchange capacity of colloidal material is an important factor in coagulation phenomenon. The capacity of ion adsorption and ion exchange differs with the type of colloid (Kawamura, 1976).

Kawamura (1976) conducted a series of jar tests to determine the influence of the type of turbidity materials. The results indicated that turbidity materials with low base exchange capacities required smaller amounts of alum for clarification and had a small effective range of clarification.

2.3.5(f) Effect of Particle Size: The fineness of the particles that comprise the turbidity material is another important factor in coagulation demand.

According to Langelier *et al.* (1952), particles of 1-5 μm in diameter served as suitable structural units for building up a dense, rapidly settling floc. Particles of a 1 μm provided a binder action for flocculent growth, resulting in a porous bulky floc with a very slow settling velocity when alum was used as a coagulant. If both fractions of particle size existed in water, good floc would be provided. When raw water lacked either the colloidal or the coarse fraction, it was recommended that the particle-size distribution be adjusted by adding a colloidal clay or the other suitable material.

Cyclofloc units developed in Europe use micrograin sand (diameters of grains are a few tens of a micron) for seeding purposes with polymer and actual treatment unit, have shown good results (Gomella, 1974; Sibony, 1981).

2.3.6 Theory of Sedimentation

The impurities in water may be of different sizes and densities with different surface properties. Some of the suspended particles are unstable with respect to the suspension due to their sizes and densities and readily settleable from suspension under the influence of gravity. Smaller suspended particles are stable in the suspension mainly by electrostatic (Thermodynamic potential) and microhydrodynamic (Brownian motion) forces although some are thermodynamically unstable which take a long time to agglomerate (Weber, 1972). However, these stable particles may be coagulated in order to make them unstable and separated from the suspension by sedimentation in a reasonable detention time.

Sedimentation is the removal of solid particles from a suspension by settling under gravity. The settling characteristics are associated with the different types of suspension of solids and the process is involved with many variables that affect its efficiency. The unstable and destabilised particles settle in different ways depending upon the concentration of the suspension and the properties of the particles and the liquids.

Fitch (1958) has described the following four different types of sedimentation depending upon the concentration of the suspension and the flocculating properties of the particles:

(a) Discrete particle settling
(b) Settling of flocculent suspension
(c) Zone settling
(d) Compression settling

(a) Discrete Particle Settling: In a suspension of low concentration, particles settle discretely without changing their shape, size and mass during settling. The settling of such a particle is a function only of the properties of the fluid and the characteristics of the particle and is not affected by the presence of other particles (Weber, 1972).

An analysis of the discrete particles suspension in terms of settling velocities may be used in the design of settling basins. The settling velocity of discrete particles can be described in the light of the principles of classic mechanics by using the well-known formulations of Newton and Stokes.

For a spherical discrete particle, the general equation for the settling velocity can be derived from Newton's law and is given by

$$v_s = \left[\frac{4}{3}\frac{g}{C_D}\left(\frac{\rho_s-\rho_w}{\rho_w}\right)d_s\right]^{1/2} \tag{2.19}$$

where, g is the gravity constant, ρ_s and ρ_w are the mass densities of the particle and water, d_s is the diameter of the particle and C_D is the drag coefficient which is defined as follows:

$$C_D = \frac{24}{\mathbf{R}} + \frac{3}{\sqrt{\mathbf{R}}} + 0.34 \tag{2.20}$$

where **R** is the Reynolds number and this equation is applicable for $1<\mathbf{R}<10^4$ which includes all situations of interest in sedimentation of water containing suspended

matters (Steel and McGhee, 1979).

For 10^3 <**R**<10^5 (turbulent flow), $C_D \approx 0.4$ and the settling velocity is given by

$$v_s = 1.82 \left(\frac{\rho_s - \rho_w}{\rho_w} d_s g \right)^{1/2} \tag{2.21}$$

For **R** < 1, when the flow is laminar, $C_D = 24/\mathbf{R}$ and the corresponding settling velocity is given by Stokes' law

$$v_s = \frac{1}{18} \frac{g}{\mu} (\rho_s - \rho_w) d_s^2 \tag{1.14}$$

In practice, the particle properties like diameter and density are normally unknown and particles are irregular in shape and therefore Equations (2.19), (2.21) and (1.14) cannot be applied directly. However, the general conclusion that settling velocity depends on particle diameter, particle density and the liquid properties like density and viscosity (and hence the temperature) is useful in studying the settling behaviour.

(b) Settling of Flocculent Suspension

The settling of flocculent suspension is related to particles of different sizes and the surface characteristics settling at different rates. The faster settling particles overtake the slower settling finer particles and the colloiding particles coalesce to form a larger mass with a higher settling velocity. Therefore, in settling of flocculent suspensions, the settling velocities are changing continually with depth and the depth should be great enough to provide the opportunity for particle contact to form larger flocs. Thus, in this type of settling, the removal is dependent on the depth as well as the properties of the fluid and the particles.

As the settling velocities are changing continually in flocculent suspension, it is not possible to predict the performance of sedimentation basins from mathematical relationship (theoretical considerations). Laboratory tests for settling column analyses are required to evaluate this type of sedimentation.

Camp (1946) suggested a settling column test in which suspended solids removals are determined at various time and depths. The analysis and description of the test have also been reported by others (Weber, 1972; Clark *et al.*, 1977; Metcalf and Eddy, 1979; Reynolds, 1982; Montgomery, 1985; AWWA, 1991). Zanoni and Blomquist (1975) conducted a series of settling column tests giving particular consideration to the effect of column diameter, number of sampling ports and initial solid concentration on the overall results obtained and they recommended a standard column settling test procedure.

The settling test of flocculent suspension is done in a column having a height to the depth of sedimentation tank considered with a diameter of 300 mm. Sampling ports are provided at various depths and samples are withdrawn at selected time intervals from different depths. The concentrations of suspended solids are determined in these samples and the results are used to evaluate the removal of solids in percentage. The actual values of the fractions removed are then plotted as shown in Figure 2.3. A particular value is plotted of proper coordinates of depth and time. The fractions of

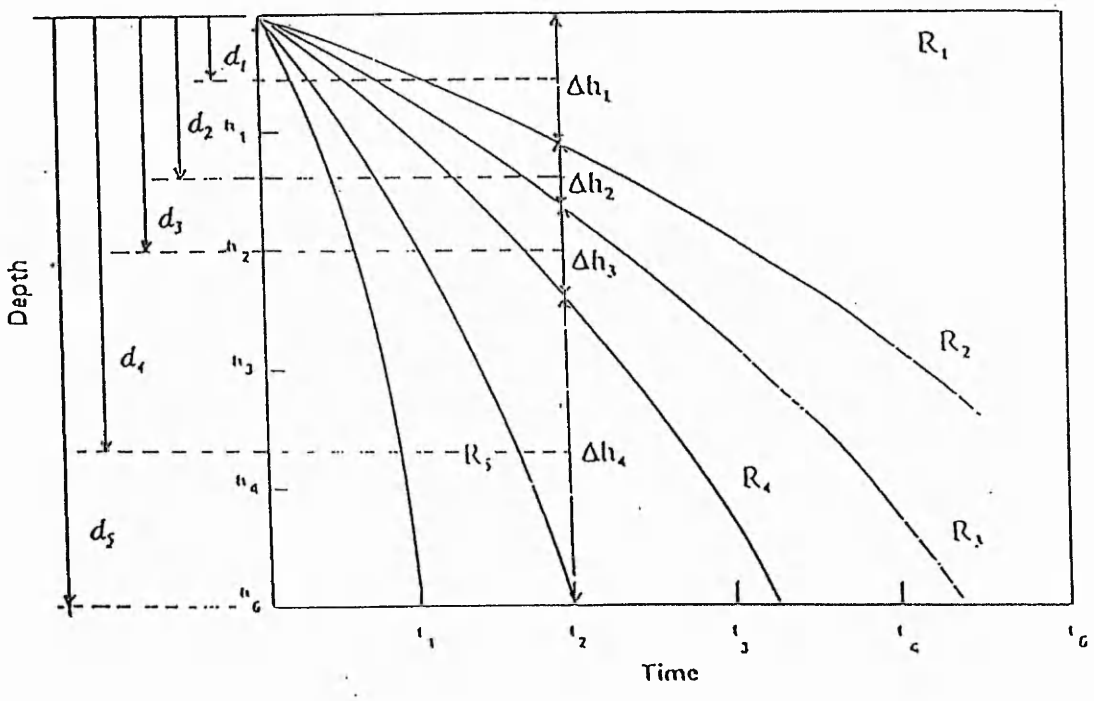

Figure 2.3 Percentage removal of flocculent particles as a function of depth and time.

particles removed at each depth at different time intervals are used to construct lines of equal fraction removal. Such lines are called isoconcentration lines which represent the maximum trajectories of settling paths for specific concentration in a flocculent suspension.

The overall removal efficiency from column settling tests for a given time is commonly evaluated using one of the following two types of equation:

Equation type 1 is referred by Metcalf and Eddy (1979) and Montgomery (1985). Removal efficiency in per cent, E at time t, is given by

$$E = \frac{\Delta h_1}{D}\frac{(R_0+R_1)}{2} + \frac{\Delta h_2}{D}\frac{(R_1+R_2)}{2} + \frac{\Delta h_3}{D}\frac{(R_2+R_3)}{2} + \frac{\Delta h_4}{D}\frac{(R_3+R_4)}{2} + \frac{\Delta h_5}{D}\frac{(R_4+R_t)}{2} \qquad (2.22)$$

where D is the distance between the lowest sampling port and the liquid surface in the test column, R_i are the curves for constant percentage removal and h_i are the depths as shown in Figure 2.3.

Equation type 2 is referred by others (Weber, 1972; Clark *et al.*, 1977; Reynolds, 1982; AWWA, 1990). Removal efficiency E in per cent at time t is given by

$$E = \frac{d_1}{D}(R_0 - R_1) + \frac{d_2}{D}(R_1 - R_2) + \frac{d_3}{D}(R_2 - R_3) + \frac{d_4}{D}(R_3 - R_4) + \frac{d_5}{D}(R_4 - R_t) + R_t \qquad (2.23)$$

It is known that the numerical results of using Equation (2.22) are the same as that of Equation (2.23). The mathematical proof by Srivastava (1992) demonstrated that the two expressions commonly used for the analysis of column settling tests for water and wastewater treatment give the same numerical results because they are essentially two seemingly different forms of the same basic relationship.

(c) Zone Settling: When the concentration of the suspension is high, the particles are sufficiently close and the interparticle forces are able to hold them in fixed

positions relative to each other (Tebbutt, 1983). As a result the particles settle as a large mass. Thus, zone settling describes a mass settling process of flocculent particles rather than the flocculent settling. In such a situation, there is an upward flow of liquid displaced by the settling particles (as the velocity fields of the fluid displaced by the settling particles) which results in a reduced settling velocity and the effect is known as hindered settling.

(d) Compression Settling: When the settling particles approach the bottom of the settling tank, they contact each other and accumulate at the bottom of the tank. The weight of the particles is supported by the lower layers of solids. This is known as compression settling.

2.4 PHYSICS AND HYDRODYNAMICS OF RISING BUBBLES

The study of gas bubbles rising through liquids is a very difficult hydrodynamic problem. As the bubble size increases, the deformations, surface oscillations and distortions to which bubbles are subjected make the analytical solution of the bubble motion practically impossible (Tapucu, 1974). The hydrodynamic behaviour of bubbles rising in liquids have been studied both theoretically and experimentally by a large number of investigators. In the subsequent sections of this chapter, the findings of these studies will be reviewed and discussed with respect to the velocity, size, shape and the path followed by the rising gas bubbles and also the properties of the liquids.

2.4.1 Rising Velocity of the Bubble: The rise of a single air bubble through different liquids of widely varying physical properties was studied by O'Brien and Gosline (1935), Robinson (1947), Datta *et al.* (1950), Peebles and Garber (1953), Garner and Hammerton (1954) Haberman and Morton (1954) and many others. These studies covered the range of Reynolds number from 10^{-5} to 3000. For the lower range of Reynolds number, i.e. $\mathbf{R} \leq 1.0$, agreement was found with Stokes' law and the theory put forth by Hadamard (1911) and Rybczynski (1911). The theory

of Hadamard-Rybczynski (1911) predicted a 50% increase in the velocity of a gas bubble in a liquid if circulation existed inside the bubble.

The velocity of a rising bubble is concerned with the bubble characteristics and also the liquid properties. Allen (1900) studied the rise velocity of small air bubbles (up to 6.0 mm) rising in water and aniline. The range of bubble size was extended by other investigators who tried to measure the terminal rise velocity and to determine its variation with equivalent bubble diameter. The rising velocity of small, medium and large sizes bubbles will be reviewed and discussed in this section. Generally, bubbles are considered as small, medium and large when the diameters are < 0.10 mm, > 0.10 mm but < 2.00 mm and > 2.00 mm respectively and the corresponding Reynolds numbers are <1.0, >1.0 but < 800 and > 800 respectively (Levich, 1962).

The motion of bubbles in different regimes of flow, i. e. at various ranges of the Reynolds number, has been treated systematically by Levich (1962). Reynolds number, **R** < 1.0 is considered as low. It was mentioned that Bowden termed the Reynolds number as moderate when a bubble moved within the range of **R** = 1.0 to **R** = 700 to 800 and Reynolds number above 800 termed as large (Levich, 1962).

2.4.1(a) Motion of Small Bubbles: The motion of very small bubbles corresponds to Reynolds number that is considered as low, i.e. **R** < 1.0, which means that the regime of liquid motion near the surface of the bubble is viscous. For a single bubble rising in an infinite medium of high viscosity with inertia forces small compared to viscous forces, Stokes' law will hold. Equating buoyant force of the bubble against the resistance to motion results in Equation (2.5).

$$v_r = \frac{1}{18}\frac{g}{\mu}(\rho_a - \rho_w)\ d_b^2 \qquad (2.5)$$

which is Stokes' law. This equation is applicable to a rising bubble when **R**<1.0 and the bubble behaves as a rigid sphere with no slip at the gas-liquid interface. Complete derivation of this mathematical formula for the rising velocity of a small bubble can be found elsewhere (Lamb, 1952; Levich, 1962).

In the initial studies of the motion of small bubbles, resistance was computed by means of the usual Stokes' formula. The motion of fluid spheres was studied independently by Hadamard and Rybczynski (1911). They found a variation in the resistance to the motion if any circulation existed inside the sphere and the rising velocity is given by Equation (1.15):

$$v_r = \frac{1}{12}\frac{g}{\mu}(\rho_a - \rho_w) d_b^2 \qquad (1.15)$$

Comparing the velocity of rise of a bubble calculated from Equation (1.15) with that calculated from Equation (2.5), i. e. from the Stokes' law, it can be seen that this is greater by the ratio of 3:2. This is due to the fact that the velocity of the liquid does not become zero at the gas-liquid interface, as it does at a solid surface (Levich, 1962).

This is the reason why the velocity difference between the motionless liquid and the surface of a bubble is smaller for a solid sphere.

Bond and Newton (1928) proposed a relationship for the critical radius at which transition from a rigid to a circulating sphere occured. Garner and Hammerton (1954) disagreed with this proposed criterion and presented data for numerous systems showing the experimental radii. However, they did not have enough data for correlation.

Haberman and Morton (1954) studied the rise of a single air bubble in various liquids and also found a transition from stagnation to circulation inside the bubbles. The drag curves of the bubbles fell between the two limiting curves, i.e. the drag curves of rigid and fluid spheres. No correlation was obtained for the transition radii.

Velocity of rise of small bubbles was investigated in the past by many workers. Allen (1900) measured the velocity of rising air bubbles in water and in aniline, presenting his data in graphic form showing the drag coefficient as a function of the Reynolds number. Allen's (1900) experimental data completely disagreed with the

theory in which the gas-liquid interface velocity was considered and led to values for drag coefficient which coincide exactly with the drag on a solid sphere. The results of measurements made by others were in good agreement with Allen's data and stressed the general conclusion that at low Reynolds number, small bubbles move like solid spheres (Levich, 1962).

Levich (1962) mentioned that the apparent "solidification" of moving bubbles is related to the effect of surface-active materials present in the liquid media. None of the experimenters took any special measures to rid the liquids of surface-active substances when conducting their measurements.

In this way, it is possible to anticipate that bubbles of very small sizes should move in the same manner as solid spheres in all liquid media that have not been specially treated to rid them of surface-active materials. This conclusion was fully confirmed in experiments conducted by A.V. Gorodetskaya (1949). Tapucu (1974) observed in his experiment that for bubbles greater than 1.34 mm, the influence of surface-active impurities was very small.

2.4.1(b) Motion of Medium-size Bubbles: The theoretical expression for the rising velocity of a medium-size bubble was given by Levich (1962) as follows:

$$v_r = \frac{1}{36}\frac{g}{\mu}\,(\rho_a-\rho_w)\,d_b^2 \qquad (2.24)$$

This expression is applicable within the range of **R** = 50 to 800 which applies to a diameter of less than 2.0 mm and the shape of the bubble is considered to be spherical. Comparing the rising velocity computed from Equation (2.24) with that of a small **R** from Equation (2.5), it is obvious that the rising velocity of a medium size air bubble is one half the value of Stokes' settling.

From a hydrodynamic viewpoint, this result appeared somewhat paradoxical. It was mentioned that for a bubble, due to the mobility of the interface, the separation point is situated so far downstream that the turbulent-wake region covers only a minute

portion of the bubble's surface. In this case, it is natural for form drag to be very small. The viscous friction is also different because of the mobility of the interface. Two assumptions were considered to form the basis of the above reasoning: (i) the bubble's shape was strictly spherical and (ii) no surface active materials were present on its surface (Levich, 1962).

The indicated relationship in Equation (2.24) was in complete disagreement with the data of many workers who studied this problem previously (Levich, 1962). In this connection, A.V. Gorodetskya (1949) conducted a special experimental study to measure the velocity of bubbles rising in water and in aqueous solutions.

The measurement of bubble rise velocity was conducted in a constant temperature vessel by the motion picture method. These experiments fully clarified the reason for the disagreement between the theory and the experimental results previously obtained (A.V. Gorodetskya, 1949).

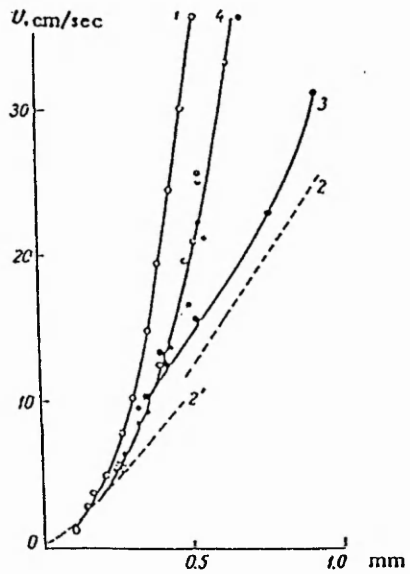

Figure 2.4 Measurements of bubble velocities in water. 1 - theoretical curve by Levich; 2 - Allen's curve; 2´ - Shabalin's curve; 3 - Luchsinger's curve; 4 - double distilled water (photographic and visual observation).
[Adapted from "Physicochemical Hydrodynamics" by Levich (1962)].

The data for bubble motion in water were presented graphically (Levich, 1962) which is shown in Figure 2.4. In this figure, the theoretical curve corresponds to Equation (2.24) and is also shown along with the experimental data of Allen, Luchsinger and Shabalin (Levich, 1962).

In examining the results of A.V. Gorodtskya's (1949) measurements, it became quite evident that the purity of water is very important. Curve 2 for ordinary tap water agreed well with Allen's data. Curve 3, obtained by Luchsinger, who used distilled water is somewhat closer to curve 1 and better than Allen's curve. Curve 4 for the special double-distilled water differs markedly from the others and , in general, corresponds to the theoretical curve 1, by Levich (1962). The discrepancy between the theoretical curve 1 and the experimental data curve 4 did not exceed 30% and could be attributed to experimental errors, residual surface-active substances, the effect of form resistance which have not been taken into account in formula (2.24) and a slight deviation in bubble shape from the spherical one.

Based on the above data and discussion, it was concluded that the theoretical consideration set forth were in complete agreement with experimental data. Earlier experimental data applied to water that had not been purified, and these data should not be used for comparison with the theory. It followed from A.V. Gorodetskya's (1949) experiments that even minute traces of surface-active substances have an effect on bubble motion.

2.4.1(c) Motion of Large Bubbles: The motion of large bubbles was studied by many investigators. When bubbles are large in size, the shape differs considerably. Levich (1962) mentioned that departure from the spherical shape occurs much sooner when **R** = 800 to 1000. Study of motion of such deformed bubbles presents difficulties, particularly in view of the fact that its shape is not strictly fixed and pulsations appear within the bubble, as a result of which its motion ceases to be steady and the bubble no longer moves in a straight line.

Levich (1962) derived the theoretical expression for the motion of large bubbles with

the diameter > 2.0 mm and the region where **R** > 800 to 1000. This expression is as follows:

$$v_r = \left(\frac{4\sigma^2 g}{\alpha\rho\mu}\frac{\rho_a}{\rho_w}\right)^{1/5} \tag{2.25}$$

where α is a numerical coefficient and other symbols as defined earlier. Equation (2.25) permits a correct estimate of the order of magnitude of the velocity of rise and the computed result was in agreement with Levich's (1962) experimental data. It should be noted, however, that the expression is not very sensitive to inaccuracies in the values of the quantities entering into it, since it contains a fifth root. It is evident that the motion of a large bubble is not a function of the bubble size.

It was noted from Levich's (1962) work that the velocity of motion of bubbles with diameters of 2.0 to 15 mm is almost independent of the bubble diameter and amounts to about 28 to 30 cm/s (**R** = 700 to 4500). Bubbles of large diameters rise at somewhat greater velocities, namely at about 35 to 40 cm/s, but are not very stable and tend to subdivide into smaller bubbles.

Variation of Rise Velocity with Height: Experiments were conducted by Aybers and Tapucu (1969) and also by Tapucu (1974) independently to determine the variation of bubble rise velocity with height, the bubble terminal velocity, the variation of the rise velocity with bubble size and the viscosity effects on the bubble velocity.

It was shown that the mean rise velocity of bubble varied with the height of liquids, in water, glycerin and water-glycerine mixtures. In these liquids, the velocity of bubbles rising on a rectilinear path, after its maximum value, decreased to an asymptotic value reached far from their originating point.

The result of Tapucu's (1974) work is shown in Figure 2.5. In glycerin and water-glycerin mixtures, the velocity of small bubbles was very low and the surface tension forces were great. Under these conditions, the bubble surface was almost completely

contaminated with surface-active impurities existing in liquid within a short distance from the originating point where they had nearly reached their maximum velocity. Since the subsequent variation of surface-active impurities concentration was small, the velocity variation would also be small. As the bubble diameter increased, the velocity increased and surface tension forces decreased. Under these circumstances, surface-active impurities on the bubble surface might not reach their maximum concentration value near the originating point. As a result, in the subsequent motion, the bubble velocity, after passing through the maximum value, decreased with increasing concentration of surface-active impurities. In the region of big bubbles, surface tension forces became very small and surface-active impurities had a vanishing effect on the velocity. Consequently, bubbles kept their maximum velocity after reaching it.

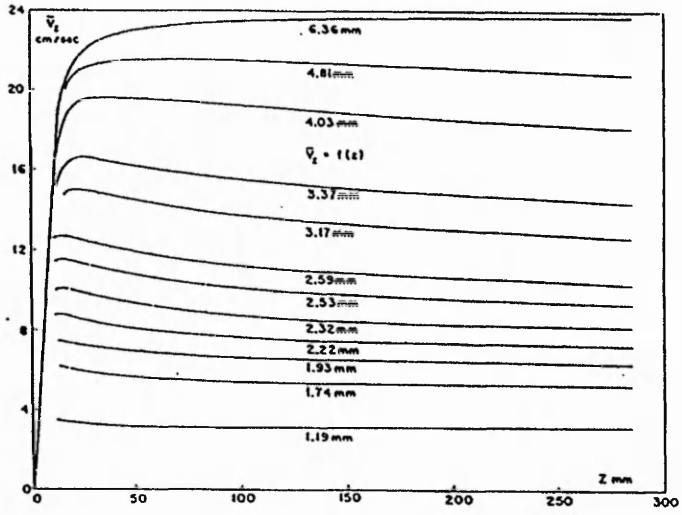

Figure 2.5 Variation of Rise velocity with Height in 25% Water - 75% Glycerine Mixture. [Adapted from Tapucu (1974)].

Variation of Rise Velocity with Bubble Diameter: In studying the velocity-diameter relationship, Tapucu (1974) used "average rise velocity" to avoid the difficulty of defining the "terminal rise velocity" due to the variation of mean rise velocity with height and defined as follows:

$$V_{z\,ave} = \frac{\int_{z_1}^{z_2} v_z\, dz}{\int_{z_1}^{z_2} dz} \qquad (2.26)$$

The variation of the average rise velocity with equivalent bubble diameters observed by Tapucu (1974) is shown in Figure 2.6. It can be seen from this figure that the viscosity effect on small bubbles is very imporant but that it decreases with increasing bubble diameter. For liquids of low and moderate viscosity and for the bubble diameters greater than 7.0 mm, the effect of viscosity on the rise velocity is negligible. Thus, it was expected that in the region of big bubbles the relation between rise velocity and bubble diameter would be independent of viscosity.

Rising velocity of a Series of Bubbles: Any velocity data reported for a stream of bubbles had shown an increase in velocity compared to that of a single bubble (Poutanen and Johnson, 1960). Haberman and Morton (1953) found that for a

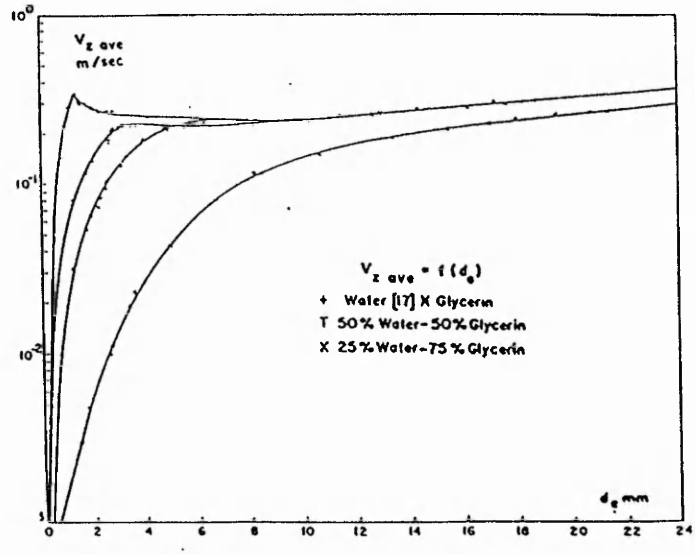

Figure 2.6 Variation of the Average Rise Velocity with Equivalent Bubble Diameters. [Adapted from Tapucu (1974)].

mineral oil with a viscosity of 58 c.p. and a density of 0.866 g/cc., increase in velocity of 9% and 39% were obtained for a bubble diameter of 0.34 cm. with the bubbles 7.7 cm. and 3.2 cm. apart respectively.

Garner and Hammerton (1954) also found an increase in velocity. For a white oil (viscosity of 198 centistokes at 20^0C) velocities 2.5 times that calculated from Stokes' law were obtained at frequencies higher than 3 bubbles per second.

At a frequency of one bubble per second, Coppock and Meiklejohn (1951) found an increase of 30% in velocity of air bubbles in water for a diameter of 2.0 mm. As the bubble diameter increased, the difference in velocity between single and multiple bubbles decreased and became the same at a diameter of 6.0 mm.

Garner and Hammerton (1954) mentioned that there was an increase of 12 to 50% in velocity for carbon dioxide bubbles in water at a frequency of 3 bubbles per second. Other workers (Owens, 1921; O'Brien and Gosline, 1935; Datta *et al.*, 1950) observed increases in velocity over that of single bubbles, but no systematic study of the effect of bubble frequency, column size, and seal height on bubble velocity has been made.

2.4.2 Shape of the Bubbles: Bubble shapes were studied by Tapucu (1974) and divided into three general categories: spherical bubbles, ellipsoidal bubbles without or with surface oscillation and spherical cap-shaped bubbles. Poutanen and Johnson (1960) mentioned that the shape has been established theoretically for a stationary bubble by equating pressure forces inside and outside the surface by the previous workers and an equation was also derived for the volume of the bubble above a given horizontal plane by balancing surface tension forces against weight and pressure forces. The work by Freud and Harkins (1929), Wark (1932) and Siemes (1954) give a good summary of bubble shape and volume.

Poutanen and Johnson (1960) studied the bubble shape and area during formation for nitrogen bubbles in water and two hydrocarbon oils. Bubble profiles were founded

to fit an empirical equation of the form

$$r^n\theta = 1 \tag{2.27}$$

where r and θ are polar co-ordinates and n is the variable power. By using this relationship, the area and the volume of the bubble were calculated as follows:

$$Area = 2\pi\int_{\theta_1}^{\pi}\frac{\sin\theta}{\theta^{2/n}}\sqrt{1+\frac{1}{n^2\theta^2}}d\theta \tag{2.28}$$

$$Volume = -\pi\int_{\theta_1}^{\pi}\frac{\sin^3\theta}{\theta^{3/n}}\left(1+\frac{1}{n\theta\tan\theta}\right)d\theta \tag{2.29}$$

Quantitative studies of bubble volume and area as a function of time were also reported (Poutanen and Johnson, 1960).

Bhaga and Weber (1981) studied the shapes of the rising air bubbles in an aqueous sugar solution and were classified as: spherical, oblate ellipsoidal, oblate ellipsoidal cap, spherical cap with open or closed wake, skirted bubbles with smooth or wavy skirts and disk-like bubbles.

The disk-like bubble was obtained for 40<**R**<70 in the least viscous solution. These bubbles were observed to wobble as they rose although both larger and smaller bubbles in the same solution rose rectilinearly. At low Reynolds number the bubble was nearly a complete oblate spheroid. With decreasing viscosity and increasing **R** it became a smaller segment of an oblate spheroid. It was a half spheroid for **R** = 25. At **R** = 45, a spherical cap shape was obtained (Bhaga and Weber, 1981).

Grace (1973) produced a generalised graphical correlation by combining data from studies of single gas bubbles rising in 21 different liquids. Data from different investigators were brought together in such a way that the regimes of bubble behaviour were clearly delineated. The correlation included boundaries between the three regimes of bubble shape (sphere, ellipsoid and spherical-cap) and allowed bubble-rise velocities to be calculated as a function of bubble size for a very wide

range of physical properties.

2.4.3 Bubble Path: Experiments were conducted by Tapucu (1974) to determine the path followed by bubbles of different diameters in liquids of different viscosities. Bubble paths observed were rectilinear, helical, first sinusoidal and then helical, sinusoidal and rectilinear with rocking depending on the viscosity of the liquids and the diameter of the bubbles.

2.4.4 Size of the Bubbles: The size of bubble formed is affected by the size of the orifice, the liquid properties and the air flow rate. It has been reported that the bubble is 10 - 100 times larger than the pore from which it escapes (Verschoor, 1950).

At low rates of gas flow previous work (Breitner, 1942; Datta *et al.*, 1950) has shown that for any given system and orifice diameter, bubble size is constant with respect to gas flow rate. At intermediate rates of gas flow bubbles are formed at a constant frequency and the bubble size is uniform and depends primarily on the rate of gas flow, the orifice diameter, and the volume of the gas chamber upstream from the orifice. At high rates of gas flow, the bubbles formed are not uniform in size (Leibson *et al.*, 1956).

CHAPTER 3

APPARATUS, MATERIALS, EXPERIMENTAL PROCEDURES AND OBSERVATIONS

3.1 INTRODUCTION

The experimental apparatus, materials and chemicals used and the procedures and observations will be described in this chapter, with the aim of investigating the validity and practical applicability of the process of pneumatic flocculation in removing the suspended particles under various initial conditions. The observed results are expected to be a contribution towards a thorough understanding and further analysis of the pneumatic flocculation process in the field of water treatment.

Experiments were conducted in a long cylindrical perspex tube receiving synthetic turbid water of a known concentration on a batch flow basis. The long tube allowed the turbid water to coagulate, flocculate and settle under various initial conditions. Sampling ports were provided to collect the sample, which were spaced at equal distances of 200 mm throughout the 2400 mm column of tested water to determine the residual turbidity at different intervals of time. Particular attention was given in flushing the pipes before collecting the sample to avoid the floc deposition in the sample collecting pipes.

Experiments were performed with air diffusion pads of various orifice sizes, different air flow rates, synthetic turbidities and coagulants and with either constant or taper agitation. Three types of synthetic turbid materials namely kaolin, lycopodium powder and polyvinyl chloride (PVC) powder and two types of coagulants namely, aluminium sulphate and ferric sulphate were used in this research work.

The pneumatic model treatment unit, peripheral equipment and instruments, synthetic turbidity materials and coagulants, sampling ports and technique, preparation of suspension, schedule of the experiments, experimental procedures and observations are all described in the following subsequent sections.

3.2 EXPERIMENTAL APPARATUS

3.2.1 Design Considerations

The pneumatic model treatment unit used in this research work has been designed to simulate, as much as possible, a water treatment plant unit used practically in the water treatment industry. This pneumatic model treatment assembly has been designed for the purposes of serving the functions of a rapid and slow mixing coagulation - flocculation chamber, settling column and to hold the energy input device (a circular diffusion pad described in section 3.2.2.(c)). The operating height of water was kept constant at 2400 mm for all the experimental runs, this is nearly equivalent to that used practically in any water treatment plant in water treatment industries. In the case of PVC turbidity, the operating height of water was limited to 2000 mm to avoid the foaming over-flow from the chamber which appeared during the application of high air flow rates required for rapid mixing for coagulation. This foaming was attributed to the long-chain molecular property of the PVC powder. The experimental work was conducted on a batch flow basis for all the runs. The number of orifices in each diffusion pad were designed to provide uniform air loading per unit area of the flocculating chamber. Removal of suspended solids was assumed to be due to pneumatic coagulation-flocculation process. However, the effect of "sweep coagulation-flocculation" was also observed and considered in removing the suspended materials.

3.2.2 Pneumatic Model Treatment Unit

The model treatment unit as shown in Figure 3.1, consisted of a 2558 mm long

cylindrical chamber of 287 mm internal diameter made of 6.0 mm thick perspex sheet with an operating water height of 2400 mm.

This model treatment unit was designed by Dr. I. H. Sholji, who is the supervisor of this research work, and made by the Heavy Structures Civil Engineering Workshop, Department of Civil and Structural Engineering, The Nottingham Trent University, England. The chamber consisted of two parts jointed together with a bolted pair of flanges and a 1 mm thick rubber gasket to prevent any leakage of water. The height of the lower part was 503 mm and that of the upper part was 2055 mm. The purpose of this arrangement was to give access to level or replace the diffusion pad of different orifice sizes for the purpose of this investigation.

Circular diffusion pads with the orifices located uniformly per unit cross sectional area of the flocculating chamber and of uniform sizes of different diameters were installed in the lower part of the chamber for inducing air bubbles from a compressor connected by flexible PVC pipes. Two air flowmeters were installed to monitor and control the high and low air flow rates required for rapid and slow mixing respectively. A wide range of air flow rates could be covered by these two flowmeters simply by changing the metering tubes and the corresponding floats in it. The rates of air flow ranging from 50 to 38, 000 cc/min. have been used in this research work. A needle valve was fitted at the inlet of each flowmeter and used for the fine adjustment of the air flows. An additional air flow controlling ball cock valve was fitted on the air supply main before the flowmeters for purging the water from the air flow piping system and diffusion pad before supplying the air to the chamber. The air flow piping system consisted of 8.0 mm internal diameter PVC pipes connected to a central manifold, to ensure the even air flow distribution to all parts of the diffusion pad. The air supply was fed from a compressed air storage tank via any appropriate air flowmeter. Four sizes of orifice were used during the experimental work, they were either 1.0, 1.5, 2.0 or 3.0 mm in diameter. Each replaced pad contains one size of the four orifices as mentioned and was supported by three levelling screws attached to the side of experimental column that could be easily adjusted from outside the column through a gland in the column wall. By

this means, the levelled diffusion pad produced a uniform air distribution across the column cross section during the course of experimental runs.

The whole assembly of the experimental apparatus used in this investigation consisted of various component parts which will be described separately in the following sections with reference to the schematic diagram shown in Figure 3.1. and Figure 3.2. Photographs of the arrangement are also shown in Figure 3.3 and Figure 3.4.

(a) Coagulation-Flocculation and Settling Chamber: This was a deep cylindrical chamber made of 6.0 mm thick perspex plastic sheet with an internal diameter of 287 mm and a height of 2558 mm allowing an operating water height of 2400 mm. The chamber consisted of two parts jointed together with a bolted pair of flanges and a 1.0 mm thick rubber gasket to prevent the leakage of water. The height of the lower part was 503 mm and that of the upper part was 2055 mm. The purpose of this arrangement was to provide easy access to the diffusion pad for initial levelling and the replacement with pads of different orifice sizes. A 20 mm internal diameter tap water inlet pipe with controlling valve was connected to the lower part of the settling chamber at a height of 394 mm from the base. The drain water pipe of 20 mm diameter was connected at the bottom of the chamber. Any one of the selected diffusion pads was installed and initially levelled using three levelling screws connected to the wall of the chamber at a height of 120 mm from the base of the chamber. The air flow piping system was connected to the diffusion pad through a manifold placed inside the chamber. Six external wall stiffeners were provided around the lower part of the upper section at the 2055 mm depth and lower section between the lower flange and the base as shown in Figure 3.3 so as to withstand the higher lateral static pressure of water column on the wall of whole chamber. There was a freeboard of 116.5 mm at the top of the upper part to allow the increase of water level during the coagulation-flocculation process due to the rising of air bubbles. An overflow weir arrangement was built on to the chamber wall at a height of 2516.5 mm with a receiving sump and this sump was connected to an overflow pipe to receive the overflow water reaching beyond the predetermined water level.

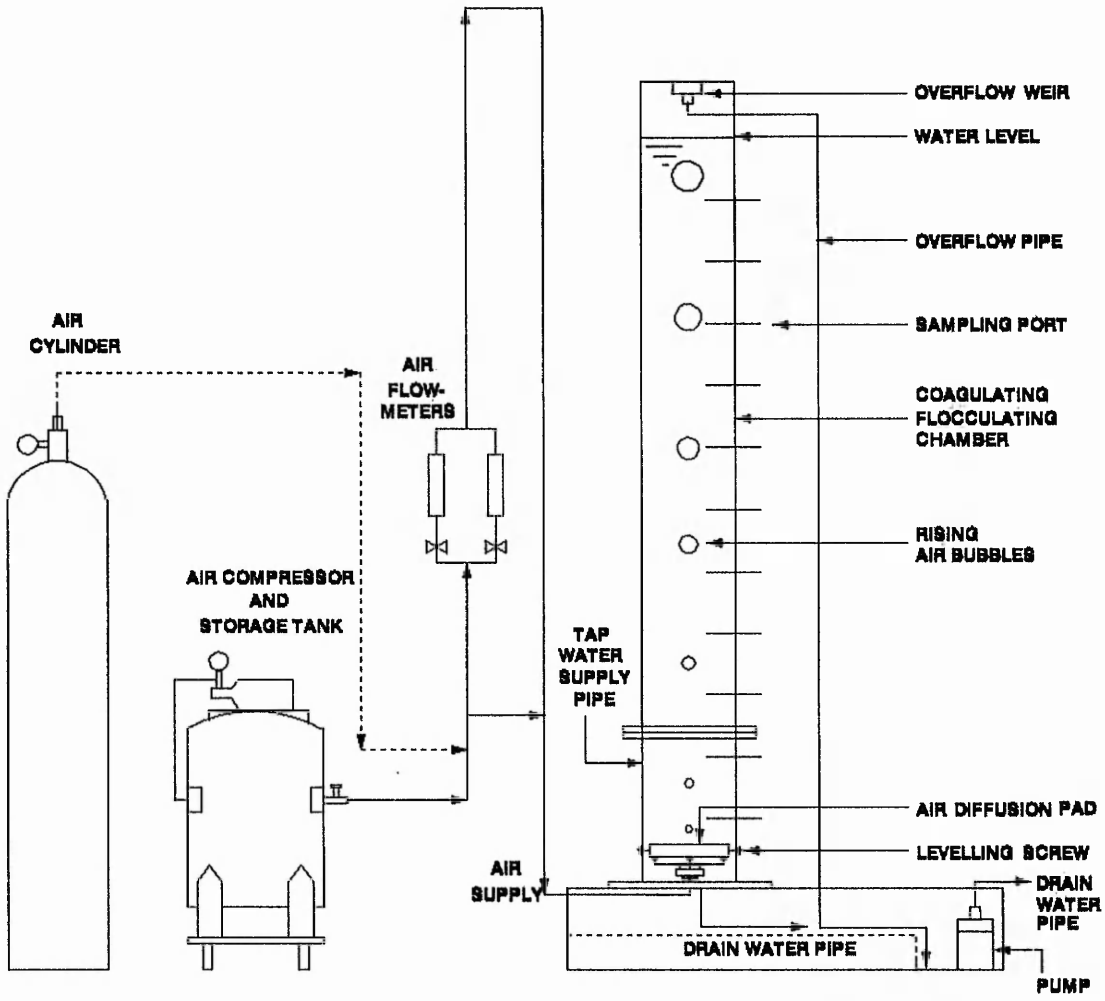

Figure 3.1 Schematic diagram of the Pneumatic Coagulation-flocculation and Settling Apparatus

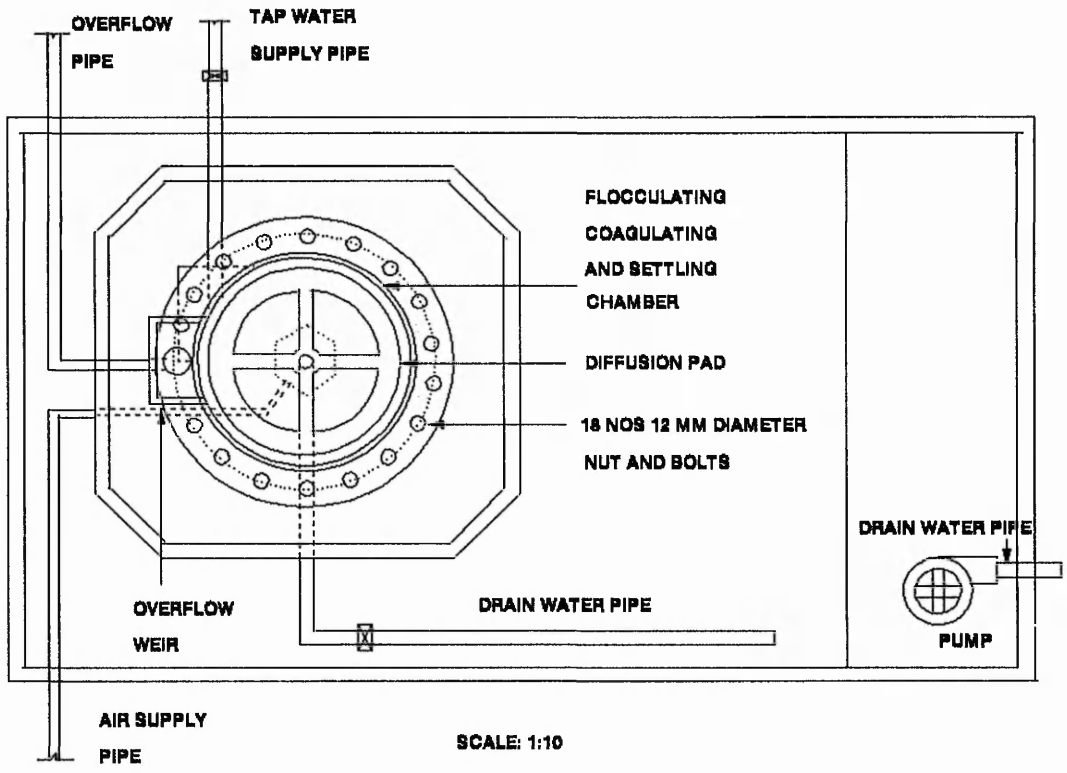

Figure 3.2 Plan of Pneumatic Coagulation-flocculation and Settling Apparatus

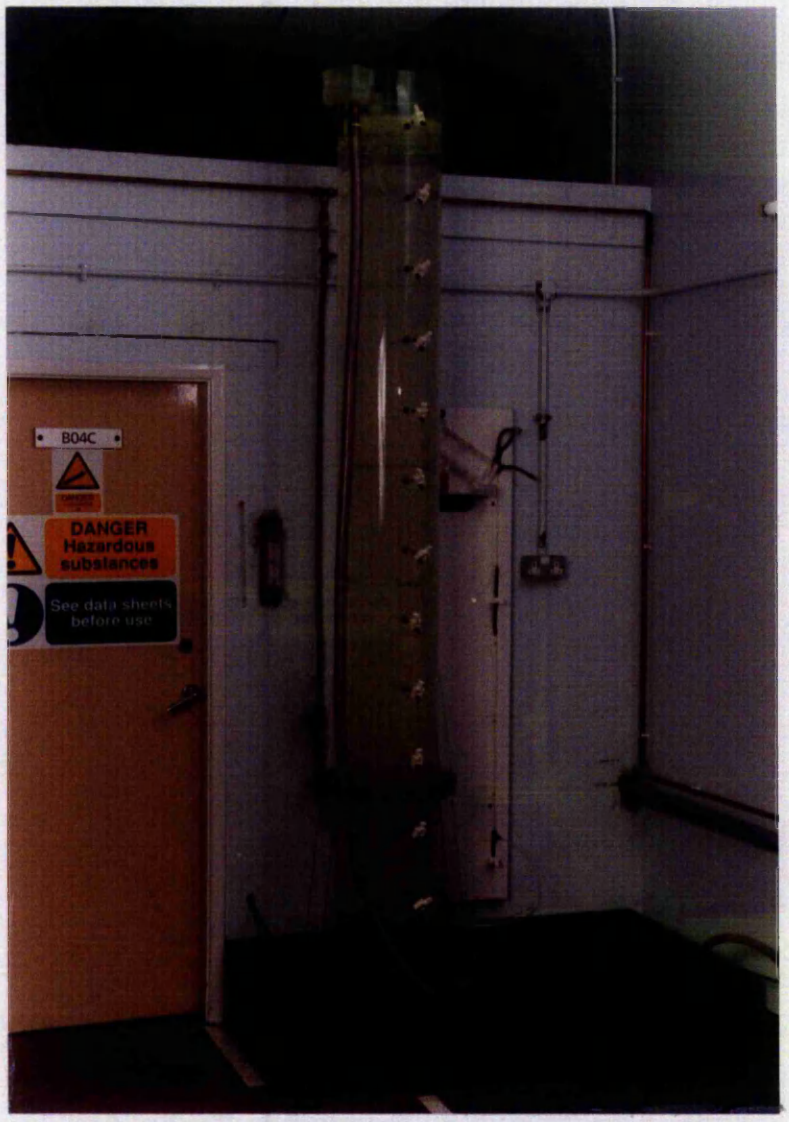

Figure 3.3 Photograph showing the Pneumatic Coagulation-flocculation and Settling Apparatus

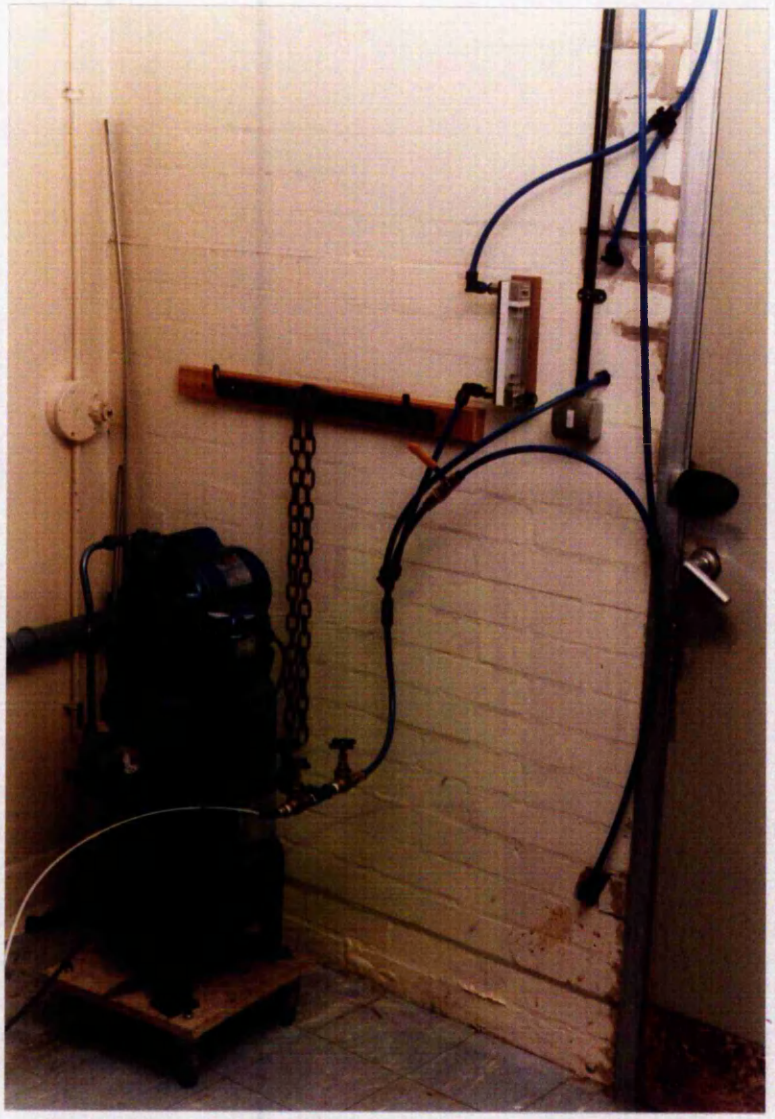

Figure 3.4 Photograph showing the Air Compressor and Storage Tank connected with the air supply system

Eleven number sample collecting pipes were inserted into the chamber all throughout its depth at equal distances of 200 mm to collect the samples for residual turbidity measurement.

The base of the chamber was mounted on a 1350 × 780 × 255 mm box made of 18 mm thick plastic coated plywood sheet which received the water from the chamber through both the drain and overflow pipes in a collecting sump. The collected water was pumped out to a near-by drain by means of a submersible pump installed as shown in the Figure 3.1. All joints of this box were sealed with resin to prevent any water leakage. The details of the experimental column and the supporting and water collecting trough (drain and overflow) box are shown in Figure 3.5.

(b) Sampling Ports: Eleven number sampling ports were installed at equal intervals of 200 mm throughout the height of the chamber to collect water samples from different depths. Details of the sampling port have been shown in Figure 3.26 and described in section 3.11. The inlets of sample collecting pipes projected into the column by a length of 2/3r, (where r is the internal radius of the chamber) thus avoiding the wall effect on the settling velocity of the floc particles and obtaining a more representative water sample. In each sampling port a 2.0 mm internal diameter stainless steel pipe was inserted into the 3.0 mm diameter flexible PVC pipes to ensure its horizontal position and maintain the proper inserted length from the inner wall. The outer projected part of the sampling port was connected to a short 5.0 mm diameter rubber tube equipped with pinch cock to enable the collection of water samples.

(c) Diffusion Pads: Circular diffusion pads made of 25 mm thick perspex sheet with orifices of different sizes and numbers were installed in the lower part of the chamber for inducing air bubbles from a compressor air storage tank via controlled air flowmeters connected by flexible pipes. There were four different diffusion pads, each pad had one size of orifices, these were either 1.0, 1.5, 2.0 or 3.0 mm in diameter. These diffusion pads were designed to provide a uniform loading of air per unit cross sectional area of the chamber.

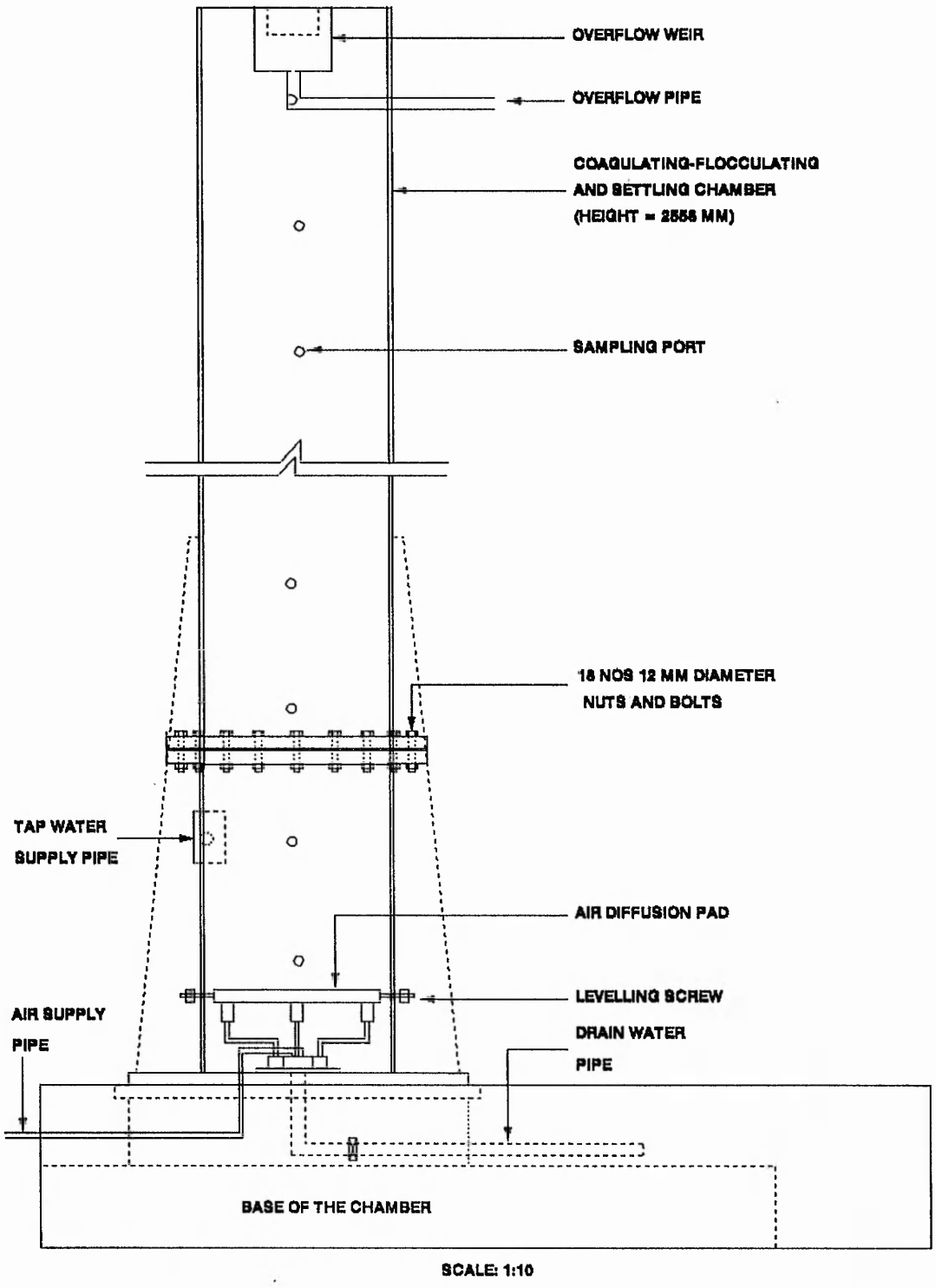

Figure 3.5 Details of the Pneumatic Coagulation-flocculation and Settling Chamber with base

All the orifices were circular and sharp edged and were located at the lower face of the pad chamfered at 45^0 to the base of the chamber to shield the orifices from any possible solid deposition which might restrict orifice openings. The orifices were placed at an angle of 45^0 as shown in Figure 3.6 to allow the release of air bubbles without any restriction. The value of the coefficient of discharge of the orifice, C_d was considered to be 0.61 (Qasim, 1985) in designing the diffusion pads. It was noted that a design value of C_d was considered as 0.68 by other workers and used in the similar works (Beek and Muttzall, 1975; Al-Hiary, 1988).

Number of Orifices: Details of the total number, distribution and spacing of orifices are given in Table 3.1 and shown in Figure 3.6 to Figure 3.9.

Table 3.1 Number of orifices and the spacing angle between adjacent orifices placed on each diffusion pad.

Diameter of orifices (mm)	Total number of orifices	No. of orifices		Spacing between orifices (degree)			
		Outer ring	Inner ring	Outer ring		Inner ring	
				Outer side	Inner side	Outer side	Inner side
1.0	58	38	20	16.32	20	30	30*
1.5	26	18	8	36	45	90	90
2.0	14	9	5	40	-	72	-
3.0	6	6	-	60	-	-	-

* 8 holes @ 30° and 60° alternatively between orifices.

(d) Air Flow System: Air was supplied by a simple compressor equipped with an air storage tank. The air tank has an automatic air pressure regulator to maintain a constant pressure of 10 kg_f/cm^2. The air was then supplied to the flocculating chamber through 8.0 mm diameter PVC piping system as shown in Figure 3.10. Two flowmeters were installed in the air piping system connected in parallel to monitor and control either the high or low air flow rates required for rapid and slow mixing respectively. The piping system was raised at a high level above the chamber's water

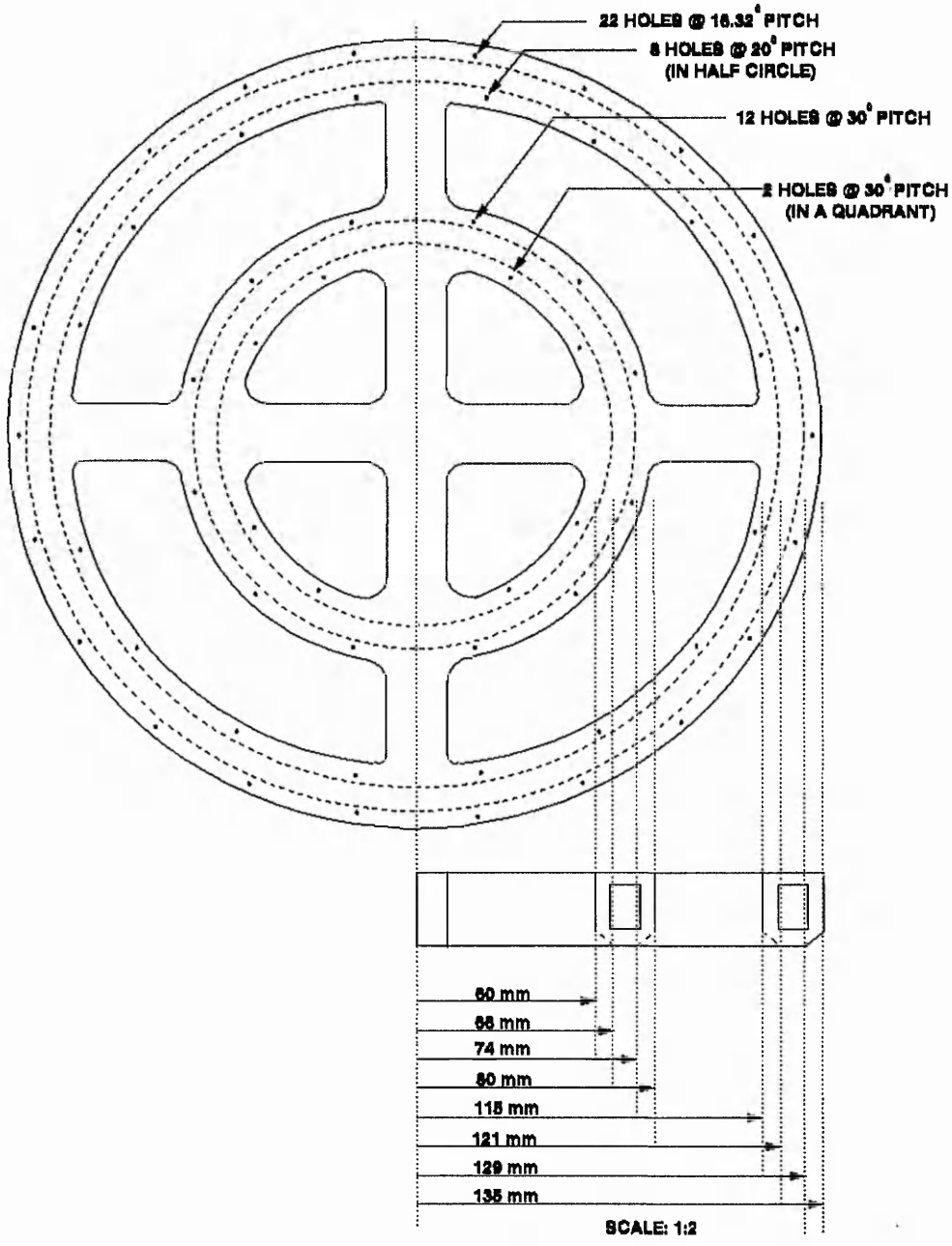

Figure 3.6 Details of 1.00 mm orifice Air Diffusion Pad

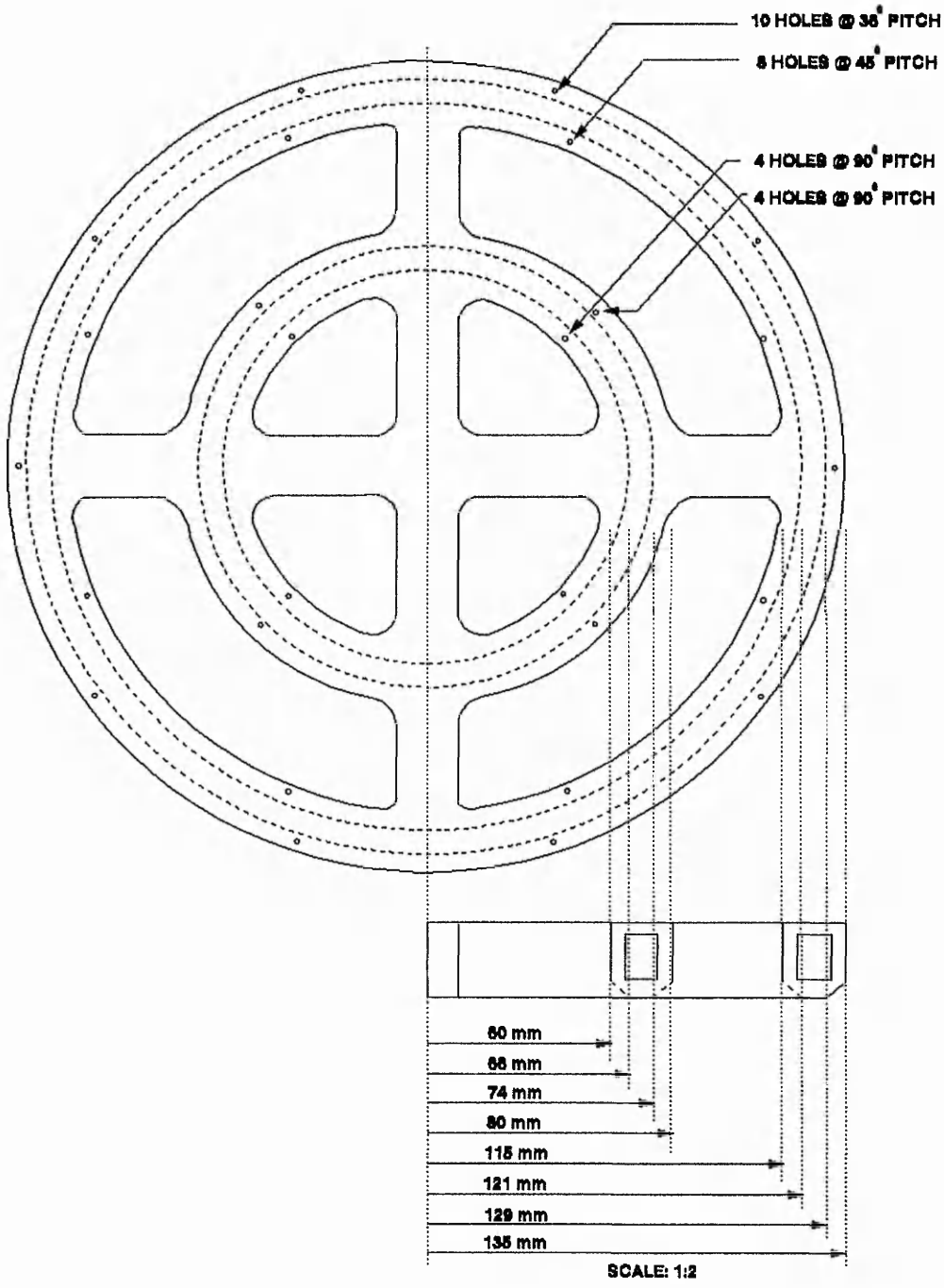

Figure 3.7 Details of 1.50 mm orifice Air Diffusion Pad

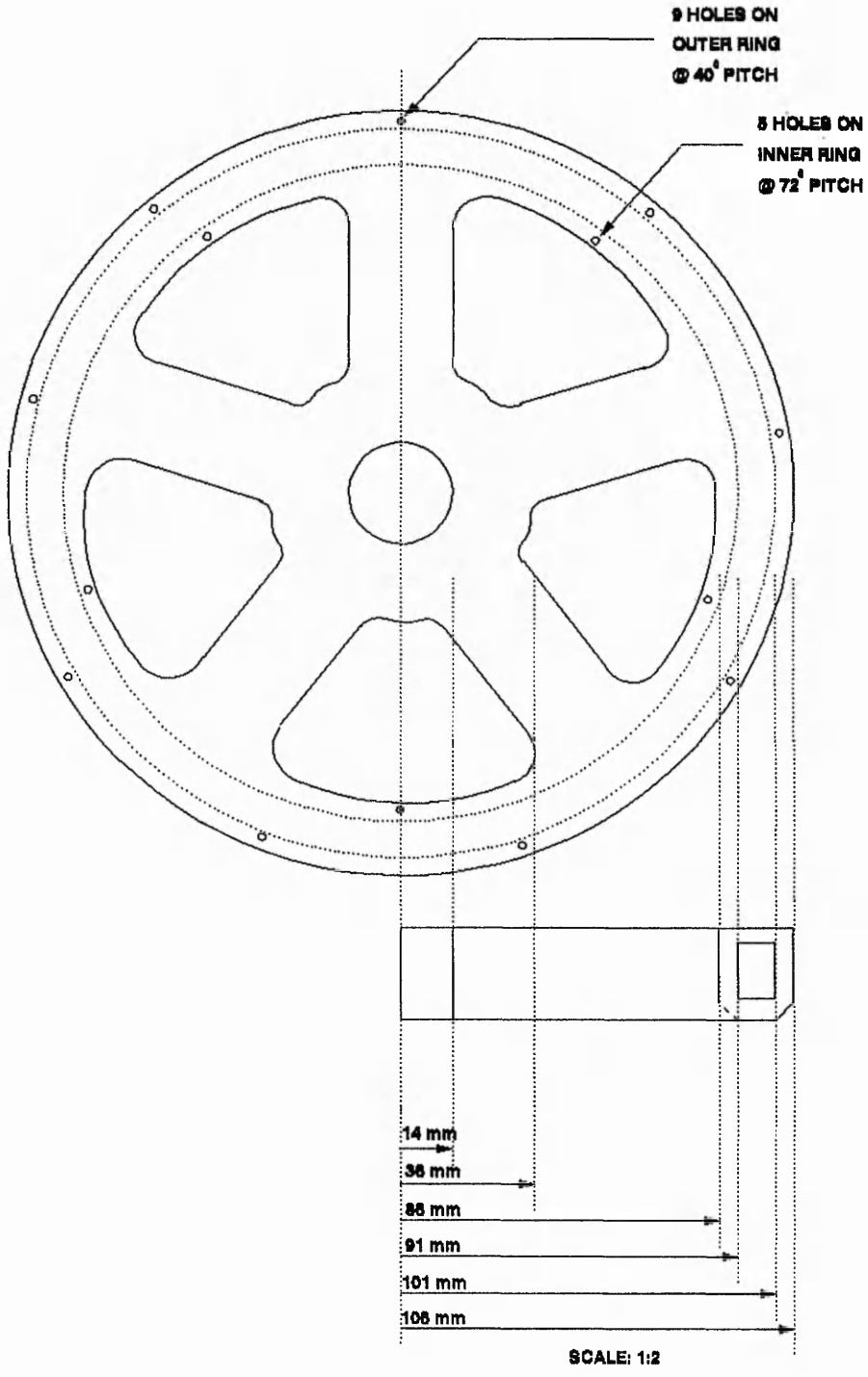

Figure 3.8 Details of 2.00 mm orifice Air Diffusion Pad

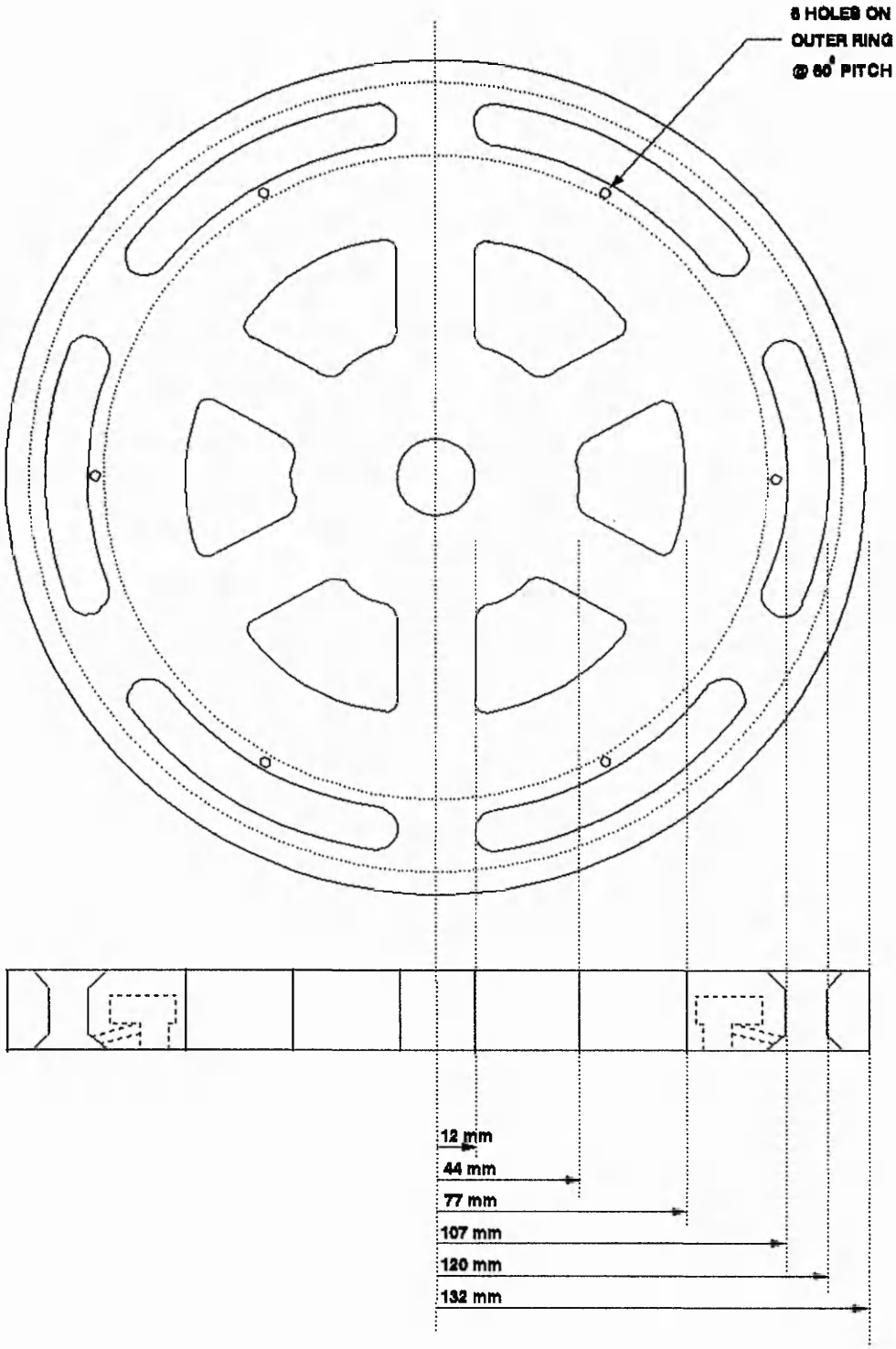

Figure 3.9 Details of 3.00 mm orifice Air Diffusion Pad

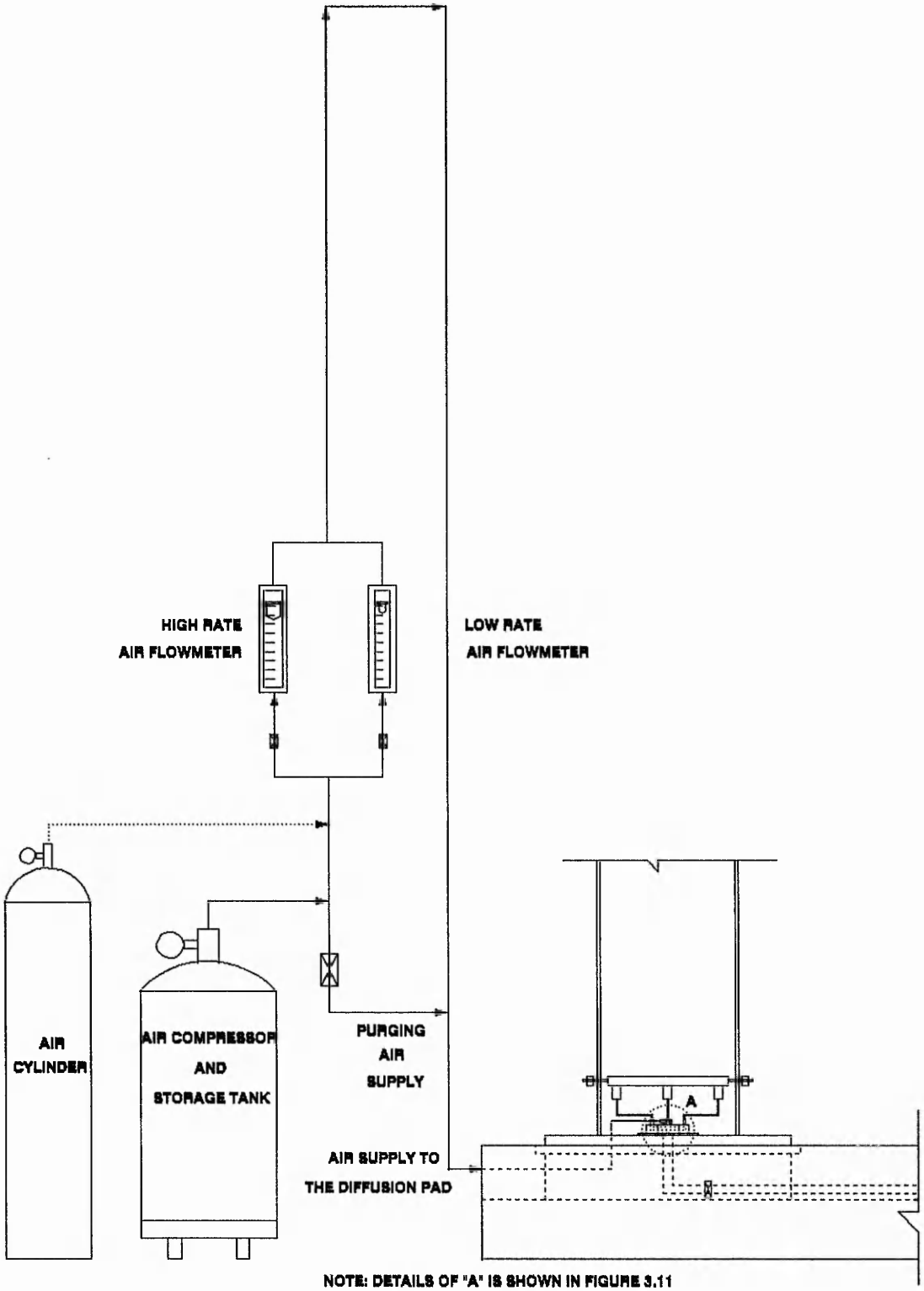

Figure 3.10 Air Supply System

surface level and brought down to be connected to the diffusion pad. This was to prevent the water from entering the air supply piping system. A ball cock was connected in parallel to the flowmeters allowing for purging the water from the air piping system before supplying the air, via flowmeters, to the chamber for coagulation and flocculation. Firstly, air entered into a hexagonal manifold which is 25 mm deep made of nylon material equipped with two 8.0 mm inlets as shown in Figure 3.11 and is then supplied to the air cavity slots of the diffusion pad through 6 number equal length 3.0 mm diameter PVC pipes connected from the manifold. Air was released through the orifices of the diffusion pad for inducing the bubbles at a required flow rate.

3.2.3 Peripheral Equipments

The peripheral equipments associated with the experimental works of this investigation will be described in this section.

(a) Air Flowmeters: Two air flowmeters, Platon, Gapmeter type GTLK, Laboratory Flowmeters were used in this work. They were supplied by "Platon Flow Control Ltd", Platon Park, Viables, Basingstoke, Hampshire, England, RG22 4BS.

A wide range of air flow rates at atmospheric temperature and pressure (ATP = 20^0C and 760 mm height of mercury) can be covered for both the rapid and slow mixing by changing the meter tubes and the float indicators. Five metering tubes and six indicating floats were provided with these flowmeters in order to control the required flow rates. The ranges of air flow rate and the corresponding combination of the metering tubes and indicating floats are shown in Table 3.2.

The float indicators were used to control the fine adjustment of air flow rates. The range of air flow rates used in this investigation were 50 to 1000 cc/min. for slow mixing and a single rate of flow of 38,000 cc/min. was used for rapid mixing during the course of the experimental works.

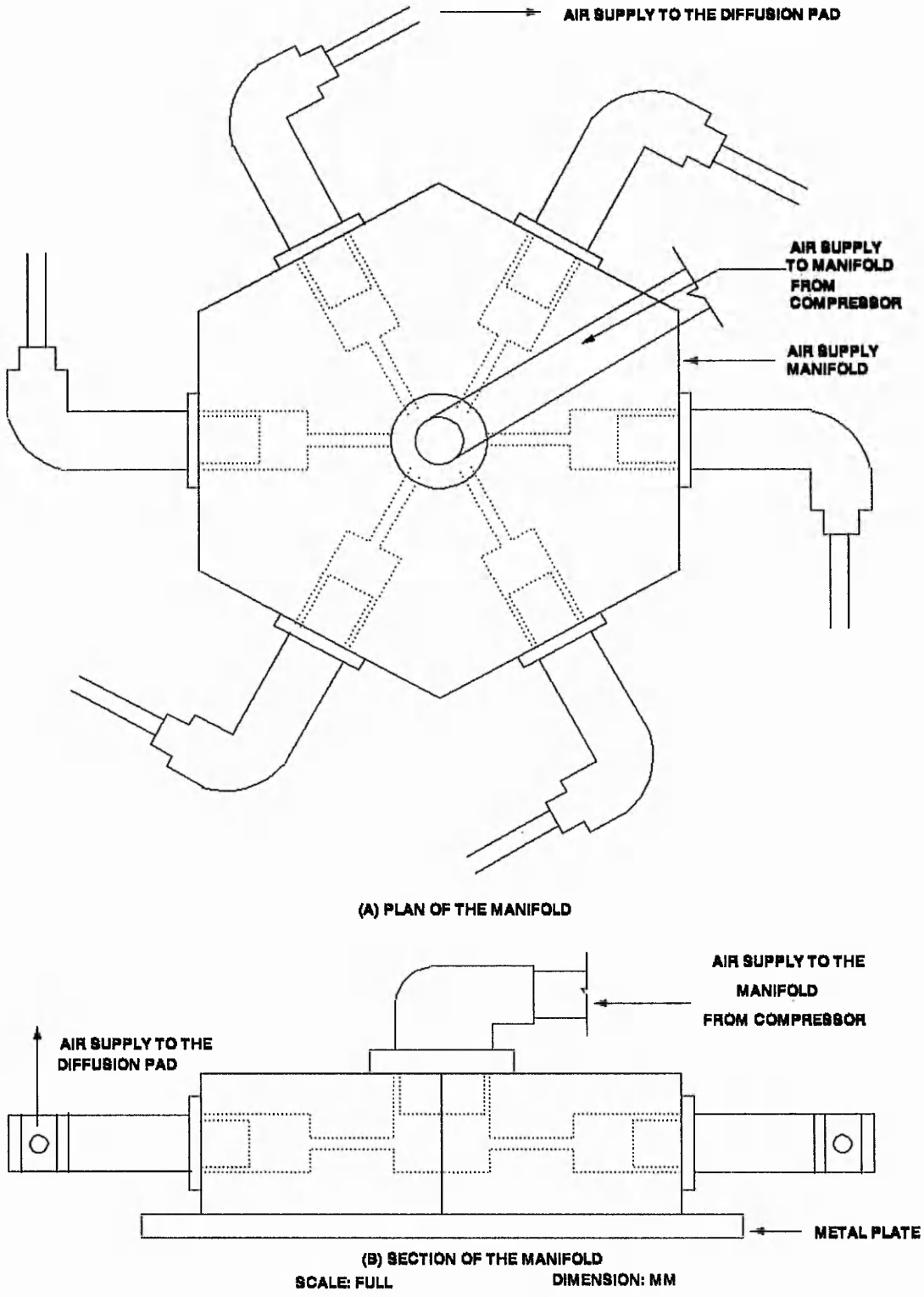

Figure 3.11 Details of air supplying Hexagonal Manifold

Table 3.2 Details of air flowmeter tubes and indicating floats

Range of Air Flow Rate (cc/minute)	Metering Tube specification	Indicating Float specification
20 - 600	A1	1/D
100 - 1200	A1	1/HS
200 - 2000	C6	6/D
200 - 4000	C6	6/HS
600 - 5000	B6	6/D
1000 - 10000	B6	6/HS
1000 - 12000	A6	6/D
2000 - 25000	A6	6/HS
6000 - 50000	A10	10/D
10000 - 100000	A10	10/HS

(b) Pump: A submersible pump of 0.22 kW, product of ABS Pumpen, 5204 Lohmar 1, West Germany was used to drain out the water after settling.

(c) Compressor: The compressor used to produce air for pneumatic flocculation was supplied by Broomwade, High Wycombe, England. It consisted of a Crompton Parkinson electric motor (BS 170, Bhp 5, volts 230, rpm 1425, amp. 3.2, single phase rating continously) and a cylindrical air storage tank of 380 mm height with a diameter of 305 mm. The compressor was equipped with an automatic regulator for on-off operation to maintain a constant pressure. The switch on and off pressures were maintained at 8.0 and 10 kg_f/cm^2 respectively during the course of experimental runs.

3.2.4 Measuring Instruments

The measuring instruments which were used during the course of the experimental works will be described in this section. The following instruments were used in this research work:

(a) Homogeniser: A product of Janke & Kunkel, GMBH & CO. KG, IKA-LABORTECHNIK, D-7813 Staufen, Br. West Germany. Type Ultra-Turrax T25 S7,

200 - 250 volts, 50/60 Hz, 600 W (input), speed range 8,000 to 24,000 rpm. This homogeniser was used to disperse the synthetic turbidity discretely without adding any dispersing chemical agents, to ensure thorough dispersion of the turbid water. The suspension was sucked in from the lower part of the mixing tube by the rotor and discharged out at the sides of the tube through the static slots. Thus the suspension was sucked into the centre of the rotor and then cast radially outward. The stator prevented the rotation of the suspension to a large extent and allowed the introduction of large mechanical energies in a very small space in between the stator and rotor as shown in Figure 3.12. In this shearing gap about 1000 times more energy was introduced into the suspension than in normal stirring. The rotor speed was selected and controlled electronically . A speed of 8,000 rpm. was selected and used to prepare the suspension during the experimental course of this investigation. Figure 3.13 shows the photograph of this homogeniser.

(b) Illuminating Floc Jar Tester: This apparatus was used to carry out the conventional coagulation-flocculation jar test. It consisted of six paddles of size 76.2 mm × 25.0 mm. The size of the paddles was standardised before using this instrument. This equipment was designed to operate from a 220/240 volts, 50 Hz/60 Hz AC supply. The stirrer provided a continuous range of near-constant stirring speeds from 0 to 300 rpm. The speed was electronically selected, controlled and regulated. The speed range of stirring used in this investigation was 30 to 65 rpm for slow mixing and a single speed of 250 rpm for rapid mixing during the experimental works. This apparatus was a product of Phipps & Bird Stirrer (Unit of General Medical Corp.), Richmond, Virginia 23228, U. S. A. Model 7790 - 402, 220 volts, 50 - 60 Hz AC supply and supplied by Camlab Limited, Nuffield Road, Cambridge CB4 1TH, England. Figure 3.14 shows the photograph of this floc tester apparatus.

(c) Turbidimeter: This equipment was a product of Hach Chemical Company, P. O. Box 907, Ames, Iowa 50010, U. S. A., Model 2100A, 190 - 270 volts, AC power supply, 50 - 60 Hz, 35 W. Figure 3.15 shows the photograph of this instrument. Turbidity ranges that could be measured were, 0 - 0.2 FTU, 0 - 1.0 FTU, 0 - 10 FTU, 0 - 100 FTU and 0 - 1000 FTU. The ranges 0 - 10, 0 - 100 and 0 - 1000 were

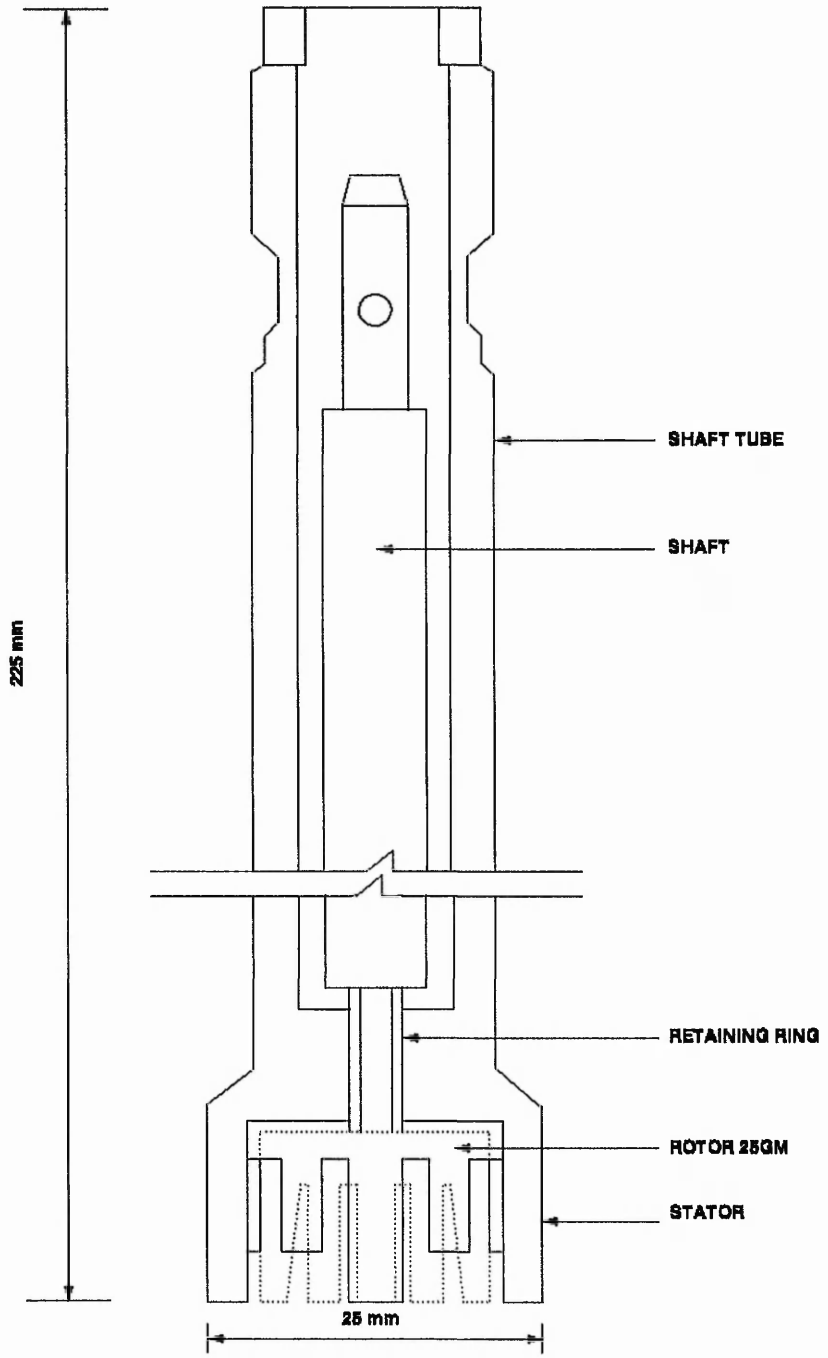

Figure 3.12 Sketch showing the details of the Dispersing Tool

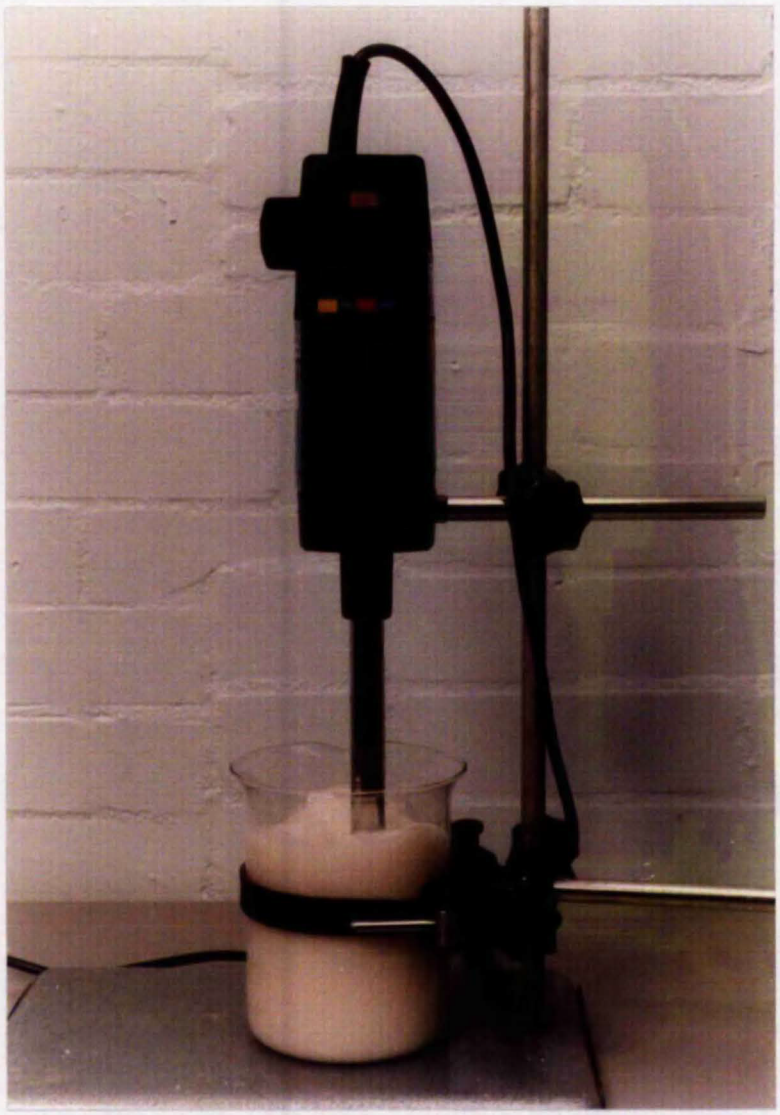

Figure 3.13 Photograph showing the Homogeniser

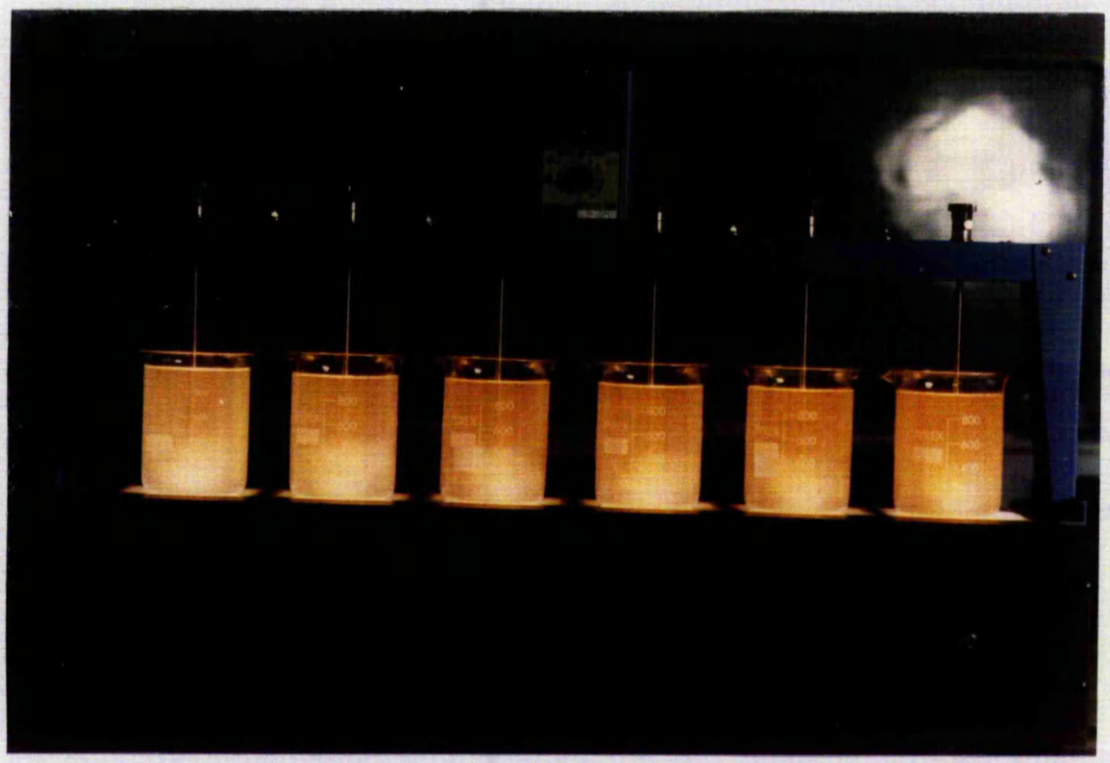

Figure 3.14 Illuminating Floc Tester

used in this research. This instrument was operated on the principle that light, passing through a substance, is scattered by particulate matter suspended in the substance. In the 2100A model, a strong light beam was sent upward through a cell containing a sample. As the beam passed through the turbidity particles, an amount of light (proportional to turbidity present) was scattered at a 90° angle to the beam and was received by a photomultiplier tube. The light energy was, in turn, converted to an electrical signal which was measured by the instrument's panel meter. It was furnished with four sample cells which were maintained in a clean condition. The sample size for all turbidity measurements were 25 (±1) ml. As the instrument was very sensitive to dirt or even finger prints left on the glass tube (sample cell) during handling of the sample, all the cells were cleaned both inside and outside and the out side was wiped with tissue paper before each reading. A cell riser was inserted into the cell holder assembly to raise the sample cell in the measurement of high turbidities in the range of (0 - 100) and (0 - 1000) FTU. The cell riser decreased the light path length which resulted in increased linearity in the measurement of high

turbidities. Calibration of this instrument was based on Formazin, a material that could be made by synthesis and reproduced repeatedly within one per cent. It was uniform in the number, size and shape of its particles which thus made it an ideal turbidity standard. The unit of measure, and thus the calibration of this instrument, was in Formazin Turbidity Units (FTU).

Standardisation: Instrument standardisation was achieved with the aid of four liquid turbidity standards, one for each range except the lowest. The turbidities of all four standards were based on Formazin dilutions. The standards (furnished with the instrument) were rated at 0.61, 10, 100 and 1000 FTU and were contained in sealed glass tubes called gel standard cells. When placed in the instrument, the inserted standards will scattered an amount of light proportional to the FTU ratings specified on the tubes. Standardisation was accomplished by selecting the desired ranged, placing the appropriate standard in the instrument and, with the light shield in place, adjusting the standardise control to obtain a meter reading equal to the FTU value of the standard.

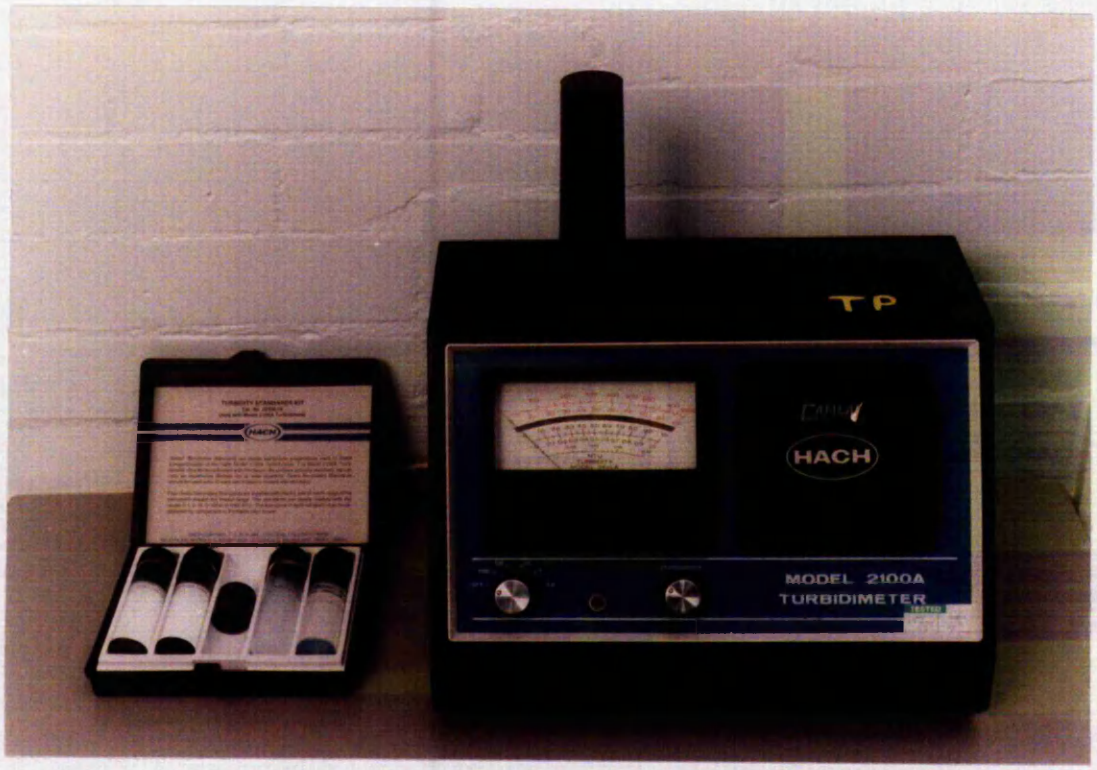

Figure 3.15 Photograph of the Turbidimeter

(d) Spectrophotometer: This equipment was a product of Hach Company, 5600 Lindbergh Drive, Loveland, Colorado 80537, U. S. A., Model DR 2000, combined microprocessor technology, optics and prepackaged reagents for colorimetric analysis. It was supplied by Camlab Limited, Nuffield Road, Cambridge CB4 1TH, England. Preprogrammed calibrations stored in the instrument's memory were used in chemical analysis during experimental work. Figure 3.16 shows the photograph of the spectrophotometer.

Figure 3.16 Photograph of the Spectrophotometer

(e) Dissolved Oxygen and pH Meter: This was a portable, microprocessor based,

pH and dissolved oxygen meter. The model used in this work was M 90, as shown in Figure 3.17, a product of Ciba Coring Diagnostics Ltd., Sudbury, Suffolk, England. The probes of this meter were checked and calibrated from time to time during the course of experimental works.

Figure 3.17 Photograph of the DO and pH Meter

(f) Analytical Balance: This equipment was an electronic analytical balance with a capacity of 120 g and with a resolution of 0.0001 g. It was supplied by GEC Avery Limited, Smethwick, Warley, West Midlands, England, B66 2LP, Model VA 124, 240/260 volts, 50/60 Hz.

In addition, thermometers, burettes and pipettes, beakers, dishes, glass bottles etc. were used during the experimental course of this investigation.

3.3 SYNTHETIC TURBIDITY MATERIALS

Three types of synthetic turbidity materials were used in this investigation of pneumatic flocculation. These turbidity materials were: Kaolin, Lycopodium powder and Polyvinyl Chloride (PVC) powder.

The physico-chemical properties of these materials will be described in the following subsequent sections. In order to verify the size range of each material used, photographs had been taken by the electronic scanning microscope in the Department of Manufacturing Engineering, The Nottingham Trent University, U. K. The photographs were taken with a magnification of 1550 times for all the materials, which are shown in Figure 3.18 to Figure 3.20, for the convenience of direct comparison, and other magnifications were also used for better views. These are shown in Figure 3.21 to Figure 3.23. Explanation of the scale reading is as shown: Four lines each have the following values $\underset{0.1}{—}$ $\underset{1}{—}$ $\underset{10}{—}$ $\underset{100}{——}$ μm. The last line in the sequence shown on the photograph indicates the size scale, for example —— for two lines only the last one is the scale length for 1 μm, for — — —— is means the last of three is 10 μm. The physico-chemical properties of the turbidity materials are summarised in Table 3.3.

Table 3.3 Physico-chemical properties of the turbidity materials

Sl No.	Turbidity Materials	Size (μm)	Density (g/cc)	Description
1	Kaolin	2 - 53	2.60	Heavy clay
2	Lycopodium powder	35	1.18	Dead fungus cells
3	PVC powder	0.5 - 1.5	1.40	Long-chain polymer

Figure 3.18 Scanning electronmicrograph of kaolin, 1550 magnification
— — —— = 10 micron

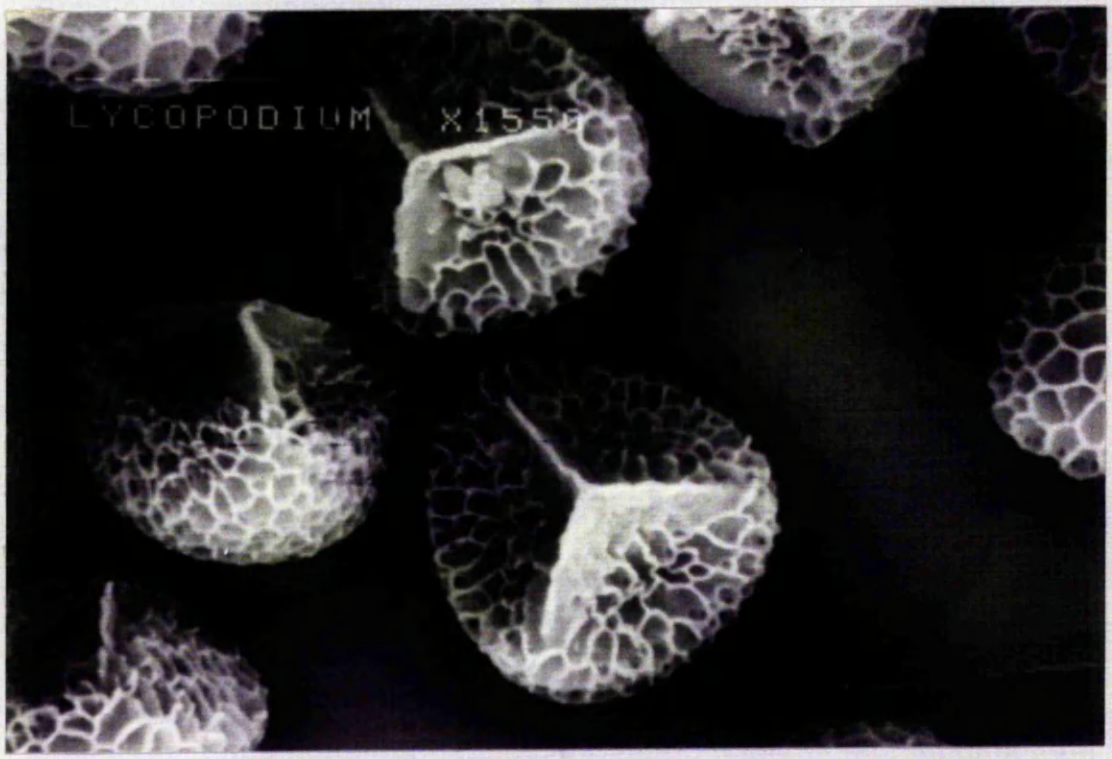

Figure 3.19 Scanning electronmicrograph of lycopodium, 1550 magnification
— — —— = 10 micron

Figure 3.20 Scanning electronmicrograph of PVC, 1550 magnification
— — —— = 10 micron

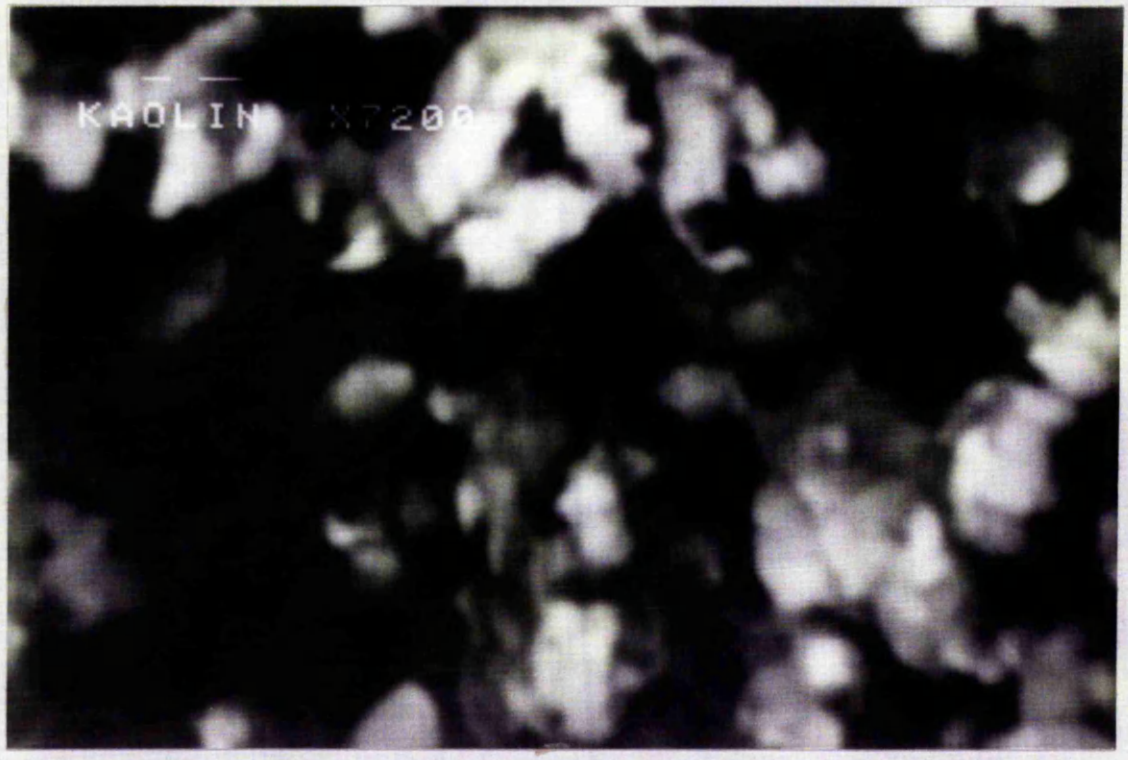

Figure 3.21 Scanning electronmicrgraph of kaolin, 7200 magnification
— —— = 1 micron

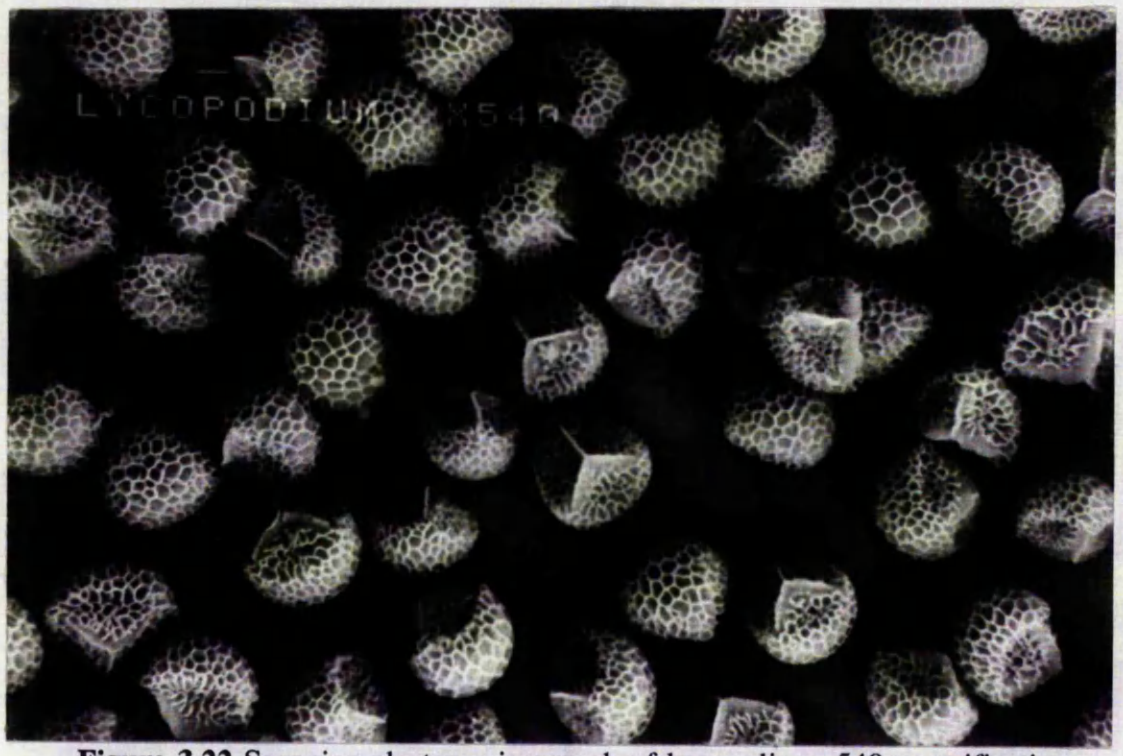

Figure 3.22 Scanning electronmicrograph of lycopodium, 540 magnification
— — —— = 10 micron

Figure 3.23 Scanning electronmicrograph of PVC, 6300 magnification
— —— = 1 micron

3.3.1 Kaolin

This material was supplied by Fisons Scientific Equipments, incorporating Griffin & George, Bishop Meadow Road, Loughborough, Leicestershire, LE11 ORG, England. Kaolin is a heavy clay powder, 2 to 53 μm in size (2 μm 80% and up to 53 μm 20%). The particles are irregular in shape with a density of 2.60 g/cc.

3.3.2 Lycopodium Powder

This material was supplied by Philip Harris Education, catalogue no. S 5103015 Lichfield, Staffordshire WS 14 OEE, England. Lycopodium powder consists of cells of dead fungus, pale yellow in colour and like a hazel nut in shape. The size of the particles is uniform, at 35 μm and its absolute density is measured as 1.18 g/cc. The procedure of measuring the density will be described in section 3.4. Particles are floated on water without being wetted. It is generally used to demonstrate Brownian motion.

3.3.3 Polyvinyl Chloride (PVC) powder

This material is commercially known as Corvic PVC Polymer. It was supplied by EVC UK Ltd., 1 Kings Court, Manor Farm Road, Runcorn, Cheshire, England. This material consisted of long-chain molecules, particles are irregular in shape and the size range is 0.5 to 1.5 μm as stated by the supplier and also verified under electronic scanning microscope during this research work as shown in Figure 3.20.

3.4 DETERMINATION OF THE ABSOLUTE DENSITY OF LYCOPODIUM TURBIDITY

The absolute density of the turbidity material was determined by using a Coulter Counter at the Science Department, The Nottingham Trent University, England. The procedure followed by the Science Department is described in this section. The

method involved dispersing a known weight of powder in a known volume of liquid. A sample was then withdrawn, diluted and analysed on the Coulter Counter. The diluted sample was stirred and 0.5 ml sample drawn through a small aperture in a tube that dipped into the sample beaker. Individual particles, as they passed through the aperture, produced a change in the resistance between two electrodes on opposite sides of the aperture, one electrode was in the beaker, the other was just above the aperture tube. Analysis was based on the variation of counts with sensitivity. At low sensitivities, none of the particles were large enough to be detected but as the sensitivity was increased increasing numbers were detected and counted.

The model used was a "D Industrial" and although far more sophisticated versions of Coulter Counter exist, the machine easily coped. The "coincidence correction" is that current when this particular machine was purchased. No blank correction had been made. The smallness of the error was obvious on comparing the blank test with the experimental data. The data was presented as a series of counts against "instrument volume", the latter effectively corresponding to 1/sensitivity provided no insidious side effects distort this convenient situation.

Experimental

5.0 g of lycopodium were mixed with a little Teepol and dispersed; several ultrasonic treatments were necessary as the lycopodium tended to clump together. These clumps usually floated to the top with the bubbles and it was often possible to see lycopodium particles streaming off them as they broke up. The 5.0 g were then made up to a total volume of 500 ml. Two ml of this were then made up to 250 ml in a filtered sodium chloride solution (9 g per litre) and counts were taken with a sample volume of 0.5 ml.

As a check on the calculations, counts @ 4500 imply 4500 particles in 0.5 ml of the "count solution", or 4500 × 500 in the 250 ml, or in 2 ml of the 500 ml, or 4500 × 500 × 250 in 5 g.

Blank	Instrument Volume
2	80
2	40
3	35
5	30
14	25
60	20
70	15
87	10
101	5

Experimental data is shown in Table 3.4 from which, it can be seen that the volume of lycopodium turbidity in 0.5 ml of the dilute sample is 68105 "instrument units".

This may be multiplied by 500 to give the total volume of lycopodium in the "count solution" and by a further factor of 250 to give the volume of 5 g of lycopodium. Instrument volume may be converted to real volumes by developing the relationship

$$d = k * (\text{instrument volume})^{0.33333}$$

where, d is a diameter (usually expressed in microns) and k is a calibration factor (that depends on the size of the aperture in the tube, 140 microns in this case). For the 140 micron tube, $k = 9.82$.

Now, volume of solid material in the sample volume = $(\pi d^3/6) = \pi/6\ [k\ (\text{instrument volume})^{0.33333}]^3 = (\pi/6)\ k^3\ (\text{instrument volume})$

Taking $\pi = 3.14159$, $k = 9.82$, cumulative volume = 68105 and allowing for the sample volume and the dilution factor and the conversion factor from cubic micron to ml, 5 g occupy a volume

$0.5236 \times (9.82^3) \times 68105 \times (10^{-6})/8 = 4.22$ ml.

This gives a particle density of 5.00/4.22 = 1.184834 or 1.18 g/ml.

Table 3.4 Determination of the Density of a Lycopodium Sample with a Coulter Counter

Count (Avg.)	Corrected Count	Inst. Volume	dn	Vav	dn × Vav	Cum. dn × Vav	Average Diameter (μm)
1	1.000006	80	0			0	0
2	2.000027	60	1.000020	70	70.00144	70.00144	40.51222
19.7	19.70266	40	17.70263	50	885.1317	955.1331	36.21402
34	34.00793	35	14.30526	37.5	536.4475	1491.580	32.90262
76	76.03962	30	42.03169	32.5	1366.030	2857.610	31.37000
195	195.2608	27.5	119.2212	28.75	3427.610	6285.221	30.11383
564	566.1821	25	370.9212	26.25	9736.683	16021.90	29.21437
1139	1147.899	22.5	581.7174	23.75	13815.79	29837.69	28.25582
1830	1852.973	20	705.0738	21.25	14982.81	44820.51	27.22741
2493	25.35.635	17.5	682.6617	18.75	12799.90	57620.42	26.11483
2860	2916.112	15	380.4768	16.25	6182.748	63803.17	24.89839
3092	3157.584	10	241.4727	12.5	3018.409	66821.57	22.81340
3256	3328.726	5	171.1417	7.5	1283.563	68105.14	19.24157

3.5 COAGULANT CHEMICALS

Two types of chemicals were used as coagulant in this research work. These chemicals are described as follows:

3.5.1 Aluminium sulphate: Aluminium sulphate, $Al_2(SO_4)_3$ $16H_2O$ was supplied in coarse powdered form by Fisons Scientific Equipment, Bishop Meadow Road, Loughborough, Leicestershire LE11 ORG, England.

3.5.2 Ferric sulphate: Ferric sulphate, $Fe_2(SO_4)_3$ + aq., was supplied in fine powdered form, yellowish in colour, also by Fisons Scientific Equipment.

3.5.3 Reagents: The following prepacked chemical reagents supplied by Camlab of U. K., which were products of Hach Company of U. S. A., were used in this research work during the course of its experimental part for the analysis of water:

(a) Nitra Ver 5 Nitrate reagent powder pillow, cat. no. 14034 - 66
(b) Ferrover Iron reagent powder pillow, cat. no. 854 - 66
(c) Ascorbic acid powder pillow, cat. no. 14577 - 16CV
(d) Alu Ver 3 Aluminium reagent powder pillow, cat. no. 14290 - 68
(e) Bleaching 3 reagent powder pillow, cat. no. 14294 - 10CM

In addition to these chemical reagents, methyl orange, 0.1N sulphuric acid and distilled water were also used.

3.6 OPTIMUM DOSES OF COAGULANTS - THE JAR TEST

The widely used jar test was performed in order to determine the optimum doses of the coagulants. There is no standardised equipment or procedure for the jar test. A typical design of the paddle and the beaker described by Ives (1978), was used in this investigation. The jar test apparatus is described in section 3.2.4(b) and shown

in Figure 3.14. The stirrer, which was standardised, is shown in Figure 3.24. A set of six beakers (1L) were stirred simultaneously after the addition of different doses of coagulant. Each sample underwent the same rapid mixing and slow stirring. The set of operating conditions are given below:

Rapid mixing: 250 rev/min. for 2 minutes.

Slow stirring: (a). Constant or fixed agitation: 50 rev/min. for 20 minutes.

(b). Stepping down agitation: 66 rev/min. for 4 minutes.
60 rev/min. for 4 minutes.
50 rev/min. for 4 "
40 rev/min. for 4 "
30 rev/min. for 4 "

Settling: 0 rev/min., 15 - 120 minutes, collecting the samples @ 15 minute intervals.

Samples were taken from supernatant liquor at a fixed depth of 30 mm and nephelometrically measured (90^0 scatter Hach 2100A turbidimeter calibrated in FTU). Jar tests were performed for both the constant stirring (will be described as "normal flocculation" in this work) and step down stirring (will be described as

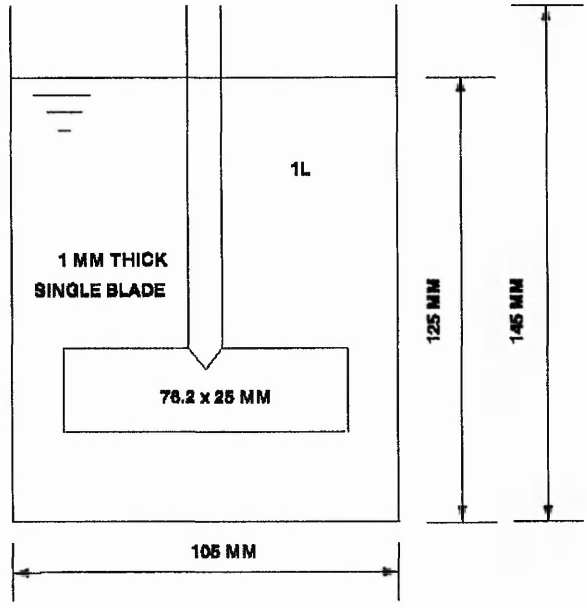

Figure 3.24 Standardised Jar Test Stirrer

"taper Flocculation") for the same value of *Gt*, the dimensionless product of the mean temporal velocity gradient and the slow mixing time which is considered as a measure of the flocculation process.

The power transmitted from the stirrer blade to the water was calculated from the drag force on the paddle blade multiplied by the relative velocity of the blade using the equation:

$$P = 0.5\ C_D A \rho u_r^3 \qquad (3.1)$$

where, P is the power dissipated, C_D is the coefficient of drag, A is the area of the blade, ρ is the mass density of water and u_r is the relative velocity of the blade.

The value of drag coefficient was assumed to be 1.20 (Rouse, 1978) for $W/L<5.0$ (where W is the width and L is the height of the blade) which was 76.2/25 ≈ 3.0 in this case. Substituting $A = 76.2 \times 25.0 \times 10^{-6}$ m^2, $\rho = 998.2$ kg/m^3 and $u_r = 0.75(2\pi rn/60)$, where r is the radius of the blade and n is the number of revolutions per minute,

$$P = 3.05 \times 10^{-8}\ n^3 \qquad (3.2)$$

The mean temporal velocity gradient G, as defined in section 1.7, was considered a basis of comparison as the design and operation has not yet been standardised for the jar test. Using this technique, the paddle stirrer shown in Figure 3.24 was calibrated at 20^{0}C, giving velocity gradients G (s^{-1}), against paddle rotation speed in rev/min. as shown in Figure 3.25 and presented in Table 3.5. The value of G was calculated using the following equation:

$$G = (P/\mu V)^{1/2} \qquad (1.3)$$

and substituting $\mu = 1.002 \times 10^{-3}$ N.s/m^2 at 20^{0}C and V, the volume of water = 1000 ml.

Table 3.5 Calibration of paddle speed for the Jar Test

Paddle speed (rpm)	Slow mixing					Rapid mixing
	30	40	50	60	66	250
Mean velocity gradients, G (s^{-1})	28.69	44.18	61.75	81.16	93.54	690.31

From this table it can be seen that the calculated *G* values correspond to the paddle speeds and are in the recommended ranges for coagulation and flocculation operation in water treatment industries (AWWA, 1969; Barnes *et al.*, 1981).

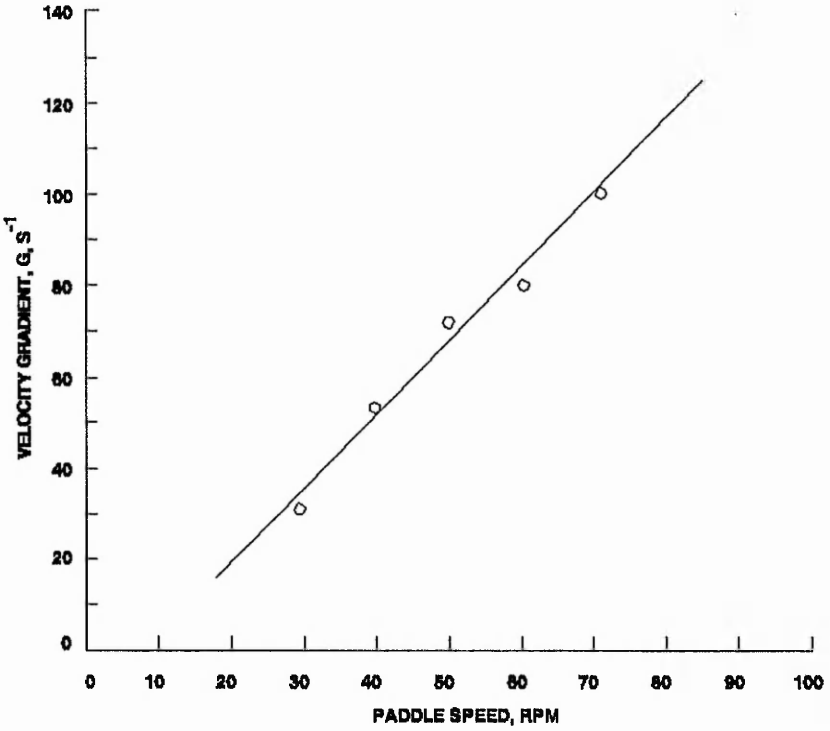

Figure 3.25 Velocity gradient produced by various speeds in paddle flocculator as shown in Figure 3.24

Jar tests were performed with constant and stepping down speed of the paddle in order to determine the optimum doses of coagulants both for the normal and taper

flocculation. In stepping down stirring, an equivalent amount of *Gt*, the dimensionless product of the velocity gradient, *G*, and the detention time, *t*, that was used in constant stirring was applied with the successively decreasing paddle speed in several stages. The *Gt* values imparted in slow stirring for constant and stepping down paddle speed are shown in Table 3.6.

Table 3.6 *Gt* distribution for constant and stepping down paddle speed in slow mixing in the Jar Test operation.

Paddle speed for constant stirring (rev./min.)	Mixing time (min.)	*Gt* values	Equivalent paddle speeds for stepping down stirring (rev./min.)	Mixing time (min.)	Equivalent *Gt* values
50	20	74,100	66	4	22,449
			60	4	19,478
			50	4	14,820
			40	4	10,603
			30	4	6,885
					74,236

The results of the Jar tests are summarised in Table 3.7 and the details are shown in Figure (B-1) to Figure (B-12) in Appendix 4.

Table 3.7 Optimum doses of the coagulants determined by the Jar Test

Synthetic Turbidity	Type of slow stirring	Optimum dose, mg/l	
		Aluminium sulphate	Ferric sulphate
Kaolin	Constant	35	42
	Taper	25	30
Lycopodium powder	Constant	35	50
	Taper	25	40
PVC powder	Constant	35	50
	Taper	35	50

3.7 PREPARATION OF SUSPENSION

The synthetic turbidity materials used were kaolin, lycopodium powder and PVC powder as described in section 3.3. A high-speed dispersing and emulsifying apparatus, the IKA Ultra Turrax T 25 homogeniser (described in section 3.2.4a) was used to prepare the homogeneously dispersed suspension of discrete particles. The medium was sucked in from below by the rotor and came out at the sides through the static slots. Thus the particles were sucked into the centre of the rotor and cast radially outward. In the shearing gap between rotor and stator about 1000 times more energy was introduced into the medium than in stirring. The speed range of the homogeniser was 8,000 to 24,000 rpm. A rotor speed of 8,000 rpm was used for 120 seconds to disperse the particles homogeneously. The procedure for the preparation of the suspension is described below:

(a) A known quantity of the turbidity material was weighed in a 250 ml beaker.

(b) 800 ml tap water was put into a 1L beaker and the beaker secured in the homogeniser with a strap clamp.

(c) The dispersing tool of the homogeniser was immersed into the beaker water in such a manner that its clearance from the bottom of the beaker was 15 mm to allow the suction and suspension entry to the rotor.

(d) The synthetic turbidity was added to the beaker and the drive unit of the homogeniser was then started at a speed of 8,000 rpm and allowed 120 seconds to disperse the turbidity materials homogeneously.

(e) The prepared suspension was then added immediately to the water in the pneumatic flocculation chamber and kept in a constant agitating state in order to maintain the homogeneous dispersion. The experimental set up was then ready for the start of the procedure.

3.8 RATES OF AIR FLOW

Compressed air was released through the orifices of the diffusion pads to generate the velocity gradients in turbid water required for rapid mixing and slow stirring. A wide range of air flow rates at ATP could be covered for this purpose by changing the air flowmeter tubes and the float indicators. The range of air flow rates used in this investigation was 50 to 38,000 cc/min. For slow stirring, the range was 50 to 1,000 cc/min. and for rapid mixing, a single air flow rate of 38,000 cc/min. was supplied for all the cases without exception. This flow rate corresponded to a G value of 300 s^{-1} which was found to be enough for uniform and homogeneous dispersion of coagulant throughout the column of water. The optimum air loading for rapid mixing was not investigated in this research work. However, some preliminary experimental works indicated that this air loading in rapid mixing produced appreciable flocs in slow mixing, that can be settled easily by sedimentation, even though the intensity of this mixing was much less than that in the jar test.

Different air flow rates (50, 100, 200, 300, 400, 500, 600, 800 and 1,000 cc/min.) were applied in the slow mixing process with the aim of investigating the optimum air loadings for turbidity removal.

In taper flocculation, an equivalent amount of Gt, the dimensionless product of the velocity gradient and the detention time, to that used in normal flocculation for a particular air flow rate, was applied with successive decreasing velocity gradients in several stages. The Gt values imparted in slow stirring for normal and taper agitation are shown in Table 3.8.

The calculations for Gt distribution in Table 3.8 were based on a standard temperature of 20°C. It was not possible to keep the water temperature constant at 20°C during the experimental runs and thus the G values were applied with a little error. However, a temperature standardisation was made for the calculation of optimum velocity gradients and for further analysis of the experimental results.

Table 3.8 Distribution of Gt for Normal and Taper agitation
(Standardised at the temperature of 20^0C)

Normal agitation			Taper agitation		
Air flow rate (cc/min.)	Mixing time (min.)	Gt values	Equivalent air flow rates(cc/min.)	Mixing time (min.)	Equivalent Gt values
50	20	12,792	100 75 50 25 21.4	4 4 4 4 4	3,616.8 3,133.2 2,556.0 1,808.8 1,677.3 --- 12,792.10
100	20	18,084	150 125 100 75 62.5	4 4 4 4 4	4,430.4 4,044.0 3,616.8 3,132.0 2,861.6 --- 18,084
200	20	25,572	300 250 200 150 124.8	4 4 4 4 4	6,266.4 5,719.2 5,114.4 4,430.4 4,041.6 --- 25,572.
300	20	31,332	400 350 300 250 218	4 4 4 4 4	7,236.0 6,768.0 6,266.4 5,719.2 5,341.7 --- 31,332.3
400	20	36,180	600 500 400 300 250.7	4 4 4 4 4	8,880.8 8,088.0 7,236.0 6,266.4 5,728.8 --- 36,180.0
500	20	40,440	700 600 500 400 341.31	4 4 4 4 4	9,571.2 8,860.8 8,088.0 7,236.0 6,684.0 --- 40,440.0

continued...

Table 3.8 Distribution of Gt for Normal and Taper agitation
(Standardised at the temperature of 20^{0}C) [continued]

Normal agitation			Taper agitation		
Air flow rate (cc/min.)	Mixing time (min.)	Gt values	Equivalent Air flowrates(cc/min.)	Mixing time (min.)	Equivalent Gt values
600	20	44,304	800 700 600 500 435.9	4 4 4 4 4	10,231.2 9,571.2 8,860.0 8,088.0 7,553.6 --------- 44,304.4
800	20	51,156	1,000 900 800 700 627.10	4 4 4 4 4	11,440.8 10,852.8 10,231.2 9,571.2 9,060.0 --------- 51,156.0
1000	20	57,204	1,200 1,100 1,000 900 823.15	4 4 4 4 4	12,532.8 11,997.6 11,440.8 10,852.8 10,380.0 --------- 57,204.0

3.9 TEMPERATURE

The ambient temperature and water temperature were recorded as they changed from day to day with the environmental changes throughout the year. It was not possible to control these temperatures in this laboratory.

3.10 TAP WATER QUALITY

The chemistry of tap water plays a significant role in the coagulation and

flocculation process particularly the sufficiency and insufficiency of alkalinity and the type of cations present. The supplied water analysis reports for the period of 01/01/1993 to 31/08/1994 were collected from Severn Trent Water Authority, for the area where the laboratory of this work is situated. These reports are presented in Appendix 2. The analysis of water of these reports were based on the quality of water collected from the sources of supply for this area.

A comparison of the analysis of tap water used for the experimental works of this investigation was made with the supplied water for the same period of 01/01/1993 to 31/08/1994. The comparison of water analysis is shown in Table 3.9. The parameters and qualifiers of the tap water are shown in the Table 3.9 and they are the average value of around 300 samples tested during the course of the experiment of this research work.

3.11 SAMPLING TECHNIQUE

The sample collecting ports were designed bearing the consideration in mind to collect truly representative samples as far as possible. The inlet of the sampling ports was projected 95.7 mm, which is equal to 2/3 of the radius of the chamber, from the inside wall of the chamber. Within this region, except very close to the wall, the average velocity of the settling particles was fairly uniform throughout the cross-sectional area of chamber.

Steel pipes of 2.0 mm internal diameter were inserted into the 3.0 mm flexible PVC sample collecting pipe to keep it straight in order to maintain the exact depth of the inlets. Rubber tubes of 5.0 mm internal diameter with regulatory pinch-cocks were connected at the outlet of the sampling ports for the convenience of collecting the samples. Details of the sampling ports are shown in Figure 3.26.

Eleven number sample collecting ports were mounted which were spaced at equal depths of 200 mm. throughout the 2400 mm column of tested water. In the case of

Table 3.9 Analysis of Water

Parameters	Severn Trent Water Authority, water analyses				TNTU* Laboratory, water analyses used for the experiment			Unit
	Period	Min.	Max.	Ave.	Min.	Max.	Ave.	
Turbidity	1993	0.1	1.0	0.2	0.4	0.4	0.4	FTU
	1994	0.3	0.3	0.3				
pH	1993	7.3	8.3	7.8	7.01	8.10	7.66	
	1994	7.4	8.2	7.8				
Tempt.	1993	6.5	22.9	12	8.70	22.60	14.00	^0C
	1994	5.5	20.1	12.5				
Alkalinity	1993	110	146	124	110	150	125	mg/l as $CaCO_3$
	1994	85	125	108				
Iron	1993	0.02	0.09	0.023	0.02	0.07	0.03	mg/l
	1994	0.02	0.03	0.021				
Nitrate	1993	11	32.8	21.6	13.64	35.20	19.58	mg/l as NO^-_3
	1994	13	34	22.5				
Dissolved Oxygen	-	-	-	-	4.80	8.00	5.60	mg/l

*TNTU = The Nottingham Trent University

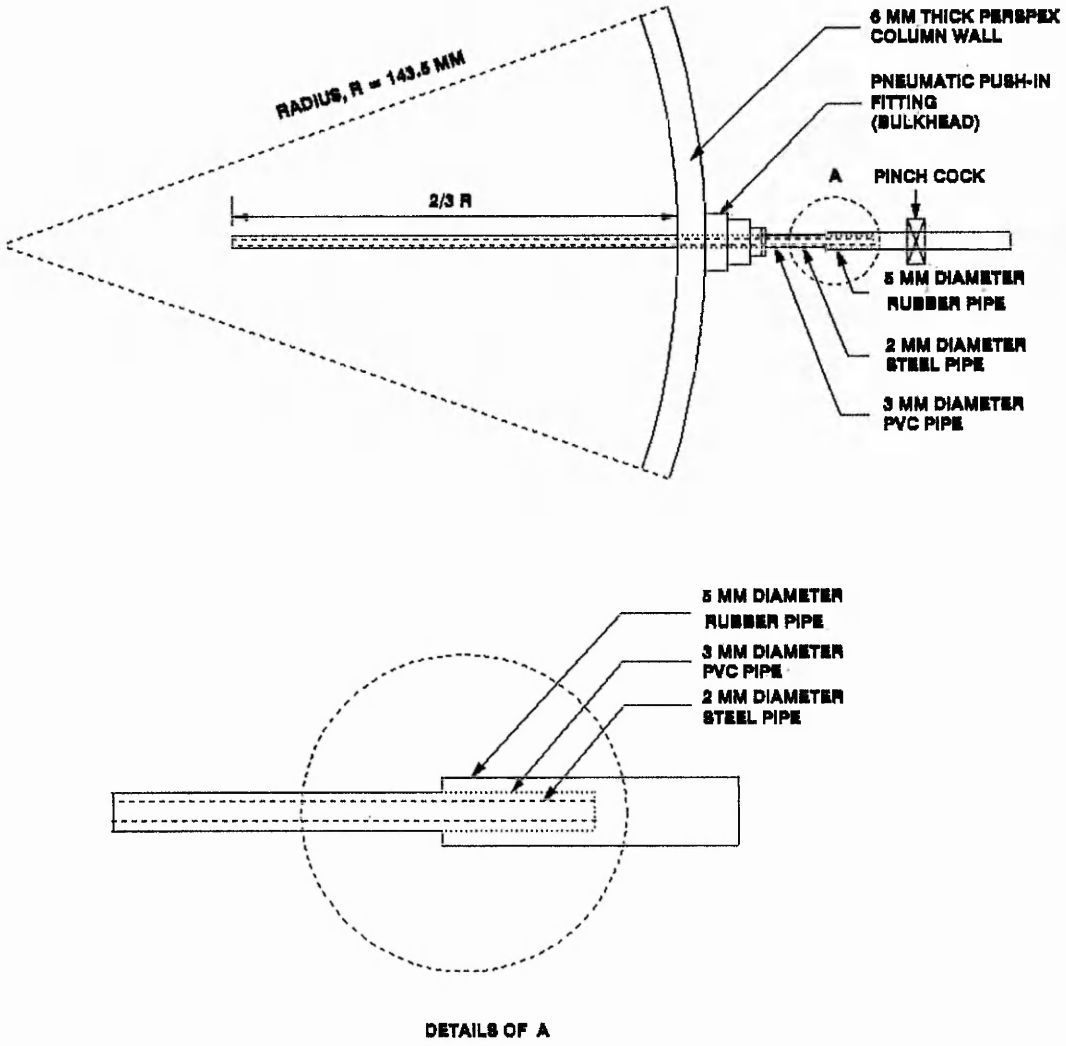

Figure 3.26 Details of Sample Collecting Port

kaolin and lycopodium powder turbidity, the operating water height was 2400 mm and the samples were collected from all of the eleven number of sampling ports at different depths. In the case of PVC powder turbidity, the operating water height was kept limited to 2000 mm to allow a free height for the rising of foam generated in the rapid mixing during the coagulation process. In this case, samples were collected from nine sampling ports at different depths. For all the cases, samples were collected at equal intervals of 30 minutes over a total settling period of 120 minutes, except in the case of lycopodium turbidity coagulated with aluminium sulphate in normal flocculation. In this particular case, samples were collected at equal intervals of 60 minutes over a settling period of 240 minutes in order to allow a longer settling time, because the flocs of lycopodium powder formed with aluminium sulphate are lighter due to the physical properties of lycopodium powder and the micro air bubble binding to floc particles. This results in a longer settling time; this phenomenon is described in chapter 5.

The sample collecting pipes were flushed every time before collecting the sample to avoid any deposition of flocs inside the pipes. Collection of samples was started from the lower port ending at the upper one, thus avoiding the fall out of flocs on the lower collecting pipes from the possible deposition on the top of the next upper collecting pipes. Disturbance to the inlet pipe could happen during the collection of samples and any deposited flocs on the upper part of the projected sampling tube might enter the next downward inlet sampling port. The inertia of the streamlines of flow at the time of sample collection could also cause some disturbances and affect the dislodgement of nested settled floc material above the projected sampling tube.

3.12 SCHEDULE OF EXPERIMENTS

Experiments were conducted to investigate the validity and applicability of the process of pneumatic flocculation at different air flow rates, different sizes of the orifice, type of synthetic turbidity materials, type of agitation (constant and taper) and type of coagulants. 284 experimental runs were performed in conjunction with

these 5 parameters in order to evaluate the efficiency and applicability of the process of pneumatic flocculation. The removal efficiency for iron, nitrogen, aluminium and the level of dissolved oxygen before and after the process were also studied in this investigation.

There are 48 experimental sets as presented in Table 3.10. Most of the sets have at least 5 experimental runs which were conducted during the course of the experimental work in the laboratory, with the aim of investigating the process of pneumatic flocculation. The details of the experimental runs are described in Appendix 1.

3.13 EXPERIMENTAL PROCEDURE

The experimental runs were conducted following the schedule described in section 3.12 and shown in Table 3.10, with the aim of investigating the validity and applicability of the process of pneumatic flocculation in water treatment. Three types of turbidity materials namely kaolin, lycopodium powder and PVC powder were used to prepare the suspensions which were coagulated and flocculated under different initial conditions as presented in Appendix 1.

The tap water from the Public Health Engineering laboratory was used to create the turbid water. The pH and the alkalinity of the tap water were checked to make sure of the suitability and sufficiency of these two parameters required for the chemical reaction before beginning the experimental run and these were also recorded. The total alkalinity in the tap water was found to be in the range of 110 - 150 mg/l as $CaCO_3$. The pH range was found to be from 7.0 to 8.1. From these values and from optimum coagulant doses determined by the conventional jar test as shown in Table 3.7, it was understood that there was sufficient alkalinity and suitable values of pH for the reaction to take place without any need for adjustment. The ambient temperature and the water temperature were recorded and converted into a suitable standard (20^0C) for data analysis.

Table 3.10 Details of the experimental sets

Set No.	Orifice Diameter(mm)	Run No.	Details of the experimental sets		
			Turbidity	Coagulant	Flocculation Type
1	1.00	01 - 09	Kaolin	A/S*	Normal
2	"	10 - 18	Kaolin	A/S	Taper
3	"	19 - 27	Kaolin	F/S*	Normal
4	"	28 - 36	Kaolin	F/S	Taper
5	"	37 - 45	Lycopodium	A/S	Normal
6	"	46 - 51	Lycopodium	A/S	Taper
7	"	52 - 60	Lycopodium	F/S	Normal
8	"	61 - 66	Lycopodium	F/S	Taper
9	"	67 - 73	PVC powder	A/S	Normal
10	"	74 - 79	PVC powder	A/S	Taper
11	"	80 - 86	PVC powder	F/S	Normal
12	"	87 - 92	PVC powder	F/S	Taper
13	1.50	93 - 97	Kaolin	A/S	Normal
14	"	98 - 102	Kaolin	A/S	Taper
15	"	102 - 107	Kaolin	F/S	Normal
16	"	108 - 112	Kaolin	F/S	Taper
17	"	113 - 117	Lycopodium	A/S	Normal
18	"	118 - 122	Lycopodium	A/S	Taper
19	"	123 - 127	Lycopodium	F/S	Normal
20	"	128 - 132	Lycopodium	F/S	Taper
21	"	133 - 137	PVC powder	A/S	Normal
22	"	138 - 142	PVC powder	A/S	Taper
23	"	143 - 147	PVC powder	F/S	Normal
24	"	148 - 152	PVC powder	F/S	Taper
25	2.00	153 - 157	Kaolin	A/S	Normal
26	"	158 - 162	Kaolin	A/S	Taper
27	"	163 - 167	Kaolin	F/S	Normal
28	"	168 - 172	Kaolin	F/S	Taper
29	"	173 - 177	Lycopodium	A/S	Normal
30	"	178 - 182	Lycopodium	A/S	Taper
31	"	182 - 187	Lycopodium	F/S	Normal
32	"	188 - 192	Lycopodium	F/S	Taper
33	"	193 - 197	PVC powder	A/S	Normal
34	"	197 - 202	PVC powder	A/S	Taper
35	"	203 - 207	PVC powder	F/S	Normal
36	"	208 - 212	PVC powder	F/S	Taper
37	3.00	213 - 220	Kaolin	A/S	Normal
38	"	221 - 227	Kaolin	A/S	Taper
39	"	228 - 233	Kaolin	F/S	Normal
40	"	234 - 239	Kaolin	F/S	Taper
41	"	240 - 246	Lycopodium	A/S	Normal
42	"	247 - 251	Lycopodium	A/S	Taper
43	"	252 - 257	Lycopodium	F/S	Normal
44	"	258 - 263	Lycopodium	F/S	Taper
45	"	264 - 269	PVC powder	A/S	Normal
46	"	270 - 273	PVC powder	A/S	Taper
47	"	274 - 278	PVC powder	F/S	Normal
48	"	279 - 284	PVC powder	F/S	Taper

*A/S = Aluminium sulphate and F/S = Ferric sulphate

The level of dissolved oxygen in the sample water was measured before and after the process of pneumatic flocculation. The concentrations of iron, nitrogen and aluminium were measured in several stages (tap water, turbid water, after flocculation and after settling) in order to evaluate the process efficiency in removing these impurities from water.

A rapid mixing duration of 120 seconds with a high rate of air flow (38,000 cc/min.) and a slow mixing time of 20 minutes with low rates of air flow (50 cc/min. to 1,000 cc/min.) were allowed for coagulation and flocculation respectively. In taper flocculation, an equivalent amount of *Gt* used in normal flocculation for a particular air flow rate was applied with successively decreasing velocity gradients in several stages as described in section 3.8. Samples were collected from eleven number of collecting ports spaced at equal distances of 200 mm throughout the chamber at an interval of 30 minutes over a settling period of 2 hours. In the case of lycopodium powder, coagulated with alum and flocculated under normal flocculation, samples were collected at an interval of 60 minutes over a settling period of 4 hours. The step by step procedure is described as follows:

1) The chamber was filled with tap water to an operating water height of 2400 mm in the case of kaolin and lycopodium powder turbidity. For PVC powder turbidity, the depth of operating water was kept at 2000 mm to provide more free height to allow for the rising of foam produced during the time of rapid mixing due to the long-chain molecular property of the suspension. Dissolved oxygen, pH and temperature (both tap water and ambient) were measured during the filling of the chamber. These parameters were also measured at the end of pneumatic flocculation.

2) Meanwhile the synthetic turbid suspension was prepared using the homogeniser. Following the procedure described in section 3.7, 0.8L of suspension was prepared in a 1L beaker to create the turbid water at a concentration of 200 mg/l in the chamber and kept ready for the test.

An 0.5% coagulant solution was also prepared in the same manner using the

optimum doses of coagulant determined by the jar test following the procedure described in section 3.6 and also kept ready for the test.

3) The ball cock of the air supply system was opened slowly and some time was allowed to purge the water from inside the air flow piping system. The air was supplied then to the chamber through the diffusion pad from the compressor following the procedure described in section 3.2.2(d) at a predetermined flow rate required for the rapid mixing, controlled and monitored by the high range air flowmeter. The bubbles were then released through the orifice of the diffusion pad for vigorous mixing. The prepared suspension of a predetermined quantity of the synthetic turbidity was then added to the surface of the water and left for 3 minutes to disperse homogeneously. Samples were then taken from the middle depth of water in the chamber for analysis.

4) The rate of air flow was checked and controlled to maintain the flow rate required for rapid mixing. The coagulant solution was then added to the top of the water surface in 0.5% solution form and was mixed vigorously with water for a period of 120 seconds.

5) After rapid mixing for 120 seconds, the air flow rate was reduced to a predetermined air flow rate required for slow mixing by controlling the air flowmeters valves and this was continued for a period of 20 minutes.

6) The air supply was stopped after 20 minutes of pneumatic flocculation and samples were collected immediately after flocculation from the middle depth of the chamber to measure the temperature, pH, dissolved oxygen, iron and nitrogen and also to determine the flocculated amount of suspended materials. The flocculated water was then left to settle for a period of two hours.

7) Following the procedure described in section 3.11, samples were collected from different depths of the chamber at equal intervals of 30 minutes over a total settling period of 2 hours and these samples were analysed for residual turbidity following

the procedure mentioned in section 3.2.4(c). In the case of lycopodium turbidity coagulated with alum in normal flocculation, samples were collected at equal intervals of 60 minutes over a total settling period of 4 hours. Depths of the sampling ports were 200, 400, 600, 800, 1000, 1200, 1400, 1600, 1800, 2000 and 2200 mm for kaolin and lycopodium turbidity. For PVC powder turbidity, the depths were 200, 400, 600, 800, 1000, 1200, 1400, 1600 and 1800 mm.

8) After the total settling period, samples were also collected to measure the alkalinity, iron, nitrogen and aluminium concentration.

9) From the obtained data as described in step 7, isoconcentration lines were constructed and removal efficiency was evaluated following the procedure described in section 3.14.

3.14 EXPERIMENTAL OBSERVATIONS

Samples were collected for analysis from different depths of the chamber at equal intervals of 30 minutes over a total settling period of 2 hours except for lycopodium turbidity coagulated with alum in normal flocculation in which samples were collected at intervals of 60 minutes over a settling period of 4 hours for the reasons mentioned in section 3.11 which will also be discussed in chapter 5. Residual turbidity was measured in FTU which was based on the optical effect of the suspended matter present in the sample. These readings in FTU were then converted into the actual amount of synthetic turbidity materials in mg/l using the calibration curves shown in Figure (A-1) to Figure (A-9) in Appendix 3 which were constructed during the early stages of this investigation.

Turbidity removal efficiency of collected samples at different depths and times were then calculated from which the isoconcentration lines were constructed for each experimental run.

The overall removal efficiency in per cent, E at any time, say t_2 of settling period can be evaluated using the following expression with respect to the Figure 3.27:

$$E = \frac{\Delta h_1}{h_5} \times \frac{R_1 + R_2}{2} + \frac{\Delta h_2}{h_5} \times \frac{R_2 + R_3}{2} + \frac{\Delta h_3}{h_5} \times \frac{R_3 + R_4}{2} + \frac{\Delta h_4}{h_5} \times \frac{R_4 + R_5}{2} \quad (2.23)$$

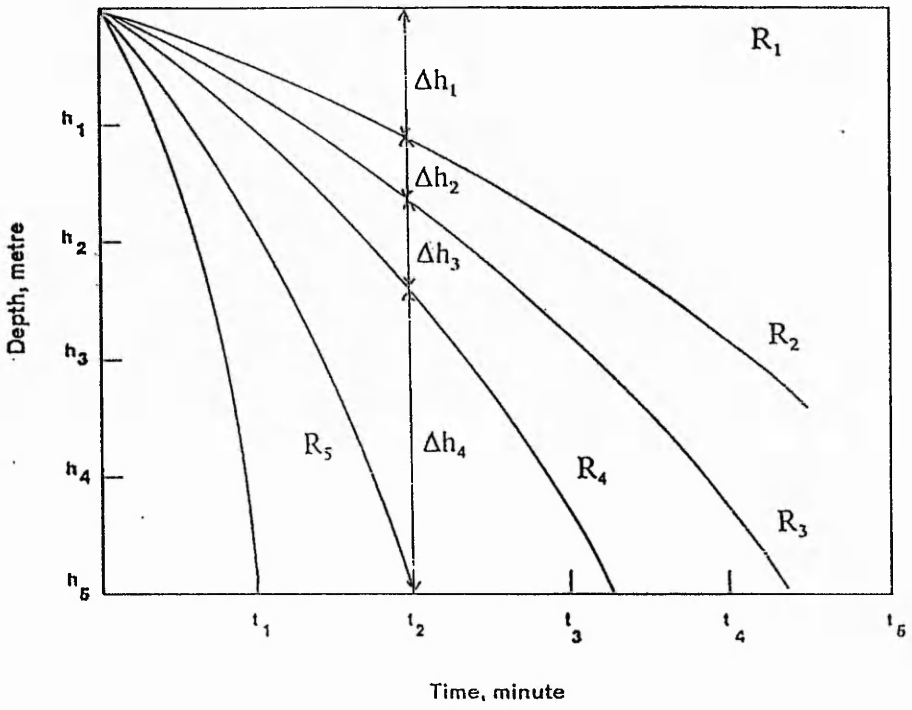

Figure 3.27 Isoconcentration lines for settled flocculent particles

There is insufficient space to present all the experimental data sheets and the settling curves, however, a few experimental data sheets covering the cases of all the three types of synthetic turbidity materials, using an air flow rate of 100 cc/min. with 1.0 mm orifice diameter air diffusion pad are attached herewith as shown in Table (C-1) to Table (C-3) in Appendix 5. The corresponding isoconcentration curves are also presented as shown in Figure (C-1) to Figure (C-3) in Appendix 6.

CHAPTER 4

THEORETICAL WORK

4.1 GENERAL

The theoretical work of this investigation consists of two parts. Part 1 is concerned with the kinetics of flocculation process employed by using diffused air to induce the required size of air bubbles through a diffusion pad. A mathematical relationship has been established to describe the kinetics of pneumatic flocculation in terms of the process variables. Extensive experimental work has been accomplished in order to verify this mathematical relationship. In all cases good agreement was found with this mathematical relationship of describing the kinetics of the process of pneumatic flocculation. It is expected that the present theoretical approach will be useful for further analysis and understanding of the pneumatic flocculation process in the field of water treatment.

Part 2 of the theoretical work is involved with the hydrodynamic behaviour of the rising air bubbles through water which are applied to generate the velocity gradients required for coagulation and flocculation. Considerable research work has been devoted theoretically and experimentally to the motion of bubbles rising in liquids by a large number of investigators in the past. But almost all of this work is related to the field of either hydrodynamics or chemical engineering. By contrast, little is known about the behaviour of rising bubbles related to the field of water treatment, primarily, about the effect of bubble characteristics on turbidity removal by pneumatic flocculation and subsequent process of sedimentation. An attempt has been made to correlate the characteristics of rising bubbles with the process variables in pneumatic flocculation.

4.2 PART 1: KINETICS OF PNEUMATIC FLOCCULATION

The work of Camp and Stein (1943) established a design criterion based on the concept of the mean temporal velocity gradient in the coagulation-flocculation process. They derived the Equation (1.3) for the mean temporal velocity gradient in a reactor containing fluid undergoing mixing:

$$G = (P/V\mu)^{1/2} \tag{1.3}$$

They also demonstrated that the rate of flocculation is directly proportional to the velocity gradient at a point. The rate of flocculation is determined by the number of contacts between floc particles (or between suspended particles and floc particles) in unit time and can be expressed by Equation (2.10)

$$J_{12} = N = G/6\ N_1N_2\ (d_1 + d_2)^3 \tag{2.10}$$

This equation shows the relationship between the velocity gradient i. e. the energy input and the number of contacts per unit volume per unit time, N, between N_1 particles of size d_1 and N_2 particles of size d_2. This equation is useful to study the speed with which small floc particles join to form larger floc particles, or it can be used to analyse the speed at which suspended particles in the raw water are entrapped by the floc particles.

Hudson (1965) developed a mathematical model based on Equation (1.3) and (2.10) describing the kinetics of flocculation as follows:

$$ln\left(\frac{N_0}{N_t}\right) = \left(\frac{\phi}{\pi}\right)V_F G t \tag{4.1}$$

which was applied for the latter situation described above and the parameters are defined as follows:

N_0 represents the suspended matter originally present

N_t represents the remaining "free" or unflocculated matter

t is the flocculation time

Φ is the sticking ratio, the portion of suspended matter adhered upon collision and

V_F is the volume of the floc per unit volume of water.

Two assumptions were made in developing the above mathematical model :

(i) based on the studies of Robeck (1963) and Riddick (unpublished), the size of the fine particles were considered very small in contrast to that of the floc particles. Therefore, the effect of d_1 on Equation (2.10) was considered to be very small and the term was omitted with little error.

(ii) the floc particles were spherical in shape.

From equation (4.1) it can be noted that the rate of entrapment of suspended matter in the floc is dependent upon the volume of the floc, not the number or the size of the floc particles.

Combining equation (1.3) and (4.1) one obtains

$$ln\left(\frac{N_o}{N_t}\right) = \frac{\phi}{\pi} V_F t \left(\frac{P}{\mu V_w}\right)^{1/2} \tag{4.2}$$

The above conception of describing the speed of floc formation can be considered in the process of pneumatic flocculation. When air is diffused into water from a compressed state, normally it expands isothermally (Fair *et al.*, 1968). Based on isothermal condition during the process the dissipated power due to the work done by the expansion of the air bubbles from compressed state to a free state in water is given by Equation (1.6),

$$P = p_a Q_a ln\left(\frac{p_c}{p_a}\right) \tag{1.6}$$

Substituting the value of P from Equation (1.6) into Equation (4.2) one obtains

$$ln\left(\frac{N_0}{N_t}\right) = \left[\frac{\phi}{\pi}\frac{V_F}{(V_w)^{1/2}}\frac{t}{(\mu)^{1/2}}\left(p_a\ ln\frac{p_{ah}+h}{p_{ah}}\right)^{1/2}\right](Q_a)^{1/2} \quad (4.3)$$

Combining all the parameters in the first term of the right hand side of Equation (4.3) and designated as a single constant K, it becomes

$$ln\left(\frac{N_0}{N_t}\right) = K(Q_a)^{1/2} \quad (4.4)$$

N_0 and N_t can be replaced by C_0 and C_t to represent the initial concentration and the concentration of any settled suspension flocculated with a detention time of t. Thus, Equation (4.4) can be rewritten as

$$ln\left(\frac{C_0}{C_t}\right) = K(Q_a)^{1/2} \quad (4.5)$$

Experiments were conducted at various initial conditions in order to verify the mathematical relationship developed in Equation (4.5). Samples were collected from a depth of 200 mm of the coagulation-flocculation and settling chamber at an interval of 30 minutes over a settling period of 120 minutes.

In this analysis, the turbidity of settled water is considered as representing the particles that escaped flocculation. The settled water might include poorly-flocculated small flocs that had a settling velocity less than 200/30 = 0.67 (for 30 minutes settling) to 200/120 = 0.16 cm/minute (for 120 minutes settling). However, these settling velocities are extremely low in comparison to that of the settling basin employed in water treatment industries. And therefore, the poorly-flocculated portion of turbidity in settled water is considered to be negligible.

When Equation 4.5 is not linearised by plotting $ln(C_0/C_t)$ against $Q_a^{1/2}$, it represents a semi-logarithmic curve with relation to a half power function. In such a case, the curve should pass through the origin theoretically at zero air flow rate i.e. $ln(C_0/C_t) = 0$ or $C_0/C_t = 1$. However, experimental data indicates an interception on $ln(C_0/C_t)$

axis even at zero air flow rate. Experimental curves are found not to be pass through the origin due to the formation of some micro flocs during the process of rapid mixing and the practicability of collecting samples for a period less than 5 minutes.

The graphs for $ln(C_0/C_t)$ versus $Q_a^{1/2}$ show a semi-logarithmic relationship. The curves become linear after a value of $Q_a^{1/2}$ upto 10 (cc/min.)$^{1/2}$ producing the following mathematical model:

$$ln\frac{C_o}{C_t} = K_1 + K(Q_a)^{1/2} \qquad (4.6)$$

The plotted curves as shown in Fig. 4.1 to 4.5, are found to be almost parallel to each other. This indicates that the lines are of constant slope which is found to be 0.01 (cc/min.)$^{-1/2}$ on average. As the concentration of the suspension is decreased with increasing settling time, the value of the interception on $ln(C_0/C_t)$ axis of these curves is also increased. The average value for each of these interceptions is found to be 1.9, 2.5, 3.0 and 3.3 corresponding to the settling times of 30, 60, 90 and 120 minutes respectively. These values are shown in Table 4.1.

Table 4.1 Average values of K (slopes) and K_1 (interceptions)

Figure No	Time, (min.)	30	60	90	120
	K,(cc/min)$^{-1/2}$	$^*K_1$	K_1	K_1	K_1
4.1	0.008	1.78	2.60	3.00	3.30
4.2	0.007	1.84	2.50	2.93	3.26
4.3	0.009	2.04	2.63	2.95	3.26
4.4	0.010	1.78	2.78	3.15	3.54
4.5	0.010	1.91	2.63	3.06	3.36
Average Values	0.010	1.90	2.50	3.00	3.30

$^*K_1$ dimensionless

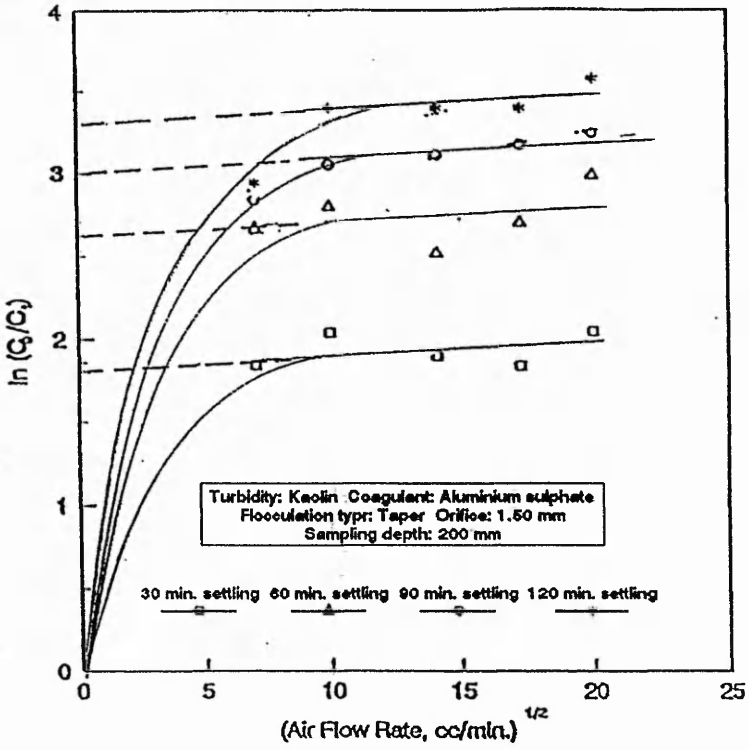

Figure 4.1 Relationship between concentration ratio and air flow rate

Calculations for the co-ordinates

Air Flow Rate, Q_a, cc/min.	Settling Time, min.	30		60		90		120	
	$(Q_a)^{1/2}$	C_{30}	$ln(C_0/C_{30})$	C_{60}	$ln(C_0/C_{60})$	C_{90}	$ln(C_0/C_{90})$	C_{120}	$ln(C_0/C_{120})$
50	7.07	31.63	1.844	13.87	2.668	11.65	2.843	10.54	2.943
100	10.00	26.08	2.037	12.21	2.796	9.43	3.054	6.66	3.402
200	14.14	29.97	1.898	16.09	2.520	8.88	3.114	6.66	3.402
300	17.32	31.63	1.840	13.32	2.700	8.32	3.179	6.66	3.402
400	20.00	25.53	2.050	9.99	2.990	7.77	3.248	5.55	3.580

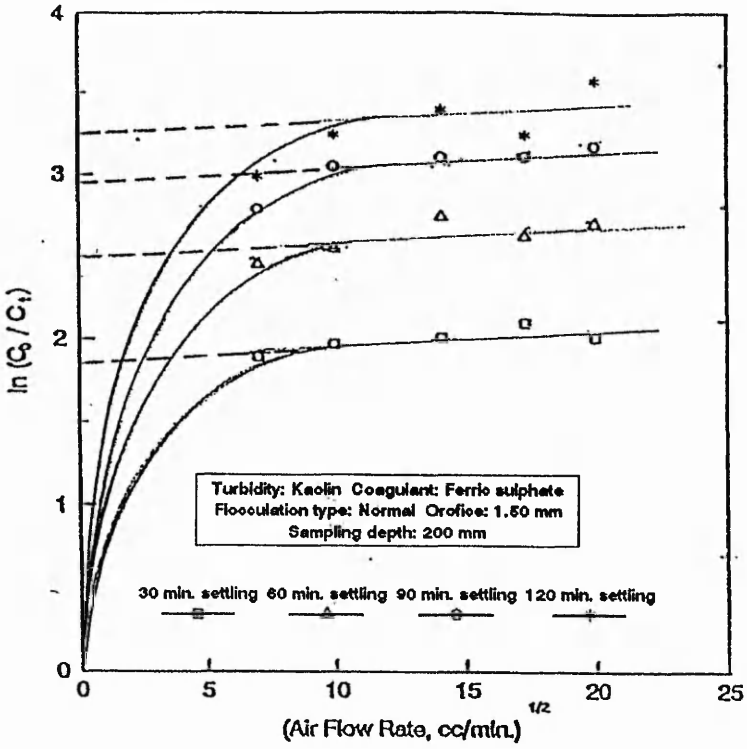

Figure 4.2 Relationship between concentration ratio and air flow rate

Calculations for the co-ordinates

Air Flow Rate, Q_a, cc/min.	Settling Time, min.	30		60		90		120	
	$(Q_a)^{1/2}$	C_{30}	$ln(C_0/C_{30})$	C_{60}	$ln(C_0/C_{60})$	C_{90}	$ln(C_0/C_{90})$	C_{120}	$ln(C_0/C_{120})$
50	7.07	29.97	1.898	17.20	2.453	12.21	2.796	9.99	2.996
100	10.00	27.75	1.975	15.54	2.554	9.43	3.054	7.77	3.248
200	14.14	26.64	2.015	12.76	2.752	8.88	3.114	6.66	3.402
300	17.32	24.42	2.102	14.43	2.629	8.88	3.114	7.77	3.248
400	20.00	26.64	2.015	13.32	2.709	8.32	3.179	5.55	3.584

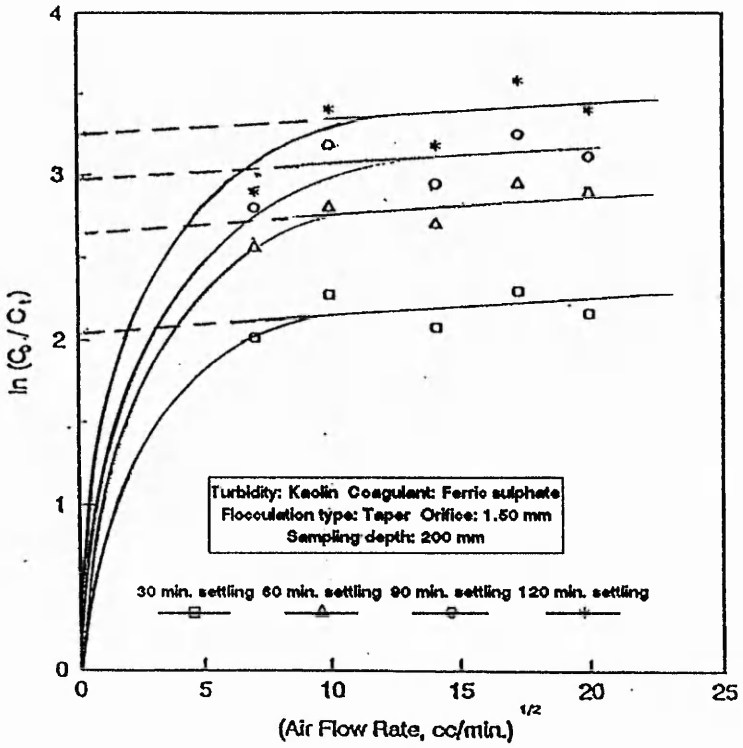

Figure 4.3 Relationship between concentration ratio and air flow rate

Calculations for the co-ordinates

Air Flow Rate, Q_a, cc/min.	Settling Time, min.	30		60		90		120	
	$(Q_a)^{1/2}$	C_{30}	$ln(C_0/C_{30})$	C_{60}	$ln(C_0/C_{60})$	C_{90}	$ln(C_0/C_{90})$	C_{120}	$ln(C_0/C_{120})$
50	7.07	26.64	2.015	15.54	2.554	12.21	2.796	11.1	2.891
100	10.00	20.53	2.276	12.21	2.796	8.32	3.179	6.66	3.402
200	14.14	24.97	2.080	13.32	2.700	10.54	2.943	8.32	3.179
300	17.32	19.98	2.303	10.54	2.943	7.77	3.248	5.55	3.584
400	20.00	22.75	2.170	11.10	2.890	8.88	3.114	6.66	3.402

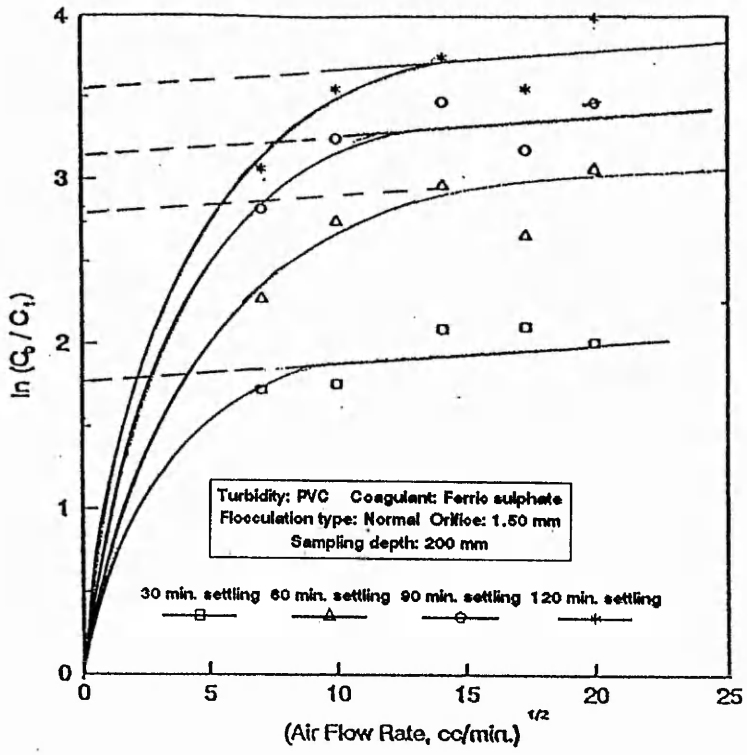

Figure 4.4 Relationship between concentration ratio and air flow rate

Calculations for the co-ordinates

Air Flow Rate, Q_a, cc/min.	Settling Time, min.	30		60		90		120	
	$(Q_a)^{1/2}$	C_{30}	$ln(C_0/C_{30})$	C_{60}	$ln(C_0/C_{60})$	C_{90}	$ln(C_0/C_{90})$	C_{120}	$ln(C_0/C_{120})$
50	7.07	35.50	1.728	20.62	2.272	11.90	2.821	9.33	3.065
100	10.00	34.47	1.758	12.92	2.739	7.79	3.245	5.74	3.550
200	14.14	24.72	2.090	10.36	2.960	6.25	3.465	4.72	3.746
300	17.32	24.21	2.111	13.95	2.662	8.31	3.180	5.74	3.550
400	20.00	26.77	2.011	9.33	3.065	6.25	3.465	3.69	3.992

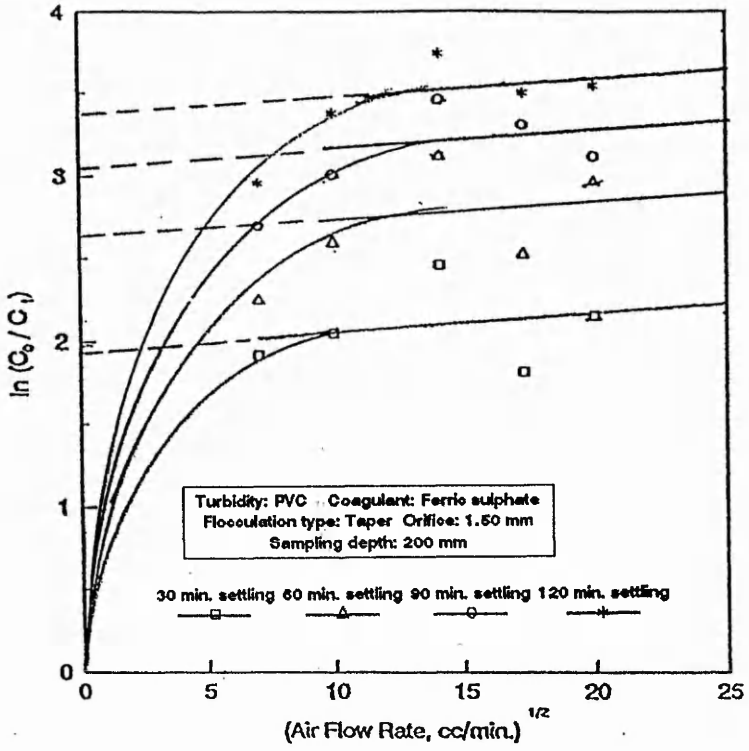

Figure 4.5 Relationship between concentration ratio and air flow rate

Calculations for the co-ordinates

Air Flow Rate, Q_a, cc/min.	Settling Time, min.	30		60		90		120	
	$(Q_a)^{1/2}$	C_{30}	$ln(C_0/C_{30})$	C_{60}	$ln(C_0/C_{60})$	C_{90}	$ln(C_0/C_{90})$	C_{120}	$ln(C_0/C_{120})$
50	7.07	29.34	1.919	21.13	2.247	13.44	2.700	10.36	2.960
100	10.00	25.75	2.049	14.98	2.591	9.85	3.010	6.77	3.385
200	14.14	17.03	2.463	8.82	3.121	6.25	3.465	4.72	3.746
300	17.32	32.42	1.819	16.00	2.525	7.28	3.313	6.00	3.506
400	20.00	23.18	2.155	10.36	2.960	8.82	3.121	5.74	3.355

4.3 PART 2: HYDRODYNAMIC ASPECTS OF PNEUMATIC FLOCCULATION

The behaviour of air bubbles rising through water is a difficult hydrodynamic problem as it is related to many variables. Although this problem has been studied from every aspect in many theoretical and experimental investigations, very little information is available on bubble behaviour concerned with the field of water treatment, particularly related to diffused air flocculation. Therefore, a systematic framework of bubble characteristics which can be used in analysing the experimental data of pneumatic flocculation has so far been lacking.

Very limited research has been devoted in the past, to pneumatic flocculation, primarily to the effect of bubble regimes on turbidity removal by subsequent sedimentation. However, any specific relationship of bubble characteristics such as size, shape or rising velocity with the process efficiency of diffused air flocculation has not yet been established.

Camp (1955) mentioned that individual bubbles rising in still water would conform to the Stokes' law for bubble diameter less than 1.4 mm and the rising velocity is given by Equation (2.5)

$$v_r = \frac{1}{18}\frac{g}{\mu}(\rho_a - \rho_w)\ d_b^2 \qquad (2.5)$$

Other investigators (Ives, 1978; Bratby, 1980) referred the same law in predicting the rising velocity of the bubble. However, neither the size of the bubble nor the flow field around the bubble in the present investigation are seen to be conformable with the condition of Stokes' law.

A series of experimental observations of the motion of an air bubble in tap water has been made using different sizes of orifice in a pneumatic coagulating- flocculating and settling chamber with the aim of investigating the flow field around the rising

bubbles. As the mean rise velocity of bubble varies with the height of liquids (Tapucu, 1974), the motion of a series of air bubbles in the middle third portion of the water column of height of 2400 mm was monitored visually. The time required to travel a height of 800 mm in the middle third portion of the water column was determined from observation using a digital electronic stop watch. The rising velocities of a series of air bubbles released from different sizes of orifices and different air flow rates were determined and analysed. The rising velocity of 100 bubbles was monitored for each different air flow rate using different sizes of orifice pads as shown in Table 4.2. An attempt has been made to evaluate the flow regimes of rising bubbles for the purpose of better understanding in further analysis.

Experimental results are summarised in Table 4.2 and shown in Figure 4.6. It can be seen from Figure 4.6 that the rising velocity of air bubbles depends on the air flow rate and the size of the orifice from which bubbles are released. The observed data are also used in further analysis of the flow field around the bubbles.

Table 4.2 Rising velocity of air bubbles through water

Air Flow Rate cc/min.	Rising velocity of Air Bubble, cm/s			
	OD*= 1.0 mm	OD = 1.5 mm	OD = 2.0 mm	OD = 3.0 mm
50	26.13	26.71	27.18	27.87
100	28.47	29.33	32.70	36.76
200	30.80	30.64	33.47	38.34
300	32.65	31.64	34.11	38.58
400	33.35	31.15	33.56	31.55
500	36.62	32.55	35.89	37.00
600	38.18	32.03	35.57	45.29

* Orifice Diameter

The size range of the rising bubble is noted from observation and used in calculating the equivalent diameter of the bubble by the iteration method considering the solid liquid and gas-liquid interface. The initial conditions and the calculations are shown in page to 136 to 139.

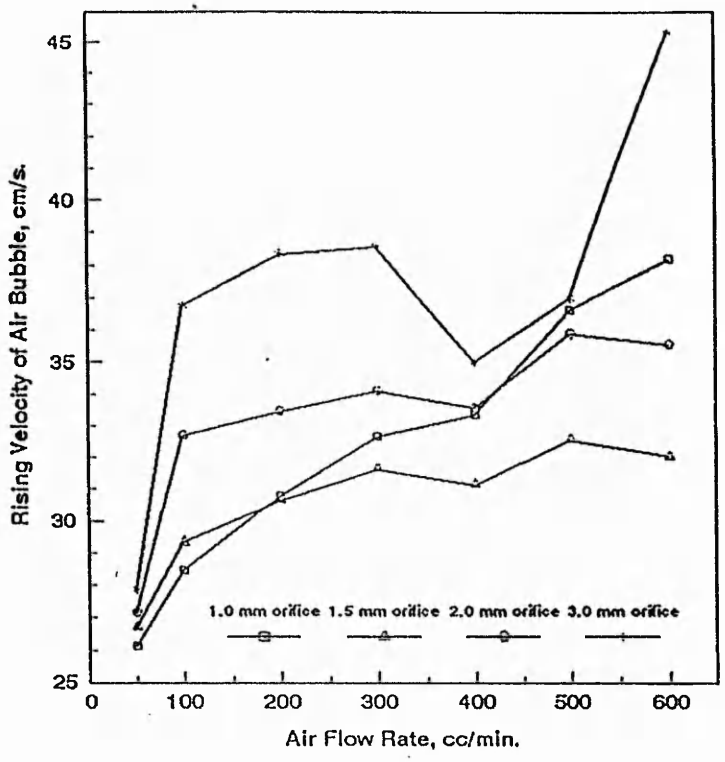

Figure 4.6 Rising velocity of air bubble versus air flow rate

The flow field around the rising bubble is shown to be turbulent both in solid liquid and gas-liquid interface. When gas-liquid interface is considered, a C_D value of 2.7 for **R**>100 is used (Bhaga and Weber, 1981). A check for C_D value is also made by using the expression for C_D value given by Bhaga and Weber (1981)

$$C_D = [(2.67)^{0.9} + (16/\mathbf{R})^{0.9}]^{1/0.9} \qquad (4.7)$$

When the gas-liquid interface is considered the calculated equivalent diameters of rising bubbles are found to be closer to that of the observed bubble in all cases. The results of these calculations led to the conclusion that the flow field around the rising bubble is not laminar in any situation of the experiment of this investigation.

Even if the case of solid-liquid interface is considered, which is the worst condition for the turbulent flow, a non-realistic bubble diameter is obtained, and this indicates that the flow is not laminar in the experimental condition.

Thus for the experimental conditions described herein, the flow is not laminar and the usual Stokes' law cannot be applied to determine the rising velocity of the air bubble in such a condition.

The calculated average equivalent diameter of the rising air bubble is plotted against orifice diameter and shown in Figure 4.7. It is evident from this figure that the calculated diameter of air bubble is increasing with the increase of orifice diameter.

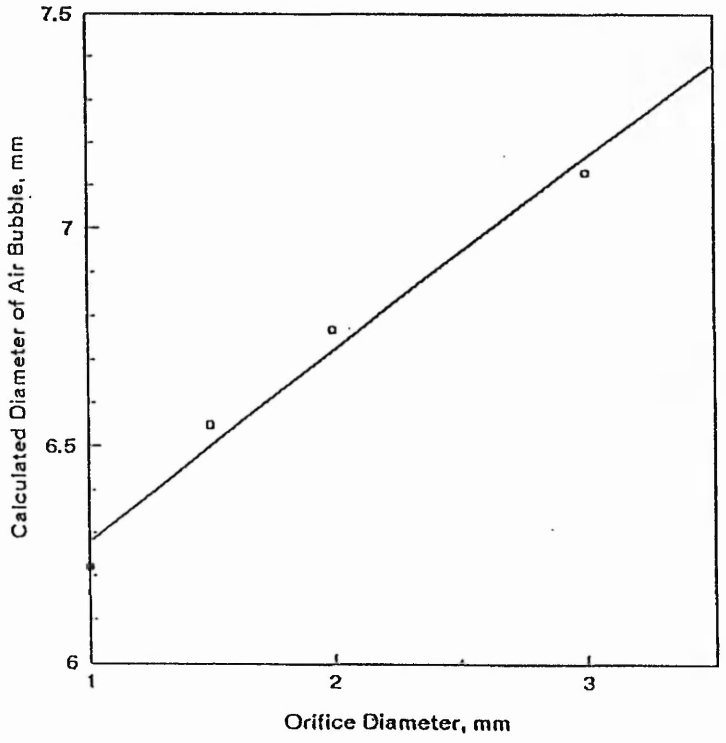

Figure 4.7 Calculated air bubble diameter versus orifice diameter

Calculation of Bubble diameter for 1.0 mm orifice

Initial conditions:

Orifice diameter = 1.0 mm Air flow rate = 50 cc/min.

Absolute viscosity of water, $\mu_w = 1.139 \times 10^{-3}$ N.s/m^2 Temperature = 15.0^{0}C

Mass density of water, ρ_w = 999.1 kg/m^3 Mass density of air, ρ_a = 1.225 kg/m^3

Observed velocity of bubble, v_a = 0.2613 m/s

Observed diameter of the bubble, d_{ob} = 5 - 10 mm

Solid-liquid interface

Assumed Diameter,mm	Reynolds Number, **R***	Drag Coefficient, $C_D$$^+$	Bubble Velocity,v_a	Calculated Diameter**
5.000	1146	0.449	0.2613	2.34
3.670	841	0.471	"	2.46
3.065	702	0.487	"	2.54
2.800	643	0.495	"	2.59
2.690	618	0.499	"	2.61
2.650	608	0.501	"	2.62
2.635	604	0.501	"	2.625
2.630	-	-		2.63

$^*\mathbf{R} = (\rho_w\, v_a\, d_{ob})/\mu_w$ $^+C_D = 24/\mathbf{R} + 3/(\mathbf{R})^{1/2} + 0.34$ **Calculated from

$$v_s^2 = (4/3.\ g/C_D.(\rho_w - \rho_a)/\rho_w)d_{ob}$$

Gas-liquid interface

For **R** > 100, C_D = 2.7. Checking the C_D value:

From Bhaga and Weber (1981), $C_D = [(2.67)^{0.9} + (16/\mathbf{R})^{0.9}]^{1/0.9}$

(a) Considering the maximum value of **R** = 1146

$C_D = [(2.67)^{0.9} + (16/1146)^{0.9}]^{1/0.9} = 2.69 \approx 2.7$

(b) Considering the minimum value of **R** = 604

$C_D = [(2.67)^{0.9} + (16/604)^{0.9}]^{1/0.9} = 2.71 \approx 2.7$

Calculation of spherical equivalent bubble diameter:

$v_s^2 = (4/3.\ g/C_D.(\rho_w - \rho_a)/\rho_w)d_{e(cal)}$

$d_{e(cal)} = 0.00522 \times C_D = 0.00522 \times 2.7 = 14$ mm

Since, $v_s = 1.5\ v_a$, therefore, $d_e = 4/9 \times 14 = 6.22$ mm.

Calculation of Bubble diameter for 1.5 mm orifice

Initial conditions:

Orifice diameter = 1.5 mm Air flow rate = 50 cc/min.

Absolute viscosity of water, $\mu_w = 1.094 \times 10^{-3}$ N.s/m^2 Temperature = 16.5^{0}C

Mass density of water, $\rho_w = 998.8$ kg/m^3 Mass density of air, $\rho_a = 1.225$ kg/m^3

Observed velocity of bubble, $v_a = 0.2671$ m/s

Observed diameter of the bubble, $d_{ob} = 7.5$ - 15 mm

Solid-liquid interface

Assumed Diameter,mm	Reynolds Number, **R***	Drag Coefficient, $C_D$$^+$	Bubble Velocity, v_a	Calculated Diameter**
7.50	1828	0.423	0.2671	2.31
4.90	1196	0.446	"	2.44
3.67	895	0.467	"	2.55
3.11	758	0.480	"	2.62
2.86	697	0.488	"	2.66
2.75	673	0.491	"	2.68
2.71	662	0.492	"	2.69
2.70	-	-		2.70

$^*\mathbf{R} = (\rho_w v_a d_{ob})/\mu_w$ $^+C_D = 24/\mathbf{R} + 3/(\mathbf{R})^{1/2} + 0.34$ **Calculated from

$$v_s^2 = (4/3.\ g/C_D.(\rho_w - \rho_a)/\rho_w)d_{ob}$$

Gas-liquid interface

For $\mathbf{R} > 100$, $C_D = 2.7$

From Bhaga and Weber (1981), $C_D = [(2.67)^{0.9} + (16/\mathbf{R})^{0.9}]^{1/0.9}$

(a) Considering the maximum value of $\mathbf{R} = 1828$

$C_D = [(2.67)^{0.9} + (16/1828)^{0.9}]^{1/0.9} = 2.69 \approx 2.7$

(b) Considering the minimum value of $\mathbf{R} = 662$

$C_D = [(2.67)^{0.9} + (16/662)^{0.9}]^{1/0.9} = 2.71 \approx 2.7$

Calculation of spherical equivalent bubble diameter:

$v_s^2 = (4/3.\ g/C_D.(\rho_w - \rho_a)/\rho_w)d_{e(cal)}$

$d_{e(cal)} = 0.005461 \times C_D = 0.005461 \times 2.7 = 14.74$ mm

Since, $v_s = 1.5\ v_a$, therefore, $d_e = 4/9 \times 14.74 = 6.55$ mm.

Calculation of Bubble diameter for 2.0 mm orifice

Initial conditions:

Orifice diameter = 2.0 mm Air flow rate = 50 cc/min.

Absolute viscosity of water, $\mu_w = 1.139 \times 10^{-3}$ N.s/m^2 Temperature = 15.0^{0}C

Mass density of water, $\rho_w = 999.1$ kg/m^3 Mass density of air, $\rho_a = 1.225$ kg/m^3

Observed velocity of bubble, $v_a = 0.2718$ m/s

Observed diameter of the bubble, d_{ob} = 10 - 15 mm

Solid-liquid interface

Assumed Diameter,mm	Reynolds Number, **R***	Drag Coefficient, $C_D$$^+$	Bubble Velocity, v_a	Calculated Diameter**
10.00	2384	0.411	0.2718	2.32
6.16	1469	0.434	"	2.45
4.30	1027	0.456	"	2.58
3.44	820	0.474	"	2.67
3.05	729	0.484	"	2.73
2.80	668	0.492	"	2.77
2.76	658	0.493	"	2.78
2.77	-	-	-	2.77

$^*\mathbf{R} = (\rho_w V_a d_{ob})/\mu_w$ $^+C_D = 24/\mathbf{R} + 3/(\mathbf{R})^{1/2} + 0.34$ ** Calculated from

$V_s^2 = (4/3.\ g/C_D.(\rho_w - \rho_a)/\rho_w)d_{ob}$

Gas-liquid interface

For $\mathbf{R} > 100$, $C_D = 2.7$

From Bhaga and Weber (1981), $C_D = [(2.67)^{0.9} + (16/\mathbf{R})^{0.9}]^{1/0.9}$

(a) Considering the maximum value of $\mathbf{R} = 2384$

$C_D = [(2.67)^{0.9} + (16/2384)^{0.9}]^{1/0.9} = 2.69 \approx 2.7$

(b) Considering the minimum value of $\mathbf{R} = 658$

$C_D = [(2.67)^{0.9} + (16/658)^{0.9}]^{1/0.9} = 2.71 \approx 2.7$

Calculation of spherical equivalent bubble diameter:

$V_s^2 = (4/3.\ g/C_D.(\rho_w - \rho_a)/\rho_w)d_{e(cal)}$

$d_{e(cal)} = 0.0056491 \times C_D = 0.0056491 \times 2.7 = 15.25$ mm

Since, $v_s = 1.5\ v_a$, therefore, $d_e = 4/9 \times 15.25 = 6.77$ mm.

Calculation of Bubble diameter for 3.0 mm orifice

Initial conditions

Orifice diameter = 3.0 mm Air flow rate = 50 cc/min.

Absolute viscosity of water, $\mu_w = 1.139 \times 10^{-3}$ N.s/m^2 Temperature = 15.0^{0}C

Mass density of water, $\rho_w = 999.1$ kg/m^3 Mass density of air, $\rho_a = 1.225$ kg/m^3

Observed velocity of bubble, $v_a = 0.2787$ m/s

Observed diameter of the bubble, d_{ob} = 15 - 20 mm

Solid-liquid interface

Assumed Diameter,mm	Reynolds Number, **R***	Drag Coefficient, $C_D$$^+$	Bubble Velocity, v_a	Calculated Diameter**
15.00	3667	0.396	0.2787	2.35
10.00	2444	0.410	"	2.44
5.00	1222	0.445	"	2.64
3.82	935	0.463	"	2.75
3.00	733	0.483	"	2.87
2.93	717	0.485	"	2.88
2.90	-	-	-	2.90

$^*\mathbf{R} = (\rho_w\, v_a\, d_{ob})/\mu_w$ $^+C_D = 24/\mathbf{R} + 3/(\mathbf{R})^{1/2} + 0.34$ ** Calculated from

$$v_s^2 = (4/3.\ g/C_D.(\rho_w - \rho_a)/\rho_w)d_{ob}$$

Gas-liquid interface

For $\mathbf{R} > 100$, $C_D = 2.7$

From Bhaga and Weber (1981), $C_D = [(2.67)^{0.9} + (16/\mathbf{R})^{0.9}]^{1/0.9}$

(a) Considering the maximum value of $\mathbf{R} = 3667$

$C_D = [(2.67)^{0.9} + (16/3667)^{0.9}]^{1/0.9} = 2.685 \approx 2.7$

(b) Considering the minimum value of $\mathbf{R} = 717$

$C_D = [(2.67)^{0.9} + (16/717)^{0.9}]^{1/0.9} = 2.71 \approx 2.7$

Calculation of spherical equivalent bubble diameter:

$v_s^2 = (4/3.\ g/C_D.(\rho_w - \rho_a)/\rho_w)d_{e(cal)}$

$d_{e(cal)} = 0.005947 \times C_D = 0.005947 \times 2.7 = 16.05$ mm

Since, $v_s = 1.5\ v_a$, therefore, $d_e = 4/9 \times 16.05 = 7.13$ mm.

It will be shown in section 5.4 that for each combination of initial experimental conditions, there exists one optimum size of orifice and hence the size of the bubble in removing the suspended solids by pneumatic flocculation. This phenomenon is also related to the hydrodynamics of the rising bubble. The impact of bubble characteristics on turbidity removal cannot be interpreted unless the hydrodynamic behaviour of the rising bubbles is well studied and their relative tendencies to coagulate and flocculate the turbidity are known.

CHAPTER 5

ANALYSIS OF THE EXPERIMENTAL WORK

5.1 GENERAL

Extensive experimental work was scheduled and carried out during the course of this investigation in order to provide sufficient information to evaluate and examine the validity of the process of pneumatic flocculation. Fundamental experiments were conducted using the pneumatic model treatment unit as described in section 3.2.2 under various initial conditions following the procedure described in section 3.13. Three types of synthetic turbidity materials were used, they were kaolin, lycopodium powder and polyvinyl chloride (PVC) powder. Two chemical coagulants were used, they were aluminium sulphate and ferric sulphate. Different air flow rates were applied through uniform sized and uniformly distributed orifices on each diffusion pad. Each pad has a different orifice diameter. The flow rate of applied air was either at a constant rate (for normal flocculation) or at a successively decreasing rate of flow (for taper flocculation). The prepared suspensions from different synthetic turbidity materials were coagulated and flocculated as described in section 3.13 and were allowed to settle under gravity. Samples of settled water were collected from different sampling ports spaced at equal distances of 200 mm throughout the operating water height of 2400 mm of the experimental column at different intervals of time and the residual turbidity was recorded. Isoconcentration lines were produced and drawn from the data. All the FTU turbidity readings were converted to turbidity in mg/l by using calibration curves as mentioned in section 3.14 and shown in Appendix 3. The efficiency of turbidity removal was determined by the procedure detailed in section 3.14.

Two hundred and eighty-four experimental runs were conducted in conjunction with three different types of synthetic turbidity materials, two types of chemical

coagulants, two types of sequence of agitation (normal and taper), four sizes of orifice diameter either 1.0, 1.5, 2.0 or 3.0 mm and different air flow rates ranging from 50 to 1000 cc/min. The details of the experimental runs are shown in Appendix 1. The total number of the experimental runs are grouped into 48 Experimental Sets as presented in Table 3.10, and most of the experimental sets have at least 5 experimental runs so that the optimum air flow rate can be evaluated for each experimental set.

The main factors affecting pneumatic flocculation are:

Air Flow rates
Orifice Sizes
Synthetic Turbidities
Chemical Coagulants
Sequences of Agitation

The effects of the above parameters on efficiency of turbidity removal will be analysed and discussed in this chapter. The impact of the pneumatic coagulation-flocculation on the level of dissolved oxygen (DO), iron, nitrogen and aluminium and other physicochemical properties of water will also be analysed and discussed in the following sections.

5.2 REMOVAL EFFICIENCY VERSUS SETTLING TIME

The overall removal efficiency was determined for each experimental run from the plotted isoconcentration lines (the settling curves) after a settling period of either 120 minutes (for kaolin and PVC turbidity) or 240 minutes (for lycopodium with aluminium sulphate under normal flocculation), depending upon the nature of the synthetic turbidity and the coagulant and the type of flocculation. Samples were collected from different depths of the settling column at equal intervals of 30 minutes over a total settling period of 120 minutes in all the cases except

lycopodium suspension coagulated with aluminium sulphate under normal flocculation. In this special situation, a longer settling period of 240 minutes was allowed in order to achieve a significant removal of turbidity and samples were collected at equal intervals of 60 minutes over this settling period. The physicochemical properties of lycopodium turbidity imposed the requirement of a longer settling time.

There is a unique settling phenomenon which occurs from the combination of: the low density of the lycopodium; the aluminium sulphate coagulant; the associated micro air bubbles produced during the application of pneumatic flocculation; and the carbon dioxide gas bubbles generated by the chemical reaction of the natural alkalinity and the coagulant used. These four factors all contribute to possible forms of grouping of lycopodium-aluminium sulphate floc particles. When the flocculated water was left in quiescent condition to allow the floc particles to settle under gravity, three different groups of the agglomeration of the floc particles emerged as shown in Figure 5.1.

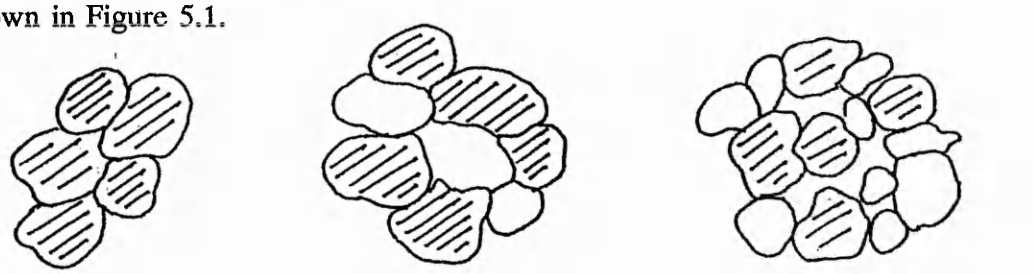

5 flocs No air or gas bubble **Group 1**	5 flocs with 3 air or gas bubbles **Group 2**	5 flocs with more than 3 air or gas bubbles **Group 3**

$$\rho_{G1} > \rho_{G2} > \rho_{G3}$$

Figure 5.1 Different groups of floc agglomeration.

Group 1 cluster of floc, floc particles are attached and bonded together to form a large mass of agglomeration of flocs free of air or gas bubbles.

Some micro bubbles of air and carbon dioxide gas produced due to the chemical

reaction of the coagulant may exist in the flocculated water, but do not have the chance to adhere to the floc formation shown for group 1 cluster. This is the most dense and heaviest group of agglomerated flocs and settle down easily and in the quickest time relative to the other type of formations.

Group 2 cluster of flocs, some micro bubbles of air and carbon dioxide gas may have combined with the floc agglomeration and hindered the settling. If the flocs originated from the synthetic turbidity of low density such as lycopodium powder, this hindered action would be more effective and consequently, the cluster of flocs would required a longer settling time.

Group 3 cluster of floc is formed with a very few floc particles which were entrapped by some more micro bubbles of air and carbon dioxide gas. The agglomeration of flocs which originated from low density synthetic turbidity like lycopodium and combined with such micro bubbles would rise upward rather than settling. Due to the upward movement of this group of floc cluster, the settling velocity of floc clusters group 1 and 2 would be hindered and these two groups of floc cluster will take a longer time to settle.

The settling behaviour of lycopodium turbidity coagulated with aluminium sulphate under normal flocculation has a unique phenomenon which can be explained as follows. Due to the physicochemical properties of lycopodium turbidity and the low density of the flocs formed in this situation, the combination of micro bubbles of air and other gases produced by the chemical reaction forms the cluster of group 3. Then the agglomeration of flocs rise up rather than settle down due to the overall lower density over the medium of water.

When dealing with this type of flocculated suspension of lycopodium turbidity, the settling behaviour is observed to be somehow different to other denser synthetic turbidities because of the micro bubbles entrapment in the agglomeration of floc particles. Immediately after flocculation, the initial concentration of the floc particles is uniform throughout the overall depth of settling column. As the settling time

progresses, the floc agglomeration of group 1 begins to settle in the quiescent body of flocculated suspension under gravity due to their reduced surface area to mass ratio in the upper part of water column. Concurrently, the floc clusters of group 3 rise upward in the lower part of water column and they are hindered by the adjacent settling clusters of group 1 and some are attached to these settling flocs. As a result, a slow moving layer of higher floc concentration is formed resulting from the combination of these two groups of floc clusters and settle as a whole mass rather than settling as an individual floc agglomeration as shown in Figure 5.2.

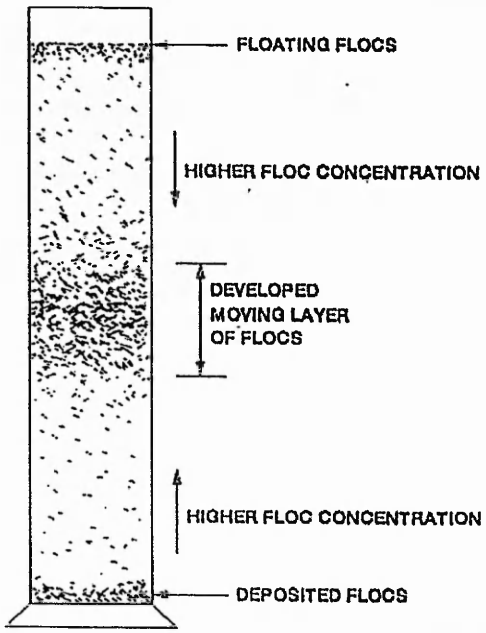

Figure 5.2 Settling of Lycopodium flocculent particles.

Some of the floc agglomeration of group 3, above the moving layer, are not hindered and rise upward freely, which then float on the surface of the water and form a scum. Similarly, some floc agglomerations of group 1, below this moving layer, settle and are deposited at the bottom of the settling column. As the settling time progresses, some floc agglomerations of group 1 above this moving layer settle and cause a gradual increase in floc concentration towards the higher concentrated moving layer. In a similar fashion, some floc agglomerations of group 3, below this moving layer, do rise and produce a gradual increase in concentration towards this

layer. This feature is illustrated in Figure 5.2. As a result of this type of settling behaviour, differently shaped isoconcentration curves are obtained as shown in Figure 5.3.

Figure 5.3 represents the isoconcentration lines for removal of suspended solids of lycopodium turbidity coagulated with aluminium sulphate under normal flocculation. This figure illustrates the feature described above.

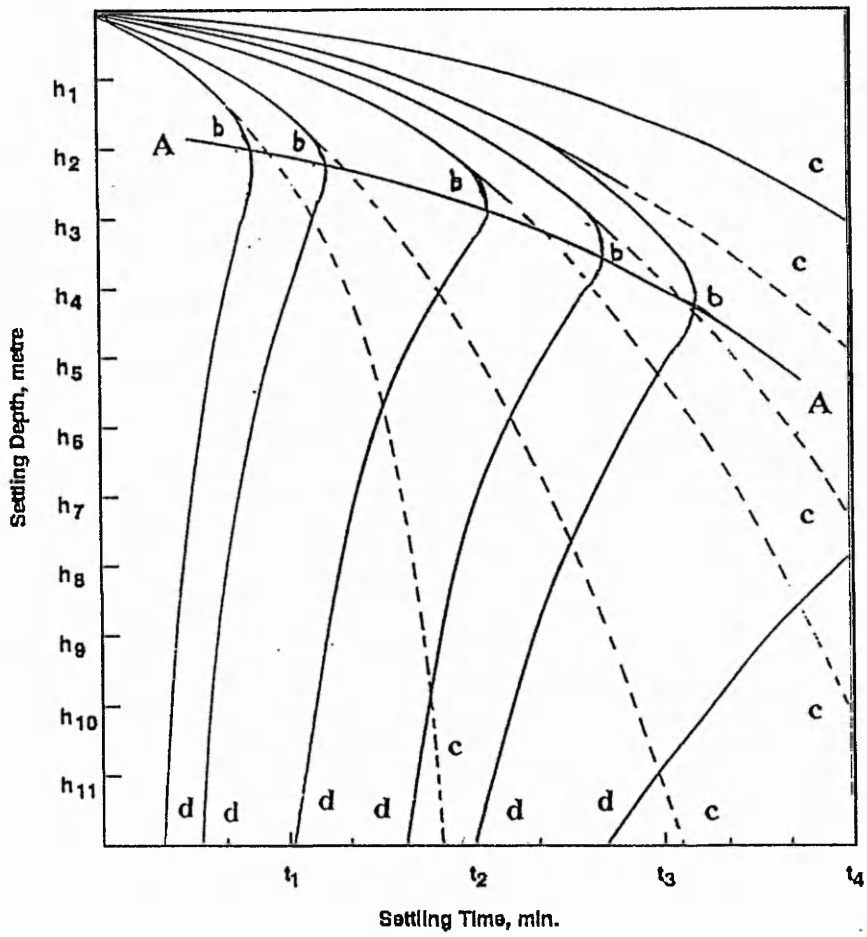

Figure 5.3 Isoconcentration lines for removal of suspended solids of lycopodium turbidity (developed from a pneumatic flocculation)

The nature of the settling curves for flocculent particles generally obtained by column settling test are shown by **abc** curves. The experimental settling curves for flocculent particles of lycopodium turbidity are shown by **abd** curves. The segments

ab and **bd** of the experimental curves represent the settling in the region of above and below the developed moving layer respectively. The settling curve of the moving layer, curve **A-A^1**, can be obtained by connecting all the points presented by **b**. The nature of the **A-A^1** curve indicates that as the settling time progresses, the layer is moving downward as a whole mass in the settling column. In such a case, removing efficiency was calculated considering the settling curves above the line **A-A^1.**

The influence of orifice sizes on the settling behaviour: Removal efficiency was determined from isoconcentration lines with the aim of investigating the settling behaviour of different types of synthetic turbidity coagulated with either aluminium sulphate or ferric sulphate and flocculated either under normal or taper agitation by diffusing the air through either 1.0, 1.5, 2.0 or 3.0 mm orifice diameter pad. The overall removal efficiency for the full depth of water column, taking into consideration the depth of water column of 2400 mm used for kaolin and lycopodium turbidity and 2000 mm for PVC turbidity as stated in section 3.2.1, at different settling times of 30, 60, 90 and 120 minutes was evaluated and the relationship was then plotted. These relationships are shown in Figure 5.4 to Figure 5.31.

After examining all the optimum values of air flow rate to produce the optimum removal of turbidity by pneumatic flocculation, as shown in Table 5.14 to Table 5.17, it is found that the frequency of the rate of air flow of 100 cc/min. prevail over the others in 20 cases out of 48. Therefore, for testing the impact of orifice diameter and for establishing a better comparison of settling behaviour, the experimental runs, those conducted with the air flow rate of 100 cc/min. under different initial conditions, were adopted from each experimental set, as shown in Table 3.10, for the purpose of analysis.

Figure 5.4 to Figure 5.15 show the performance of different sizes of orifices. To simplify the comparison, the performance of all sizes of orifices at the same air flow rate of 100 cc/min. are shown in the same figure.

The performance of different sizes of orifice show the same trend of settling behaviour of flocculated particles under all conditions mentioned above, but, in the behaviour of settling shown in Figure 5.4 to Figure 5.7 and also in Figure 5.12 to Figure 5.15 for kaolin and PVC turbidity respectively, the removal efficiency increased steeply in the first 30 minutes of settling and, between 60 and up to 90 minutes, a noticeable decrease in the increasing of removal efficiency is obvious, then curves tend to become asymptotic for all the orifice sizes.

It is worth mentioning that towards the end of 120 minutes of settling time the removal efficiency tends to come closer to one value of efficiency and after this there is insignificant change in the improvement of water quality. The best removal efficiency was obtained in almost all the cases with the orifice of sizes of either 1.5 or 2.0 mm.

It is evident from Figure 5.4 to Figure 5.7 and also Figure 5.10 to Figure 5.13 that the 1.0 mm orifice diameter pad gives the worst efficiency results of removing the kaolin and PVC turbidity.

In the case of lycopodium turbidity, it behaves differently with each of the coagulants used and under the type of agitation, i.e. normal and taper flocculation, as shown in Figure 5.8 to Figure 5.11.

After a general examination of the curves shown on the above mentioned figures it is apparent that the 1.0 mm orifice pad produced the worst removal efficiency after 120 minutes under most conditions.

The trend in the removal efficiencies was an almost steep increase in the first 30 minutes matching the kaolin and PVC turbidity and the steepness of the lycopodium curves produced progressed up to 90 minutes, and this is obvious as shown in Figure 5.9 to Figure 5.11.

The best removal efficiency has been dominated at 120 minutes when 1.5 and 2.0

mm orifice pads were used and even the 3.0 mm orifice pad for normal flocculation using ferric sulphate as coagulant produced an improved removal efficiency as shown in Figure 5.10.

The merging phenomenon was clear under some conditions for up to 120 minutes, although it was mentioned in section 5.2 that both settling time and efficiency were recorded up to 240 minutes and the ongoing trend of the curves would become closer when becoming asymptotic and the efficiency of removal levelled out and showed no further improvement as shown in Figure 5.8.

The influence of turbidity materials on the settling behaviour: Three synthetic turbidities were utilised with an air flow of 100 cc/min. but under different initial conditions as shown in Figure 5.16 to Figure 5.31. The plotted curves as shown in the figures mentioned above showed the steeply increasing tendency of the removal efficiency in the first 30 minutes and similar behaviour as discussed previously. After a settling period of 30 minutes, the difference in removal efficiencies becomes less, with appreciable decrease of the increase of the removal efficiency, and ultimately becoming asymptotic in a similar manner to that obtained with different orifice sizes as explained previously. However, under some circumstances, a great difference in the turbidity removal efficiency for lycopodium turbidity was noticed in comparison to kaolin and PVC turbidity and even after a settling period of 120 minutes.

In Figure 5.16 to Figure 5.19, it is clear that a better removal efficiency is obtained for PVC and kaolin turbidity when compared with lycopodium turbidity when using 1.0 mm orifice pad. The settling of lycopodium turbidity is found to be much slower than PVC and kaolin turbidity, even after a longer settling period. Particularly, when alum is used as a coagulant, as shown in Figure 5.16 and Figure 5.17, the settling behaviour of lycopodium is found to be somehow different in trend and even slower than that of kaolin and PVC turbidity. This is attributed to the low density of lycopodium turbidity in association with aluminium sulphate coagulant and grouping of lycopodium flocs with micro bubbles of gas and air.

When ferric sulphate with various orifice sizes was used to coagulate and flocculate the lycopodium suspension, an improvement in settling behaviour was obtained, as shown in Figure 5.18 and Figure5.19, due to the formation of heavier flocs because of the higher density of ferric sulphate compared with alum. However, the worst results in the removal efficiency of turbidity was found to be for lycopodium turbidity compared to others, even when using ferric sulphate, due to the physicochemical properties of the turbidity materials.

In Figure 5.16 to Figure 5.19, it is obvious that the best result obtained for PVC turbidity, compared to kaolin, occurs when using the 1.0 mm orifice size. This could be attributed to the finer size of PVC turbidity. As the particles are very fine, they have a larger specific area for chemical reaction and produce dense flocs, thus enhancing the settling efficiency.

In the case of 1.5 and 2.0 mm orifice size, as shown in Figure 5.20 to Figure 5.28, the best results are obtained when removing kaolin turbidity. In the case of using a larger size of orifice of 3.0 mm, the removal efficiences are almost the same, both for kaolin and PVC turbidity at any settling period, as shown in Figure 5.28 to Figure 5.31.

This indicates that there is an existing relationship between the physicochemical properties of the turbidity materials and the size of the air bubbles.

From the above discussions, it is evident that PVC powder is able to produce more compact and dense floc than kaolin and lycopodium powder. This could be attributed to the physicochemical properties of the colloidal particles. The effect of the hydrodynamic behaviour of the rising bubble in this aspect is also significant. The ultimate removal efficiency after 120 minutes was the same value.

Al-Hiary (1988) also observed the same settling behaviour of kaolin and silica turbidity coagulated with alum which were flocculated and settled in a 0.4 × 0.4 × 2.30 m deep pneumatic model treatment chamber.

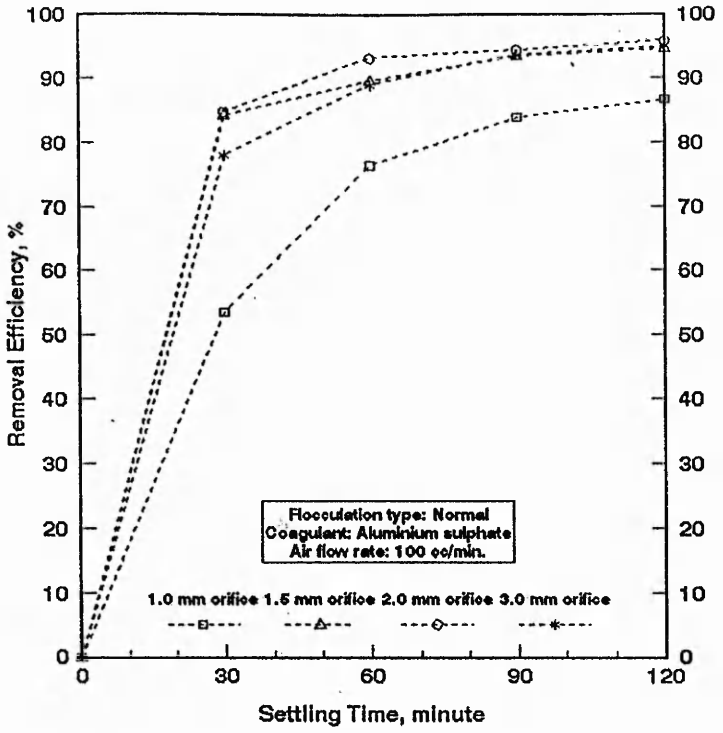

Figure 5.4 Settling behaviour of kaolin turbidity at various initial conditions in pneumatic flocculation

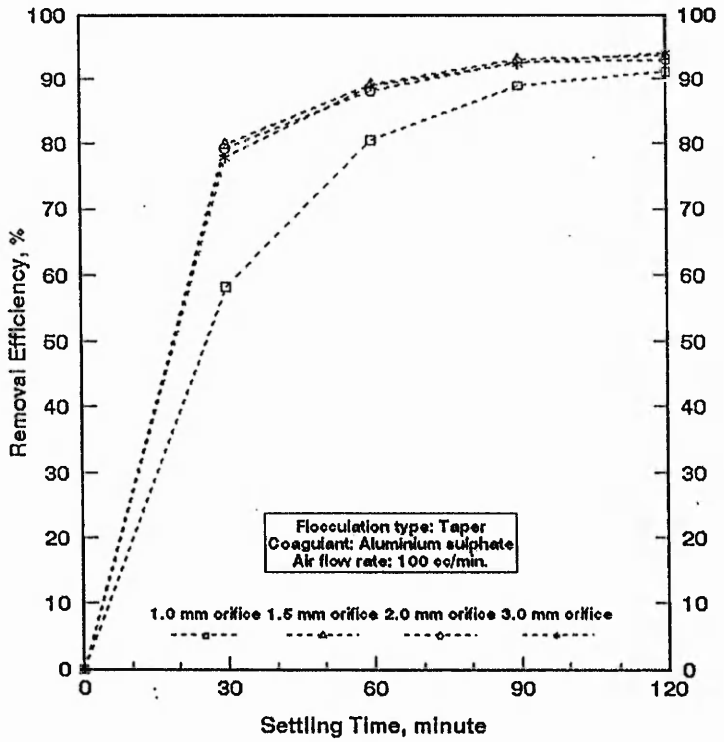

Figure 5.5 Settling behaviour of kaolin turbidity at various initial conditions in pneumatic flocculation

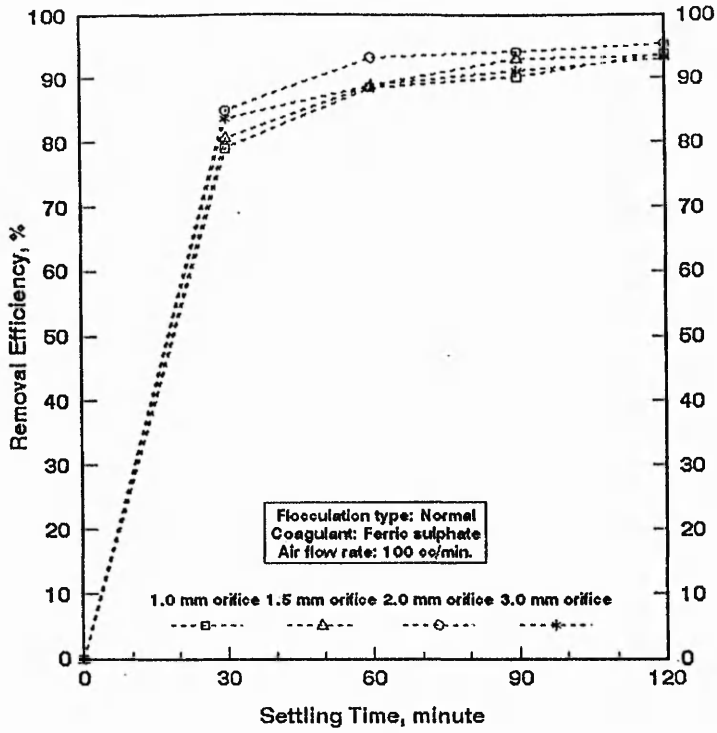

Figure 5.6 Settling behaviour of kaolin turbidity at various initial conditions in pneumatic flocculation

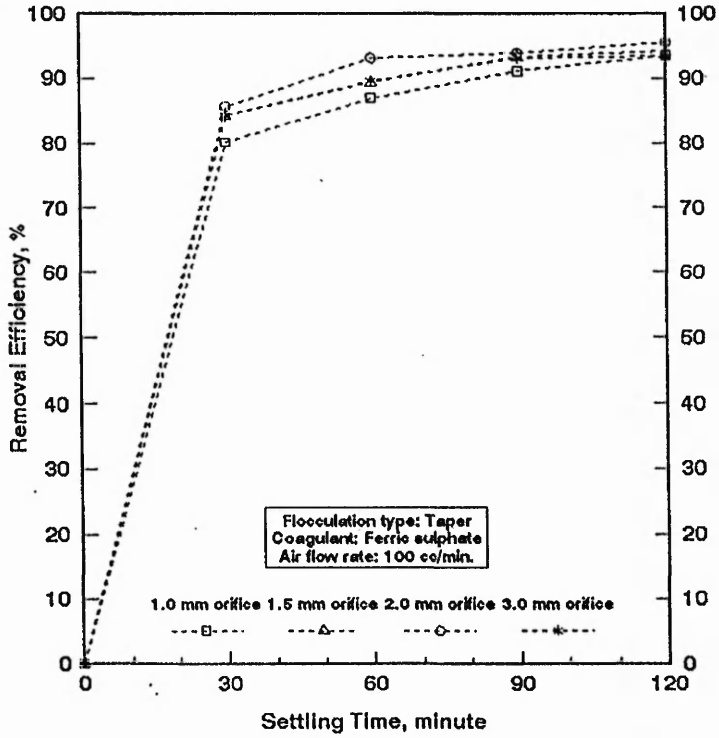

Figure 5.7 Settling behaviour of kaolin turbidity at various initial conditions in pneumatic flocculation

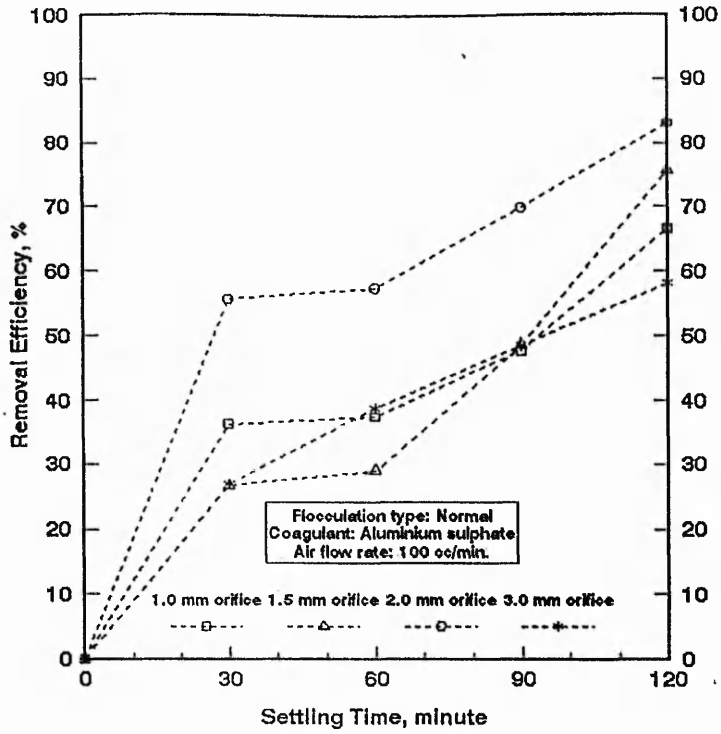

Figure 5.8 Settling behaviour of lycopodium turbidity at various initial conditions in pneumatic flocculation

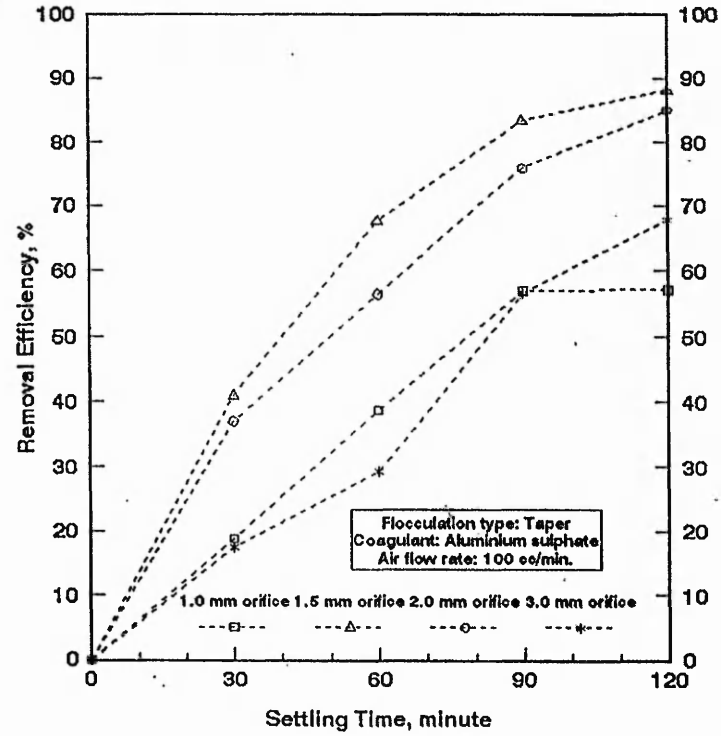

Figure 5.9 Settling behaviour of lycopodium turbidity at various initial conditions in pneumatic flocculation

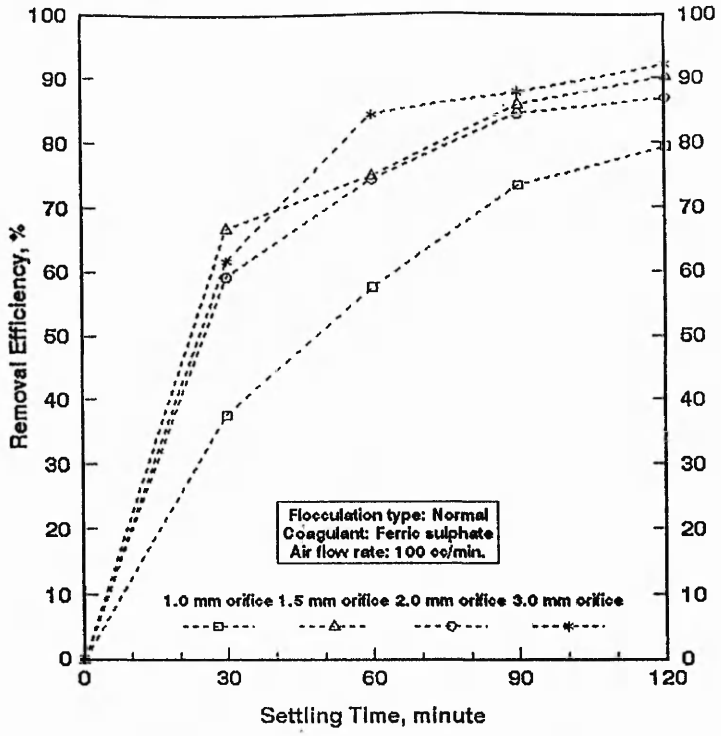

Figure 5.10 Settling behaviour of lycopodium turbidity at various initial conditions in pneumatic flocculation

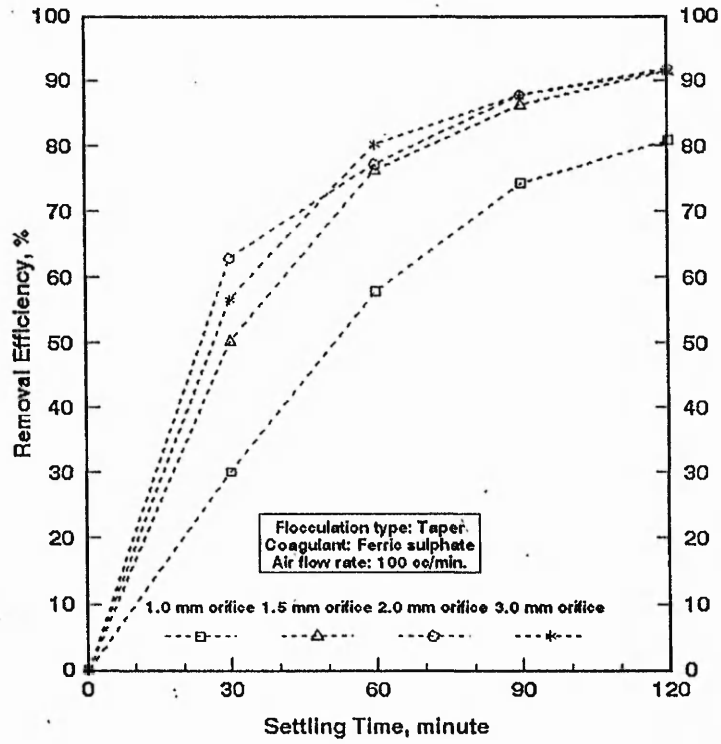

Figure 5.11 Settling behaviour of lycopodium turbidity at various initial conditions in pneumatic flocculation

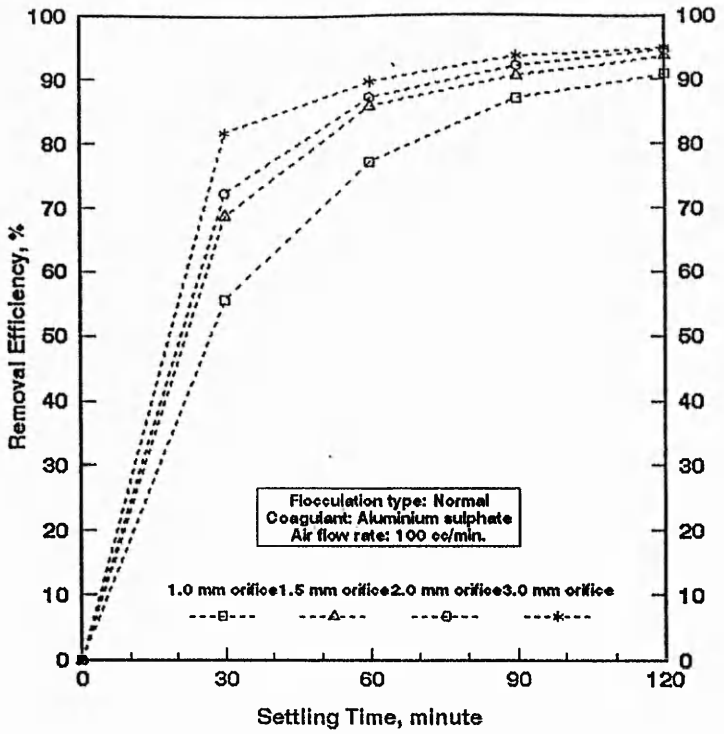

Figure 5.12 Settling behaviour of PVC turbidity at various initial conditions in pneumatic flocculation

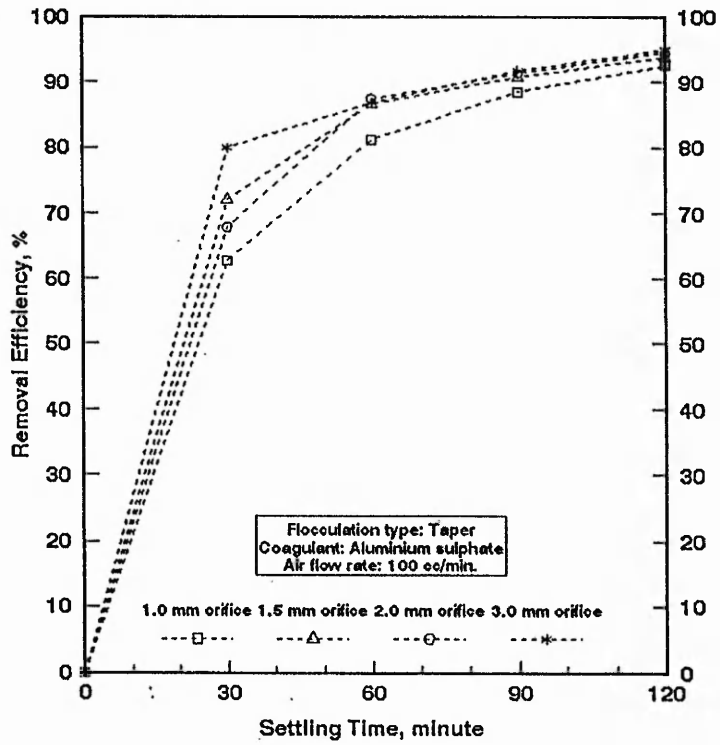

Figure 5.13 Settling behaviour of PVC turbidity at various initial conditions in pneumatic flocculation

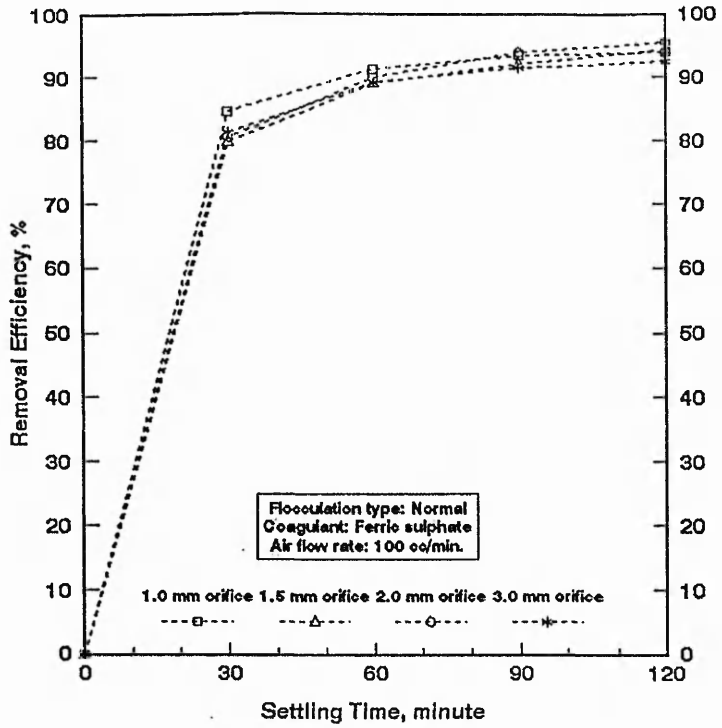

Figure 5.14 Settling behaviour of PVC turbidity at various initial conditions in pneumatic flocculation

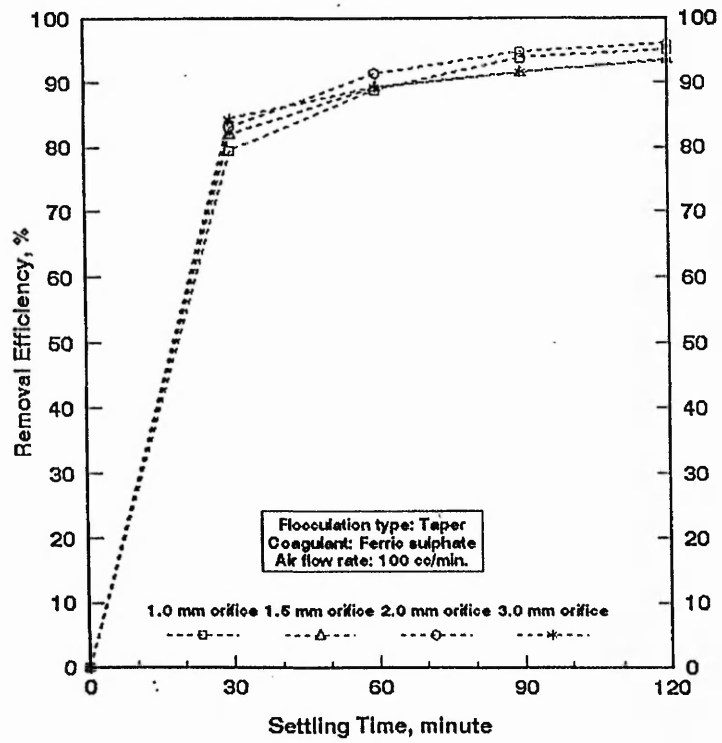

Figure 5.15 Settling behaviour of PVC turbidity at various initial conditions in pneumatic flocculation

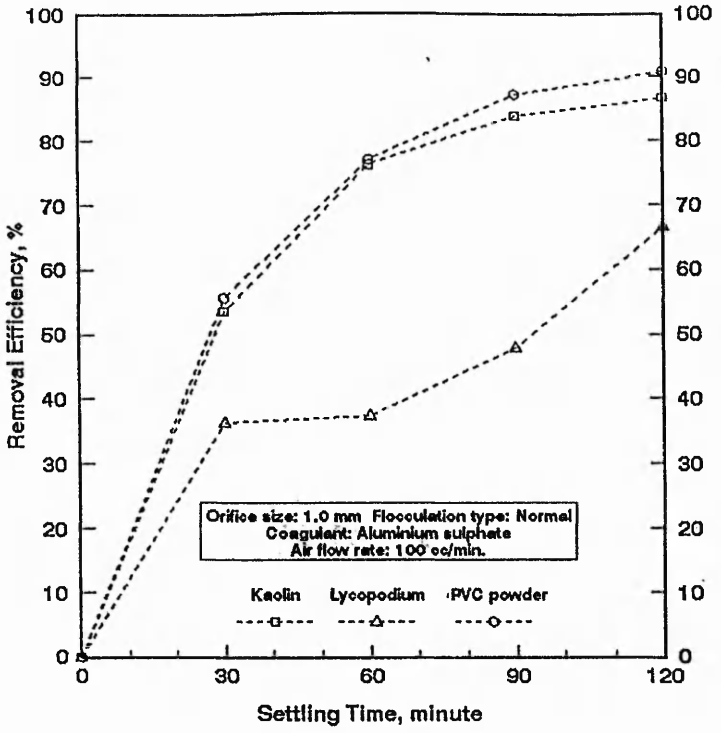

Figure 5.16 Settling behaviour of different types of synthetic turbidities in pneumatic flocculation

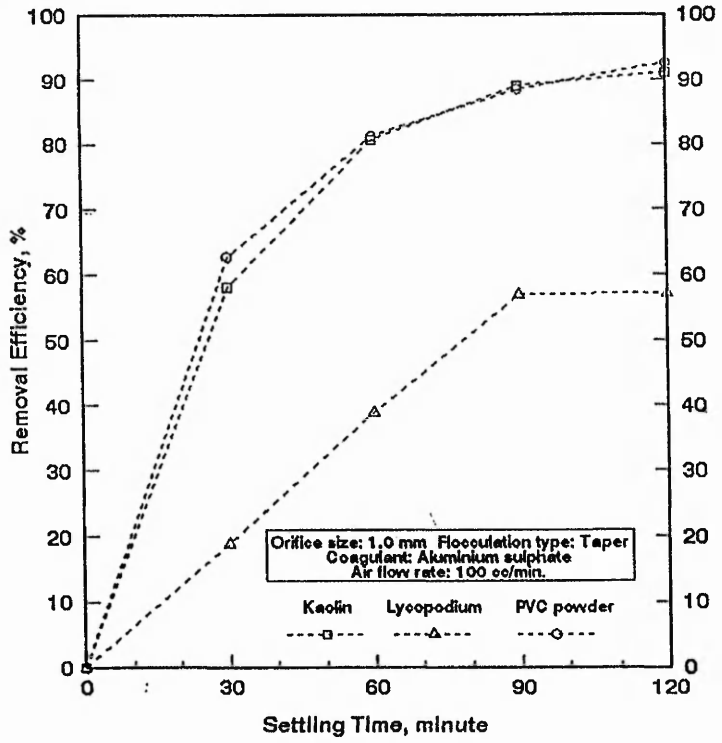

Figure 5.17 Settling behaviour of different types of synthetic turbidities in pneumatic flocculation

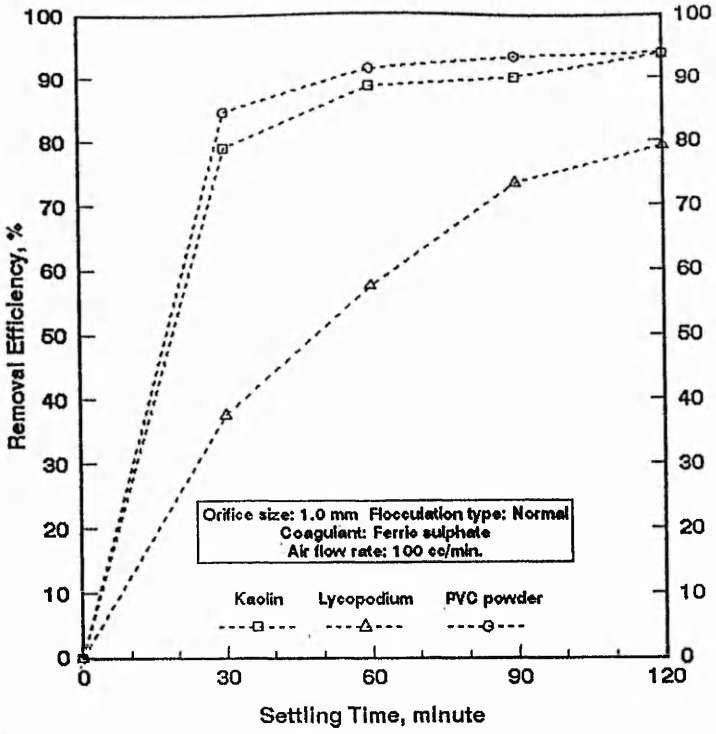

Figure 5.18 Settling behaviour of different types of synthetic turbidities in pneumatic flocculation

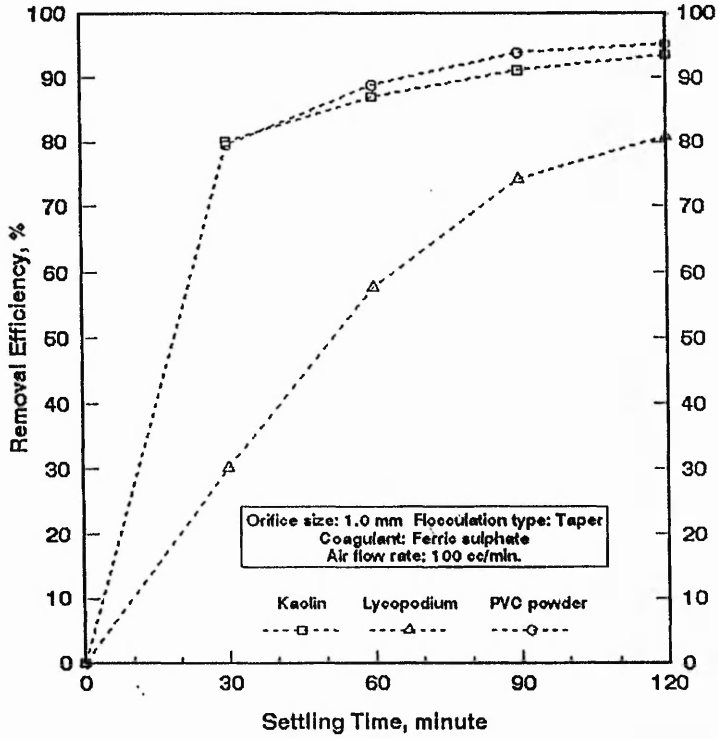

Figure 5.19 Settling behaviour of different types of synthetic turbidities in pneumatic flocculation

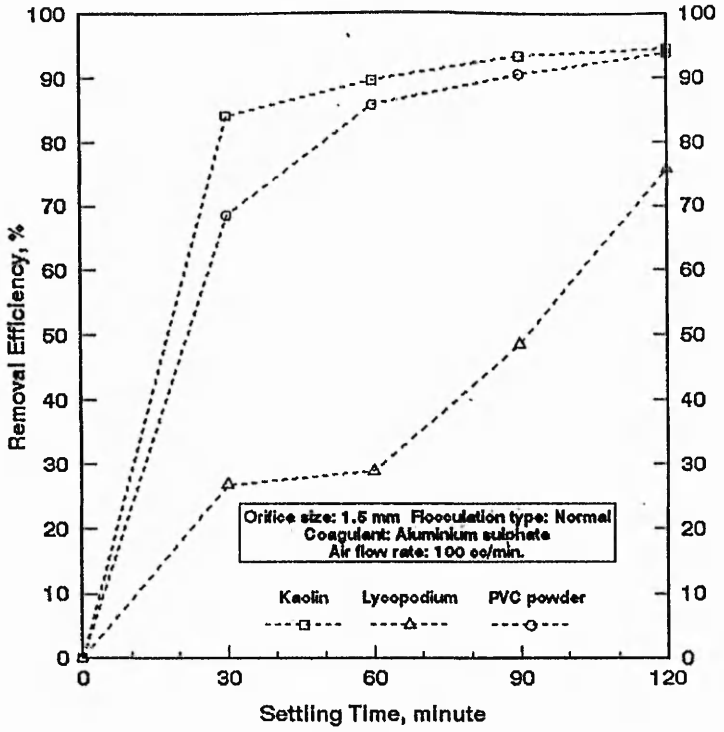

Figure 5.20 Settling behaviour of different types of synthetic turbidities in pneumatic flocculation

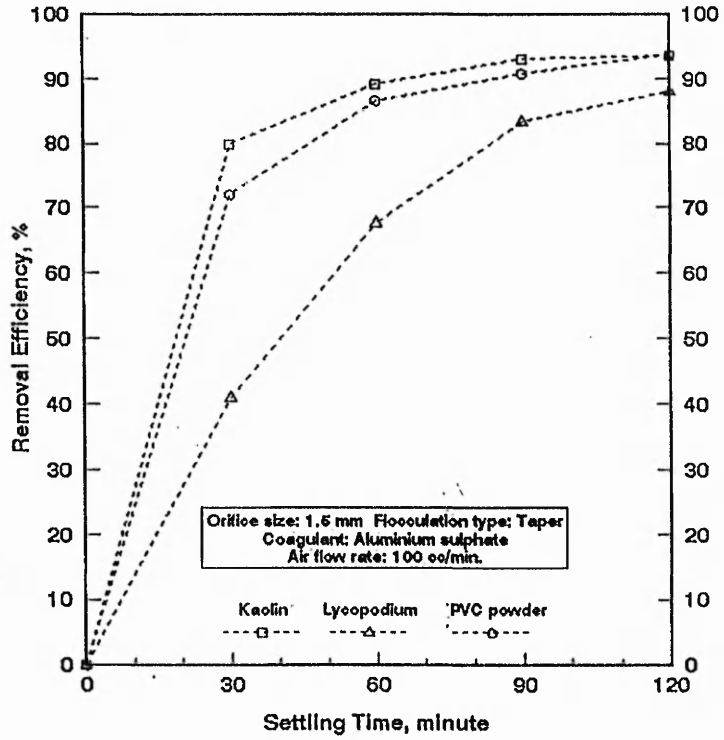

Figure 5.21 Settling behaviour of different types of synthetic turbidities in pneumatic flocculation

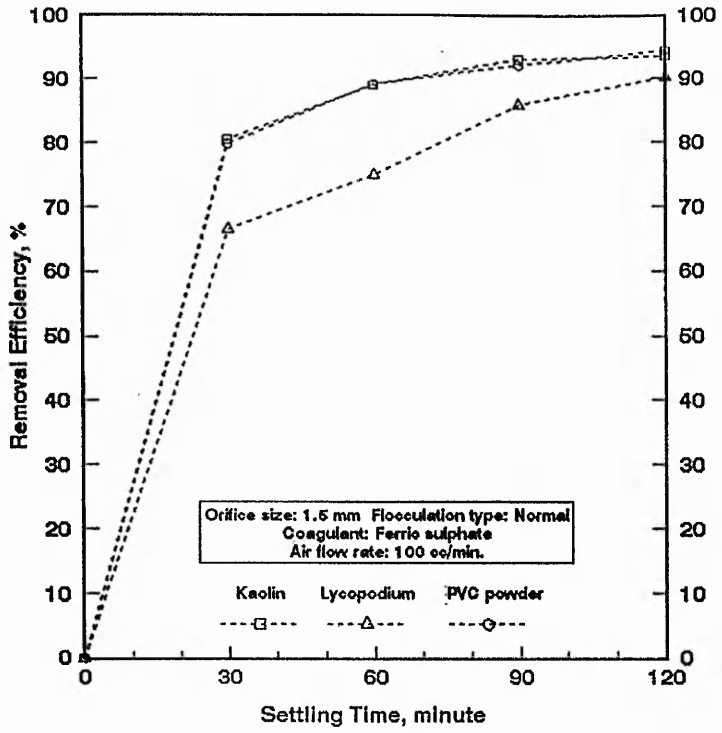

Figure 5.22 Settling behaviour of different types of synthetic turbidities in pneumatic flocculation

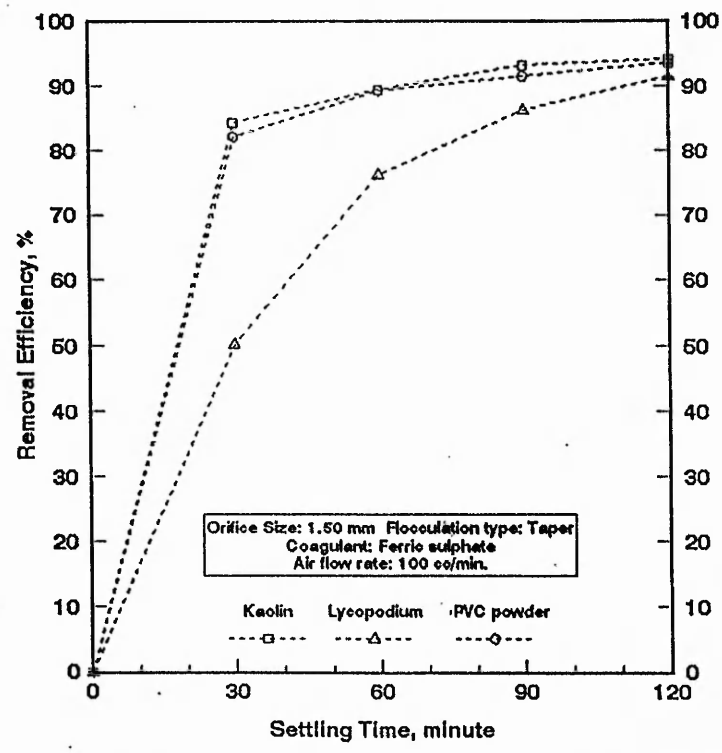

Figure 5.23 Settling behaviour of different types of synthetic turbidities in pneumatic flocculation

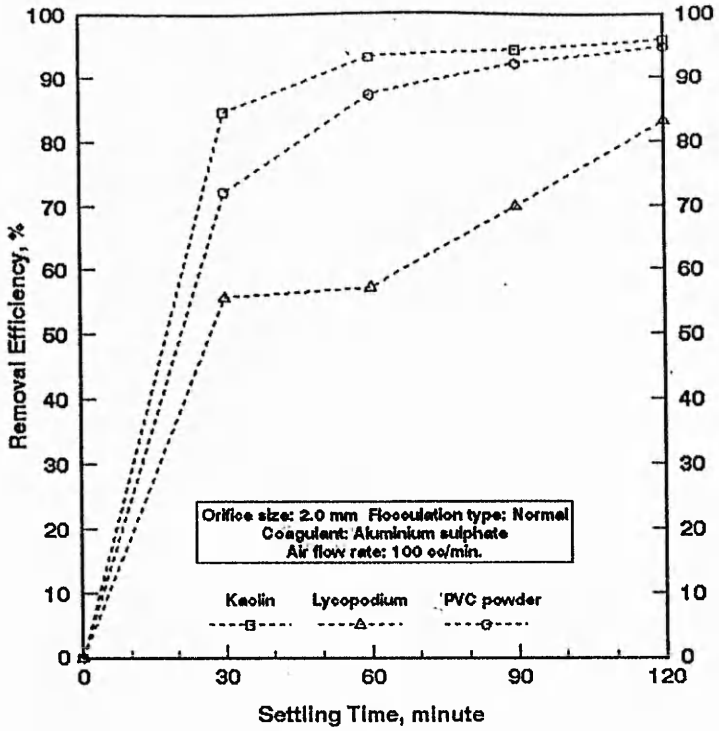

Figure 5.24 Settling behaviour of different types of synthetic turbidities in pneumatic flocculation

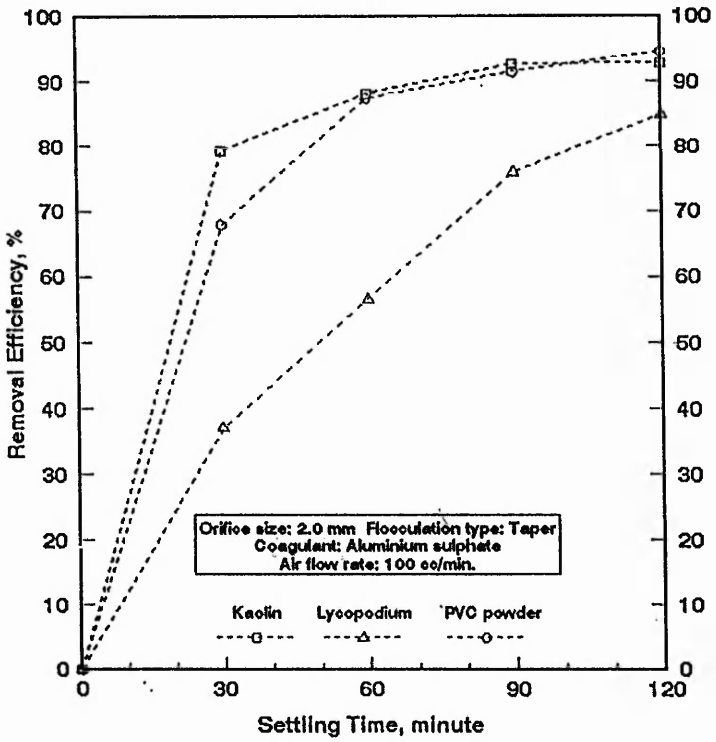

Figure 5.25 Settling behaviour of different types of synthetic turbidities in pneumatic flocculation

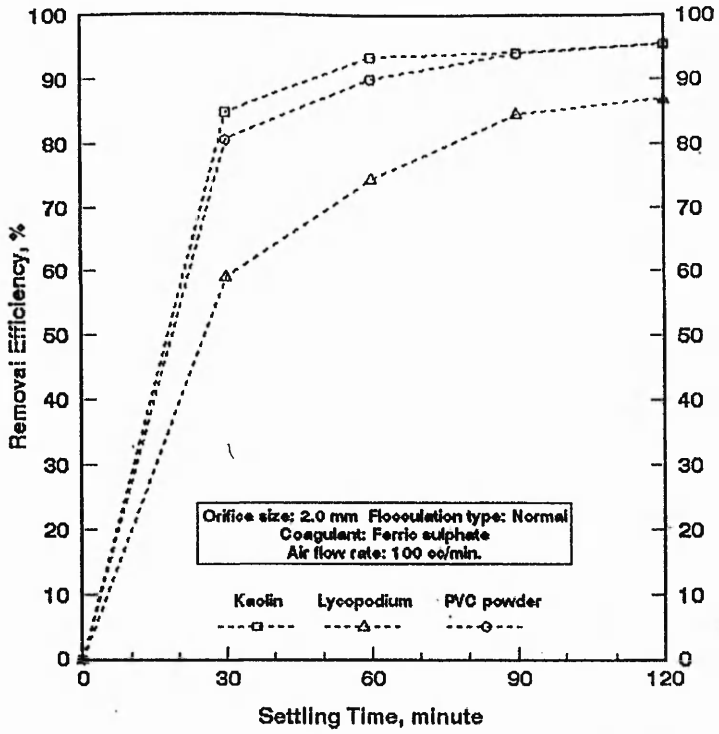

Figure 5.26 Settling behaviour of different types of synthetic turbidities in pneumatic flocculation

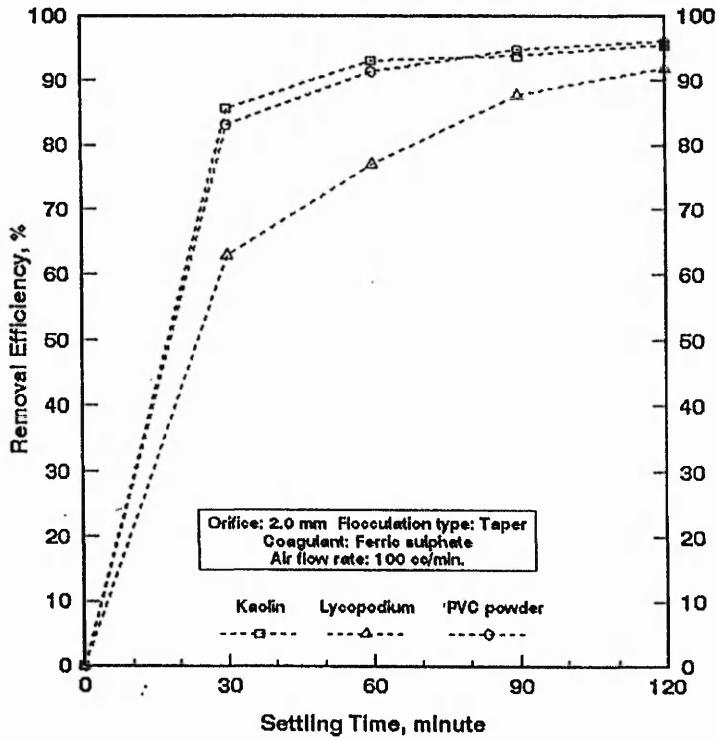

Figure 5.27 Settling behaviour of different types of synthetic turbidities in pneumatic flocculation

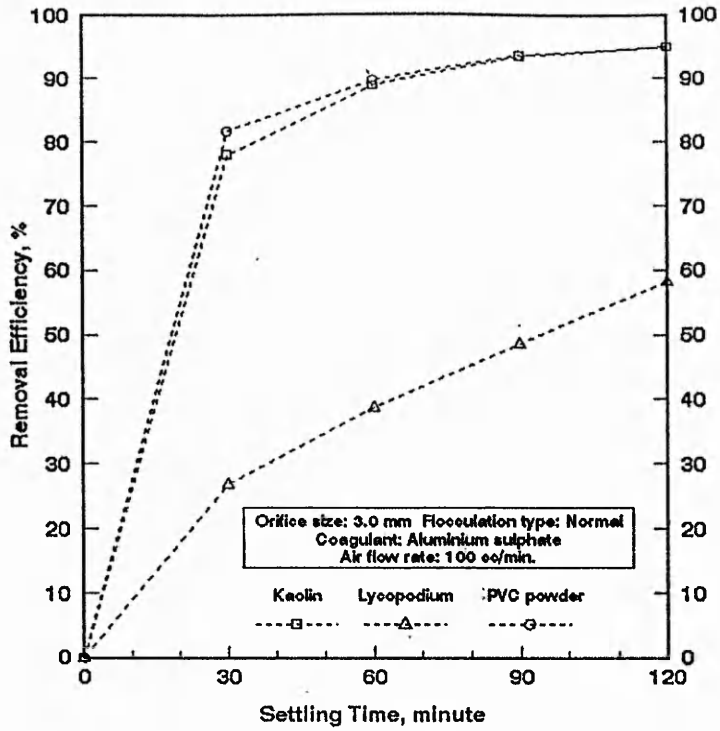

Figure 5.28 Settling behaviour of different types of synthetic turbidities in pneumatic flocculation

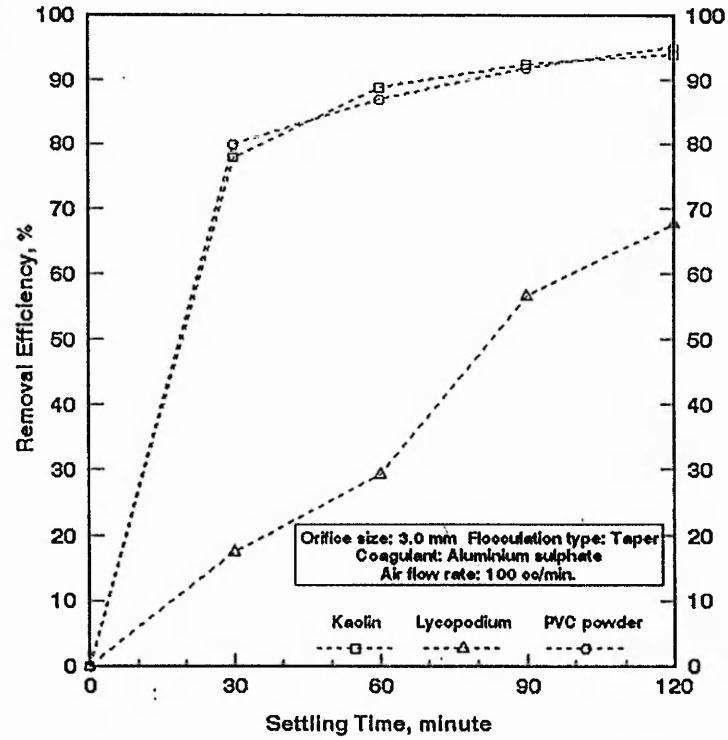

Figure 5.29 Settling behaviour of different types of synthetic turbidities in pneumatic flocculation

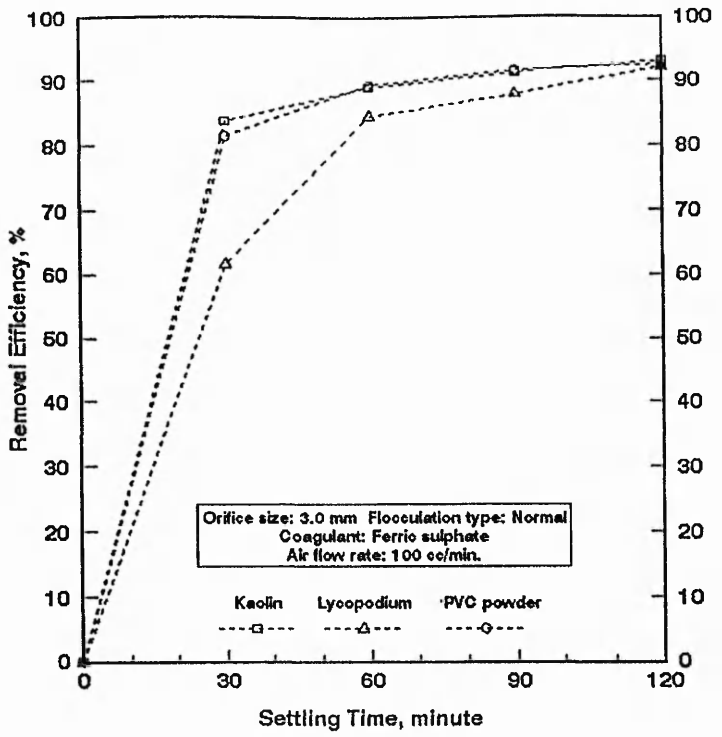

Figure 5.30 Settling behaviour of different types of synthetic turbidities in pneumatic flocculation

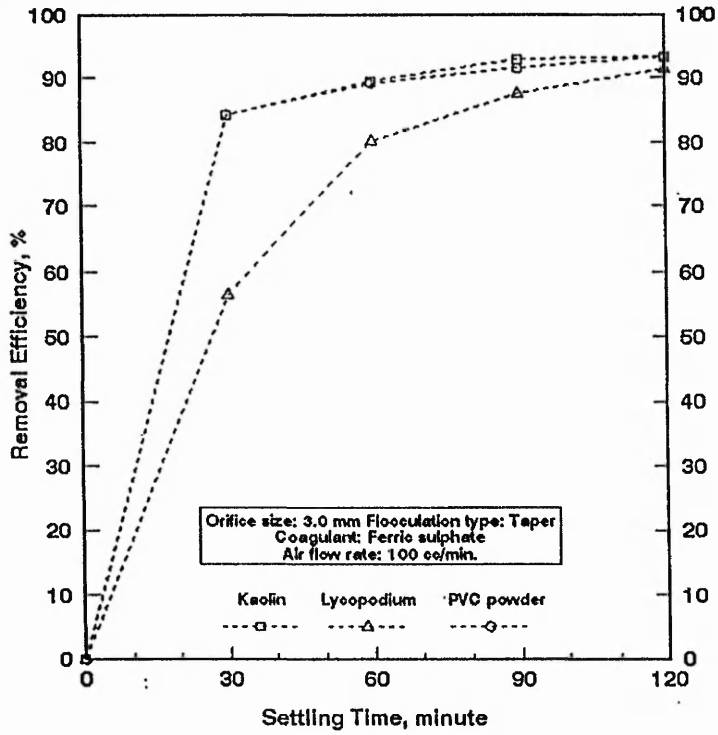

Figure 5.31 Settling behaviour of different types of synthetic turbidities in pneumatic flocculation

5.3 REMOVAL EFFICIENCY VERSUS AIR FLOW RATES

The overall removal efficiency was determined from isoconcentration lines for each experimental run scheduled in Appendix 1 with the sole aim of determining the optimum air flow rate using different orifice size, flocculation type, coagulants and turbidity materials. The relationship of removal efficiencies with different air flow rates are then plotted for each experimental set as described in Table 3.10 and shown in Figure (D-1) to Figure (D-48) in Appendix 7. It is imperative to state here that in the case of taper flocculation, the relationship of removal efficiencies with air flow is plotted with the amount of air flow rate, which is equivalent to the dimensionless product of the velocity gradient, and the flocculation time for four minutes interval and successively decreasing the air flow rate to produce the same amount of *Gt* value used under normal flocculation as shown in Table 3.8.

Experimental results and the analyses revealed that an optimum air flow rate would produce an associated maximum removal efficiency under the recorded initial conditions. The air flow rates and the corresponding removal efficiencies for different experimental conditions are shown in Table 5.1 to Table 5.12. These relationships are plotted and shown in Figure 5.32 to Figure 5.43. For each experimental set, covering all sizes of orifice diameter, the optimum air flow rate is determined from this relationship.

Figure 5.32 shows that the optimum air flow rate is a 100 cc/min. for the orifice sizes of 1.5, 2.0 and 3.0 mm when kaolin suspension is coagulated and flocculated with alum under normal agitation, while an optimum air flow rate of 500 cc/min. is associated with the orifice of 1.0 mm diameter. This optimum air flow rate of 500 cc/min. may be associated with the second peak of removal efficiency.

After a thorough examination of Figure 5.32 to Figure 5.43, it is obvious that each curve would produce a lower and upper optimum air flow depending on its oscillation and on reflection of what has been said above about the optimum air flow rate of 500 cc/min. under 1.0 mm orifice size. It is evident that this optimum is not

the first peak. During the experimental stage, special care was taken in applying a low air flow rate of 50 cc/min., as shown in Table 5.1, which produce a lower removal efficiency of kaolin as shown in Figure 5.32 and the plotted point did not show a peak. It was unfortunate that the practical range of the flowmeter sets used could not go below a 50 cc/min. and under such circumstances the first peak could not be produced and the air flow rate of 50 cc/min. is considered to be the first peak of removal efficiency.

Smaller sizes of bubbles generate a relatively low local *G* value which might affect the flocculation process in this case. However, a relatively low air flow rate of 100 cc/min. is found to be the optimum in other cases of kaolin suspension as shown in Figure 5.33 to Figure 5.35. Figure 5.33 to Figure 5.43 show two peaks of removal efficiency at two different air flow rates. This phenomenon could be explained in the light of destabilisation and restabilisation of the flocs at different air flow rates. The initial rate of floc formation is proportional to the air flow rates. However, higher air flow rates generate high-velocity shear gradients that cause large flocs to be broken as a result of either internal tension, or surface shear stress erosion, or both. Afterwards, when the air flow rate is increased broken floc particles are reformed again as shown in nearly all the figures mentioned above. Under the best economical situation the first peak removal efficiency yields the lowest air flow and produces a lower energy requirement, and the overall efficiency difference with other peaks is insignificant.

Lycopodium suspension, as shown in Figure 5.36 to Figure 5.39, is somehow found to show a different settling behaviour to that of kaolin and PVC suspension. When lycopodium suspension is coagulated and flocculated with aluminium sulphate under normal agitation, a high fluctuation in removal efficiency is observed as shown in Figure 5.36. This indicates that the lycopodium flocs when coagulated with alum, are very sensitive to the power variation due to their physicochemical properties. Lycopodium is less dense than kaolin and PVC turbidity and its density is comparatively low. When lycopodium combined with microbubbles of gas and air, some unstable groups were formed which could be sensitive to power variation. In

the case of using ferric sulphate as coagulant, lycopodium formed heavier flocs, which are not too sensitive to the power variations like the lycopodium flocs coagulated with alum, due to a higher density and strength of the flocs. In such cases, the fluctuation in the removal efficiency is not influenced to the same degree of sensitivity.

The mean velocity gradients corresponding to these first optimum air flow rates produced from the above mentioned experiments were calculated by using the following equation:

$$P = 101.3 \times 10^3 \, Q_a \ln\frac{10.3+h}{10.3} \qquad (1.7)$$

Substituting h = 2.40 metre for kaolin and lycopodium turbidity as mentioned in section 3.2.1 and h = 2.00 metre for PVC powder turbidity and taking Q_a in cc/min., will lead to:

For kaolin and lycopodium turbidity, power, $P = 3.527 \times 10^{-4} \, Q_a$ (5.1a)

For PVC powder turbidity, power, $P = 2.988 \times 10^{-4} \, Q_a$ (5.1b)

Noting that the volume of water for kaolin and lycopodium turbidity is

$V = \pi(0.287)^2 /4 \times 2.40 = 0.15525 \text{ m}^3$

and the volume of water for PVC powder turbidity is

$V = \pi(0.287)^2/4 \times 2.0 = 0.12938 \text{ m}^3$

Then, for kaolin and lycopodium turbidity, $G = (22.718 \times 10^{-4} \, Q_a / \mu)^{1/2}$ (5.2a)

And for PVC turbidity, $G = (23.0947 \times 10^{-4} \, Q_a / \mu)^{1/2}$ (5.2b)

The analysed results are summarised in Table 5.13 showing the overall removal

efficiency after a settling period of 120 minutes, optimum air loading and optimum G value at the respective temperatures recorded during the time of flocculation. Hazen's approximation (1892) of the variation of viscosity with temperature within the normal temperature range from 0 to 25^{0}C is

$$\mu_T / \mu_{50} = 60 /(T + 10) \qquad (5.3)$$

where, T is the temperature in ^{0}F and the subscripts of μ denote the viscosities at temperatures of T^{0}F and 50^{0}F, was used to work out the absolute viscosities at the recorded temperatures and the mean velocity gradients were calculated. For the simplicity of direct comparison, G values are standardised at 20^{0}C and shown in the same table.

The working ranges of minimum and maximum first optimum air flow rates were found to be 50 to 300 cc/min. for kaolin and lycopodium turbidity and 50 to 400 cc/min. for PVC turbidity.

It is evident from the calculated optimum G values that lycopodium turbidity required a relatively lower level of power input than PVC and kaolin turbidity. This could be attributed to the differences in densities and other physicochemical properties of the synthetic turbidities as detailed in section 3.3. The calculated optimum G values are found to be in the recommended ranges (AWWA, 1969; Kawamura, 1973). In the case of high range air loading, say up to 1000 cc/min., particularly for lighter synthetic turbidity like lycopodium, it is found that removal efficiency is oscillatory with respect to air flow rates for a constant flocculation period. This is due to floc rupture caused by high-velocity shear gradients which cause large flocs to be ripped apart as a result of either internal tension or surface shear stress erosion or both (Barnes *et al.,* 1981). This phenomenon is similar to the oscillating floc growth process with respect to the product Gt or G for constant agitation period studied by Fair and Gemmell (1964). It is observed that lycopodium flocs are more sensitive to power variations than that of kaolin and PVC turbidity. This could be due to the strength of the flocs.

Table 5.1 Removal efficiency versus air flow rate and the percussion of orifice sizes (Normal flocculation of kaolin suspension with aluminium sulphate)

Air flow rate cc/min.	Removal efficiency, %			
	1.00 mm	1.50 mm	2.00 mm	3.00 mm
50	85.83	93.11	95.41	93.75
100	86.67	94.57	95.83	95.00
200	89.06	93.53	95.41	93.95
300	89.81	93.27	95.00	93.75
400	90.66	93.04	94.57	93.61
500	91.12			93.55
600	90.89			93.50
800	89.95			93.68
1000	89.30			

Table 5.2 Removal efficiency versus air flow rate and the percussion of orifice sizes (Taper flocculation of kaolin suspension with aluminium sulphate)

Air flow rate cc/min.	Removal efficiency, %			
	1.00 mm	1.50 mm	2.00 mm	3.00 mm
50	88.87	92.77	92.81	93.16
100	91.09	93.57	92.88	93.95
200	89.43	93.53	93.74	93.68
300	89.75	93.33	93.27	94.10
400	90.95	93.74	93.33	94.02
500	91.03			93.85
600	90.10			91.75
800	90.12			
1000	90.00			

Table 5.3 Removal efficiency versus air flow rate and the percussion of orifice sizes (Normal flocculation of kaolin suspension with ferric sulphate)

Air flow rate cc/min.	Removal efficiency, %			
	1.00 mm	1.50 mm	2.00 mm	3.00 mm
50	92.80	92.91	94.16	92.77
100	93.75	93.47	95.41	93.12
200	91.84	94.16	95.00	93.95
300	93.43	93.74	95.83	94.66
400	93.60	93.95	95.23	94.37
500	93.33			94.58
600	91.45			
800	93.00			
1000	93.22			

Table 5.4 Removal efficiency versus air flow rate and the percussion of orifice sizes (Taper flocculation of kaolin suspension with ferric sulphate)

Air flow rate cc/min.	Removal efficiency, %			
	1.00 mm	1.50 mm	2.00 mm	3.00 mm
50	91.84	92.87	94.78	93.75
100	93.43	94.16	95.41	93.33
200	93.18	93.20	95.83	94.58
300	93.95	94.43	95.68	94.16
400	93.33	93.74	95.20	94.44
500	92.91			93.75
600	91.47			
800	91.63			
1000	92.02			

Table 5.5 Removal efficiency versus air flow rate and the percussion of orifice sizes (Normal flocculation of lycopodium suspension with aluminium sulphate)

Air flow rate cc/min.	Removal efficiency, %			
	1.00 mm	1.50 mm	2.00 mm	3.00 mm
50	75.93	78.00	76.34	76.20
100	66.62	75.79	83.18	58.22
200	13.57	75.92	83.09	76.74
300	67.46	75.41	76.85	67.91
400	18.28	76.13	75.82	76.17
500				76.25
600				58.28

Table 5.6 Removal efficiency versus air flow rate and the percussion of orifice sizes (Taper flocculation of lycopodium suspension with aluminium sulphate)

Air flow rate cc/min.	Removal efficiency, %			
	1.00 mm	1.50 mm	2.00 mm	3.00 mm
50	67.83	83.27	83.30	67.56
100	57.18	88.15	85.00	67.78
200	75.56	80.42	82.25	88.26
300	83.24	78.50	88.12	83.03
400	73.38	76.56	76.17	84.46
500	66.57			

Table 5.7 Removal efficiency versus air flow rate and the percussion of orifice sizes (Normal flocculation of lycopodium suspension with ferric sulphate)

Air flow rate cc/min.	Removal efficiency, %			
	1.00 mm	1.50 mm	2.00 mm	3.00 mm
50	78.21	87.93	89.60	91.21
100	79.31	90.15	86.88	92.16
200	85.20	89.30	90.28	93.55
300	86.93	88.95	89.94	93.64
400	79.17	87.56	91.03	90.87
500	74.47			89.72
600	79.69			
800	82.17			
1000	80.38			

Table 5.8 Removal efficiency versus air flow rate and the percussion of orifice sizes (Taper flocculation of lycopodium suspension with ferric sulphate)

Air flow rate cc/min.	Removal efficiency, %			
	1.00 mm	1.50 mm	2.00 mm	3.00 mm
50	80.45	87.53	90.64	90.39
100	80.80	91.39	91.87	91.37
200	82.63	87.63	90.74	91.68
300	81.31	90.76	89.63	91.63
400	82.92	88.46	91.79	91.55
500	82.47			90.06

Table 5.9 Removal efficiency versus air flow rate and the percussion of orifice sizes (Normal flocculation of PVC suspension with aluminium sulphate)

Air flow rate cc/min.	Removal efficiency, %			
	1.00 mm	1.50 mm	2.00 mm	3.00 mm
50	91.73	93.80	94.12	94.50
100	90.90	93.70	94.71	95.00
200	91.64	95.21	94.60	95.62
300	92.69	94.63	94.26	95.00
400	92.76	93.50	95.00	95.50
500	91.60			95.31
600	89.47			

Table 5.10 Removal efficiency versus air flow rate and the percussion of orifice sizes (Taper flocculation of PVC suspension with aluminium sulphate)

Air flow rate cc/min.	Removal efficiency, %			
	1.00 mm	1.50 mm	2.00 mm	3.00 mm
50	91.10	94.50	93.78	93.16
100	92.57	93.79	94.50	95.00
200	92.37	95.40	94.78	93.00
300	91.85	94.00	95.10	93.35
400	92.50	93.24	94.59	
500	92.02			

Table 5.11 Removal efficiency versus air flow rate and the percussion of orifice sizes (Normal flocculation of PVC suspension with ferric sulphate)

Air flow rate cc/min.	Removal efficiency, %			
	1.00 mm	1.50 mm	2.00 mm	3.00 mm
50	93.82	93.09	94.81	92.06
100	94.00	94.37	95.50	92.46
200	94.53	94.70	96.00	95.40
300	95.00	94.50	95.70	95.30
400	94.50	94.45	95.87	94.87
500	95.07			
600	94.44			

Table 5.12 Removal efficiency versus air flow rate and the percussion of orifice sizes (Taper flocculation of PVC suspension with ferric sulphate)

Air flow rate cc/min.	Removal efficiency, %			
	1.00 mm	1.50 mm	2.00 mm	3.00 mm
50	94.35	92.98	94.00	92.90
100	95.07	93.50	96.00	93.31
200	95.20	94.81	95.50	94.00
300	95.50	93.88	95.90	95.00
400	95.07	94.20	96.00	95.70
500	94.57			94.51

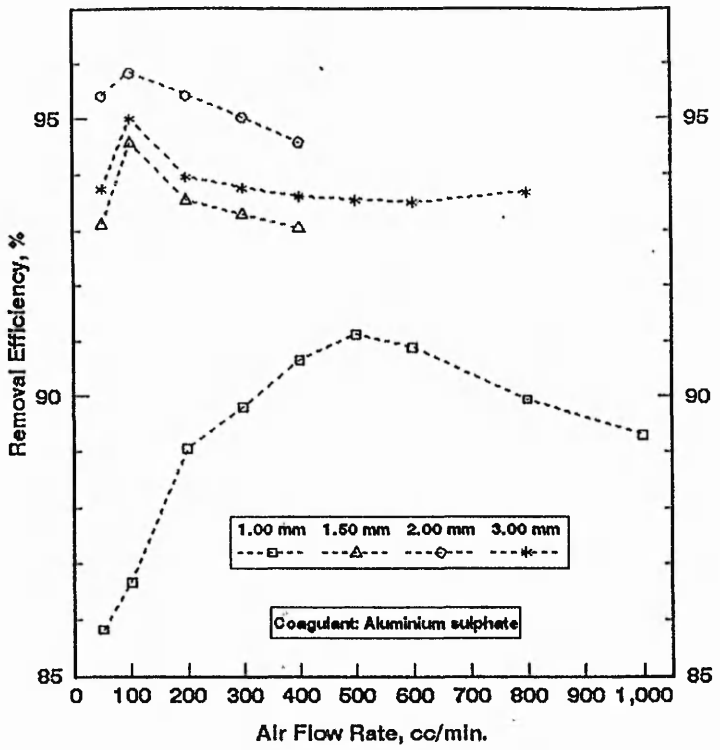

Figure 5.32 Removal efficiency versus air flow rate and the percussion of orifice size (normal flocculation of kaolin turbidity)

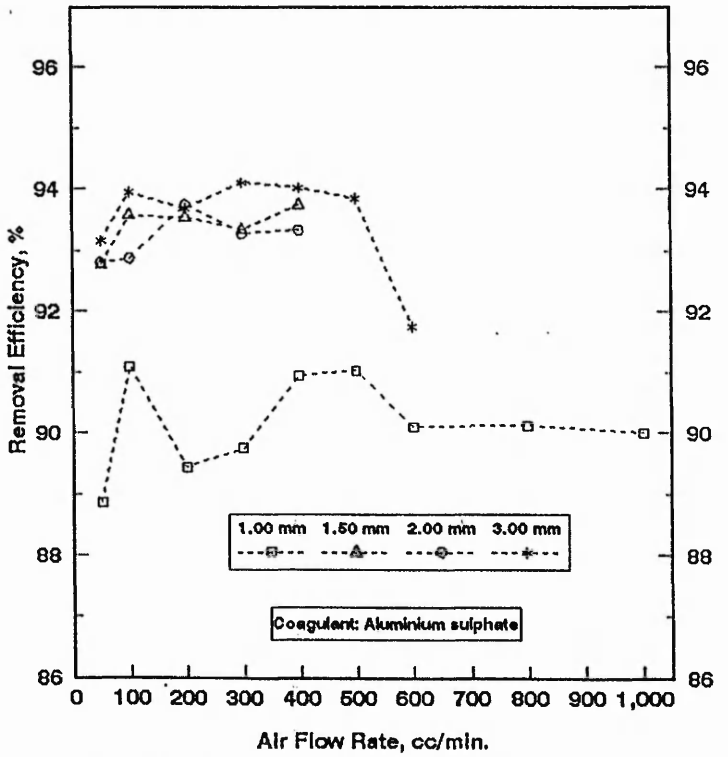

Figure 5.33 Removal efficiency versus air flow rate and the percussion of orifice size (taper flocculation of kaolin turbidity)

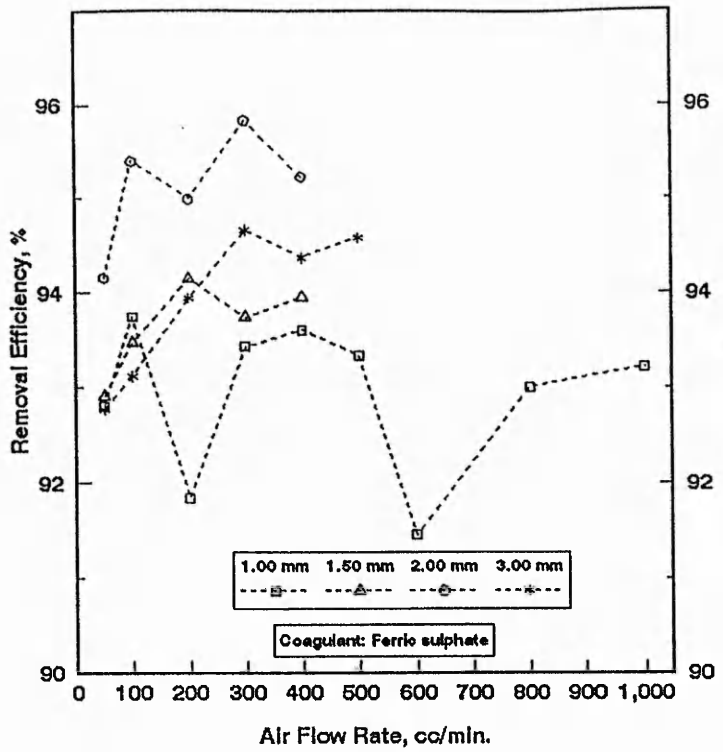

Figure 5.34 Removal efficiency versus air flow rate and the percussion of orifice size (normal flocculation of kaolin turbidity)

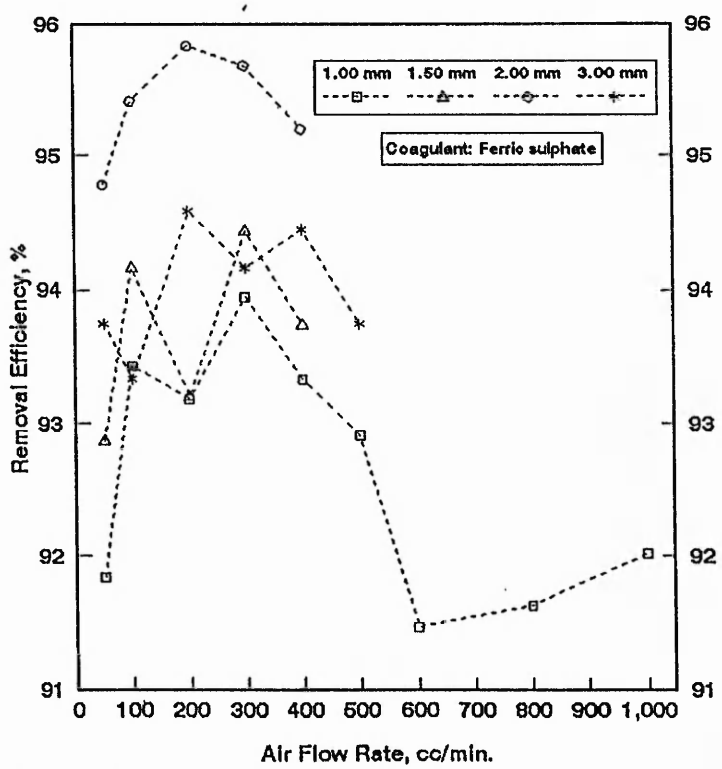

Figure 5.35 Removal efficiency versus air flow rate and the percussion of orifice size (taper flocculation of kaolin turbidity)

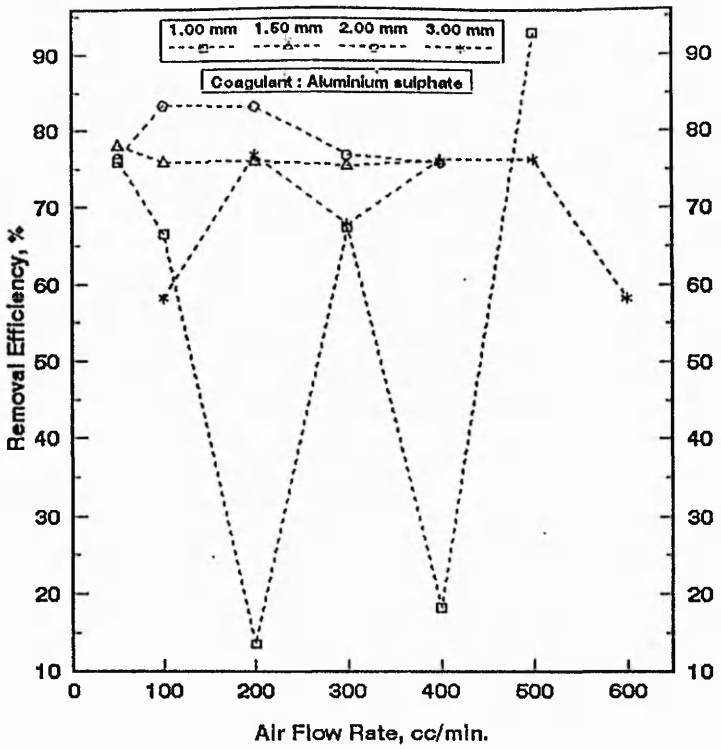

Figure 5.36 Removal efficiency versus air flow rate and the percussion of orifice size (normal flocculation of lycopodium turbidity)

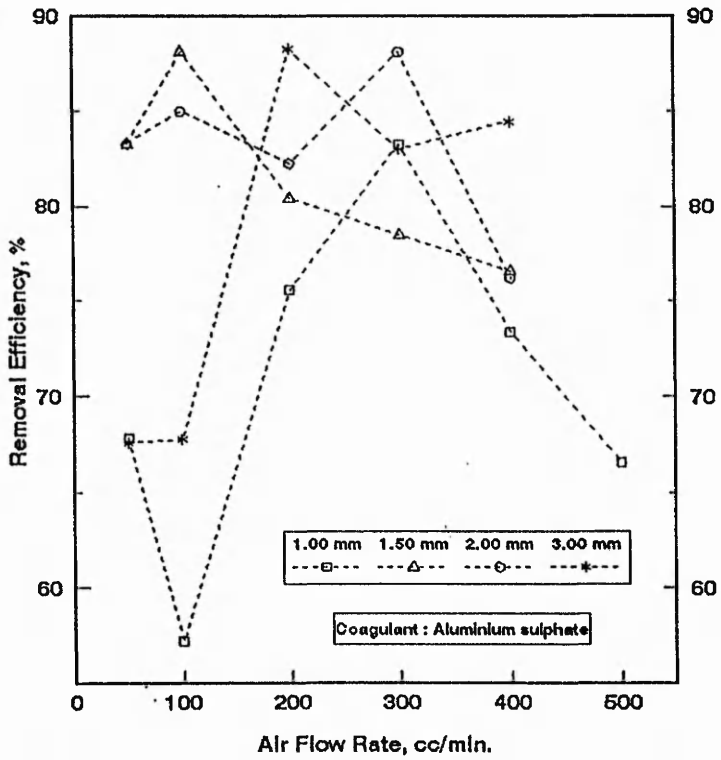

Figure 5.37 Removal efficiency versus air flow rate and the percussion of orifice size (taper flocculation of lycopodium turbidity)

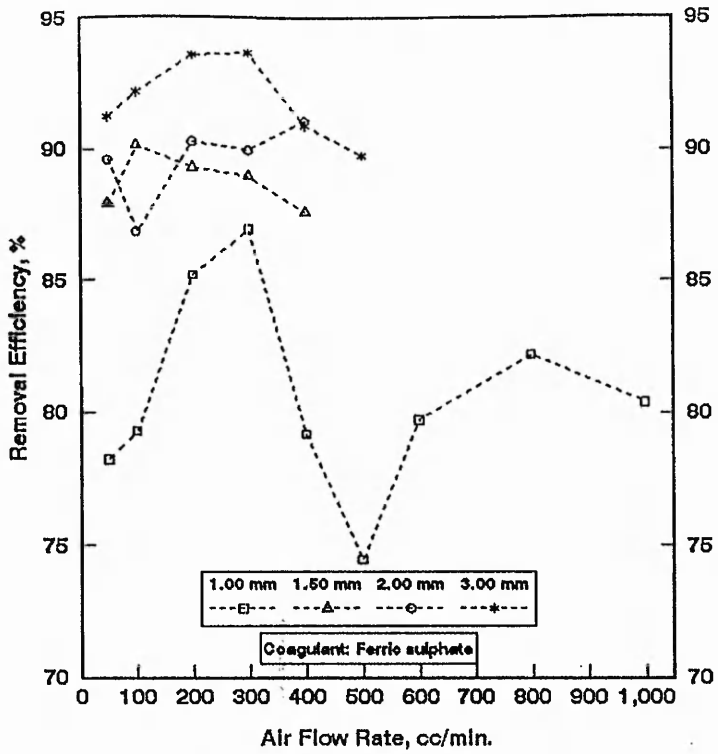

Figure 5.38 Removal efficiency versus air flow rate and the percussion of orifice size (normal flocculation of lycopodium turbidity)

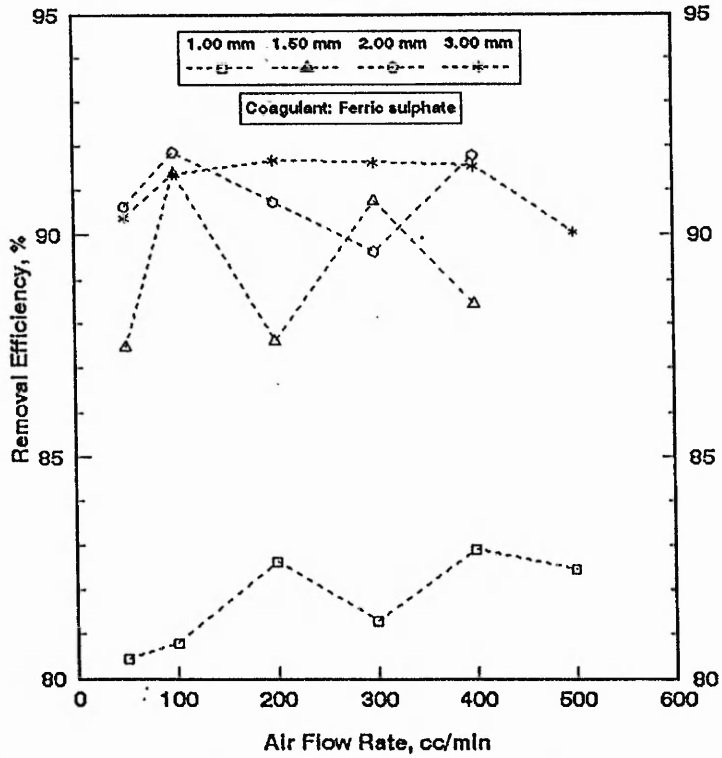

Figure 5.39 Removal efficiency versus air flow rate and the percussion of orifice size (taper flocculation of lycopodium turbidity)

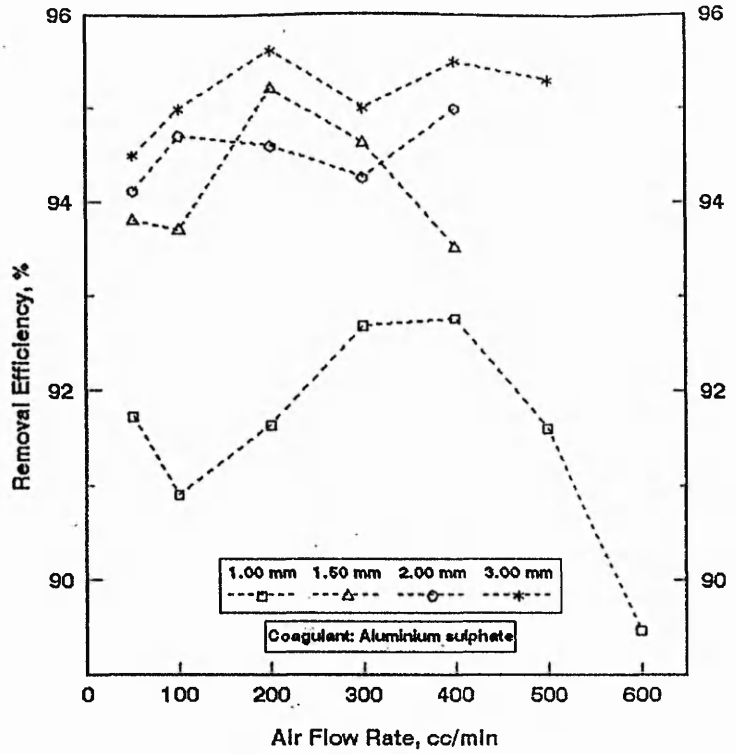

Figure 5.40 Removal efficiency versus air flow rate and the percussion of orifice size (normal flocculation of PVC turbidity)

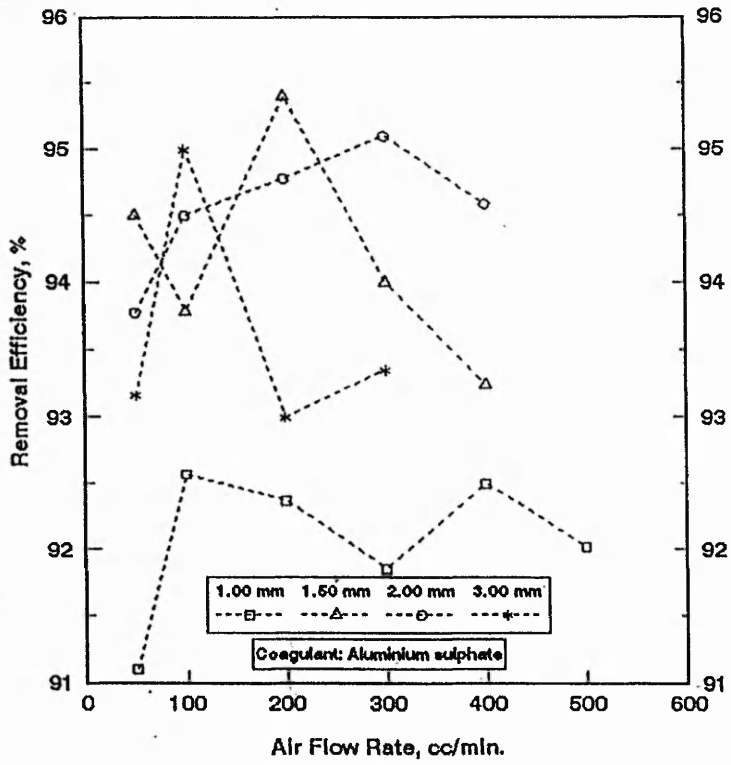

Figure 5.41 Removal efficiency versus air flow rate and the percussion of orifice size (taper flocculation of PVC turbidity)

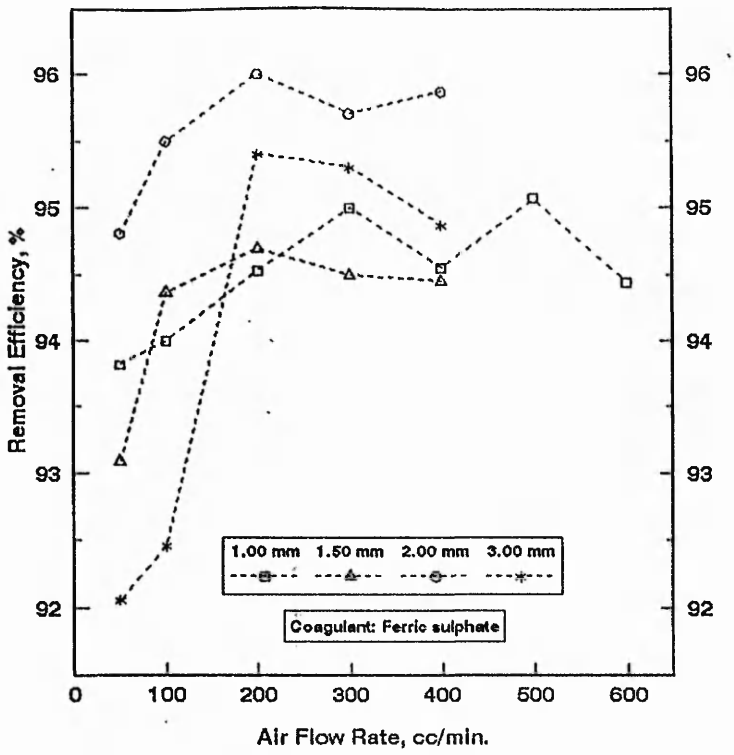

Figure 5.42 Removal efficiency versus air flow rate and the percussion of orifice size (normal flocculation of PVC turbidity)

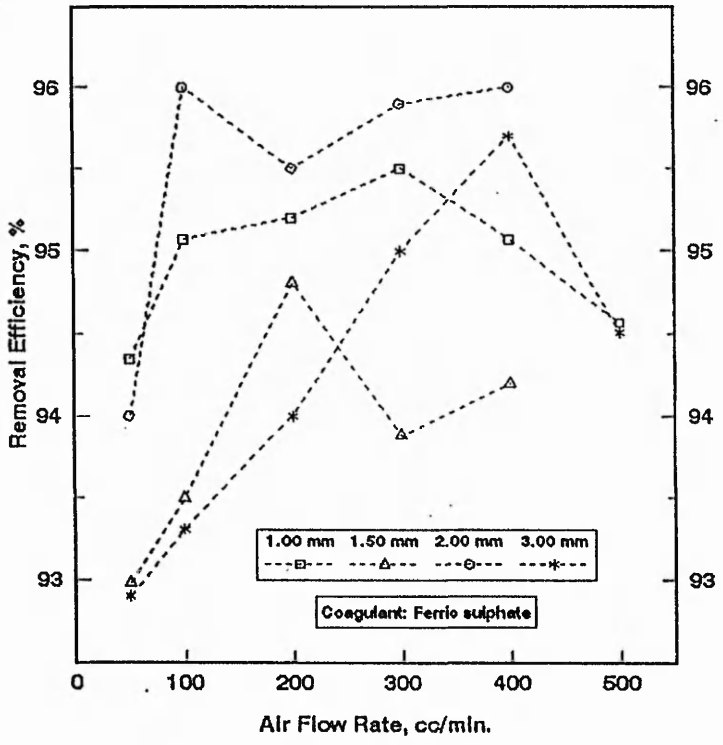

Figure 5.43 Removal efficiency versus air flow rate and the percussion of orifice size (taper flocculation of PVC turbidity)

Table 5.13 Optimum Air loading and the *G* values.

Set No.	Opt. Removal Efficiency (%)	Opt. Air Flow rates (cc/min.)	Air loading per unit area (cc/sq.cm-min)	Temp. (^{0}C)	Opt. *G* value (s^{-1})	*G* value, s^{-1} standardised at 20^{0}C
1	85.83	50	0.077	10.35	9.32	10.65
2	91.09	100	0.154	13.78	13.91	15.05
3	93.75	100	0.154	13.90	13.93	15.05
4	93.43	100	0.154	13.00	13.76	15.05
5	75.93	50	0.077	13.53	9.80	10.65
6	67.83	50	0.077	15.57	10.07	10.65
7	86.93	300	0.463	15.52	24.65	26.08
8	82.63	200	0.309	13.77	19.67	21.30
9	91.73	50	0.077	16.43	10.26	10.73
10	92.57	100	0.154	17.53	14.71	15.18
11	95.00	300	0.463	17.43	25.46	26.29
12	95.50	300	0.463	16.95	25.31	26.29
13	94.57	100	0.154	15.42	14.21	15.05
14	93.57	100	0.154	17.21	14.53	15.05
15	94.16	200	0.309	16.07	20.27	21.30
16	94.16	100	0.154	15.95	14.31	15.05
17	78.00	50	0.077	16.58	10.20	10.65
18	88.14	100	0.154	16.25	14.36	15.05
19	90.15	100	0.154	15.95	14.31	15.05
20	91.39	100	0.154	16.10	14.33	15.05
21	93.80	50	0.077	15.37	10.04	10.73
22	94.50	50	0.077	16.45	10.18	10.73
23	94.70	200	0.309	14.75	20.09	21.47
24	94.81	200	0.309	13.30	18.15	21.47
25	95.83	100	0.154	16.57	14.42	15.05
26	93.74	200	0.309	16.40	20.35	21.30
27	95.41	100	0.154	15.35	14.20	15.05
28	95.83	200	0.309	16.37	20.34	21.30
29	83.18	100	0.154	15.57	14.24	15.05
30	85.00	100	0.154	14.25	13.99	15.05
31	89.60	50	0.077	17.40	10.30	10.65
32	91.87	100	0.154	15.57	14.24	15.05
33	94.71	100	0.154	17.60	14.73	15.18
34	95.10	300	0.463	14.00	24.36	26.29
35	96.00	200	0.309	12.47	19.48	21.49
36	96.00	100	0.154	13.75	14.02	15.18
37	95.00	100	0.154	18.20	14.71	15.05
38	93.75	100	0.154	19.05	14.86	15.05
39	94.66	300	0.463	19.85	25.97	26.08
40	93.75	50	0.077	20.37	10.07	10.65
41	75.20	50	0.077	19.50	10.66	10.65
42	88.26	200	0.309	20.37	21.34	21.30
43	93.64	300	0.463	21.52	26.48	26.08
44	91.68	200	0.309	21.05	21.51	21.30
45	95.62	200	0.309	19.38	21.27	21.47
46	95.00	100	0.154	16.50	14.53	15.18
47	95.40	200	0.309	15.70	20.34	21.47
48	95.70	400	0.618	17.30	29.35	30.36

5.4 THE IMPACT OF ORIFICE SIZE ON REMOVAL EFFICIENCY BASED ON OPTIMUM AIR FLOW RATE

The performance of different sizes of orifice was studied and analysed under various initial conditions. The results for optimum air flow rates are summarised in Table 5.14 to Table 5.17. The performance of different sizes of orifice at these optimum air flow rates were plotted and shown in Figure 5.44 to Figure 5.47. The best result in removing the kaolin turbidity is found with the orifice sizes of 1.5 or 2.0 mm, as shown in Figures 5.44 to 5.47. When PVC turbidity is coagulated with alum, better removal efficiency is obtained with higher orifice size as shown in Figure 5.44 and Figure 5.45. On the other hand, when PVC turbidity is coagulated with ferric sulphate, a minimum optimum removal efficiency is found with 1.5 mm orifice, although a better removal with more acceptable efficiency removal is obtained when 1.0 mm orifice size is used, as indicated in Figure 5.46 and Figure 5.47, and treated as first peak reading, because no experiments were conducted with orifice sizes smaller than 1.0 mm in diameter. A second peak in optimum removal efficiency is obtained with the 2.0 mm orifice as shown in Figure 5.46 and Figure 5.47. However, the corresponding size of the orifice of these optimum removal efficiences, i.e. 2.0 mm, is not considered as the best size for turbidity removal from an economic point of view to yield a lower energy value. In the case of lycopodium turbidity, the best optimum removal efficiency is obtained with an orifice size of 1.5 or 2.0 mm as shown in Figure 5.44 to Figure 5.47.

From the experimental results discussed above it can be concluded that for each combination of initial conditions, there exists one optimum size of orifice. This corresponds to the intensity of local maximum velocity gradients produced by different sizes of the bubbles associated with their orifice size and also the physicochemical properties of the turbidity materials.

Operating under constant air flow and not optimum for various orifice sizes, well defined curves are produced for the removal efficiency versus orifice diameter as shown in Figures 5.48 to 5.59. The removal efficiency of kaolin turbidity is found

to be increased with the increasing air flow rates within the limited range of air flow through 1.0 mm orifice only, and no smaller size is used as mentioned before in this section, which is shown in Figure 5.48. The behaviour of air flow and removal efficiency with the 1.5, 2.0 and 3.0 mm diameter orifice differs somehow from the 1.0 mm diameter orifice mentioned above and defines the prevailing 100 cc/min. over the three sizes used. Generally the best removal efficiency was obtained with 2.0 mm orifice at any air flow rates in the range of 50 to 400 cc/min. The best removal efficiency is related to the 2.0 mm orifice size after which it started to decline with the 3.0 mm orifice size. This could be attributed to the increase in the local velocity gradient at the bubble surface for larger sizes, which would cause the floc to be broken by the surface erosion or internal tension.

In some other cases under differently stated initial conditions for removal efficiency versus orifice diameter as shown in Figure 5.49 and Figures 5.53 to 5.57, the best removal efficiency is obtain with 1.5 mm size of orifice. But, in most cases, 2.0 mm orifice produced the best results at different corresponding air flow rates. In general it can said that at any air flow rate within the range used in this investigation, better removal is experimentally obtained with the orifice sizes of 1.5 to 2.0 mm.

The experimental data and analyses of results revealed the existence of an optimum size of the orifice in removing any of the turbidities in the pneumatic flocculation process. This phenomenon is related to the size, shape, path followed by the bubbles, frequency and velocity of the rising air bubbles originated from different sizes of the orifices and also to the properties of the synthetic turbidity used and eventually normal and taper mixing. In fact, the optimum size of the orifice depends on the unique combination of the initial conditions like the nature of the turbidity and coagulants, type of flocculation, rates of air flow etc.

No definite and precise relationship exists between the size of orifice and the size and shape of the rising air bubbles and any other variable which might be involved in this process. In general, it is well known that bubble size increases with the increase of orifice diameter and this phenomenon is also noticed in this investigation.

There is no existing relationship of the bubble size, orifice size and the related mixing intensity G available for wide application.

However, Camp (1955) has suggested the following equation, for limited application, giving the maximum velocity gradient, G_{max} , produced by a bubble of diameter d_b:

$$G_{max} = \frac{1}{6}\frac{g}{\mu}(\rho_b - \rho_w)\, d_b \qquad (2.6)$$

where g is the gravitional acceleration, μ is the absolute viscosity, ρ_b and ρ_w are the mass density of the air bubble and the water respectively. This equation is applicable only for Stokes' law region, i. e. under the laminar flow condition where $\mathbf{R} < 1.0$, and employed for the bubbles which are less than 0.1 mm (Levich, 1962). The bubbles administered under this investigation are obviously much greater than the 0.1 mm size and do not follow the same trend of proportionality between G_{max} and d_b as stated in Equation (2.6).

From Figure 5.44 to Figure 5.47, it can be seen that the optimum removal efficiency is achieved with a relatively larger size of orifice (say, 1.5 and 2.0 mm diameter) at any constant air flow rate. This indicates that the removal efficiency is controlled by orifice size and hence by the size of rising bubbles even with a constant intensity of mixing. This could be associated with the hydrodynamic behaviour like the shape, size, path, frequency and rising velocity of the bubbles and their impact on mixing process and ultimately on the removal of turbidity from water.

Table 5.14 Effect of orifice sizes on removal efficiency (Normal flocculation with aluminium sulphate)

Orifice Diameter (mm)	Kaolin		Lycopodium powder		PVC powder	
	Optimum air flow rate cc/min.	Optimum Removal efficiency %	Optimum air flow rate cc/min.	Optimum Removal efficiency %	Optimum air flow rate cc/min.	Optimum Removal efficiency %
1.00	50	85.83	50	75.93	50	91.73
1.50	100	94.57	50	78.00	50	93.80
2.00	100	95.83	100	83.18	100	94.71
3.00	100	95.00	50	75.20	200	95.62

Table 5.15 Effect of orifice sizes on removal efficiency (Taper flocculation with aluminium sulphate)

Orifice Diameter (mm)	Kaolin		Lycopodium powder		PVC powder	
	Optimum air flow rate cc/min.	Optimum Removal efficiency %	Optimum air flow rate cc/min.	Optimum Removal efficiency %	Optimum air flow rate cc/min.	Optimum Removal efficiency %
1.00	100	91.09	50	67.83	100	92.57
1.50	100	93.57	100	88.14	50	94.50
2.00	200	93.74	100	85.00	300	95.10
3.00	100	93.95	200	88.26	100	95.00

Table 5.16 Effect of orifice sizes on removal efficiency
(Normal flocculation with ferric sulphate)

Orifice Diameter (mm)	Kaolin		Lycopodium powder		PVC powder	
	Optimum air flow rate cc/min.	Optimum Removal efficiency %	Optimum air flow rate cc/min.	Optimum Removal efficiency %	Optimum air flow rate cc/min.	Optimum Removal efficiency %
1.00	100	93.75	300	86.90	300	95.00
1.50	200	94.16	100	90.15	200	94.70
2.00	100	95.41	50	89.60	200	96.00
3.00	300	94.66	300	93.64	200	95.40

Table 5.17 Effect of orifice sizes on removal efficiency
(Taper flocculation with ferric sulphate)

Orifice Diameter (mm)	Kaolin		Lycopodium powder		PVC powder	
	Optimum air flow rate cc/min.	Optimum Removal efficiency %	Optimum air flow rate cc/min.	Optimum Removal efficiency %	Optimum air flow rate cc/min.	Optimum Removal efficiency %
1.00	100	93.43	200	82.63	300	95.50
1.50	100	94.16	100	91.39	200	94.81
2.00	200	95.83	100	91.87	100	96.00
3.00	50	93.75	200	91.68	400	95.70

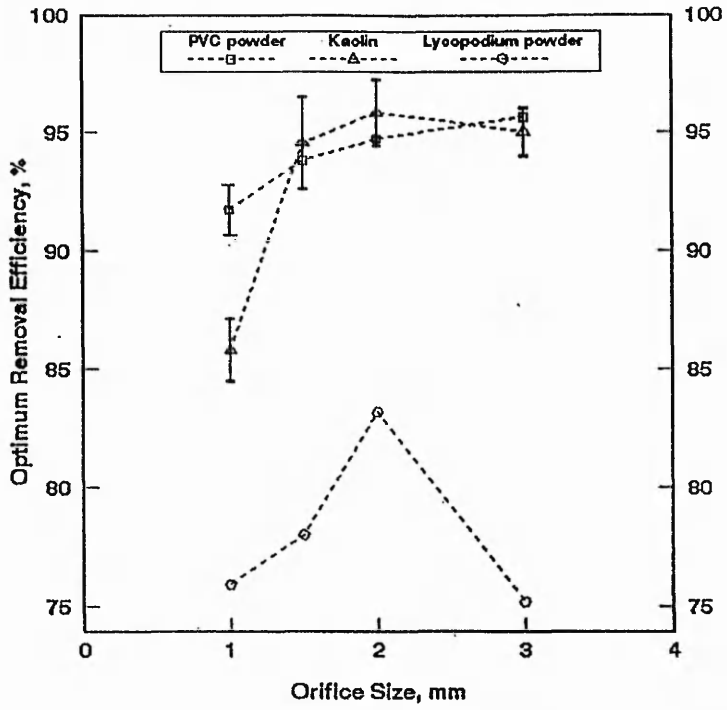

Figure 5.44 Effect of orifice size on removal efficiency (normal flocculation with aluminium sulphate)

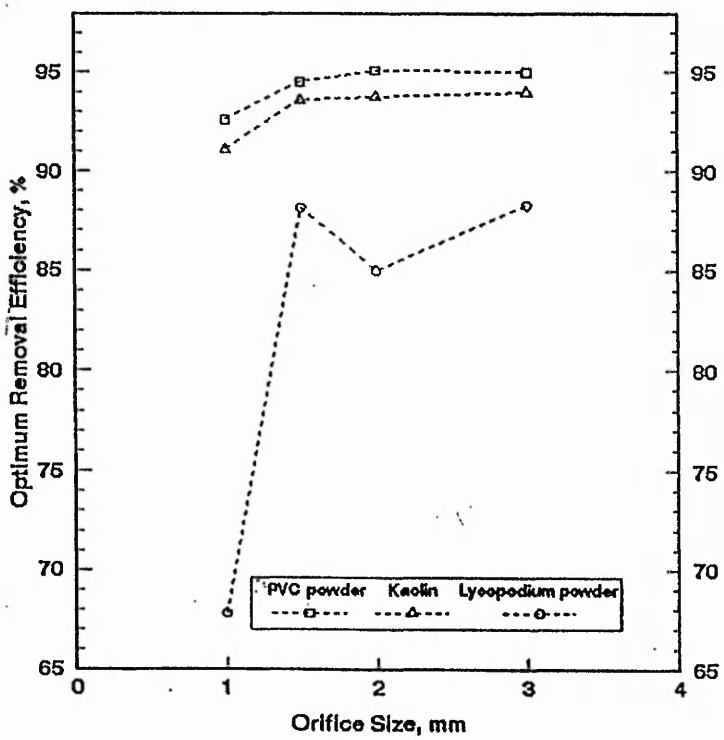

Figure 5.45 Effect of orifice size on removal efficiency (taper flocculation with aluminium sulphate)

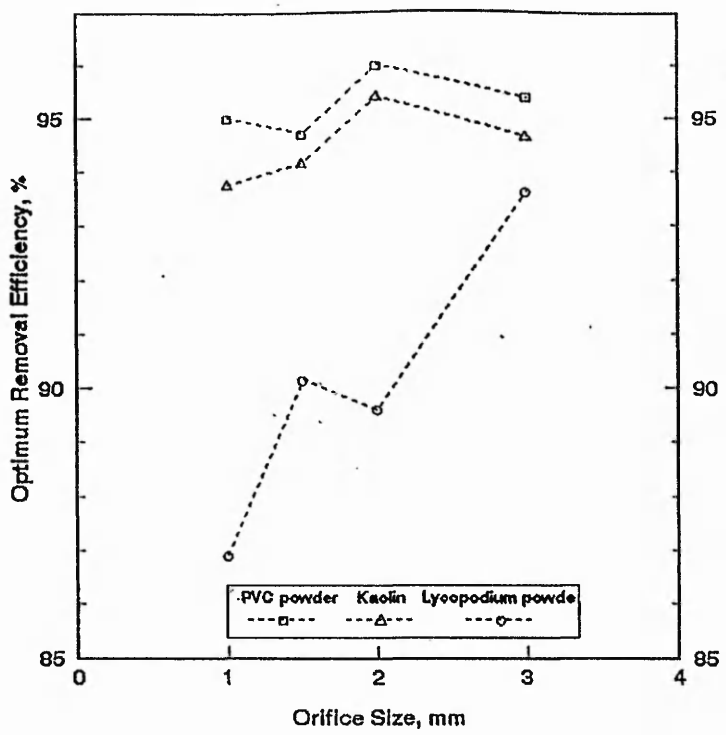

Figure 5.46 Effect of orifice size on removal efficiency (normal flocculation with ferric sulphate)

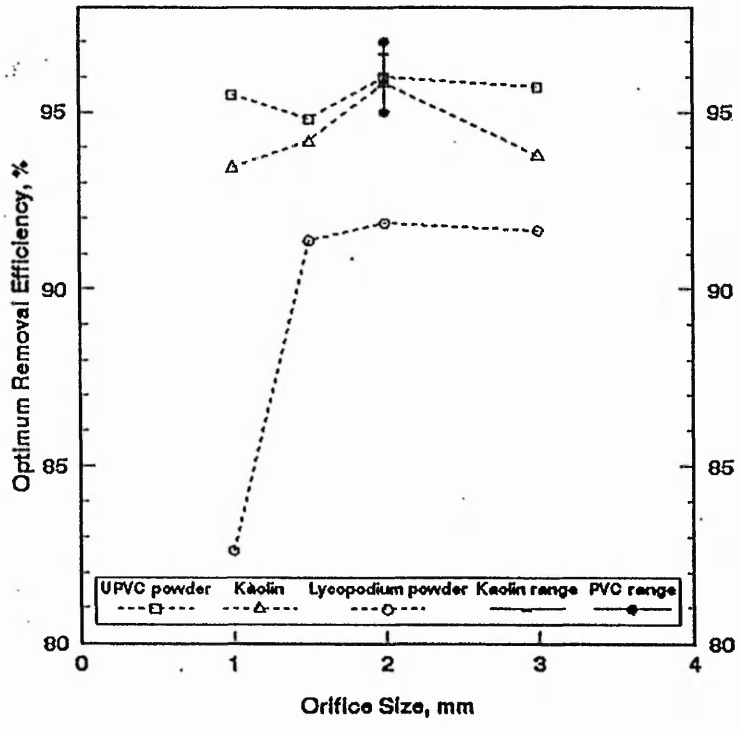

Figure 5.47 Effect of orifice size on removal efficiency (taper flocculation with ferric sulphate)

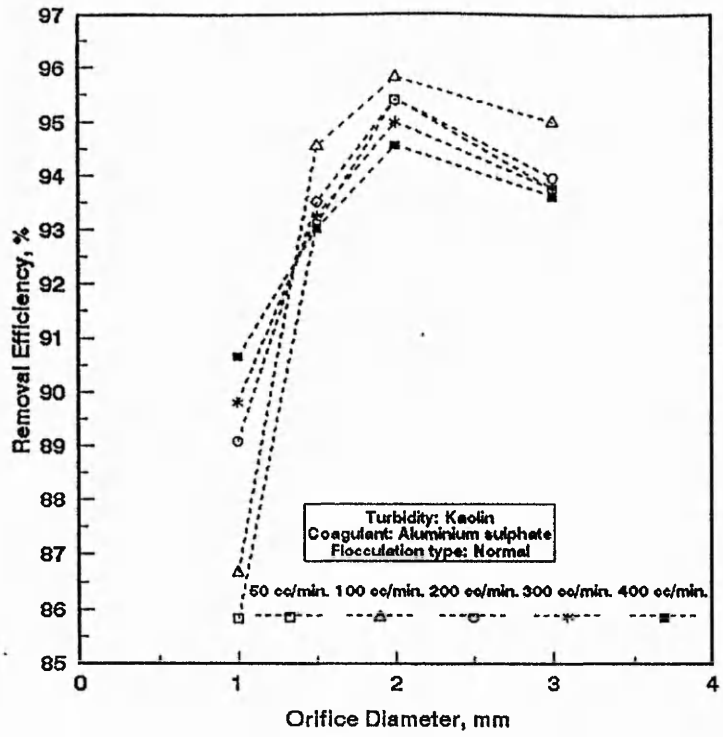

Figure 5.48 Removal efficiency versus orifice diameter

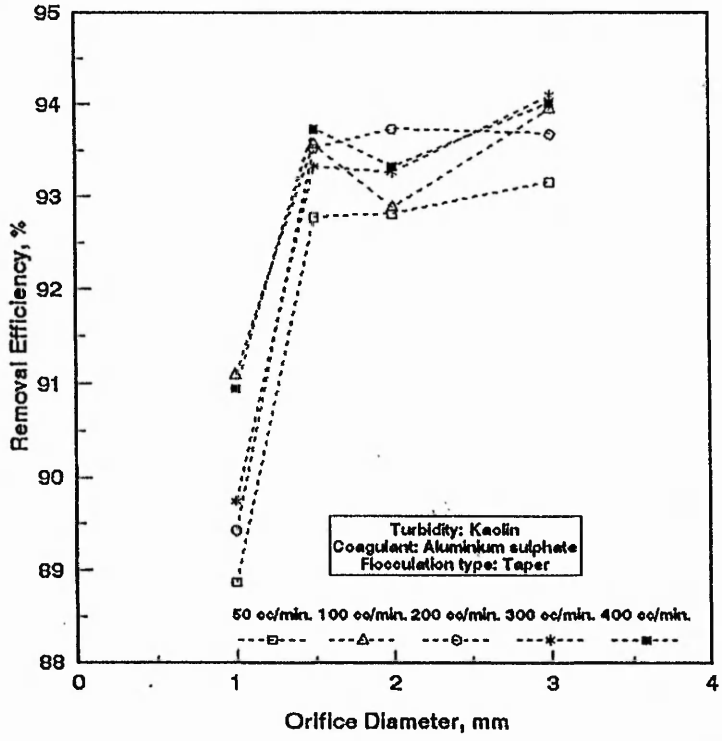

Figure 5.49 Removal efficiency versus orifice diameter

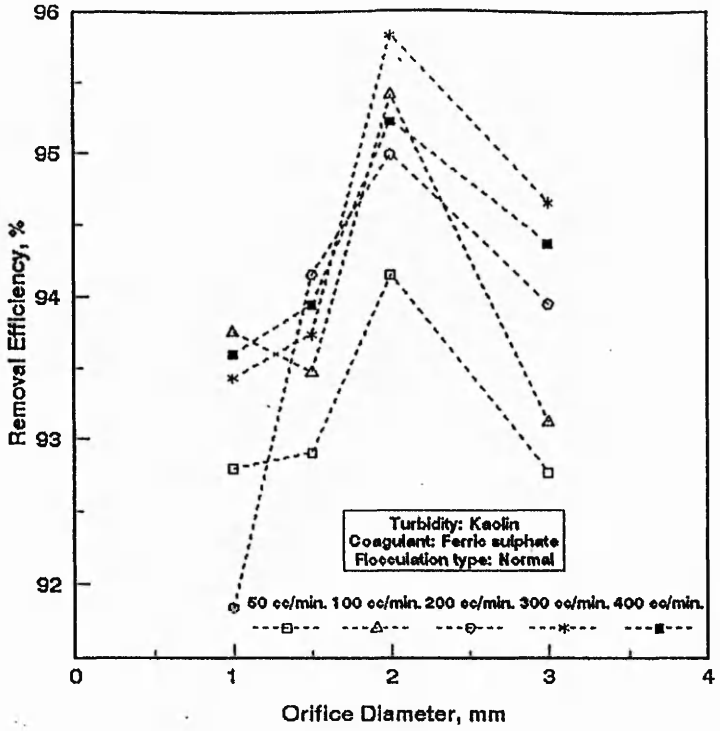

Figure 5.50 Removal efficiency versus orifice diameter

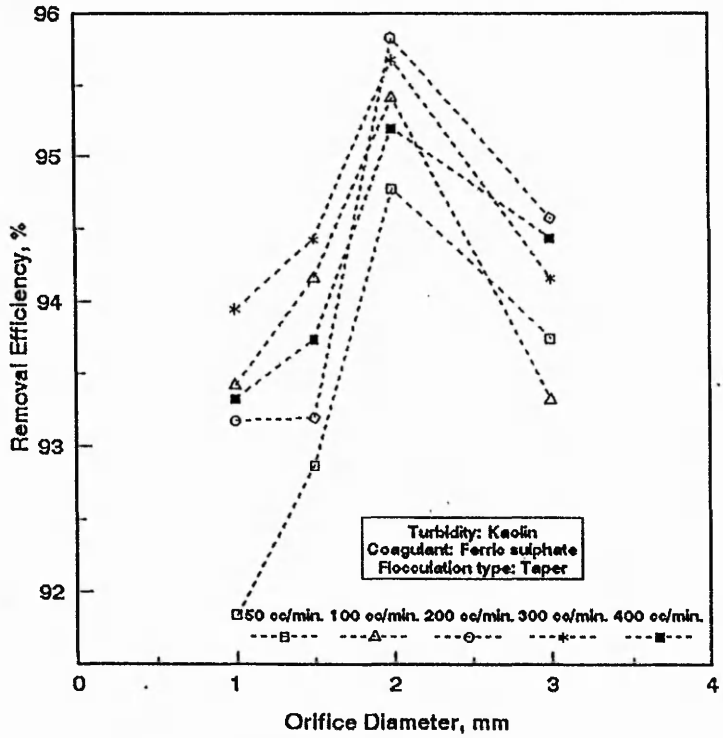

Figure 5.51 Removal efficiency versus orifice diameter

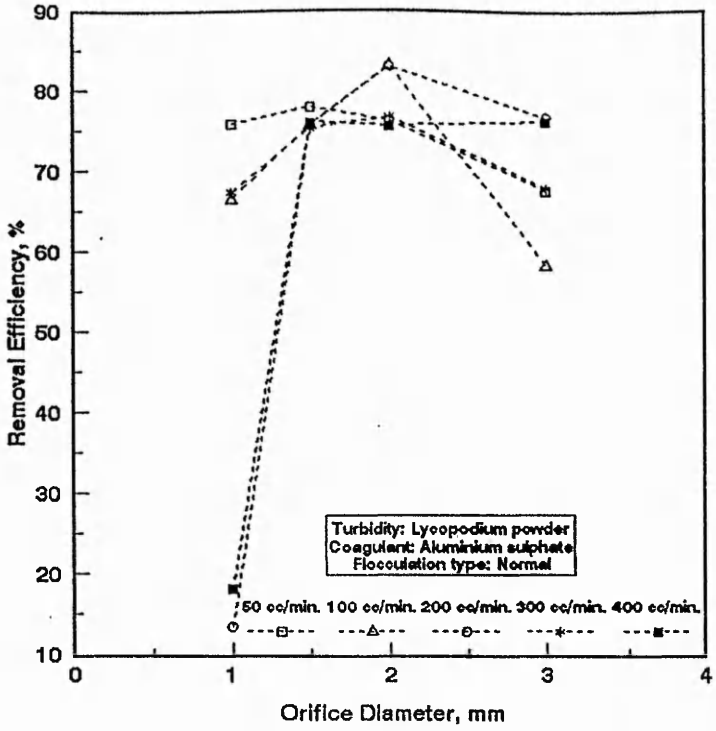

Figure 5.52 Removal efficiency versus orifice diameter

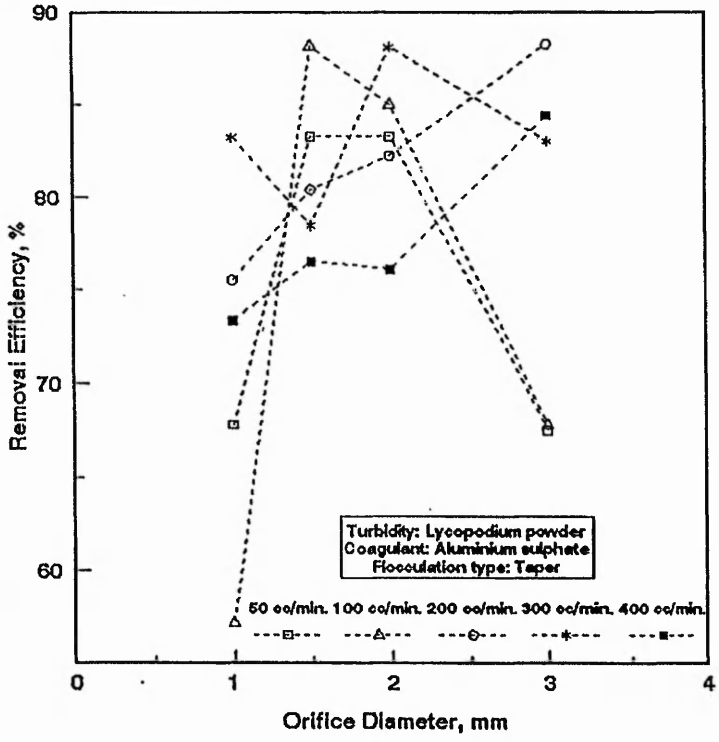

Figure 5.53 Removal efficiency versus orifice diameter

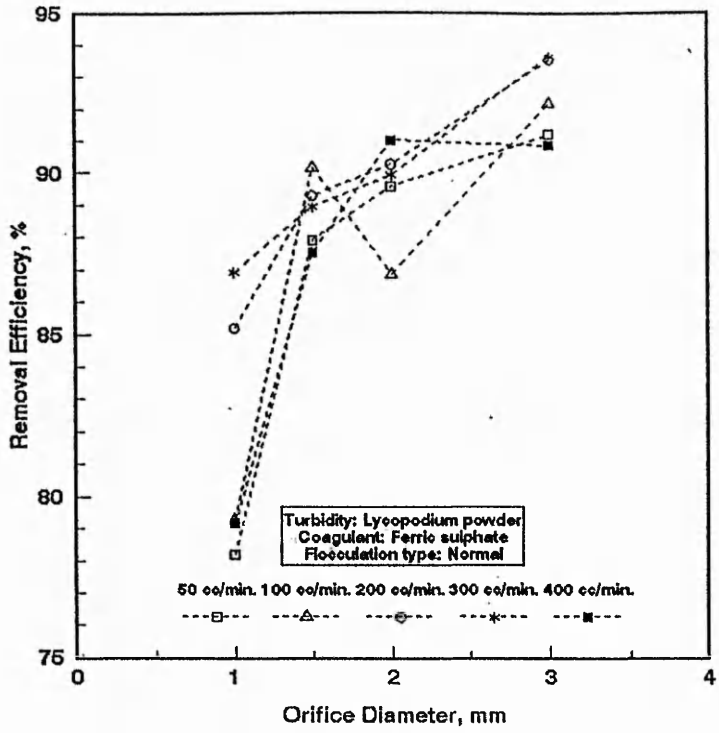

Figure 5.54 Removal efficiency versus orifice diameter

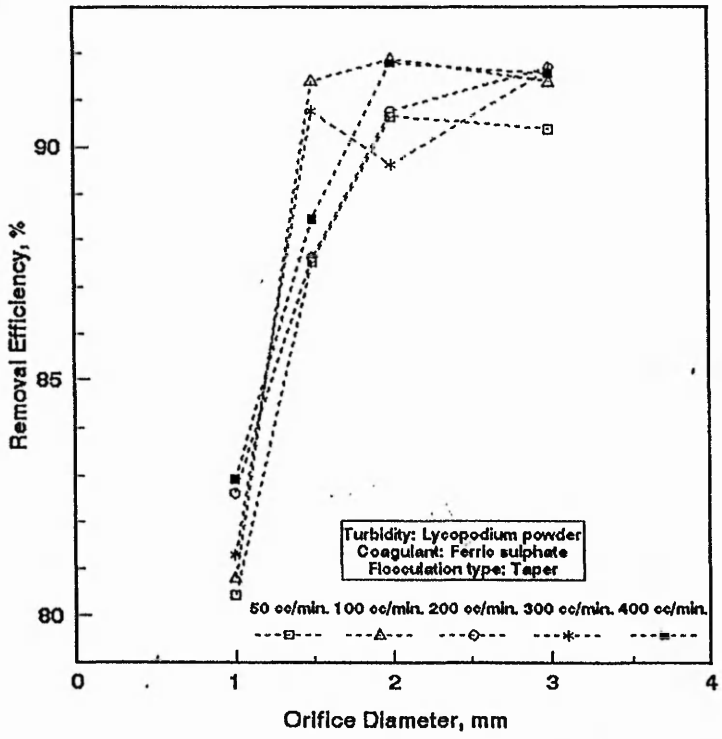

Figure 5.55 Removal efficiency versus orifice diameter

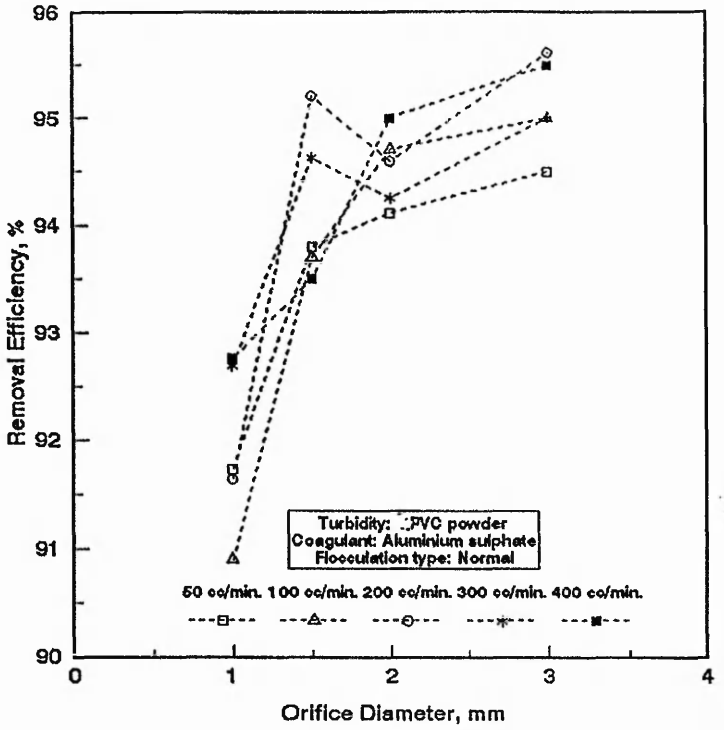

Figure 5.56 Removal efficiency versus orifice diameter

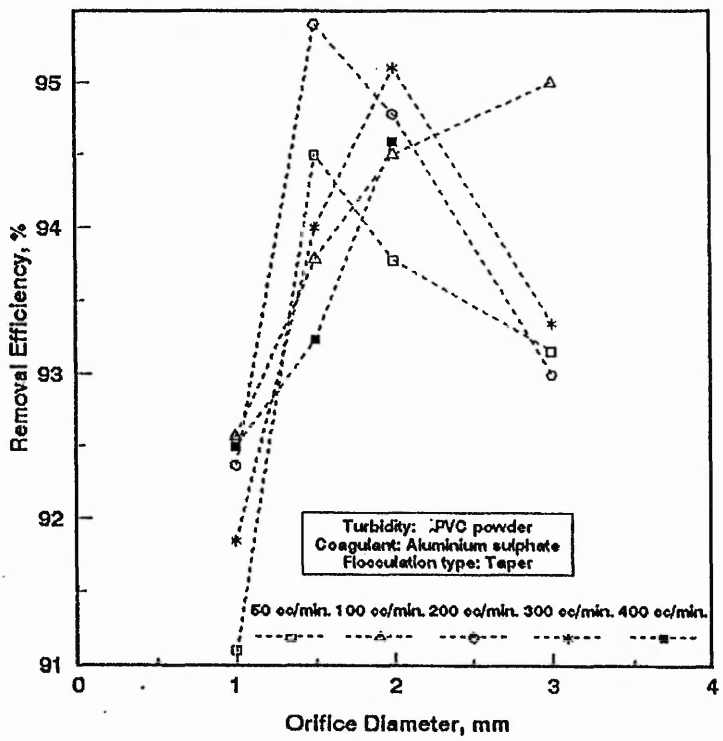

Figure 5.57 Removal efficiency versus orifice diameter

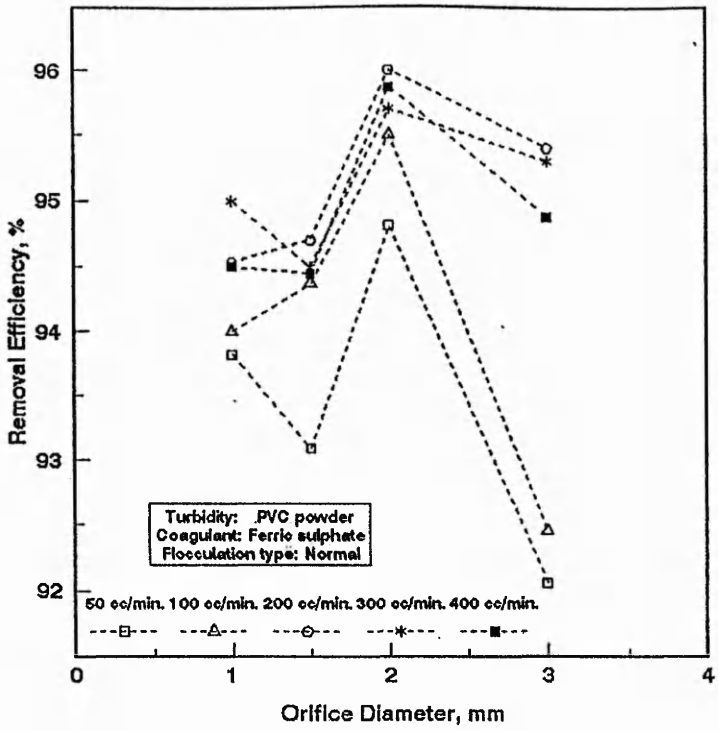

Figure 5.58 Removal efficiency versus orifice diameter

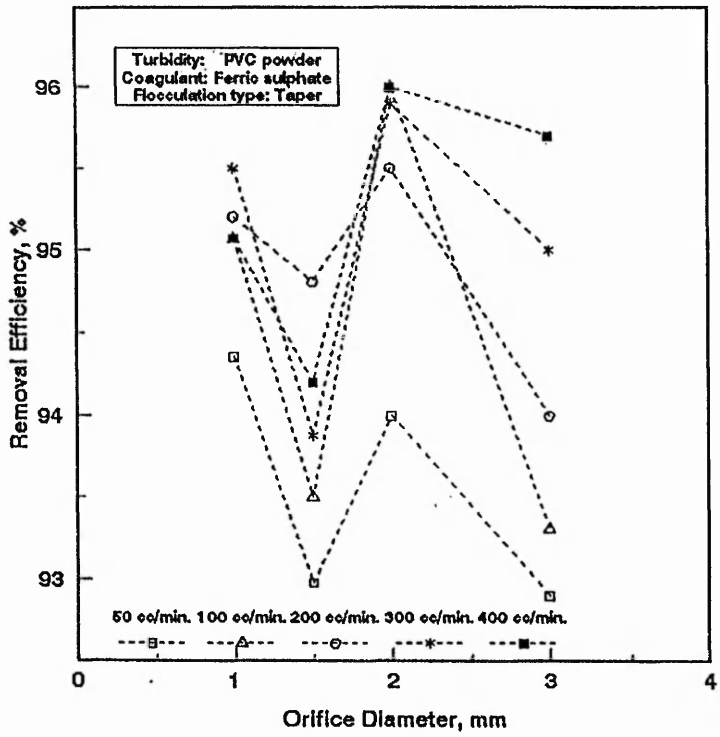

Figure 5.59 Removal efficiency versus orifice diameter

5.5 THE NATURE OF SYNTHETIC TURBIDITY AND THE REMOVAL EFFICIENCY

The physicochemical properties of the synthetic turbidity materials influence the process of pneumatic flocculation in removing the turbidity from water. The influence of the nature of synthetic turbidity materials on the removal efficiency is also shown in Figure 5.44 to Figure 5.47. From these figures it can be seen that the maximum removal efficiencies are achieved with PVC turbidity in comparison to the kaolin and lycopodium as described in section 5.2, although there is a discrepancy as shown in Figure 5.44 in which the best removal is obtained for kaolin turbidity with the orifice size of 2.0 mm. This could be attributed to the physicochemical properties of the suspension. The minimum removal efficiency is achieved in case of lycopodium turbidity. The experimental results, shown in Figure 5.44 to Figure 5.47, indicate that PVC is able to produce more settleable flocs than kaolin and lycopodium powder. This phenomenon could be explain with respect to the colloidal size or fineness of the particles. The size range of the PVC particles is the smallest (0.50 to 1.50 μm) and thus the particles have the largest specific surface area to react with the counterions of the coagulant species. As a result, more suspended particles are destabilised to produce the settleable flocs and better removal of turbidity is achieved. The particles of lycopodium powder are comparatively coarser (35 μm) and less turbidity removal was observed in this case due to the same reason mentioned above and also because of its low density as mentioned in section 3.3.

Al-Hiary (1988) obtained the best removal of silica turbidity than kaolin and he found that the rate of settling for silica flocs was faster than that of kaolin flocs at the same air flow rate.

Due to the difference in physicochemical properties of different types of synthetic turbidities, contrasting behaviour of kaolin, lycopodium and PVC has been observed during the experimental course of this investigation.

5.6 EFFECTS OF THE TYPE OF COAGULANTS

Two types of chemical coagulants namely, aluminium sulphate and ferric sulphate, were used to destabilise the colloidal suspended particles in order to produce the settleable floc by the process of pneumatic flocculation. The effects of coagulants on removal efficiency have been studied and the results are shown in Figures 5.60 to 5.65. In most cases, better removal of turbidity is achieved with ferric sulphate. This could be due to the physicochemical properties of the coagulants. Ferric sulphate is denser than aluminium sulphate and thus the flocs produced with ferric sulphate could be heavier than that of aluminium sulphate and settle faster and result in better removal of turbidity from water.

However, there are some discrepancies in some situations as shown in Figure 5.60 and Figure 5.64. In Figure 5.60, better results are obtained in removing the kaolin turbidity coagulated with alum under normal agitation with 1.5, 2.0 and 3.0 mm diameter orifice. As shown in Figure 5.64, a slightly higher optimum removal efficiency is obtained with the 3.0 mm orifice when alum is used to coagulate PVC turbidity under normal agitation, although a better trend of removal is noticed when ferric sulphate is used as coagulant.

Aluminium sulphate was the traditional coagulant used in water treatment industries before the advent of ferric sulphate. Ferric sulphate is now increasingly becoming the coagulant for replacement of aluminium sulphate or for new treatment plants in UK because of its effectiveness, particularly for the removal of humic and fulvic acids from waters (Water Services, 1975). In the pneumatic flocculation process ferric sulphate is expected to result in better performances over aluminium sulphate in water treatment industries. However, ferric sulphate results a high level of iron in the settled water and a further treatment is required to reduce the amount of iron in order to achieve the recommended level.

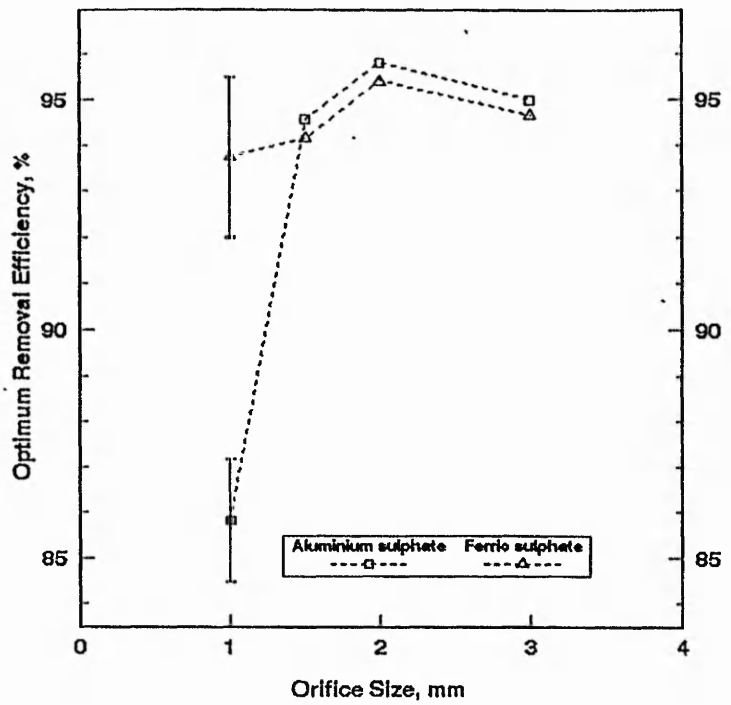

Figure 5.60 Effect of coagulant on removal efficiency (normal flocculation of kaolin turbidity)

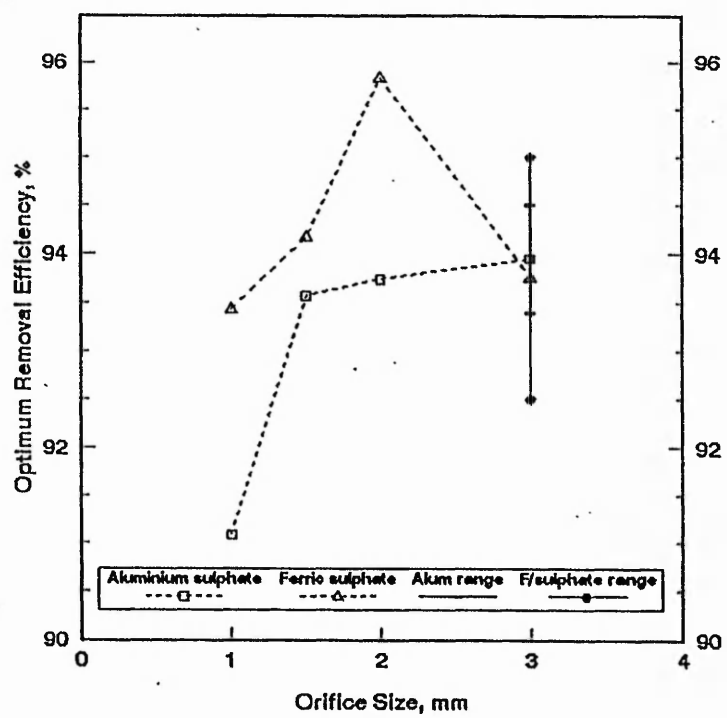

Figure 5.61 Effect of coagulant on removal efficiency (taper flocculation of kaolin turbidity)

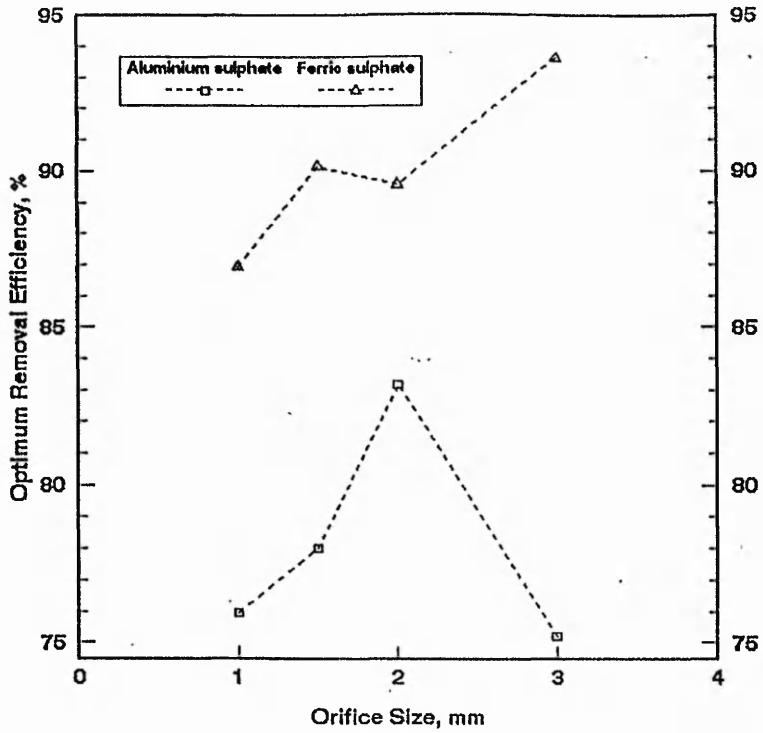

Figure 5.62 Effect of coagulant on removal efficiency (normal flocculation of lycopodium turbidity)

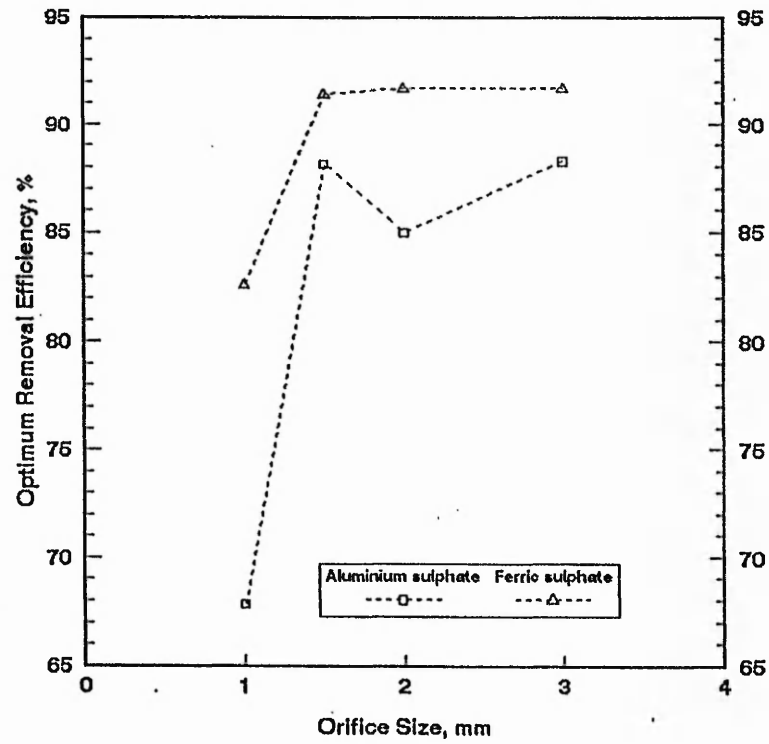

Figure 5.63 Effect of coagulant on removal efficiency (taper flocculation of lycopodium turbidity)

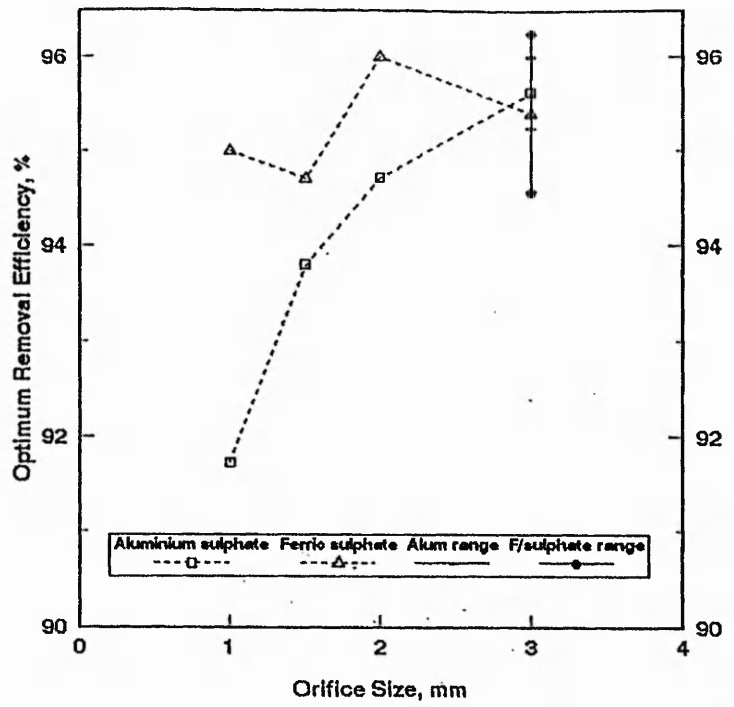

Figure 5.64 Effect of coagulant on removal efficiency (normal flocculation of PVC turbidity)

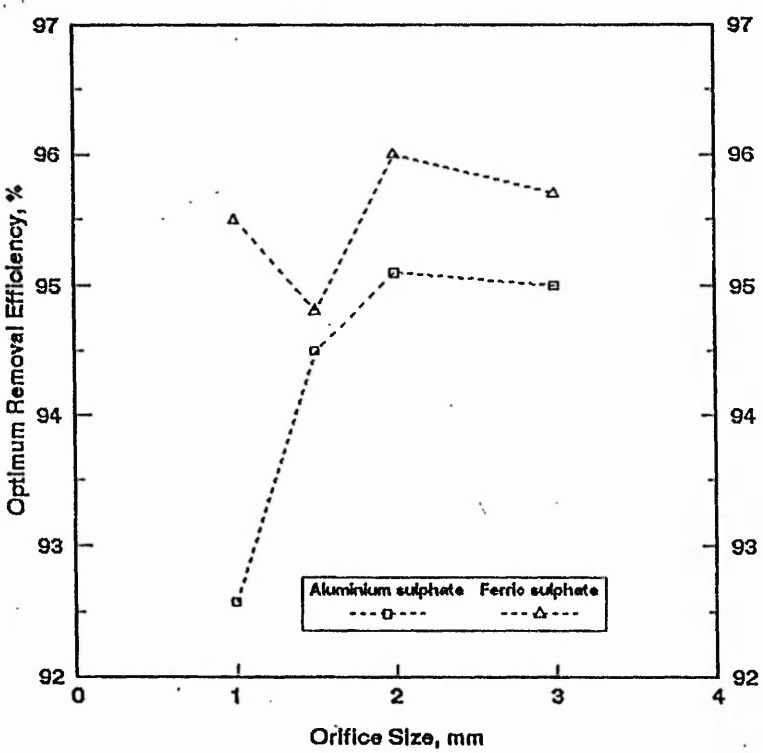

Figure 5.65 Effect of coagulant on removal efficiency (taper flocculation of PVC turbidity)

5.7 EFFECTS OF THE TYPE OF FLOCCULATION

Air was supplied at constant and step-down rates with the aim of investigating the effect of the fixed and tapered energy input in the process of pneumatic flocculation. Experimental data were analysed and the effect of normal and taper agitation on the removal of turbidity are shown in Figure 5.66 to Figure 5.71. Better performances were achieved with taper flocculation either in terms of economy or the process efficiency or both. Normal pneumatic flocculation requires less expertise and knowhow for both operation and maintenance during the running of the plant.

In some cases, as shown in Figure 5.67 and Figure 5.71, removal efficiencies are almost the same for 1.5 and 2.0 mm orifice respectively. In some other cases, as shown in Figure 5.66, Figure 5.69 and Figure 5.70, better removal is obtained in normal flocculation under the same initial conditions. However, when economy is considered, taper flocculation is found to be much better than normal flocculation as lower amounts of coagulants are required to obtain either the same or slight lower removal efficiency as in normal flocculation.

Camp and Stein (1943) stated that the rate of floc formation is directly proportional to the velocity shear gradients. However, high velocity shear gradients can cause the large flocs to be broken by either internal tension or surface shear stress erosion of the flocs or both. Applying the air in several stages with initial high flow-rate and progressively decreasing as the floc particles grow in size, the break of the flocs was prevented with stepping down taper flocculation and better results of turbidity removal were obtained. The application of tapered energy input in coagulation-flocculation process has long been recommended and used as an improved process of turbidity removal over constant energy input, but requires a higher skill and knowhow. The results of this investigation indicate that the consideration of taper agitation in the process of pneumatic flocculation is equally significant and applicable as in other conventional processes of coagulation-flocculation which are generally employed in water treatment industries.

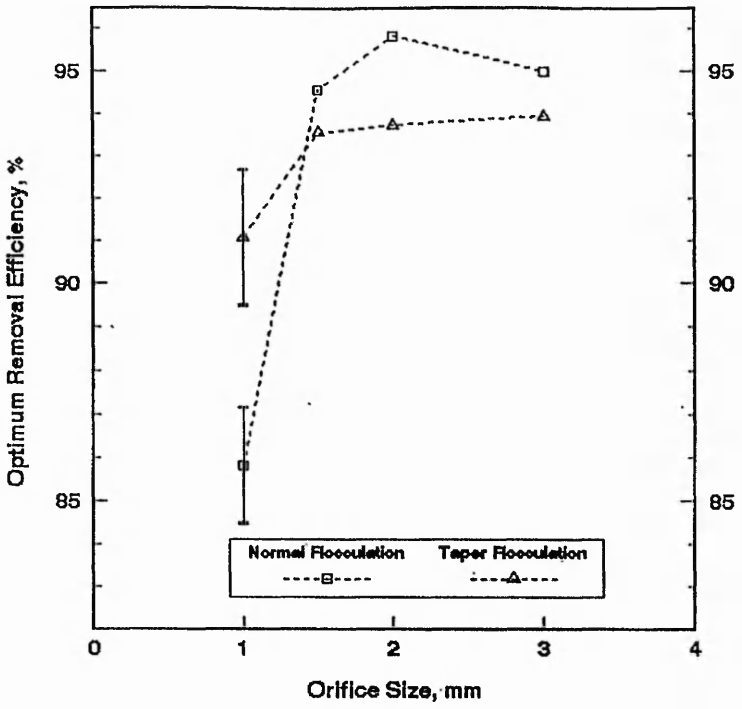

Figure 5.66 Effect of flocculation type on removal efficiency (kaolin with aluminium sulphate)

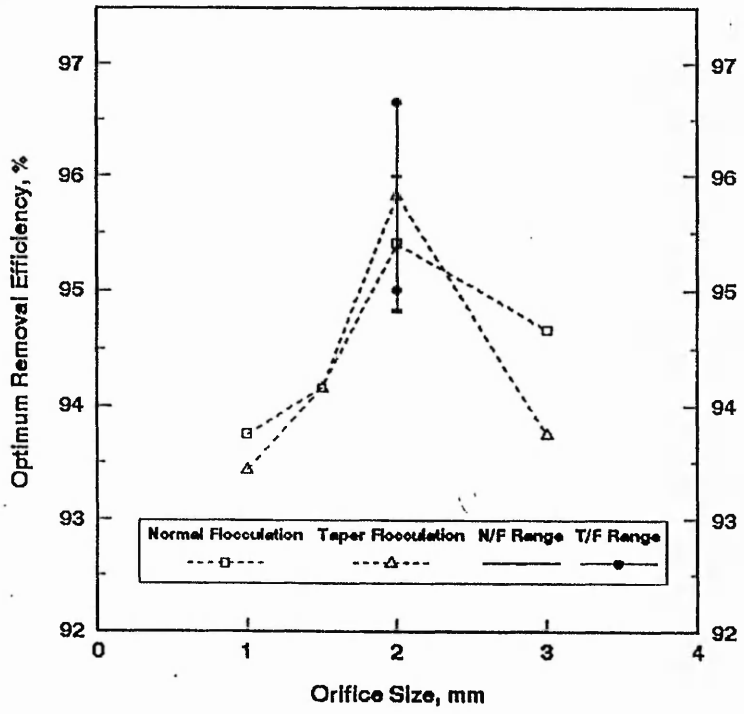

Figure 5.67 Effect of flocculation type on removal efficiency (kaolin with ferric sulphate)

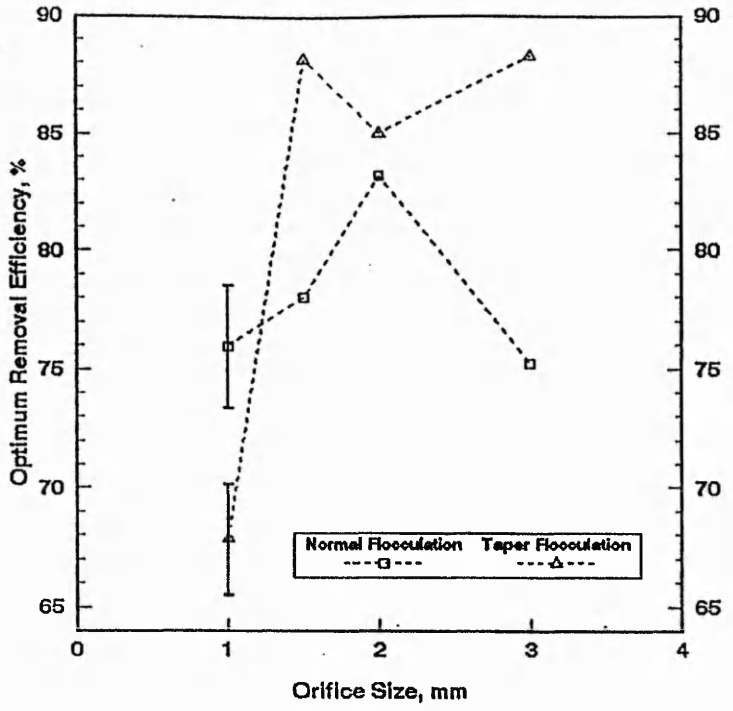

Figure 5.68 Effect of flocculation type on removal efficiency (lycopodium with aluminium sulphate)

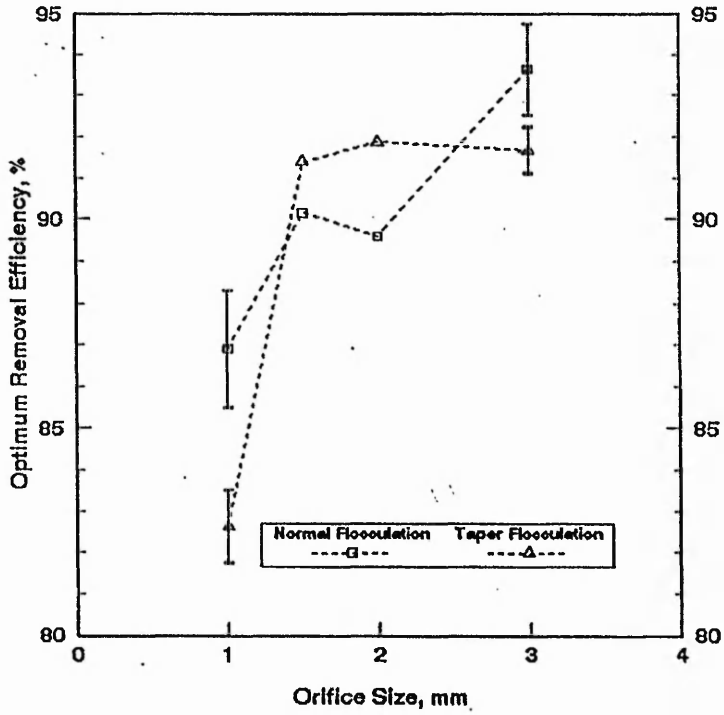

Figure 5.69 Effect of flocculation type on removal efficiency (lycopodium with ferric sulphate)

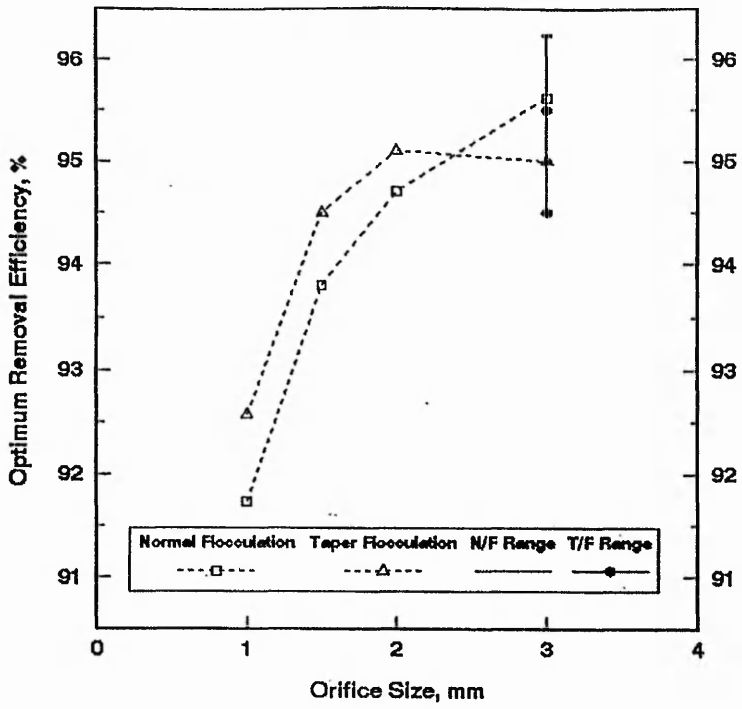

Figure 5.70 Effect of flocculation type on removal efficiency (PVC with aluminium sulphate)

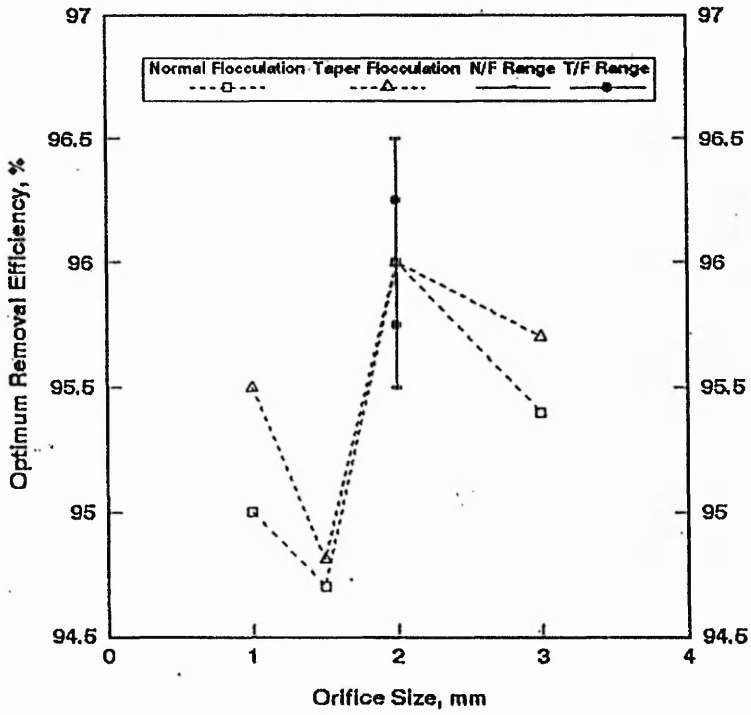

Figure 5.71 Effect of flocculation type on removal efficiency (PVC with ferric sulphate)

5.8 DISSOLVED OXYGEN CONTENT

Dissolved oxygen (DO) was measured by a portable, microprocessor based, M 90 model dissolved oxygen meter, as described in section 3.2.4 (e), before and after the pneumatic coagulation and flocculation process.

Dissolved oxygen of tested water (tap water) and that of flocculated water were recorded for each of the experimental runs as shown in Table (C - 1) to Table (C - 3) in Appendix 5. In almost all of the cases, an increase in the level of dissolved oxygen is found after the pneumatic coagulation and flocculation process. In most cases, an increase of 0.50 to 1.00 mg/l in DO content was recorded, part of which can be seen in Table (C - 1) to (C - 3) in Appendix 5.

The increase of oxygen content enhances the quality of water by inhibiting the anaerobic conditions and also oxidising the soluble impurities. The oxidisable soluble impurities like iron, nitrogen, manganese, aluminium etc. are oxidised, coagulated, flocculated and precipitated, resulting in an improved quality of water.

Thus simultaneous aeration was also achieved by pneumatic flocculation, although it is reported that aeration of water using compressed air through the orifice is of low efficiency (Pattle, 1950). An increase in DO level by diffused air flocculation is also noted by Al-Hiary (1988).

5.9 REMOVAL OF IRON

Total iron content was measured in different stages of the experimental process (tap water, before and after flocculation of turbid water and after settling) by using Hach Spectrophotometer, model DR 2000, based on microprocessor technology and combined with optics and prepackaged reagents for colorimetric analysis. The standard procedure of determining the total iron, as described in the reference (Hach, 1989), was followed and the experimental data was recorded as shown in Table

(C - 1) to Table (C - 3) in Appendix 5.

In almost all cases, a substantial reduction in the amount of iron content after settling was recorded, part of which is shown in Table (C - 1) to (C - 3) as mentioned above. This is attributed to oxidation of soluble iron, transformed into insoluble oxides and precipitated in the process of pneumatic flocculation followed by sedimentation.

A comparison of iron content in tap water and kaolin suspension was made and a higher level of iron content was found in kaolin suspensions. This indicates that kaolin turbidity contained some mineral iron impurities which was liberated due to the solubility. On the other hand, no iron was found to be liberated in lycopodium suspension, however, a trace amount was detected in PVC suspension.

When using alum coagulant, the recommended drinking standard level of iron content (EC Directive, 1980; WHO, 1984) was achieved for all the experimental runs after settling. A higher level of iron content was found in settled water when ferric sulphate was used as coagulant, which needed a further treatment for reducing the iron in order to achieve the acceptable standard as mentioned above. A reduction of iron content from 0.20 to 0.02 mg/l was recorded during the course of the experimental work of this investigation.

5.10 REMOVAL OF NITROGEN

Nitrogen exists in water in four different forms: organic nitrogen, ammonia nitrogen, nitrite nitrogen and nitrate nitrogen. The relative concentrations of the different forms of nitrogen give a useful indication of the nature and strength of the sample. The nitrogen level was measured at different stages of the experimental process in order to evaluate the process efficiency in removing nitrogen. Four measurements of the nitrogen concentration were made. Firstly, of the incoming tap water, as an initial reading; secondly, after addition of turbidity to the tap water; thirdly, after pneumatic

flocculation; and finally after settling. It was measured in the form of nitrate (NO^-_3), which is the final oxidation form of nitrogen by using Hach Spectrophotometer, model DR 2000, as mentioned in section 5.9. The step by step procedure of determining high range nitrate (0 to 30.0 mg/l NO^-_3-N) described in the reference (Hach, 1989) was followed to determine the level of nitrate. The content of nitrate was determined at different stages of the experimental run as shown in Table (C - 1) to (C - 3) in Appendix 5.

It was measured as the total nitrogen in the nitrogen nitrate which was then converted to the equivalent nitrate as NO^-_3. For the whole range of experimental work, a decrease in the total nitrogen concentration was observed during the applied sequence of the four measurements mentioned above. It is obvious that the incoming tap water contains the final stabilised form of nitrogenous matter in the form of NO_3^-.

The reduction in the concentration of nitrogen in the nitrate could be attributed to the adsorption of the ions on the floc particles and ultimately removed with the sludge, leaving the settled water with a lesser concentration of the above mentioned ion. The other possibility is the formation of nitrogenous hydroxide floc which then settles and is removed.

5.11 REMOVAL OF ALUMINIUM

When using aluminium salts as coagulant, the initial and final aluminium concentrations after settling were measured in order to determine the removal efficiency of aluminium by the process of pneumatic flocculation. The procedure described in the reference (Hach, 1989) was followed to determine the level of aluminium at different stages of the experimental runs.

The final concentration of aluminium was always found to be below the maximum acceptable level of 0.20 mg/l (WHO, 1984). This indicates that the pneumatic flocculation process is very effective in removing the aluminium.

CHAPTER 6

DISCUSSIONS AND CONCLUSIONS

The main findings of the experimental and theoretical work of this investigation are discussed in this chapter and also compared and contrasted with that of previous investigators. Based on the theoretical and experimental works and the analysed results, conclusions are drawn afterwards on the process of pneumatic flocculation in water treatment industries.

6.1 Physicochemical properties of the Synthetic Turbidities

Synthetic turbidities were homogeneously dispersed using the Ultra-Turrax T25 S7 Homogeniser as described in section 3.2.4(a), following the procedure described in section 3.7 in order to produce the reproducible suspension of discrete particles. During the preparation of the suspension it was borne in mind that the shearing intensity and mixing time would change the nature of the suspension. This view was confirmed by the author during the early stages of the experimental work for preparation of the calibration curves of synthetic turbidities. It is significant to mention that the use of the dispersing agent was avoided in this research work. This was due to the belief that the dispersing agent could influence the physical and chemical behaviour of the coagulation and flocculation process. In order to produce reproducible, homogeneous, discrete particle suspension, the shearing intensity was kept constant (8,000 rpm) over a constant period of time i.e. 120 seconds. In the shearing gap between rotor and the stator of the homogeniser, about 1000 times more energy was introduced into the suspension medium than in normal mechanical stirring as mentioned in section 3.7 and it is believed that the particles of synthetic turbidities were suspended discretely in the suspension and there was no possibility

of the cluster of particles in the suspension.

The suspensions are used immediately after preparation in order to avoid any physicochemical change in the nature of the turbidity. This change in nature is particularly significant for lycopodium turbidity, because lycopodium swells during the wetting process. This swelling was observed at the time of the determination of the density of lycopodium with a Coulter Counter.

The size range of the particles given by the suppliers was verified by the electronic scanning microscope using the wet method of preparation as mentioned in section 3.3 and shown in Table 3.3. It was taken into consideration that the fineness of the particles that comprise the turbidity material is an important variable in coagulant demand (Kawamura, 1976). Langelier *et al.* (1952) stated that particles of 1-5 μm in diameter serve as suitable structural units for building up a dense, rapidly settling floc. Particles of about 1 μm provide a binding action for flocculent growth, resulting in a porous bulky floc with a very slow settling velocity when alum is used as a coagulant. If both fractions of particle size exist in water, good flocs would occur and when raw water lacks either the colloidal or the coarse fraction, it is recommended that the particle size distribution be adjusted by adding a colloidal clay or other suitable material (Kawamura, 1976).

Cyclofloc units developed in Europe use micrograin sand (the diameter of grains are a few tens of a micron) for seeding purposes with polymer and actual treatment units have shown good results (Gomella, 1974; Sibony, 1981).

The physicochemical properties of the synthetic turbidity materials influence the process of pneumatic flocculation in removing the turbidity from water. Due to the difference in the physicochemical properties of different types of the synthetic turbidities, contrasting behaviour of kaolin, lycopodium and PVC has been observed during the experimental work of this investigation.

The maximum removal efficiencies are achieved with PVC turbidity in comparison

to kaolin and lycopodium, although the operating water height was reduced to 2000 mm from 2400 mm as explained in section 3.2.1. As the removal efficiency also depends on the height of the water column (Weber, 1972), it could be said that more removal efficiency could be obtained if the same water height was maintained as for kaolin and lycopodium, i.e. 2400 mm.

The experimental results indicate that PVC was able to produce more settleable floc than kaolin and lycopodium. This phenomena could be explained with respect to the colloidal size or fineness of the particles. As shown in Figure 3.20 and 3.23, the size range of the PVC particles was the smallest i.e. 0.5 to 1.5 μm and thus the particles had the largest specific surface area to react with the counter-ions of the coagulant species. As a result, more suspended particles were destabilised to produce settleable flocs and the better removal of turbidity was achieved. The growth of individual particles enhances removal rates, because the larger particles created a reduced surface-area-to-mass ratio and thus the drag forces opposing subsidence were reduced (Weber, 1972).

The particles of lycopodium turbidity were comparatively coarser, with a uniform size of 35 μm as shown in Figure 3.19 and 3.22 and less removal was noticed in this case. Settling of lycopodium flocs was found to be much slower than that of kaolin and PVC. This is attributed to the low density of lycopodium turbidity in association with aluminium sulphate coagulant and the grouping of lycopodium flocs with micro bubbles of gas and air.

Lycopodium turbidity was found to show somehow a different settling behaviour to that of kaolin and PVC suspension. When lycopodium turbidity was coagulated and flocculated with aluminium sulphate under normal agitation, a high fluctuation in removal efficiency with the air flow rates was observed. This indicates that the lycopodium flocs when coagulated with alum, are very sensitive to the power variation due to their physicochemical properties.

6.2 Settling behaviour of Synthetic Turbidities

The removal efficiency of all types of synthetic turbidities increased steeply in the first 30 minutes of settling as shown in Figure 5.4 to Figure 5.31. Between 60 to 90 minutes, a noticeable decrease in the increasing of removal efficiency was observed, then the curve tended to become asymptotic for all types of synthetic turbidities and all sizes of the orifice diameters. Towards the end of 120 minutes of settling time, the removal efficiency tended to come closer to one value of efficiency after which there was insignificant change in the improvement of water quality. Al-Hiary (1988) reported the same nature of settling in removing silica and kaolin turbidity coagulated with alum using diffused air as power in mixing.

From the experimental results and previous investigations, it is evident that the removal efficiency tends to become the same at a longer settling time irrespective of the type of synthetic turbidities and orifice sizes.

A unique settling behaviour was observed which occurred from the combination of: the low density of the lycopodium; the aluminium sulphate coagulant; the associated micro air bubbles produced during the application of pneumatic flocculation; and, the carbon dioxide gas bubbles generated by the chemical reaction of the natural alkalinity and the coagulant used. It is possible that these four factors all contributed to the formation of three groups of lycopodium-aluminium sulphate floc particles as shown in Figure 5.1.

The settling behaviour of lycopodium turbidity coagulated with aluminium sulphate under normal flocculation showed a unique behaviour due to the formation of these three groups of flocs as, described in section 5.2. When dealing with this type of flocculated suspension of lycopodium turbidity, the settling behaviour was observed to be somehow different to other denser synthetic turbidities because of the micro bubble entrapment in the agglomeration of porous floc particles. A slow moving layer of higher floc concentration formed, resulting from the combination of the floc cluster of group 1 and group 2, and settled as a whole mass rather than settling as

an individual floc agglomeration as shown in Figure 5.2. As a result of this type of settling behaviour, differently shaped isoconcentration curves were obtained as shown in Figure 5.3.

The nature of the settling curve of the moving layer, represented by curve $A\text{-}A^1$ in Figure 5.3, indicates that, as the settling time progresses, the developed moving layer is going downward as a whole mass in the settling column. In such a case, removing efficiency was calculated considering the isoconcentration lines above the curve $A\text{-}A^1$ as shown in Figure 5.3.

To conclude, the author believes that the physicochemical properties of the synthetic turbidities, e.g. the nature, shape, size, density, shearing strength etc., are all significant in the study of pneumatic flocculation. The effect of the hydrodynamic behaviour of the rising bubble is also influenced by those properties, which will be discussed later.

6.3.1 Coagulant Concentration

The optimum doses of coagulants were determined by the jar test as described in section 3.6 and shown in Table 3.7. At the time of preparing the coagulant solution, it was considered that the alum solution concentration is a significant factor in coagulation-flocculation. Some investigators revealed that there is a relationship between alum concentration and the residual turbidity following flocculation and sedimentation (Kitano and Kawamura, 1954; Griffith and William, 1972; Letterman *et al.*, 1973; Kawamura, 1976). Kawamura (1976) stated that it is generally agreed that the concentration of alum solution to be fed to raw water should be low (<0.5 per cent solution). In order to obtain the best result, a 0.5 per cent alum solution was used in this investigation. Griffith and William (1972) showed that reasonable dilution might offer some mixing advantages that promoted rapid and uniform coagulant dispersion. They showed that dilution of alum down to 1.5 per cent solution did not impair its effectiveness as a coagulant.

Walker (1971) performed extensive tests and demonstrated the practicability of dilution to about a 0.6 per cent alum solution. However, below a dilution of about 0.3 per cent Walker (1971) found a "decisive fall-off in coagulation effect".

Kawamura (1973) tested the effect of ferric sulphates and ferric chlorides concentration on flocculation, but no significant difference was detected with the limited number of tests performed. Therefore, about 0.5 per cent ferric sulphate solution was used in this investigation.

6.3.2 Location of the Point of Application of coagulant

The importance of the location of the point of application of coagulant solution was considered during the experimental work of this investigation. In the experimental work conducted by Moffett (1968), it was found that 27 per cent more alum was required to obtain zero zeta potential when the coagulant was introduced on the surface of water rather than at the agitator blade level of a Phipps-Bird jar tester. However, Kawamura (1973) believed that the reported big difference in required alum could become insignificant if a low or a high concentration alum were fed into the more efficient type of mixing unit.

Coagulant solution was added at the top of the water surface in 0.5 per cent solution and was mixed vigorously for 120 seconds. It is believed that this concentration of the coagulant solution and the mixing efficiency by diffused air did not affect significantly the location of the point of application of the alum solution.

6.4 Rapid Mixing Time and Intensity

The main objective of rapid mixing was to disperse the coagulants uniformly and intimately throughout the volume of water in order to allow adequate contact between the coagulant and the suspended particles prior to completion of hydrolysis. The mixing time of coagulants, t, and the intensity of mixing, i.e. velocity gradients,

G, were considered as the controlling (design) parameters in rapid mix operation.

Although the reactions which occurred in the destabilisation of the colloidal particles are very rapid, they are believed to occur in less than a second (Weber, 1972), the rapid mix detention times of 30-60 seconds are traditional. According to a survey of 15 water treatment plants reported by Hubbell (1969), a rapid mix time of 1.9 minutes was being used in water treatment industries. Letterman *et al.* (1973) found in their studies that the optimum rapid mix time is 9 seconds to 2.5 minutes for a turbidity range of 10 to 100 mg/l with a *G* value of 1000 s^{-1}. The theoretical detention time is much less than that adopted in treatment plants for many reasons such as the quality of raw water, intensity of mixing, prevention of short-circuiting flow, type, dose and concentration of coagulants etc. Several ranges of the *G* values from 250 to 1000 s^{-1} were suggested by the previous investigators, which are shown in Table 2.1.

Based on the theory and from a practical point of view as discussed above, it was decided to work with a rapid mix detention time of 120 seconds, both in mechanical stirring (Jar test) and the diffused air agitation (Pneumatic flocculation), throughout the experimental work of the present investigation. The corresponding *G* values of 690 s^{-1} and 300 s^{-1} were applied for the mechanical and pneumatic agitation respectively.

An air flow rate of 38,000 cc/min. was applied during the operation of the rapid mixing in pneumatic coagulation-flocculation. The corresponding mixing intensity, at a *G* value of 300 s^{-1}, was hoped to be enough to disperse the coagulant thoroughly and homogeneously throughout the chamber to produce appreciated settleable flocs after slow mixing under initial standardised conditions.

6.5 Slow Mixing in Pneumatic Flocculation

A slow mixing duration of 20 minutes with low rates of air flow ranging from 50

to 1000 cc/min. was applied for flocculation in this investigation. The corresponding G values standardised at 20°C ranged from 10.65 to 30.65 s^{-1}.

For slow mixing, mean G values of between 20 and 100 s^{-1} and flocculation times of 20 to 40 minutes are commonly used (Barnes *et al.*, 1981). The recommended values of flocculation time are 20 to 60 minutes and that of G are 5 to 100 s^{-1} (AWWA, 1969). Camp (1955) has reported that the G value ranged from 20 to 74 s^{-1} and the flocculation time ranged from 10 to 100 minutes for 20 operating water treatment plants in USA.

The slow mixing time and the intensity of mixing were also studied by many other investigators (Black *et al.*, 1961; Argaman and Kaufman, 1970; Ives and Bhole, 1973). Hudson (1965) has noted that previous publications have indicated the existence of a maximum velocity gradient. Mixing intensities beyond this maximum appeared to be detrimental to floc formation (Villegas and Letterman, 1976). Several publications (Camp, 1955; Griffith and William, 1972; Letterman *et al.*, 1973) have noted the observation of an optimum velocity gradient. The optimum value of G and flocculation time t, depend on the chemical composition of the water and the nature and amount of colloids present; this optimum G tends to decrease with increasing turbidity (Barnes *et al.*, 1981). Kawamura (1973) also observed an optimum mixing intensity in his work which, in general, decreased as the alum concentration was increased.

Considering the factors and conditions highlighted above, the author of the present investigation believes that the duration of 20 minutes and the intensity of slow mixing of 10.65 to 30.36 s^{-1} applied in this investigation were reasonable and quite similar to that used in the practical field in water treatment industries.

To indicate the intensity of turbulence and the degree of flocculation, many investigators used the dimensionless product of G and t, sometimes called "Camp Number". It is more convenient to use the Gt value in the sense that just any number can be used. The optimum value of Gt was set between the limits of 10^4 and 10^5 in

order to achieve a satisfactory flocculation based on observational data from twenty water works in the USA (Camp, 1955). Practical experience by Kawamura (1958) has indicated that a *Gt* value of 4.5×10^4 usually results in satisfactory alum flocculation. In the present investigation, a range of *Gt* value of 1.27×10^4 to 5.72×10^4 was used, as shown in Table 3.8, throughout the experimental work.

In taper flocculation, an equivalent amount of *Gt* to that used in normal flocculation for a particular air flow rate was applied with successively decreasing velocity gradients in several stages as described in section 3.8 and shown in Table 3.8. The calculations for *Gt* distribution in Table 3.8 were based on a standardised temperature of 20^0C. This was taken into consideration as *G* values were applied with a little error due to change in temperature, it was not possible to keep the water temperature constant at 20^0C during the experimental runs. However, a temperature standardisation was made for the calculation of optimum velocity gradient and for further analysis of the experimental results as shown in Table 5.13.

Ives (1978) mentioned that the Camp Number, *Gt*, is not a sufficient criterion to cover all cases of flocculation, particularly those of the floc blanket clarification. To overcome this shortcoming it was suggested that the effect of particle or floc concentration should be included in any assesment of flocculation adequacy. Ives (1981) and others have pointed out the need to include the volume concentration of suspended particles in the dimensionless product yielding *GtC*, where *C* is the suspended particles volume concentration. He suggested a design value for *GtC* of about 100 for solid contact clarifiers. However, in the present work *C* was kept constant so only *Gt* is used.

Edzwald (1993) has recently discussed the characteristics of the effectiveness of the flocculation process. O'Melia (1972) argued that particle stability should be included in the dimensionless product yielding $\alpha_p GtC$. Edzwald and Lawler (1983) suggested that good flocculation (prior to conventional settling) occurs when $\alpha_p GtC$ is 1 or greater. Edzwald (1993) used a 30 minute flocculation time and a *G* of 50 s^{-1} for the Cyclotella suspension, giving a product of 0.1 for $\alpha_p GtC$, where α_p is the collision

efficiency factor, in which improving flocculation can be accomplished by increasing C or t.

The conception of these two groups of dimensionless products was not applied in the present investigation because of the constant initial concentration of the particles throughout the experimental work.

6.6 Air Flow Rates

Different air flow rates of 50, 100, 200, 300, 400, 500, 600, 800 and 1,000 cc/min. were applied in the slow mixing process as described in section 3.8 and shown in Table 3.8 with the aim of investigating the optimum air loadings for turbidity removal under different initial conditions. For rapid mixing, a single air flow rate of 38,000 cc/min. was applied for all cases without exception. This flow rate corresponded to a G value of 300 s^{-1} which was hoped to be enough for uniform and homogeneous dispersion of coagulant throughout the column of water. Some preliminary experimental work indicated that this air loading in rapid mixing produced appreciable flocs in the slow mixing phase that can be settled easily by sedimentation, even though the intensity of this mixing was much less than that in the jar test (690 s^{-1}).

After examining all the values of air flow rate to produce the optimum removal of turbidity for each experimental set, as shown in Table 3.10, by pneumatic flocculation, it was found that the frequency of the rate of air flow of 100 cc/min. prevailed over the others in 20 cases out of 48.

It is imperative to state here that in the case of taper flocculation, the relationship of removal efficiencies with air flow is plotted with the amount of air flow rate, which is equivalent to the dimensionless product of the velocity gradient and mixing time in normal flocculation. The taper flocculation time of four minute intervals and the successive decrease of the air flow rate produces the same amount of Gt value

used under normal flocculation as shown in Table 3.8.

Experimental results and the analyses revealed that an optimum air flow rate would produce an associated maximum removal efficiency under the recorded initial conditions. The air flow rates and the corresponding removal efficiencies for different experimental conditions are shown in Table 5.1 to Table 5.12.

It was found that each curve would produce a lower and upper optimum air flow depending on its oscillation. In some cases, the upper optimum air flow rate was found to be in the higher range, say, 500 cc/min. (Figure 5.32), it is evident that this optimum was not the first peak. As mentioned in section 5.3, that special care was taken in applying a low air flow rate, 50 cc/min., which produced a lower efficiency and the plotted point did not show a peak. It was unfortunate that the practical range of the flowmeters used could not go below a 50 cc/min.; under such circumstances the first peak could not be reproduced and the air flow rate of 50 cc/min. was considered to be the first peak of removal efficiency.

In other cases, as shown in Figure 5.33 to Figure 5.43, two peaks of removal efficiency at two different air flow rates were found. This phenomenon could be explained in the light of destabilisation and restabilisation of the flocs at different air flow rates. Although the initial rate of floc formation is proportional to the air flow rates, the higher air flow rates generate high-velocity shear gradients that cause large flocs to be broken as a result of either internal tension, or surface shear stress erosion, or both. Afterwards, when a high air flow rate is applied, finer and smaller floc particles are reformed again.

It is well known that better removal has been achieved upon increasing the power input (Tekippe and Ham, 1971; Al-Hiary, 1988; Dharmappa, 1993). This is due to the reformation of the broken flocs and better compaction characteristics of the new and existing flocs. Also, adsorption rate of micro-flocs on large ones and collision rates between the micro-flocs themselves are increased. Furthermore, Fair and Gemmell (1964) have found from their studies that the floc growth process is

oscillatory with respect to the product *Gt*, or *G* for constant flocculation period.

For the best economical situation, the first peak removal efficiency yields the lowest air flow and produces a lower energy requirement, the overall efficiency difference with other peaks is insignificant.

In fact, there is a maximum size of floc particles associated with each velocity gradient and the removal efficiency depends on the size of floc formed. The rate of air flow required to coagulate and flocculate the colloidal suspension is greatly dependent on the nature of the turbidity. Experiments by Hubley *et al.* (1950) showed that suspension of aged latex particles in water had very little tendency to flocculate at a *G* exceeding 10 s^{-1}, whereas suspension of wood pulp fibres required *G* in excess of 50 s^{-1} to break up the flocs appreciably.

Al-Hiary (1988) conducted his experiments with a range of air flow from 200 to 10,000 cc/min. He found the working range for silica to be 1000 to 2000 cc/min. and that for kaolin to be 400 to 1000 cc/min. In the present investigation, the working ranges of air flow rate were found to be 50 to 300 cc/min. for kaolin and lycopodium turbidity and 50 to 400 cc/min. for PVC turbidity, which are much lower than those of Al-Hiary's work. Al-Hiary (1988) did not conduct the experiments with a low range of air flow rate down to 200 cc/min. and possibly he missed obtaining the first peak as discussed above. McConnachie (1984) found an optimum air loading of 0.16 cc/sq.cm-min. in removing the kaolin turbidity while he conducted the experiment with a chamber of 92 mm internal diameter and a depth of 315 mm. If this optimum air loading of 0.16 cc/sq.cm-min. is compared and converted to the air flow rate for the present experimental chamber, it would become 103.44 cc/min. which is almost equivalent to the optimum air flow rate in most of the cases in the present investigation.

To conclude, it can be said that the pneumatic flocculation process is very effective even at low range of air flow rate.

6.7 Impact of Orifice Sizes

The performance of different sizes of orifice show the same trend of settling behaviour of flocculated particles under all the initial experimental conditions. The best settling was obtained in almost all cases with the orifice size of either 1.5 or 2.0 mm. A 1.0 mm orifice size pad results in the worst settling of different types of synthetic turbidities. In the case of using a larger size of orifice of 3.0 mm, the removal efficiencies are almost the same both for kaolin and PVC turbidity.

The settling behaviour of turbidities flocculated by diffused air through different sizes of orifice indicates that a relationship exists between the physicochemical properties of the turbidity materials and the size of the air bubble (and hence the size of the orifice).

From the optimum removal point of view, the best results in removing kaolin and lycopodium turbidity were found with the orifice sizes of 1.5 or 2.0 mm. When PVC turbidity is coagulated with alum, better removal efficiency was obtained with higher sizes of orifice. On the other hand, when PVC was coagulated with ferric sulphate, a minimum optimum removal efficiency was found with a 1.5 mm orifice although a better removal with more acceptable removal efficiency was obtained when a 1.0 mm orifice size was used. A second peak in optimum removal efficiency was obtained with 2.0 mm orifice. However, the corresponding size of the orifice of these optimum removal efficiencies, i.e. 2.0 mm, was not considered as the best size for turbidity removal from an economic point of view, to yield a lower energy value as discussed previously.

McConnachie (1984) conducted an experiment of the same nature as the present investigation with kaolinite suspension using a coagulating-flocculating chamber of 92 mm internal diameter and a height of 315 mm. He confirmed the use of bubbles as a source of mixing for flocculation. However, he used three different bubble sizes, 0.2 to 0.5 mm, 0.5 to 1.5 mm and 1.5 to 4.0 mm effective diameter, using a sintered glass filter funnel of maximum pore diameter of 5 - 10 μm and a 0.9 mm diameter

hypodermic needle. Obviously, in his case, the bubbles were not uniform in size as he used different ranges of bubble size. At the end of his investigation, he concluded that the efficiency of flocculation was affected by the size of the bubble and out of the three size ranges used, 0.5 to 1.5 mm gave the best turbidity removal.

Al-Hiary (1988) conducted experimental work to study the validity of using optimal introduced air flow rates and orifice diameter in the process of diffused air flocculation. Perforated metal pipes were used as the diffusers and four different sizes of orifice 1.0, 2.0, 3.0 and 4.0 mm in diameter and different air flow rates ranging from 200 to 10,000 cc/min. were applied in his investigation. Al-Hiary (1988) performed the experiments to remove silica and kaolin turbidity coagulated and flocculated with aluminium sulphate under normal agitation. He found the best removal of silica with a 1.0 mm orifice diameter and that of kaolin with a 3.0 mm orifice diameter. The removal of kaolin with a 2.0 mm orifice diameter was found to be almost the same as that with a 3.0 mm orifice diameter. Therefore, in his case, the range of the effective diameter of the orifice was found to be 1.0 to 2.0 mm diameter, in removing the kaolin and silica turbidity.

From the experimental results of the present investigation and the discussion above, it can be concluded that for each combination of the initial conditions, there exists an optimum size of orifice, corresponding to the intensity of local maximum velocity gradients produced by different sizes of the bubble associated with this orifice size and also the physicochemical properties of the turbidity materials.

The experimental data and analysis of results revealed the existence of an optimum size of the orifice in removing any of the turbidities in the pneumatic flocculation process. This phenomenon is related to the size, shape, path followed by the bubbles, frequency and velocity of the rising air bubbles which originated from different sizes of orifice and also to the properties of the synthetic turbidities used and eventually normal and taper mixing. In fact, the optimum size of the orifice depends on the unique combination of the initial conditions like the nature of the turbidity and coagulants, type of flocculation, rates of air flow etc. The intricate phenomena of the

released air bubble might have a significant effect on the pneumatic flocculation and is a separate field of research.

It can be seen that the optimum removal efficiency was achieved with a relatively larger size of orifice (say, 1.5 and 2.0 mm diameter) at any constant air flow rate. This indicates the removal efficiency was controlled by orifice sizes and hence by the size of rising bubbles even with a constant intensity of mixing. This could be associated with the hydrodynamic behaviour like shape, size, path, frequency and rising velocity of the bubbles and their impact on mixing process and ultimately on the removal of turbidity from water. The impact of these parameters cannot be interpreted unless the hydrodynamic behaviour of the rising bubbles is well studied and their relative tendencies to coagulate and flocculate the turbidity are known.

Another research project to study the hydrodynamic behaviour of rising bubbles and their impact on turbidity removal has been initiated by the Department of Civil and Structural Engineering, The Nottingham Trent University. The research programme is being carried out under the direction of Dr. I.H. Sholji and it is expected that the outcome of the investigation will be beneficial and useful to interprete the hydrodynamic aspects of rising bubbles related to pneumatic flocculation.

6.8 Effects of the Type of Flocculation

The application of taper energy input in the flocculation process has long been known and used as an improved process of turbidity removal over constant energy input (Langelier, 1921; Priesing, 1962; Walker, 1968; Kawamura, 1976; McConnachie, 1984). Recently, some investigators recommended the process for better results in removing the turbidity from raw water (Ives, 1974; Bhargava and Ojha, 1993; McConnachie, 1993).

Experiments were conducted in which air was supplied at step down rates with the aim of investigating the effect of taper energy input over fixed energy input in the

process of pneumatic flocculation. From experimental data and analyses as shown in Figure 5.66 to Figure 5.71, it is evident that better performances were achieved with taper flocculation either in terms of economy or the process efficiency or both.

In some cases, removal efficiencies were found to be almost the same either in taper or normal flocculation. In some other cases, better removal was obtained in normal flocculation under some initial conditions. However, when economy was considered, taper flocculation was found to be much better than normal flocculation as lower amounts of coagulant were required, as shown in Table 3.7, to obtain either the same or slightly lower removal efficiency as the normal flocculation.

McConnachie (1984) also studied the effect of taper energy input using large bubbles at higher air flow rates followed by small bubbles at lower air flow rates. In his study, the lowest residual turbidity of kaolin was produced by tapered agitation. He confirmed the use of bubbles as a source of mixing for flocculation with taper agitation giving significant improvement in efficiency over fixed agitation.

Camp and Stein (1943) stated that the rate of floc formation is directly proportional to the velocity shear gradients. However, high velocity shear gradient can cause the large flocs to be broken by either internal tension or surface shear stress erosion of the flocs or both. Applying the air in several stages with an initial high flow rate which progressively decreased as the flocs particles grew in size prevented break up of the flocs and better results of turbidity removal were obtained.

The experimental results and analysis of this investigation and the above discussion indicate that the consideration of taper agitation in the process of pneumatic flocculation is equally important and significant and also applicable as in other conventional processes of coagulation-flocculation which are generally employed in water treatment industries.

6.9 Effects of Coagulants

Aluminium sulphate and ferric sulphate were used to destabilise the colloidal suspended particle with the aim of investigating the effect of different types of coagulants on pneumatic flocculation. In most cases, as can be seen from Figure 5.60 to Figure 5.65, the better removal of turbidity was achieved when ferric sulphate was used as the coagulant. This could be attributed to the physicochemical properties of the coagulants. Ferric sulphate is denser than aluminium sulphate and thus the flocs produced with ferric sulphate could be heavier than that of aluminium sulphate, settle faster and result in better removal of turbidity from water.

Aluminium sulphate is the most widely used water treatment coagulant (Edzwald, 1993) and popular because it is relatively inexpensive and the water treatment industry has experience and confidence in use of alum (Dempsey, 1995). It was the traditional coagulant used in water treatment industries before the advent of ferric sulphate. Ferric sulphate is now increasingly becoming the coagulant for the replacement of aluminium sulphate or for new treatment plants in U.K. because of its effectiveness, particularly for the removal of humic and fulvic acids from waters (Water Services, 1975).

In the pneumatic flocculation process, ferric sulphate is expected to produce a better perfomance over aluminium sulphate in water treatment industries. However, a higher level of iron content was found in settled water when ferric sulphate was used, which needed a further treatment for reducing the iron in order to achieve the acceptable standard. This will be discussed later.

6.10 Dissolved Oxygen content

The level of dissolved oxygen (DO) was measured at different stages (before and after pneumatic flocculation) of the experimental run as described in section 5.8. In almost all cases, an increase in the level of dissolved oxygen was found after the

pneumatic coagulation-flocculation process. In most cases, an increase of 0.50 to 1.0 mg/l in DO content was recorded. Dissolved oxygen content was increased due to aeration of water when coagulated and flocculated by diffused air. An increase in the level of dissolved oxygen in water while flocculating with diffused air was also noticed by Al-Hiary (1988). In his case, the water almost reached saturation level in the prevailing laboratory conditions. Thus, simultaneous aeration was achieved by pneumatic flocculation, although it is reported that aeration of water using compressed air through orifice is of low efficiency (Pattle, 1950).

Oxygen is a most important element in water quality control (Tebbutt, 1983). All aerobic treatment processes depend upon the presence of dissolved oxygen (Sawyer and McCarty, 1978). Increasing the oxygen content is favourable, especially if the water is organically polluted, or in the case of treating groundwater. The increase of oxygen content enhances the quality of water by inhibiting the anaerobic conditions and also oxidising the soluble impurities. The oxidisable soluble impurities like iron, nitrogen, manganese, aluminium etc. are oxidised, coagulated, flocculated and precipitated, resulting in an improved quality of water. However, a high level of dissolved oxygen is a significant factor in the corrosion of iron and steel, particularly in a water distribution system and in steam boilers (Sawyer and McCarty, 1978). Such higher levels of oxygen content was not experienced in the present investigation and would not be expected in practice.

6.11 Removal of Iron

The level of iron content was measured at different stages (tap water, turbid water, flocculated water and settled water) of the experimental run with the aim of investigating the reduction in iron content by pneumatic flocculation, as discussed in section 5.9.

A higher level of iron content was found in the kaolin suspension when compared with that of tap water. This indicated that kaolin contained some mineral iron

impurities which were liberated in the suspension due to the solubility. No iron was found to be liberated in the lycopodium suspension but a trace amount was detected in the PVC suspension.

A substantial reduction in the amount of iron content was recorded after settling. This was attributed to the oxidation of soluble iron, transformed into insoluble oxides and precipitated in the process of pneumatic flocculation followed by sedimentation.

In the case of using alum coagulant, recommended drinking standard level of iron content i.e. 0.3 mg/l (WHO, 1984) or 0.05 mg/l (EC Directive, 1980) was achieved in all cases after settling. A higher level of iron content was found in settled water when ferric sulphate was used as the coagulant, which needed further treatment for reducing the iron in order to achieve the acceptable standard mentioned above.

A reduction of iron content from 0.20 to 0.02 mg/l was recorded during the course of the experimental work of this investigation.

6.12 Removal of Nitrogen

The level of total nitrogen converted to NO^-_3 was measured at different stages of the experimental process, as described in section 5.10, in order to evaluate the process efficiency in removing nitrogen. It was measured in the form of nitrate nitrogen (NO_3^--N) which is the final oxidation form of nitrogen.

Almost a 50% reduction in nitrate nitrogen was found in settled water. This could be attributed to the floc removal and precipitated by sedimentation.

Several methods are available to reduce the nitrite-nitrate concentration. Two common processes are demineralisation and biological removal under controlled conditions using denitrifying bacteria. Ion-exchange with Cl^- is also used at full-scale. It is expected that the process of pneumatic flocculation can be applied to

reduce the nitrite-nitrate concentration in large scale treatment of water. Further investigation is required in this aspect.

6.13 Level of Aluminium

The level of aluminium was measured at different experimental stages described in section 5.11. When aluminium sulphate was used as the coagulant, the final aluminium concentration was recorded in order to investigate the reduction of aluminium by pneumatic flocculation followed by sedimentation.

Ideally water going into supply should contain less than 0.05 mg/l aluminium as Al, with a maximum acceptable concentration of 0.2 mg/l (Twort *et al.*, 1985). Levels of aluminium in the final water above about 0.3 mg/l usually reflect faults in the coagulation, flocculation and sedimentation or filtration stages of treatment (WHO, 1984).

The final concentration of aluminium was always found to be below the recommended level of 0.20 mg/l (WHO, 1984). The experimental results indicate that the pneumatic flocculation process is very effective in removing the aluminium and there are no faults in coagulation, flocculation and sedimentation process.

6.14 Rising Velocity of Air Bubbles

The velocity of rising bubbles has been studied both theoretically and experimentally by a large number of investigators in the field of hydrodynamics (Datta *et al.*, 1950; Peebles and Garber, 1953; Garner and Hammerton, 1954; Haberman and Morton, 1954). A limited theoretical approach was mentioned by Camp (1955) and others (Bratby, 1980; Ives, 1981) to evaluate the rising velocity of the bubble through fluid using the well known Stokes' formula:

$$v_r = \frac{1}{18}\frac{g}{\mu}(\rho_a - \rho_w) d_b^2 \qquad (2.5)$$

However, neither the shape of the bubble nor the flow field around the bubble in the present investigation were observed to be conformable to Stokes' law, since the bubbles were found not to be spherical (visual observation) and the flow was found not to be laminar (shown in section 4.3) which are the two basic conditions of the Stokes' law.

A series of experimental observations were made of the motion of an air bubble in water under different initial conditions as described in section 4.3. The average rising velocity of the air bubble has been found to be in the range of 26.10 to 45.30 cm/s depending on the air flow rate and the size of the orifices. The impact of orifice size and the air flow rates has been discussed previously. The relationship of the bubble rising velocity with the size of orifice and the rate of air flow indicates that the bubble rising velocity is somehow related to the removal of turbidity in diffused air flocculation. The impact of the rising velocity of air bubbles on removal of turbidity in pneumatic flocculation cannot be established unless the hydrodynamic behaviour of the rising bubbles are studied as mentioned previously.

In general, rising velocity increases with increasing the rate of air flow and the size of the orifice. However, there exists an optimum air flow rate corresponding to the maximum rising velocity for all sizes of orifice as shown in Figure 4.6.

6.15 Flow Field around the Bubbles

An attempt was made to predict the flow condition around the rising bubble with the aim of investigating the hydrodynamic behaviour of the rising bubble and to correlate this with the process of pneumatic flocculation. Experiments were conducted under different initial conditions to determine the rising velocity of the bubbles as described in section 4.3 and the results are shown in Table 4.1. The range of average rising velocities of the bubbles was found to be 26.13 to 45.29 cm/s

covering all the initial conditions. In order to predict the flow condition, the rising velocity corresponding to an air flow rate of 50 cc/min. was taken into account which produced the least intensity of turbulence as the bubble sizes are comparatively smaller at low air flow rate.

The rising velocity of the bubbles obtained experimentally and its observed size (the equivalent spherical diameter) have been used to calculate the Reynolds number in order to determine the flow condition around the rising bubble. Both the conditions of solid-liquid and gas-liquid interface were considered in the calculations. A check for C_D value was also made in the case of gas-liquid interface using the following expression given by Bhaga and Weber (1981):

$$C_D = [(2.67)^{0.9} + (16/\mathbf{R})^{0.9}]^{1/0.9} \qquad (4.7)$$

The flow field around the bubble has not been found to be laminar under any experimental conditions of this investigation and the shape of the bubble is essentially not spherical. Therefore, Stokes' law cannot be applied to evaluate the rising velocity described in this investigation.

6.16 Kinetics of Pneumatic Flocculation

The mathematical relationship shown in Equation (4.3) is based on Hudson's (1965) work and established by using the principle of rate of flocculation given by Camp and Stein (1943). This equation described the kinetics of pneumatic flocculation in terms of the process variables.

$$ln\frac{N_0}{N_t} = \left[\frac{\phi}{\pi}\cdot\frac{V_F}{(V_w)^{1/2}}\cdot\frac{t}{(\mu)^{1/2}}\left(p_a \ln\frac{p_{ah}+h}{p_{ah}}\right)^{1/2}\right](Q_a)^{1/2} \qquad (4.3)$$

The two assumptions made by Hudson (1965) were reconsidered in establishing this equation and they were:

(i) that the effect of the diameter of suspended particles was considered to be very small compare to that of the floc particles and was omitted with little error.

(ii) that the floc particles were considered to be spherical.

All the parameters in the first term of the right hand side of Equation (4.3) can be combined together, as represented by K in Equation (4.4) and (4.5) i.e.

$$ln\left(\frac{N_0}{N_t}\right) = K(Q_a)^{1/2} \tag{4.4}$$

$$K=\frac{\phi}{\pi}\cdot\frac{V_F}{(V_w)^{1/2}}\cdot\frac{t}{(\mu)^{1/2}}\cdot\left(p_a ln\frac{p_{ah}+h}{p_{ah}}\right)^{1/2}$$

Then, Equation (4.3) takes the form of

$$ln\frac{C_0}{C_t} = K(Q_a)^{1/2} \tag{4.5}$$

Experiments were conducted under various initial conditions in order to verify the above mathematical relationship and experimental results are shown in Figure 4.1 to Figure 4.5. When Equation 4.5 is not linearised by plotting $ln(C_0/C_t)$ against $Q_a^{1/2}$, it represents a semi-logarithmic curve with relation to a half power function. In such a case, the curve should pass through the origin theoretically at zero air flow rate i.e. $ln(C_0/C_t) = 0$ or $C_0/C_t = 1$. However, experimental data indicates an interception on $ln(C_0/C_t)$ axis even at zero air flow rate. Experimental curves are found not to be pass through the origin due to the formation of some micro flocs during the process of rapid mixing and the practicability of collecting samples for a period less than 5 minutes.

The graphs for $ln(C_0/C_t)$ versus $Q_a^{1/2}$ show a semi-logarithmic relationship. The curves become linear after a value of $Q_a^{1/2}$ upto 10 $(cc/min.)^{1/2}$ producing the following mathematical model:

$$ln\frac{C_o}{C_t} = K_1 + K(Q_a)^{1/2} \qquad (4.6)$$

The plotted curves as shown in Fig. 4.1 to 4.5, are found to be almost parallel to each other. This indicates that the lines are of constant slope which is found to be 0.01 (cc/min.)$^{-1/2}$ on average. As the concentration of the suspension is decreased with increasing settling time, the value of the interception on $ln(C_0/C_t)$ axis of these curves is also increased. The average value for each of these interceptions is found to be 1.9, 2.5, 3.0 and 3.3 corresponding to the settling times of 30, 60, 90 and 120 minutes respectively. These values are shown in Table 4.1.

6.17 Economical Considerations:

(1) Power consumption: A comparison of the power consumption of the pneumatic flocculator and the usual mechanical paddle stirrer flocculator has been made which is shown below:

(a) Pneumatic flocculator:

Power, $P = 3.527 \times 10^{-4}\ (Q_a)$ (5.1a)

where Q_a is the rate of air flow in cc/min. Considering the optimum air flow rate of 100 cc/min. in most of the cases in of this investigation,

Power, $P = 3.527 \times 10^{-4}\ (100) = 0.03527$ watt.

This is the power required to treat 155.26 litres of water.

(b) Mechanical paddle flocculator:

Power, $P = 0.5C_D A\rho u_r^3 = 3.049 \times 10^{-8}\ n^3$,

where n is the number of revolution of the blade per minute. Considering a revolution of 50 per minute for slow mixing,

$P = 3.049 \times 10^{-8} (50)^3 = 0.003812$ watt.

This is the power required to treat 1 litre of water. To treat 155.26 litres of water, the required power for the mechanical paddle will be 0.5918 watt which can be compared to that of 0.03527 watt required by the pneumatic flocculator to treat the same amount of water.

From the above example, it can be seen that the pneumatic flocculation required much less power than the mechanical paddle stirrer flocculator to treat the equivalent amount of water in order to achieve the same degree of treatment under similar initial conditions. Following the calculation shown above and considering the statistical mean of power ratio for all optimum air flow rates as shown in Table 5.13, it is found that the pneumatic flocculator required 1/16 of the power required for the mechanical flocculator.

Comparison was also made by McConnachie (1984) who found less power consumption in the diffused air flocculator than in the mechanical flocculator.

(2) Initial costs: Air compressors are cheaper, available extensively and easy to use. Hence, a saving in the initial cost can be made.

Pneumatic flocculation also offers less mechanical maintenance and operational staff.

6.18 Application

The use of compressed air as a source of power required in the coagulation-flocculation process in reducing the turbidity has been shown to be very effective and economical. This new technique could be promoted and used widely in most

conventional water treatment plants to replace the usual mechanical mixing and stirring.

The method is very simple and easy to implement practically. Perforated metal pipes can be used as diffusers and can be laid out at the bottom of a rectangular tank. Air can be supplied from a compressor connected to the electric power supply. Where mains electricity is not available, a generator or compressed air cylinders can be used for small community water supply. Alternatively, air can be generated manually by using a bellows or foot-pump, and can be stored in a storage tank. Air can be supplied from the storage tank to the flocculating chamber via appropriate flowmeters to control the air flow rate.

As taper flocculation produces the better result, the rectangular tank can be split into several chambers by perforated baffles which will promote a uniform horizontal flow over the vertical plane. The rate of air flow, size of the bubble and the detention time would be assessed from tests of the actual water to be tested. A higher velocity gradient can be applied in the first chamber and it can be decreased successively in the other chambers in order to obtain better removal of turbidity.

6.19 Conclusions

1. According to the procedure described in this thesis, as detailed in chapter 3 and the results obtained experimentally, the process of pneumatic flocculation is valid to coagulate and flocculate turbid waters under the recorded laboratory conditions.

2. Due to the differences in physicochemical properties of different types of synthetic turbidities, contrasting behaviour of the kaolin, lycopodium and PVC turbidities have been observed.

The physicochemical properties of synthetic turbidity materials influence the process of pneumatic flocculation in removing the turbidity from water. The best results were

obtained in the settling of PVC turbidity. The experimental results indicate that PVC turbidity is able to produce more compact and dense floc than kaolin and lycopodium due to the fineness of the suspended particles.

Settling of lycopodium floc, particularly when coagulated with alum, was found to be much slower than that of kaolin and PVC. This is attributed to the low density of lycopodium turbidity in association with aluminium sulphate coagulant and grouping of lycopodium flocs. Differently shaped isoconcentration lines, as shown in Figure 5.3, should be considered in assessing the removal efficiency of this nature of turbidity.

Flocs made up of kaolin and PVC turbidity are more settleable and less sensitive to power variations than those made up of lycopodium. This can be attributed to differences in shape, size, density and electrical properties of the particles and the structure and strength of the flocs.

3. The settling behaviour of turbidities flocculated by diffused air through different sizes of orifice indicates that there exists a relationship between the physicochemical properties of the turbidity materials and the size of the air bubbles.

The best removal was obtained in almost all the cases with orifice diameters of either 1.5 or 2.0 mm. The orifice size of 1.0 mm resulted in the worst removal of different types of synthetic turbidities. In the case of using a larger size orifice of 3.0 mm, the removal efficiencies are almost the same both for kaolin and PVC turbidity at any settling period.

4. The working range of air flow rate per unit area of the coagulating and flocculating chamber is 0.077 to 0.463 cc/sq.cm-min. for kaolin and lycopodium turbidity and is 0.077 to 0.618 cc./sq.cm-min. for PVC turbidity.

5. The working range of air flow rate per unit area of the chamber is 0.077 to 0.463, 0.077 to 0.309 and 0.077 to 0.618 cc/sq.cm-min. for the diffusion pads of orifice

sizes of 1.0 and 2.0 mm., 1.5 mm and 3.0 mm respectively.

6. The range of experimentally found optimum removal efficiencies are 85.83 to 95.00%, 67.83 to 93.64% and 91.73 to 96.00% for kaolin, lycopodium and PVC turbidity respectively.

7. The range of experimentally found optimum removal efficiencies are 67.83 to 95.50%, 78.00 to 94.81%, 83.18 to 96.00% and 75.20 to 95.70% for 1.0, 1.5, 2.0 and 3.0 mm orifice respectively.

8. The conditions for the best (maximum) turbidity removals are:

(i) For kaolin turbidity:
Orifice: 2.0 mm
Air flow rate: 100 cc/min.
Coagulant: Aluminium sulphate
Flocculation type: Normal
Removal: 95.83% after 120 minutes of settling

(ii) For lycopodium turbidity:
Orifice: 3.0 mm
Air flow rate: 300 cc/min.
Coagulant: Ferric sulphate
Flocculation type: Normal
Removal: 93.64% after 120 minutes of settling

(iii) For PVC turbidity:
Orifice: 2.0mm
Air flow rate: 100 cc/min.
Coagulant: Ferric sulphate
Flocculation type: Taper
Removal: 96.00% after 120 minutes of settling

9. The working range of velocity gradients are 10.65 to 26.08 s^{-1} for kaolin and lycopodium turbidity and that for PVC is 10.73 to 30.36 s^{-1} which are standardised at 20^0C. These ranges are also the range of experimentally found optimum velocity gradients for different turbidities in the order mentioned above.

10. The turbidity removal efficiency follows an oscillatory shape with respect to the orifice diameter. The first optimum peak was selected for a lower energy requirement.

11. The rate of settling for PVC and kaolin was faster than that of lycopodium flocs at the same air flow rate, because of the lower density of lycopodium.

12. Simultaneous aeration was achieved by pneumatic flocculation and the dissolved oxygen (DO) content was increased by aerating the water. An increase in DO of 0.50 to 1.0 mg/l was recorded.

13. The transformation to hydroxide floc of soluble material like iron, aluminium and nitrogenous compounds, during the pneumatic flocculation, contributes to the final reduction in concentration of these materials in the settled water. The major concentration of this matter is removed in the sludge.

14. Ferric sulphate results in better removal of turbidity than aluminium sulphate in pneumatic flocculation owing to a higher density of ferric sulphate. However, a higher level of iron content was obtained in the settled water when using ferric sulphate, and the settled water then required further treatment in order to achieve an acceptable standard of iron in the water.

15. Taper agitation in the process of pneumatic flocculation produced better removal of turbidity over the experimental range than normal agitation.

16. The rising velocity of the air bubble increased with increasing rate of air flow and the size of the orifice. However, there exists an optimum rising velocity

depending on the rates of air flow and the size of the orifice.

17. The flow field around the rising bubble was not laminar under the experimental conditions and the shape of the observed bubble was not spherical. Therefore, Stokes' law cannot be applied to evaluate the rising velocity of the bubble used in this investigation.

18. A mathematical relationship has been established to describe the kinetics of pneumatic flocculation in terms of the process variables.

19. Pneumatic flocculation required much less calculated power than the mechanical paddle stirrer flocculator to treat the equivalent amount of water in order to achieve the same degree of treatment under similar condition. The pneumatic flocculator required 1/16 of the power required for the mechanical flocculator.

20. The process of pneumatic flocculation is very simple, flexible, powerful, economical and requires less maintenance and less knowhow. This new technique could be promoted and used widely both in developed and developing countries in most conventional water treatment plants to replace the usual mechanical mixing and stirring.

It is recommended that the process of pneumatic flocculation should be applied in water treatment plants because of the low cost of operation, maintenance and improvement of water quality.

BIBLIOGRAPHY

Al-Hiary, S.M. (1988)
Pneumatic Flocculation.
M.Sc. Engg. Thesis, Department of Civil Engineering, University of Jordan.

Allen, H.S. (1900)
The Motion of a Sphere in a Viscous Fluid.
Phil. Mag., 50, 323 - 338, 519 - 534.

Amirtharajah, A. (1988)
Design of Rapid Mix Units in Sanks, R. L. (ed), *Water Treatment Plant Design,*
Ann Arbor Science,
Ann Arbor, Mich.

Argaman, Y. and Kaufman, W.J. (1968)
Turbulence in Orthokinetic Flocculation.
Sanitary Engineering Research Laboratory (SERL), Report no. 68-5, Berkeley: SERL, Univ. Calif., Berkeley, Calif., July.

Argaman, Y. and Kaufman, W.J. (1970)
Turbulence and Flocculation.
J. San. Eng. Div. ASCE., 96, SA2, Proc. Paper 7201, 223 - 241.

AWWA (1969)
Water Treatment Plant Design.
ASCE and Conference of State San. Engrs. (1969)
New York.

AWWA (1971)
Water Quality and Treatment.
Third edition, New York, McGraw-Hill Book Company.

Barnes, D., Bliss, P.J., Gould, B.W. and Vallentine, H.R. (1981)
Water and Wastewater Engineering Systems
Pitman Publishing Inc., London.

Beek, W. J. and Muttzall, K.M.K. (1975)
Transport Phenomena.
London, John Wiley & Sons Ltd., 84.

Bhaga, D. and Weber, M. E. (1981)
Bubbles in viscous liquids: shape, wakes and velocities

J. Fluid Mechanics, vol. 54, 167 - 173.

Bhargava, D.S. and Ojha, C.S.P. (1993)
Models for design of flocculating baffled channels
Water Research, 27, 3, 465 - 475.

Black, A.P. and Willems, D.G. (1961)
Electrophoretic Studies of Coagulation for Removal of Organic Colour.
J. AWWA, May, 589 - 604.

Black, A.P. Singley, J.E., Whittle, G.P. and Maulding, J.S. (1963)
Stoichiometry of Coagulation of Color-causing Compounds with ferric sulfate.
J. AWWA., 55, Oct., 1347 - 1366.

Black, A.P. and Chen, C. (1965)
Electrophoretic Studies of Coagulation and Flocculation of River Sediment Suspensions with Aluminium sulfate.
J. AWWA, 57, 354 - 362.

Bond, N.W. and Newton, D.A. (1928)
Bubbles, Drops and Stokes' Law
Phil. Mag. 5, 794.

Bratby, J. (1980)
Coagulation and Flocculation
Croydon, England, Uplands Press Ltd.

Camp, T.R. and Stein, P.C. (1943)
Velocity gradients and internal work in fluid motion
J. of the Boston Society of Civil Engineers, 30, 4, 219 - 237.

Camp, T.R. (1946)
Sedimentation and the design of settling tanks.
Trans., ASCE, 111, paper no. 2285, 895 - 958.

Camp, T.R. (1955)
Flocculation and Flocculation Basins
Trans. of ASCE, 120, paper no. 2722, 1 - 16.

Camp, T.R. (1968)
Floc volume concentration
J. AWWA, vol. 60, no. 6, 656.

Camp, T. R. (1969)
Discussion to *Agglomerate size change in coagulation*
San. Engg. Dir. ASCE, SA, Dec. 1210 - 1214.
(Cited by Bratby, 1980)

Clark, J.W., Viessman, W.Jr. and Hammer, M.J. (1977)
Water Supply Pollution Control.
3rd edition, New York, N.Y., Harper and Row.

Coppock, P.D. and Meiklejohn, G.T. (1951)
The behaviour of gas bubbles in relation to mass transfer
Trans. Inst. Chem. Engrs. 29, 75 - 86.

Cox, C.R. (1969)
Operation and Control of Water Treatment Processes.
Geneva, World Health Organization.

Datta, R.L., Napier, D.G. and Newitt, D.M. (1950)
The properties and behaviour of gas bubbles formed at a circular orifice
Trans. Inst. Chem. Engrs., 28, 14 - 26.

Degre'mont (1991)
Water Treatment Handbook.
6th edition, France, Lavoisier Publishing, vol. 1.

Dempsey, B.A. (1995)
Current and future use of coagulants in water treatment in the USA
Proc. on Role of coagulants in water and wastewater treatment
Ouki, S.K. and Graham N.J.D. (ed.)
Lonsdale Press Ltd., London.

Deryagin, B.V. and Landau, L.D.(1941)
Theory of the stability of strongly charged lyphobic sols and of the adhesion of strongly charged particles in solutions of electrolutes.
Acta Physico-chim. USSR., 14, 733 - 762.
(Cited by Gregory, 1993)

Dharmappa, H.B. (1993)
Optimal design of a flocculator
Water Research, 27, 3, 513 - 519.

Edzwald, J.K. (1993)
Algae, bubbles, coagulants, and dissolved air flotation
Wat. Sci. Tech., 27, 10, 67 - 81.

Edzwald, J.K. and Lawler, D.F. (1983)
Mechanics of particle destabilization for polymers in water treatment.
Proc. of AWWA seminar on use of organic polyelectrolytes in water treatment, AWWA, Denver.

Ernest, A.N., Bonner, J.S. and Autenrieth, R.L. (1995)
Determination of particle collision efficiencies for flocculent transport models
J. Env. Eng. vol. 121, no. 4.

Fair, G.M. and Gemmell, R.S. (1964)
A Mathematical model of coagulation
J. of Colloid Science, 19, 360 - 372.

Fair, G.M., Geyer, J.G. and Okun, D.A. (1968)
Water and Wastewater Engineering
John Wiley & Sons, inc., U.S.A., vol. 2.

Fitch, E.B. (1958)
Sedimentation Process Fundamentals.
Brother Joseph McCabe & W W Eckenfelder. Jr (edited)
Biological Treatment of Sewage and Industrial Waste.
New York, Reinhold Publishing Corporation, Volume II, 159 - 170.

Freud, B.B. and Harkins, W.D. (1929)
The Shapes of Drops, and the determination of Surface Tension.
J. Phys. Chem 33, 1217.

Garner, F.H. and Hammerton, D. (1954)
Circulation inside gas bubbles.
Chem. Eng. Sci., 3, 1.

Gorodetskaya, A.V. (1949)
Velocity of Rise of Bubble in Water and Aqueous Solutions at High Reynolds Number.
J. Phys. Chem. (USSR), 23, 71 - 77.

Gomella, C. (1974)
Recent Developments Related to Preclarification.
Special commission on the pollution and protection of water sources, London, England.

Grace, J.R. (1973)
Shapes and velocities of bubbles rising in infinite liquids
Trans. Inst. Chem. Engrs., vol. 51, 116 - 120.

Gregory, J. (1993)
The role of colloid interactions in solid-liquid separation
Wat. Sci. Tech., 27, 10, 1 - 17.

Griffith, J.D. and William, R.G. (1972)
Application of Jar Test Analysis at Phoenix, Ariz
J. AWWA, 64, 12, 825 - 830.

Haberman, W.L. and Morton, R.K.(1954)
An experimental study of bubbles moving in liquids.
Proc. ASCE, 80, 387(1 - 25).

HACH Company (1989)
Water Analysis Handbook.
Colorado, U.S.A., Hach Company.

Hadamard, J. S. (1911)
Mouvement Permenant Lent d'une Sphere Liquide et Visqueuse dans un Liquide Visqueux.
Compt. Rend. Acad. Sci., Paris, 152, 1735 - 1738.
(Cited by Levich, 1962)

Harris, H.S. and Kaufman, W.J. (1966)
Orthokinetic Flocculation of Polydispersed System.
SERL Report no. 66-2, Berkeley: SERL, Univ. Calif., Berkeley, Calif., July.

Harris, H.S., Kaufman, W. J. and Krone, R.B. (1966)
Orthokinetic Flocculation in Water Purification.
J. San. Eng. Div., Proc., ASCE., 92, SA6. 95 - 111.

Hazen, A. (1892)
Annual Report of the Massachusetts State Board of Health.
(Cited by Fair *et al.*, 1968)

Hubbell, G.E. (1969)
Initial Mixing.
Paper presented at the short course for water treatment plant operators, sponsored by *AWWA,* Evanston, I11.
(Cited by Letterman *et al.*, 1973).

Hubley, C.E. and Robertson, A.A. (1950)
Flocculation in suspensions of large particles
Canadian J. of Res. B, 28, 770 - 787.

Hudson, H.E. (1965)
Physical aspects of Flocculation
J. AWWA, 57, 7, 885 - 892.

Hudson, H.E., JR. and Wolfner, J.P. (1967)
Design of mixing and flocculating basins
J. AWWA, 59, 10, 1257 - 1267.

Ives, K.J. (1978)
Experimental Methods (2)
In: *The Scientific Basis of Flocculation.*
Netherlands, Sijthoff & Noordhoff.

Ives, K.J. (1981)
Coagulation and flocculation Part II - orthikinetic flocculation
In: *Solid-Liquid Separation.*

Svarovsky, L. (ed.), 2nd edition, London, Butterworth and Co. Ltd.

Ives, K.J. (1995)
Personal communication, Department of Civil and Environmental Engineering, University College London.

Ives, K.J. and Bhole, A.G. (1973)
Theory of flocculation for continous flow system.
J. of the Env. Engg. Div. ASCE, 99, EE1, 18 - 33.

Jiang, J.Q., Graham, N.J.D. and Harward, C. (1995)
Pilot-plant evaluation of polyferric sulphate as a coagulant for drinking water treatment
Proc. on Role of coagulants in water and wastewater treatment.
Ouki, S.K. and Graham, N.J.D. (ed.)
Lonsdale Press Ltd., London.

James M. Montgomery (1985)
Water Treatment Principles and Design.
New York, John Wiley and Sons.

Kawamura, S. (1959)
Effectiveness of Various Coagulant Aids and pH Adjustment on Alum Flocculation for Low Turbidity Waters.
J. AWWA., 302, 303, 10, 34.

Kawamura, S. (1967)
Removal of Color by Coagulation Part I & II.
W. Sew. Wks., 130, 131.

Kawamura, S. (1973)
Coagulation Considerations
J. AWWA, 65, 6, 417 - 423.

Kawamura, S. (1976)
Considerations on Improving Flocculation
J. AWWA, June, 328 - 336.

Kitano, Y. and Kawamura, S. (1954)
Studies on Water Purification Mechanism.
J. Jap. WWA., 239, 15.
(Cited by Kawamura, 1973).

Lagvankar, A.L. and Gemmell, R.S. (1968)
A Size Density Relationship for Flocs
J. AWWA., 60, 1040 - 1046.

Lamb, H. (1952)
Hydrodynamics.
6th edition, Cambridge University Press.

Langelier, W.F. (1921)
Coagulation of Water with Alum by Prolonged Agitation
Engineering News-Record, 86, 22, 924 - 928.

Langelier, W.F. (1952)
Flocculation phenomena in turbid water clarification
ASCE Proc., 78, 118, 1 - 18.

Leibson, I., Holcomb, E.G., Cacoso, A.G. and Jacmic, J.J. (1956)
Rate of flow and mechanics of bubble formation from single submerged orifices
J. A.I. Ch. E., vol. 2, no. 3, 296 - 306.

Letterman, R.D., Quon, J.E. and Gemmell, R.S. (1973)
Influence of Rapid mix parameters on Flocculation
J. AWWA, 65, 11, 716 - 722.

Levich, A.G. (1962)
Physicochemical Hydrodynamics.
New Jersey, Prentice-Hall.

Manley, R.S.J. and Mason, S.G. (1952)
Particle motions in sheared suspension II. Collisions of uniform spheres.
J. of Colloid Science, 7, 354 - 369.

McConnachie, G.L. (1984)
Flocculation and Turbulence from bubble-induced mixing
J. of the Instn. of Wat. Engrs. & Scientists, 38, 4, 337 - 347.

Metcalf and Eddy (1979)
Wastewater Engineering: Treatment, Disposal, Reuse.
2nd edition, New York, N.Y., McGraw-Hill Book Co.

Michaels, A.S. and Bolger, J.C. (1962)
Settling Rates and Sediment Volumes of Flocculated Kaolin Suspensions.
Industrial and Engineering Chemistry Fundamentals, Quarterly serial journal commenced 1962, published by American Chemical Society, Washington, D.C. (U55 16th St. NW), 1, 69.

Moffett, W.J. (1968)
The Chemistry of high rate water treatment.
J. AWWA, 60, 11, 1255 - 1270.

O'Brien, M.P. and Gosline, J.E. (1935)
Velocity of large bubbles in vertical tubes

Ind. Eng. Chem., 27, 1436 - 1440.

O'Melia, C.R. (1972)
Coagulation and flocculation
In: *Physicochemical Processes for Water Quality Control,* W.J. Weber, Jr. (ed). Wiley-Interscience, New York, 61 - 109.

Overbeek, J. Th. G. (1952)
Kinetics of Flocculation, Chapter VII in *Colloid Science, Vol. 1, Irreversible System.*
H.R. Kruyt, Ed.
Elsevier, Amsterdam.

Owens, J.S. (1921)
Experiments on air lift pumping
Engineering 112, 458 - 461.

Packham, R.F. (1963)
The coagulation process: A review of some recent investigations
Proc. Soc. Water Exam., vol. 12, no. 15.

Pattle, R.E. (1950)
The aeration of liquids
J. Trans. Inst. Chem. Eng., vol. 28, 27 - 31.

Patwardhan, S.V. (1975)
Low cost water treatment for developing countries.
2nd international conference on environmental health engineering in hot climates.

Peavy, H.S., Rowe, D.R. and Tchobanoglous, G. (1987)
Environmental Engineering.
Singapore, McGraw-Hill Book Company.

Peebles, F.N. and Garber, H.J. (1953)
Studies on the motion of gas bubbles in liquid
Chem. Eng. Prog., 49, 88 - 97.

Poutanen, A.A. and Johnson, A.I. (1960)
Studies of bubble formation and rise
The Canadian J. of Chem. Engg., vol. 38, no. 4, 93 - 101.

Priesing, C.P. (1962)
Design theory in flocculation and mixing equipment
Ind. & Engg. Chemistry, 54, 9, 54 - 55

Qasim, S.R. (1985)
Wastewater Treatment Plants, Planning, Design and Operation
CBS International edition

CBS Publishing Japan Ltd., New York.

Reynolds, T.D. (1982)
Unit Operations and Processes in Environmental Engineering.
Brooks/Cole Engrg. Div., Monterey, Calif.

Riddick, T.M. (unpublished)
Water Filtration Plant, Governeur, N.Y.
(Cited by Hudson, 1965).

Ritchie, A.R. (1956)
Theoretical Aspects of Flocculation Coagulation.
Proceedings of the Society for Water Treatment & Examination, 5, 81.

Robeck, G.G. (1963)
High rate filtration study at Gatfney, South Carolina, Water Plant, USPHS, R.A. Taft. San. Eng. Centre, Cincinnati.
(Cited by Hudson, 1965).

Robinson, J.V. (1947)
The rise of air bubbles in lubricating oils
J. Phys. and Colloid Chem., 51, 401, 431 - 437.

Root, D.A., Bhoota, B.V. and Camp, T.R. (1940)
Effects of Temperature on Rate of Floc Formation.
J. AWWA, 32, 1913.
(Cited by Camp, 1943).

Rouse, Hunter (1978)
Elementary Mechanics of Fluids
New York
Dover Publications, Inc.

Rybczynski, W. (1911)
Uber die Forschreitende Bewegung einer Flussigen Kugel in einem Zahen Medium.
Bull. Acad. Sci. Cracorie., Ser. A, 40 - 46.
(Cited by Levich, 1962).

Sawyer, C. N. (1960)
Chemistry for Sanitary Engineers.
New York, N. Y.
McGraw-Hill Book Company.

Sawyer, C.N. and McCarty, P.L. (1978)
Chemistry for Environmental Engineers
Third edition
New York

McGraw-Hill Book Company

Sholji, I.H. (1994)
Physicochemical treatment of water
B. Engg. lecture notes, Department of Civil and Structural Engineering, The Nottingham Trent University, England.

Sibony, J. (1981)
Clarification with microsand seeding. A state of the art.
Water Research, vol. 15, 1281 - 1290.

Siemes, W. (1954)
Gasblasen in Flussigkeiten Teil I : Entstehung von Gasblasen an nach oben gerichteten Kreisformigen Dusen
Chem. Ing. Tech. vol. 26, no. 479 - 496.

Simpson, A.M., Brockbank, M. and Hatton, W. (1995)
Aluminium and iron compounds
Proc. on Role of coagulants in water and wastewater treatment.
Ouki, S.K. and Graham, N.J.D. (ed.)
Lonsdale Press Ltd., London.

Smethurst, G. (1979)
Basic Water Treatment.
London, Thomas Telford Ltd.

Srivastava, R.M. (1992)
Type II sedimentation: Removal efficiency from column settling tests
J. Environ. Engrg., (U.S.), 118, 3, 438 - 441.

Steel, E.W. and McGhee, T.J. (1979)
Water Supply and Sewerage.
5th edition,

Swift, D.L. and Friedlander, S.K. (1964)
The coagulation of hydrosols by Brownian motion and laminar shear flow.
J. of Colloid Science, vol. 19, 621.

Tapucu, A. (1974)
Viscosity effects on the motion of gas bubbles rising through stagnant liquids
Trans. of CSME, vol. 2, no. 3, 151 - 159.

Tebbutt, T.H.Y. (1983)
Principles of Water Quality Control.
3rd edition, England, Pergamon Press.

Tekippe, R.J. and Ham, R.K. (1971)
Velocity Gradient paths in Coagulation

J. AWWA, 63, 7, 439 - 448.

Tolman, S.L. (1942)
Water Conditioning by Flocculation
J. AWWA, 34, 3, 404 - 411.

Tsuge, H. and Hibino, S. (1981)
Bubble formation from a submerged orifice in liquids
Proc. 2nd World congress of Chemical Engrs., Montreal, vol. V. 307 - 311.

Twort, A.C., Law, F.M. and Crowley, F.W. (1985)
Water Supply.
3rd edition, Australia, Edward Arnold Ltd.

Verschoor, H (1950)
Some aspects of the motion of a swarm of gas bubbles rising through a vertical liquid column.
Trans. Inst. Chem. Engrs., vol. 28, 52 - 57.

Verwey, E.J. and Overbeek, J.Th. G. (1948)
Theory of the stability of Lyophobic Colloids.
Amsterdam
Elsevier.

Villegas, R.A. and Letterman, R. D. (1976)
Optimizing Flocculator Power Input
J. ASCE, 102, EE2, 251 - 263.

Von Smoluchowski M. (1916)
Drei Vortrage uber Diffusion, Brownshe Molekular Beweging und Koagulation von Kolloidteilchen,
Physik. Z. 17, 557.
(Cited by Bratby, 1980)

Von Smoluchowski M. (1917)
Versuch einer Mathematischen Theorie der koagulationskinetik Kolloid Losungen.
Z. Physik. Chem., 92, 155.

Walker, J.D. (1968)
High-Energy Flocculation Units
J. AWWA, 60, 1271 - 1279.

Walker, J.D. (1971)
InstoMix for Instantaneous and Uniform Blending of Coagulants in Water Treatment.
Walker Process Equipment, Div., Chicago Bridge & Iron Co. Tech. Bull. CBT No. 5225.

Wark, I.W. (1932)
Physical chemistry of flotation. I
J. Phys. Chem., vol. 37, 623 - 644.

Water Services (1975)
Chemicals for use in water treatment
Water Services (GB), 79, 950, 141 - 156.

Weber, W. J. (1972)
Physicochemical Processes for Water Quality Control.
New York, John Wiley & Sons Inc.

World Health Organisation (1984)
Guidelines for Drinking - Water Quality
Geneva
WHO
Volume 2.

Zanoni, A.E. and Blomquist, M.W. (1975)
Column settling tests for flocculant suspensions
J. Envr. Engg. Div., ASCE, 101, EE3, 309 - 318.

Appendix 1 Details of the Experimental Runs

Table (A-1) Details of the Experimental Runs

Run No.	Set No.	Experimental Details				
		Air Flow rate (cc/min.)	Synthetic Turbidity	Chemical Coagulant	Orifice Diameter (mm)	Type of Flocculation
1	1	50	Kaolin	Aluminium sulphate	1.00	Normal
2	"	100	"	"	"	"
3	"	200	"	"	"	"
4	"	300	"	"	"	"
5	"	400	"	"	"	"
6	"	500	"	"	"	"
7	"	600	"	"	"	"
8	"	800	"	"	"	"
9	"	1000	"	"	"	"
10	2	50	"	"	"	Taper
11	"	100	"	"	"	"
12	"	200	"	"	"	"
13	"	300	"	"	"	"
14	"	400	"	"	"	"
15	"	500	"	"	"	"
16	"	600	"	"	"	"
17	"	800	"	"	"	"
18	"	1000	"	"	"	"
19	3	50	"	Ferric sulphate	"	Normal
20	"	100	"	"	"	"
21	"	200	"	"	"	"
22	"	300	"	"	"	"
23	"	400	"	"	"	"
24	"	500	"	"	"	"
25	"	600	"	"	"	"
26	"	800	"	"	"	"
27	"	1000	"	"	"	"
28	4	50	"	"	"	Taper
29	"	100	"	"	"	"
30	"	200	"	"	"	"
31	"	300	"	"	"	"
32	"	400	"	"	"	"
33	"	500	"	"	"	"
34	"	600	"	"	"	"
35	"	800	"	"	"	"
36	"	1000	"	"	"	"
37	5	50	Lycopodium	Aluminium sulphate	"	Normal
38	"	100	"	"	"	"
39	"	200	"	"	"	"
40	"	300	"	"	"	"
41	"	400	"	"	"	"
42	"	500	"	"	"	"

Continued...

Table (A-1) Details of the Experimental Runs

Run No.	Set No.	Experimental Details				
		Air Flow rate (cc/min.)	Synthetic Turbidity	Chemical Coagulant	Orifice Diameter (mm)	Type of Flocculation
43	5	600	Lycopodium	Aluminium sulphate	1.00	Normal
44	"	800	"	"	"	"
45	"	100	"	"	"	"
46	6	50	"	"	"	Taper
47	"	100	"	"	"	"
48	"	200	"	"	"	"
49	"	300	"	"	"	"
50	"	400	"	"	"	"
51	"	500	"	"	"	"
52	7	50	"	Ferric sulphate	"	Normal
53	"	100	"	"	"	"
54	"	200	"	"	"	"
55	"	300	"	"	"	"
56	"	400	"	"	"	"
57	"	500	"	"	"	"
58	"	600	"	"	"	"
59	"	800	"	"	"	"
60	"	1000	"	"	"	"
61	8	50	"	"	"	Taper
62	"	100	"	"	"	"
63	"	200	"	"	"	"
64	"	300	"	"	"	"
65	"	400	"	"	"	"
66	"	500	"	"	"	"
67	9	50	PVC powder	Aluminium sulphate	"	Normal
68	"	100	"	"	"	"
69	"	200	"	"	"	"
70	"	300	"	"	"	"
71	"	400	"	"	"	"
72	"	500	"	"	"	"
73	"	600	"	"	"	"
74	10	50	"	"	"	Taper
75	"	100	"	"	"	"
76	"	200	"	"	"	"
77	"	300	"	"	"	"
78	"	400	"	"	"	"
79	"	500	"	"	"	"
80	11	50	"	Ferric sulphate	"	"
81	"	100	"	"	"	"
82	"	200	"	"	"	"
83	"	300	"	"	"	"

Continued...

Table (A-1) Details of the Experimental Runs

Run No.	Set No.	Experimental Details				
		Air Flow rate (cc/min.)	Synthetic Turbidity	Chemical Coagulant	Orifice Diameter (mm)	Type of Flocculation
84	11	400	PVC powder	Ferric sulphate	1.00	Normal
85	"	500	"	"	"	"
86	"	600	"	"	"	"
87	12	50	"	"	"	Taper
88	"	100	"	"	"	"
89	"	200	"	"	"	"
90	"	300	"	"	"	"
91	"	400	"	"	"	"
92	"	500	"	"	"	"
93	13	50	Kaolin	Aluminium sulphate	"	Normal
94	"	100	"	"	"	"
95	"	200	"	"	"	"
96	"	300	"	"	"	"
97	"	400	"	"	"	"
98	14	50	"	"	"	Taper
99	"	100	"	"	"	"
100	"	200	"	"	"	"
101	"	300	"	"	"	"
102	"	400	"	"	"	"
103	15	50	"	Ferric sulphate	"	Normal
104	"	100	"	"	"	"
105	"	200	"	"	"	"
106	"	300	"	"	"	"
107	"	400	"	"	"	"
108	16	50	"	"	"	Taper
109	"	100	"	"	"	"
110	"	200	"	"	"	"
111	"	300	"	"	"	"
112	"	400	"	"	"	"
113	17	50	"	Aluminium sulphate	"	Normal
114	"	100	"	"	"	"
115	"	200	"	"	"	"
116	"	300	"	"	"	"
117	"	400	"	"	"	"
118	18	50	"	"	"	Taper
119	"	100	"	"	"	"
120	"	200	"	"	"	"
121	"	300	"	"	"	"

Continued...

Table (A-1) Details of the Experimental Runs

Run No.	Set No.	Experimental Details				
		Air Flow rate (cc/min.)	Synthetic Turbidity	Chemical Coagulant	Orifice Diameter (mm)	Type of Flocculation
122	18	400	Lycopodium	Aluminium sulphate	1.50	Taper
123	19	50	"	Ferric sulphate	"	Normal
124	"	100	"	"	"	"
125	"	200	"	"	"	"
126	"	300	"	"	"	"
127	"	400	"	"	"	"
128	20	50	"	"	"	Taper
129	"	100	"	"	"	"
130	"	200	"	"	"	"
131	"	300	"	"	"	"
132	"	400	"	"	"	"
133	21	50	PVC powder	Aluminium sulphate	"	Normal
134	"	100	"	"	"	"
135	"	200	"	"	"	"
136	"	300	"	"	"	"
137	"	400	"	"	"	"
138	22	50	"	"	"	Taper
139	"	100	"	"	"	"
140	"	200	"	"	"	"
141	"	300	"	"	"	"
142	"	400	"	"	"	"
143	23	50	"	Ferric sulphate	"	Normal
144	"	100	"	"	"	"
145	"	200	"	"	"	"
146	"	300	"	"	"	"
147	"	400	"	"	"	"
148	24	50	"	"	"	Taper
149	"	100	"	"	"	"
150	"	200	"	"	"	"
151	"	300	"	"	"	"
152	"	400	"	"	"	"
153	25	50	"	Aluminium sulphate	2.00	Normal
154	"	100	"	"	"	"
155	"	200	"	"	"	"
156	"	300	"	"	"	"
157	"	400		"	"	"
158	26	50	"	"	"	Taper
159	"	100	"	"	"	"

Continued...

Table (A-1) Deatils of the Experimental Runs

Run No.	Set No.	Experimental Details				
		Air Flow rate (cc/min.)	Synthetic Turbidity	Chemical Coagulant	Orifice Diameter (mm)	Type of Flocculation
160	26	200	Kaolin	Aluminium sulphate	Taper	2.00
161	"	300	"	"	"	"
162	"	400	"	"	"	"
163	27	50	"	Ferric sulphate	Normal	"
164	"	100	"	"	"	"
165	"	200	"	"	"	"
166	"	300	"	"	"	"
167	"	400	"	"	"	"
168	28	50	"	"	Taper	"
169	"	100	"	"	"	"
170	"	200	"	"	"	"
171	"	300	"	"	"	"
172	"	400	"	"	"	"
173	29	50	Lycopodium	Aluminium sulphate	Normal	"
174	"	100	"	"	"	"
175	"	200	"	"	"	"
176	"	300	"	"	"	"
177	"	400	"	"	"	"
178	30	50	"	"	Taper	"
179	"	100	"	"	"	"
180	"	200	"	"	"	"
181	"	300	"	"	"	"
182	"	400	"	"	"	"
183	31	50	"	Ferric sulphate	Normal	"
184	"	100	"	"	"	"
185	"	200	"	"	"	"
186	"	300	"	"	"	"
187	"	400	"	"	"	"
188	32	50	"	"	Taper	"
189	"	100	"	"	"	"
190	"	200	"	"	"	"
191	"	300	"	"	"	"
192	"	400	"	"	"	"
193	33	50	PVC powder	Aluminium sulphate	Normal	"
194	"	100	"	"	"	"
195	"	200	"	"	"	"
196	"	300	"	"	"	"
197	"	400	"	"	"	"
198	34	50	"	"	Taper	"

Continued...

Table (A-1) Details of the Experimental Runs

Run No.	Set No.	Experimental Details				
		Air Flow rate (cc/min.)	Synthetic Turbidity	Chemical Coagulant	Orifice Diameter (mm)	Type of Flocculation
199	34	100	PVC powder	Aluminium sulphate	2.00	Taper
200	"	200	"	"	"	"
201	"	300	"	"	"	"
202	"	400	"	"	"	"
203	35	50	"	Ferric sulphate	"	Normal
204	"	100	"	"	"	"
205	"	200	"	"	"	"
206	"	300	"	"	"	"
207	"	400	"	"	"	"
208	36	50	"	"	"	Taper
209	"	100	"	"	"	"
210	"	200	"	"	"	"
211	"	300	"	"	"	"
212	"	400	"	"	"	"
213	37	50	Kaolin	Aluminium sulphate	3.00	Normal
214	"	100	"	"	"	"
215	"	200	"	"	"	"
216	"	300	"	"	"	"
217	"	400	"	"	"	"
218	"	500	"	"	"	"
219	"	600	"	"	"	"
220	"	800	"	"	"	"
221	38	50	"	"	"	Taper
222	"	100	"	"	"	"
223	"	200	"	"	"	"
224	"	300	"	"	"	"
225	"	400	"	"	"	"
226	"	500	"	"	"	"
227	"	600	"	"	"	"
228	39	50	"	Ferric sulphate	"	Normal
229	"	100	"	"	"	"
230	"	200	"	"	"	"
231	"	300	"	"	"	"
232	"	400	"	"	"	"
233	"	500	"	"	"	"
234	40	50	"	"	"	Taper
235	"	100	"	"	"	"
236	"	200	"	"	"	"
237	"	300	"	"	"	"
238	"	400	"	"	"	"
239	"	500	"	"	"	"

Continued...

Table (A-1) Details of the Experimental Runs

Run No.	Set No.	Experimental Details				
		Air Flow rate (cc/min.)	Synthetic Turbidity	Chemical Coagulant	Orifice Diameter (mm)	Type of Flocculation
240	41	50	Lycopodium	Aluminium sulphate	3.00	Normal
241	"	100	"	"	"	"
242	"	200	"	"	"	"
243	"	300	"	"	"	"
244	"	400	"	"	"	"
245	"	500	"	"	"	"
246	"	600	"	"	"	"
247	42	50	"	"	"	Taper
248	"	100	"	"	"	"
249	"	200	"	"	"	"
250	"	300	"	"	"	"
251	"	400	"	"	"	"
252	43	50	"	Ferric sulphate	"	Normal
253	"	100	"	"	"	"
254	"	200	"	"	"	"
255	"	300	"	"	"	"
256	"	400	"	"	"	"
257	"	500	"	"	"	"
258	44	50	"	"	"	Taper
259	"	100	"	"	"	"
260	"	200	"	"	"	"
261	"	300	"	"	"	"
262	"	400	"	"	"	"
263	"	500	"	"	"	"
264	45	50	PVC powder	Aluminium sulphate	"	Normal
265	"	100	"	"	"	"
266	"	200	"	"	"	"
267	"	300	"	"	"	"
268	"	400	"	"	"	"
269	"	500	"	"	"	"
270	46	50	"	"	"	Taper
271	"	100	"	"	"	"
272	"	200	"	"	"	"
273	"	300	"	"	"	"
274	47	50	"	Ferric sulphate	"	Normal
275	"	100	"	"	"	"
276	"	200	"	"	"	"
277	"	300	"	"	"	"
278	"	400	"	"	"	"

Continued...

Table (A-1) Details of the Experimental Runs

Run No.	Set No.	Experimental Details				
		Air Flow rate (cc/min.)	Synthetic Turbidity	Chemical Coagulant	Orifice Diameter (mm)	Type of Flocculation
279	48	50	PVC powder	Ferric sulphate	3.00	Taper
280	"	100	"	"	"	"
281	"	200	"	"	"	"
282	"	300	"	"	"	"
283	"	400	"	"	"	"
284	"	500	"	"	"	"

Appendix 2 Local Authority Water Quality Report

Severn Trent Water

WATER SUPPLY ZONE :- N08A WHITEM & SHER RISE 93/94

REPORTING PERIOD :- 01/01/1993 TO 31/12/1993

AREA:- Forest Fields, Whitemoor, Sherwood, Hyson Green, Bobbers Mill, Radford

POPULATION:- 35,550

SUPPLY SOURCES:- BASFORD BH,BESTWOOD BH,BOUGHTON BH,CHUR WILNE WTW FAR BAULKER BH, HALAM BH,OMPTON BH,BAMFORD (DV) HOMESFORD WSW ,

AUTHORISED SUPPLY POINT:-

GENERAL COMMENTS:-

Lead The exceedance of the PCV for lead was a result of pick up from the pipes between the water main and the customer's tap. As detailed below actions are in hand to alleviate the problem. The relevant Environmental Health Officer and the customer were informed.

ACTION TAKEN TO COMPLY WITH SECTION 19 (1) (B) UNDERTAKINGS:-

Reference	Nature of Contravention	Steps to be taken	Statutory completion date
ST.41(D)	Occasional exceedances of the iron and turbidity parameters	Where appropriate air scour, flush or otherwise clean the system. and	Ongoing as necessary
		Carry out mains refurbishment programme using any acceptable process. Estimates are that approx 5500km require refurbishment in the priority zones by 31 December 1994	Continuing
ST.40(L)	Due to the presence of lead service pipes, a significant proportion of which is not the responsibility of Severn Trent Water there is a risk that on occasions the prescribed concentration may be exceeded	Identify zones where - the prescribed risk relates to an insignificant part of the zone or treatment is not reasonably practicable	December 1991 (complete)
		In zones not so identified investigate potential treatment methods to determine whether a significant reduction in lead concentrations can be achieved	December 1991 (complete)
		In the light of the above investigations install treatment where appropriate	December 1995

22/03/94 19:46:47

Severn Trent Water

WATER SUPPLY ZONE :- N08A WHITEM & SHER RISE 93/94

REPORTING PERIOD :- 01/01/1993 TO 31/12/1993

01/01/1993 TO 31/12/1993

DETAILS OF SAMPLES WHICH BREACHED A STANDARD:-

DATE	RESULT			LOCATION
18/05/93	LEAD	=	818	NOTTINGHAM ROAD DMA

Severn Trent Water

WATER SUPPLY ZONE :- N08A WHITEM & SHER RISE 93/94

REPORTING PERIOD :- 01/01/1993 TO 31/12/1993

Parameter And Qualifiers		No. Of Samples Taken In Period	Samples Greater Than P.C.V.		Concentration Or Value				
			Number	Percent	Minimum	Maximum	Mean	PCV	Units
TOTAL COLIFORMS		96	----	------	0	0	0	--------	-----
TOTAL COLIFORMS	4	96	0	0.00	0	0	0	0.0	100ML
FAECAL COLIFORMS		96	0	0.00	0	0	0	0.0	100ML
PLATE COUNT (AT 21C)		53	0	0.00	0	>300	>6	NONE	ML
PLATE COUNT (AT 37C)		53	0	0.00	0	>300	>7	NONE	ML
FREE CHLORINE		96	0	0.00	<0.01	0.43	<0.05	NONE	MG/L
TOTAL CHLORINE		96	0	0.00	<0.01	0.54	<0.06	NONE	MG/L
COLOUR		48	0	0.00	<1	3	<1	20	HAZEN
TURBIDITY	U	48	0	0.00	<0.1	1	<0.2	4	F.T.U
TEMPERATURE		96	0	0.00	6.5	22.9	12	25	DEG C
PH		48	0	0.00	7.3	8.3	7.8	5.5-9.50	
CONDUCTIVITY		96	----	------	248	705	391	--------	-----
CONDUCTIVITY	1	96	0	0.00	378	405	389	1500	MICSM
QUALITATIVE TASTE		96	----	------	----------	----------	----------	--------	
QUANTITATIVE TASTE		48	0	0.00	0	0	0	3	
TASTE (NATURE)		46	----	------	----------	----------	----------	--------	
QUALITATIVE ODOUR		96	----	------	----------	----------	----------	--------	
QUANTITATIVE ODOUR		48	0	0.00	0	1	0	3	
ODOUR (NATURE)		47	----	------	----------	----------	----------	--------	
AMMONIUM		48	0	0.00	<0.05	<0.05	<0.05	0.5	MG/L
NITRITE		48	0	0.00	<0.01	<0.01	<0.01	0.1	MG/L
NITRATE		48	0	0.00	11	32.8	21.6	50	MG/L
CHLORIDE		1	----	------	70	70	70	--------	-----
CHLORIDE	1	1	0	0.00	53	53	53	400	MG/L
SULPHATE		1	0	0.00	102	102	102	250	MG/L
FLUORIDE		4	0	0.00	<100	390	<243	1500	UG/L
PHOSPHORUS		1	0	0.00	<30	<30	<30	2200	UG/L
ALKALINITY		4	0	0.00	110	146	124	NONE	MG/L
TOTAL HARDNESS		4	0	0.00	164	265	213	NONE	MG/L
CALCIUM		1	----	------	78	78	78	--------	-----
CALCIUM	1	1	0	0.00	55	55	55	250	MG/L
MAGNESIUM		1	0	0.00	17	17	17	50	MG/L
SODIUM		1	----	------	49	49	49	--------	-----
SODIUM	2	2	0	0.00	49	49	31	150	MG/L
POTASSIUM		1	0	0.00	5	5	5	12	MG/L
IRON	U	48	0	0.00	<20	90	<23	200	ug/l
MANGANESE		48	0	0.00	<10	<10	<10	50	UG/L
ALUMINIUM		48	0	0.00	<20	80	<21	200	UG/L
COPPER		1	0	0.00	43	43	43	3000	UG/L
ZINC		1	0	0.00	13	13	13	5000	UG/L
LEAD	U	24	1	4.16	<1	818	<40	50	UG/L

22/03/94 19:46:47

QUALIFIER KEY ***

A SECTION 19 UNDERTAKING APPLIES

COMPLIANCE WITH THE PCV IS BASED ON THE AVERAGE CONCENTRATION OR VALUE OVER THE PRECEDING 12 MONTHS

COMPLIANCE WITH THE PCV IS BASED ON 80 PERCENT OF THE SAMPLES OVER THE PRECEDING 36 MONTHS

COMPLIANCE WITH THE PCV REQUIRES THAT 95 PERCENT OF SAMPLES WITHIN THE YEAR (OR THE LAST 50 SAMPLES WHICHEVER IS THE GREATER) ARE FREE OF COLIFORMS IN 100ML

Severn Trent Water

WATER SUPPLY ZONE :- N08A WHITEM & SHER RISE 93/94

REPORTING PERIOD :- 01/01/1993 TO 31/12/1993

Parameter And Qualifiers		No. Of Samples Taken In Period	Samples Greater Than P.C.V.		Concentration Or Value				
			Number	Percent	Minimum	Maximum	Mean	PCV	Units
CADMIUM		1	0	0.00	<0.2	<0.2	<0.2	5	UG/L
SILVER		1	0	0.00	<0.2	<0.2	<0.2	10	UG/L
BORON		1	----	------	<160	<160	<160	--------	-----
BORON	1	1	0	0.00	<90	<90	<90	2000	UG/L
BARIUM		1	----	------	80	80	80	--------	-----
BARIUM	1	1	0	0.00	190	190	190	1000	UG/L
ARSENIC		1	0	0.00	1	1	1	50	UG/L
CHROMIUM		1	0	0.00	<2	<2	<2	50	UG/L
NICKEL		1	0	0.00	3	3	3	50	UG/L
MERCURY		1	0	0.00	<0.1	<0.1	<0.1	1	UG/L
ANTIMONY		1	0	0.00	1.4	1.4	1.4	10	UG/L
SELENIUM		1	0	0.00	3.8	3.8	3.8	10	UG/L
CYANIDE		1	0	0.00	<5	<5	<5	50	UG/L
OXIDIZABILITY		1	0	0.00	1.4	1.4	1.4	5	MG/L
T.O.C.		1	0	0.00	3.2	3.2	3.2	5	MG/L
SURFACTANTS		1	0	0.00	30	30	30	200	UG/L
TRIHALOMETHANES		25	----	------	2	78	19	--------	-----
TRIHALOMETHANES	3	25	0	0.00	9	28	18	100	UG/L
TETRACHLOROMETHANE		14	----	------	<0.3	<0.3	<0.3	--------	-----
TETRACHLOROMETHANE	1	14	0	0.00	<0.3	<1.1	<0.6	3	UG/L
TRICHLOROETHENE		14	----	------	<3	<3	<3	--------	-----
TRICHLOROETHENE	1	14	0	0.00	<3	<4.7	<3.8	30	UG/L
TETRACHLOROETHENE		14	----	------	<1	<1	<1	--------	-----
TETRACHLOROETHENE	1	14	0	0.00	<1	<1	<1	10	UG/L
P.A.H. (TOTAL)		4	0	0.00	<0.005	<0.005	<0.005	0.2	UG/L
BENZ (A) PYRENE		4	----	------	<1	<1	<1	--------	-----
BENZ (A) PYRENE	1	4	0	0.00	<1	<4.6	<3.3	10	NG/L
TOTAL PESTICIDES		4	0	0.00	<0.03	<0.05	<0.05	0.5	UG/L
TOTAL MECOPROP		4	0	0.00	<0.01	<0.01	<0.01	0.1	UG/L
MCPA		4	0	0.00	<0.01	<0.01	<0.01	0.1	UG/L
IOXYNIL		4	0	0.00	<0.01	<0.01	<0.01	0.1	UG/L
BROMOXYNIL		4	0	0.00	<0.01	<0.01	<0.01	0.1	UG/L
2,4 DB		4	0	0.00	<0.01	<0.01	<0.01	0.1	UG/L
2,4 D		4	0	0.00	<0.01	<0.01	<0.01	0.1	UG/L
DICHLORPROP		4	0	0.00	<0.01	<0.01	<0.01	0.1	UG/L
DICAMBA		4	0	0.00	<0.01	<0.01	<0.01	0.1	UG/L
MCPB		4	0	0.00	<0.02	<0.02	<0.02	0.1	UG/L
2,4,5,-TCPA		4	0	0.00	<0.01	<0.01	<0.01	0.1	UG/L
2,3,6,-TBA		4	0	0.00	<0.01	<0.01	<0.01	0.1	UG/L
ATRAZINE		4	0	0.00	<0.02	<0.02	<0.02	0.1	UG/L
SIMAZINE		4	0	0.00	<0.02	<0.02	<0.02	0.1	UG/L

22/03/94 19:46:47

QUALIFIER KEY ###

COMPLIANCE WITH THE PCV IS BASED ON THE AVERAGE CONCENTRATION OR VALUE OVER THE PRECEDING 12 MONTHS
COMPLIANCE WITH THE PCV IS BASED ON THE AVERAGE CONCENTRATION OR VALUE OVER A ROLLING 3 MONTH PERIOD

Severn Trent Water

WATER SUPPLY ZONE :- N08A WHITEM & SHER RISE 93/94

REPORTING PERIOD :- 01/01/1993 TO 31/12/1993

Parameter And Qualifiers		No. Of Samples Taken In Period	Samples Greater Than P.C.V.		Concentration Or Value				
			Number	Percent	Minimum	Maximum	Mean	PCV	Units
PROMETRYNE		4	0	0.00	<0.01	<0.01	<0.01	0.1	UG/L
TRIETAZINE		4	0	0.00	<0.01	<0.02	<0.01	0.1	UG/L
TERBUTRYNE		4	0	0.00	<0.01	<0.01	<0.01	0.1	UG/L
PROPAZINE		4	0	0.00	<0.01	<0.01	<0.01	0.1	UG/L
ISOPROTURON		4	0	0.00	<0.02	<0.05	<0.04	0.1	UG/L
CHLORTOLURON		4	0	0.00	<0.02	<0.05	<0.04	0.1	UG/L
LINURON		4	0	0.00	<0.02	<0.05	<0.04	0.1	UG/L
DIURON		4	0	0.00	<0.02	<0.05	<0.04	0.1	UG/L

22/03/94 19:46:47

Severn Trent Water

WATER SUPPLY ZONE :- N08A WHITEMR/SHER RISE 93/94

REPORTING PERIOD :- 01/01/1994 TO 31/08/1994

AREA:- Forest Fields, Whitemoor, Sherwood, Hyson Green, Bobbers Mill, Radford.

POPULATION:- 36,793

SUPPLY SOURCES:- BESTWOOD BH,BOUGHTON BH,CHUR WILNE WTW, FAR BAULKER BH HALAM BH,OMPTON BH,BAMFORD (DV),HOMESFORD WSW

AUTHORISED SUPPLY POINT:-

GENERAL COMMENTS:-

Lead — The exceedances of the PCV for lead were a result of pick up from the pipes between the water main and the customer's tap. Actions are in hand to alleviate the problem as detailed problem. The relevant Environmental Health Officer and the customer were informed.

ACTION TAKEN TO COMPLY WITH SECTION 19 (1) (B) UNDERTAKINGS:-

Reference	Nature of Contravention	Steps to be taken	Statutory completion date
ST.40(L)	Due to the presence of lead service pipes, a significant proportion of which is not the responsibility of Severn Trent Water there is a risk that on occasions the prescribed concentration may be exceeded	Phosphate dosing at source or service reservior to minimise plumbosolvent characteristics of the water	December 1995
ST.41(D)	Occasional exceedances of the iron and turbidity parameters	Where appropriate air scour, flush or otherwise clean the system	Ongoing as necessary
		and Carry out mains refurbishment programme using any acceptable process. Estimates are that approximately 5500km require refurbishment in the priority zones by 31 December 1994	Continuing

Severn Trent Water

WATER SUPPLY ZONE :- N08A WHITEMR/SHER RISE 93/94

REPORTING PERIOD :- 01/01/1994 TO 31/08/1994

01/01/1994 TO 31/08/1994

DETAILS OF SAMPLES WHICH BREACHED A STANDARD:-

DATE		RESULT			LOCATION
18/01/94	LEAD	=	67		WILKINSON ST AINSLEY EST DMA
28/07/94	LEAD	=	107		CROSSLEY STREET SHERWOOD DMA

Severn Trent Water

WATER SUPPLY ZONE :- N08A WHITEMR/SHER RISE 93/94

REPORTING PERIOD :- 01/01/1994 TO 31/08/1994

Parameter And Qualifiers		No. Of Samples Taken In Period	Samples Greater Than P.C.V.		Concentration Or Value				
			Number	Percent	Minimum	Maximum	Mean	PCV	Units
TOTAL COLIFORMS (COMPLIANCE)		64	0	0.00	0	0	0	0.0	100ML
FAECAL COLIFORMS		64	0	0.00	0	0	0	0.0	100ML
PLATE COUNT (AT 21C)		35	0	0.00	0	14	1	NONE	ML
PLATE COUNT (AT 37C)		35	0	0.00	0	8	0	NONE	ML
FREE CHLORINE		64	0	0.00	0.01	0.39	0.09	NONE	MG/L
TOTAL CHLORINE		64	0	0.00	0.01	0.55	0.12	NONE	MG/L
COLOUR		7	0	0.00	<1	<1	<1	20	HAZEN
TURBIDITY	U	7	0	0.00	<0.3	<0.3	<0.3	4	F.T.U
TEMPERATURE		64	0	0.00	5.5	20.1	12.5	25	DEG C
PH		7	0	0.00	7.4	8.2	7.8	5.5-9.50	
CONDUCTIVITY (COMPLIANCE)		64	0	0.00	245	663	444	1500	MICSM
QUALITATIVE TASTE		64	----	------	----------	----------	----------	--------	
QUANTITATIVE TASTE		7	0	0.00	0	0	0	3	
TASTE (NATURE)		7	----	------	----------	----------	----------	--------	
QUALITATIVE ODOUR		64	----	------	----------	----------	----------	--------	
QUANTITATIVE ODOUR		7	0	0.00	0	0	0	3	
ODOUR (NATURE)		7	----	------	----------	----------	----------	--------	
AMMONIUM		7	0	0.00	<0.05	<0.05	<0.05	0.5	MG/L
NITRITE		7	0	0.00	<0.01	<0.01	<0.01	0.1	MG/L
NITRATE		31	0	0.00	13	34	22.5	50	MG/L
CHLORIDE (COMPLIANCE)		1	0	0.00	40	40	40	400	MG/L
SULPHATE		1	0	0.00	47	47	47	250	MG/L
FLUORIDE		3	0	0.00	<100	230	<143	1500	UG/L
PHOSPHORUS		1	0	0.00	<30	<30	<30	2200	UG/L
ALKALINITY		3	0	0.00	85	125	108	NONE	MG/L
TOTAL HARDNESS		3	0	0.00	143	197	174	NONE	MG/L
CALCIUM (COMPLIANCE)		3	0	0.00	26	48	38	250	MG/L
MAGNESIUM		3	0	0.00	15	23	19	50	MG/L
SODIUM (COMPLIANCE)		1	0	0.00	27	27	27	150	MG/L
POTASSIUM		1	0	0.00	2.9	2.9	2.9	12	MG/L
IRON	U	7	0	0.00	<20	30	<21	200	ug/l
MANGANESE		7	0	0.00	<5	<5	<5	50	UG/L
ALUMINIUM		7	0	0.00	<20	<20	<20	200	UG/L
COPPER		1	0	0.00	20	20	20	3000	UG/L
ZINC		1	0	0.00	20	20	20	5000	UG/L
LEAD	U	16	2	12.50	<1	107	<23	50	UG/L
CADMIUM		1	0	0.00	<0.5	<0.5	<0.5	5	UG/L
SILVER		1	0	0.00	<0.2	<0.2	<0.2	10	UG/L
BORON (COMPLIANCE)		1	0	0.00	60	60	60	2000	UG/L
BARIUM (COMPLIANCE)		1	0	0.00	390	390	390	1000	UG/L
ARSENIC		1	0	0.00	<1	<1	<1	50	UG/L

26/10/94 11:44:52

QUALIFIER KEY ***

A SECTION 19 UNDERTAKING APPLIES

Severn Trent Water

WATER SUPPLY ZONE :- N08A WHITEMR/SHER RISE 93/94

REPORTING PERIOD :- 01/01/1994 TO 31/08/1994

Parameter And Qualifiers	No. Of Samples Taken In Period	Samples Greater Than P.C.V.		Concentration Or Value				
		Number	Percent	Minimum	Maximum	Mean	PCV	Units
CHROMIUM	1	0	0.00	<5	<5	<5	50	UG/L
NICKEL	1	0	0.00	<2	<2	<2	50	UG/L
MERCURY	1	0	0.00	<0.1	<0.1	<0.1	1	UG/L
ANTIMONY	1	0	0.00	<1	<1	<1	10	UG/L
SELENIUM	1	0	0.00	<1	<1	<1	10	UG/L
CYANIDE	1	0	0.00	<5	<5	<5	50	UG/L
OXIDIZABILITY	1	0	0.00	0.5	0.5	0.5	5	MG/L
T.O.C.	1	0	0.00	1	1	1	5	MG/L
SURFACTANTS	1	0	0.00	<50	<50	<50	200	UG/L
TRIHALOMETHANES (COMPLIANCE)	2	0	0.00	10	57	34	100	UG/L
TETRACHLOROMETHANE (COMP.)	9	0	0.00	<0.3	<0.3	<0.3	3	UG/L
TRICHLOROETHENE (COMPLIANCE)	9	0	0.00	<3	7	<3.4	30	UG/L
TETRACHLOROETHENE (COMP.)	9	0	0.00	<1	10	<2.4	10	UG/L
P.A.H. (TOTAL)	16	0	0.00	<0.005	0.046	<0.015	0.2	UG/L
BENZ (A) PYRENE (COMPLIANCE)	16	0	0.00	<1	<1	<1	10	NG/L
TOTAL PESTICIDES	2	0	0.00	<0.02	<0.02	<0.02	0.5	UG/L
TOTAL MECOPROP	2	0	0.00	<0.01	<0.01	<0.01	0.1	UG/L
MCPA	2	0	0.00	<0.01	<0.01	<0.01	0.1	UG/L
IOXYNIL	2	0	0.00	<0.01	<0.01	<0.01	0.1	UG/L
BROMOXYNIL	2	0	0.00	<0.01	<0.01	<0.01	0.1	UG/L
2,4 DB	2	0	0.00	<0.01	<0.01	<0.01	0.1	UG/L
2,4 D	2	0	0.00	<0.01	<0.01	<0.01	0.1	UG/L
DICHLORPROP	2	0	0.00	<0.01	<0.01	<0.01	0.1	UG/L
DICAMBA	2	0	0.00	<0.01	<0.01	<0.01	0.1	UG/L
MCPB	2	0	0.00	<0.02	<0.02	<0.02	0.1	UG/L
2,4,5,-TCPA	2	0	0.00	<0.01	<0.01	<0.01	0.1	UG/L
2,3,6,-TBA	2	0	0.00	<0.01	<0.01	<0.01	0.1	UG/L
ATRAZINE	2	0	0.00	<0.02	<0.02	<0.02	0.1	UG/L
SIMAZINE	2	0	0.00	<0.02	<0.02	<0.02	0.1	UG/L
PROMETRYNE	2	0	0.00	<0.01	<0.01	<0.01	0.1	UG/L
TRIETAZINE	2	0	0.00	<0.01	<0.01	<0.01	0.1	UG/L
TERBUTRYNE	2	0	0.00	<0.01	<0.01	<0.01	0.1	UG/L
PROPAZINE	2	0	0.00	<0.01	<0.01	<0.01	0.1	UG/L
ISOPROTURON	2	0	0.00	<0.02	<0.02	<0.02	0.1	UG/L
CHLORTOLURON	2	0	0.00	<0.02	<0.02	<0.02	0.1	UG/L
LINURON	2	0	0.00	<0.02	<0.02	<0.02	0.1	UG/L
DIURON	2	0	0.00	<0.02	<0.02	<0.02	0.1	UG/L

Appendix 3 Calibration Curves

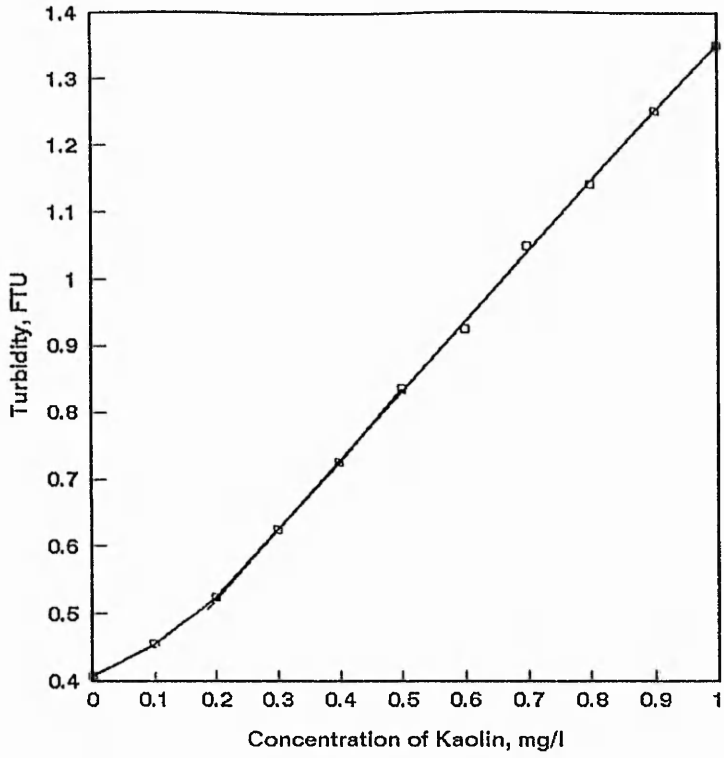

Figure (A-1) Calibration curve for kaolin turbidity, 0 - 1.0 mg/l

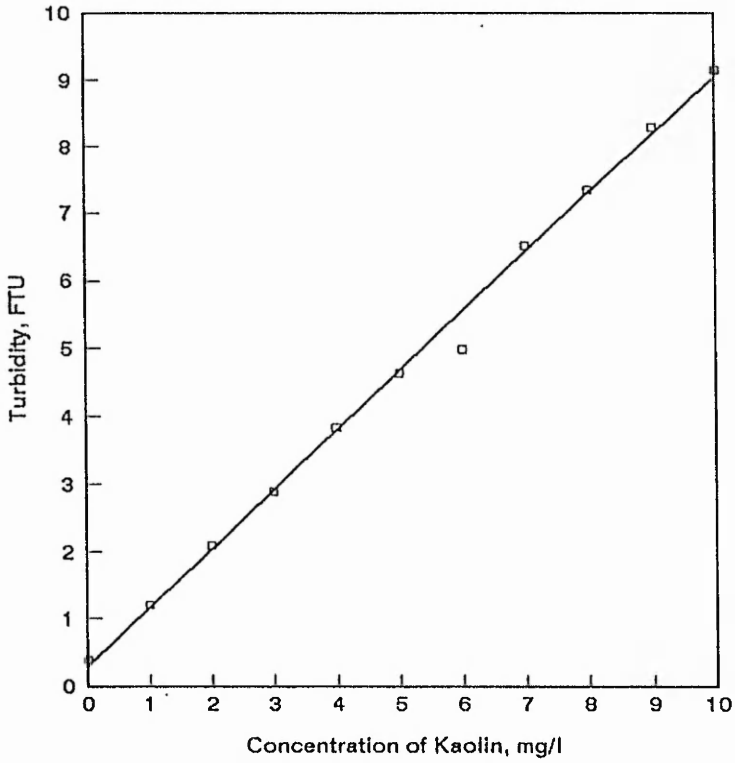

Figure (A-2) Calibration curve for kaolin turbidity, 0 - 10 mg/l

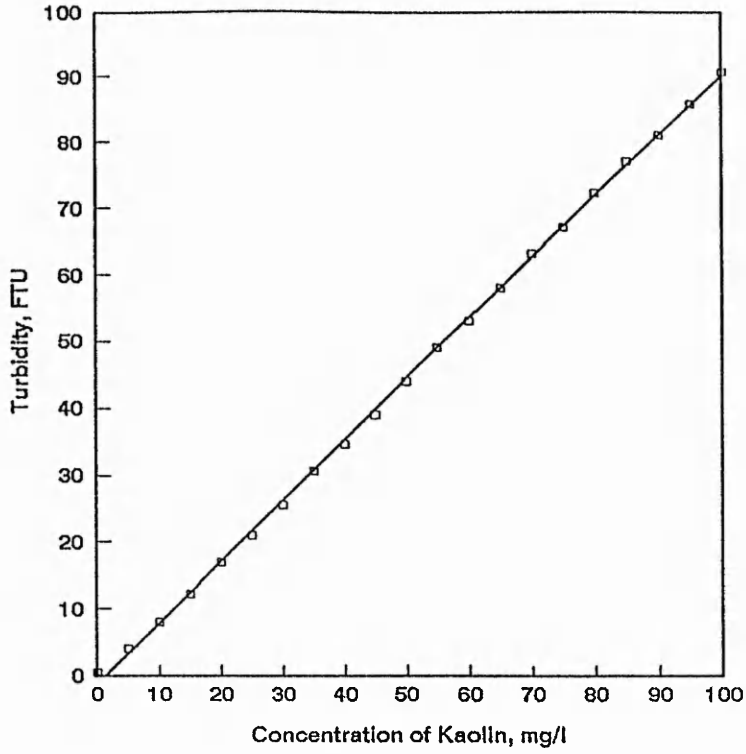

Figure (A-3) Calibration curve for kaolin turbidity, 0 - 100 mg/l

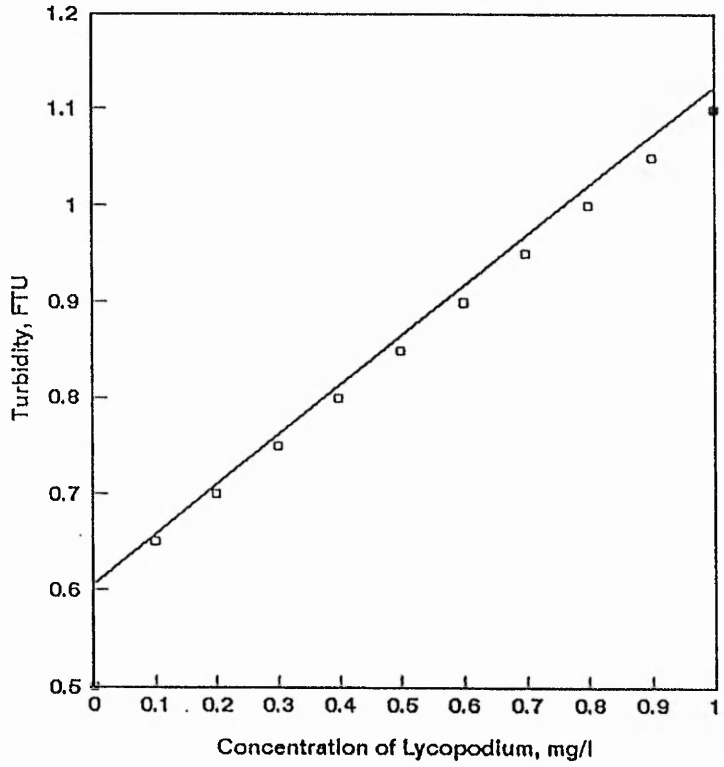

Figure (A-4) Calibration curve for lycopodium turbidity, 0 - 1.0 mg/l

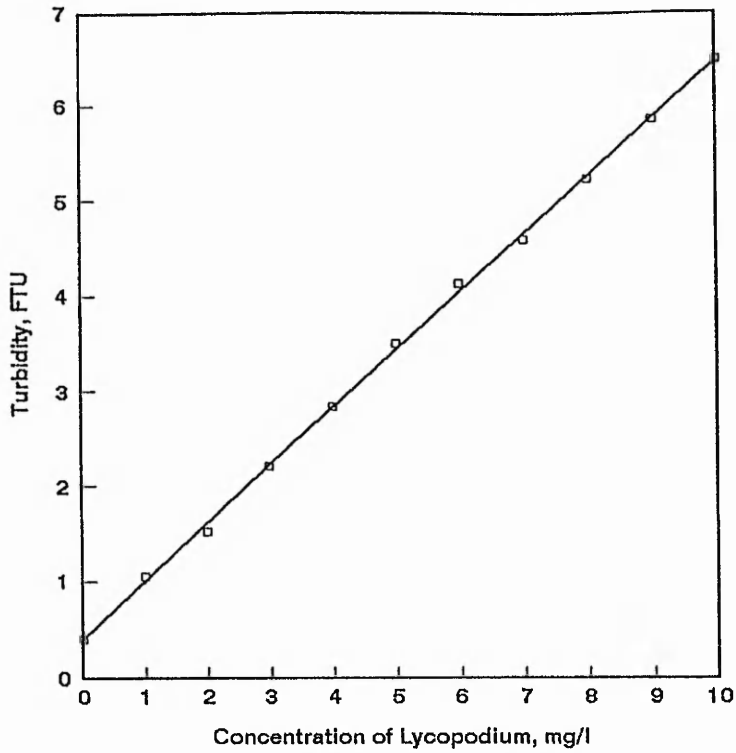

Figure (A-5) Calibration curve for lycopodium turbidity, 0 - 10 mg/l

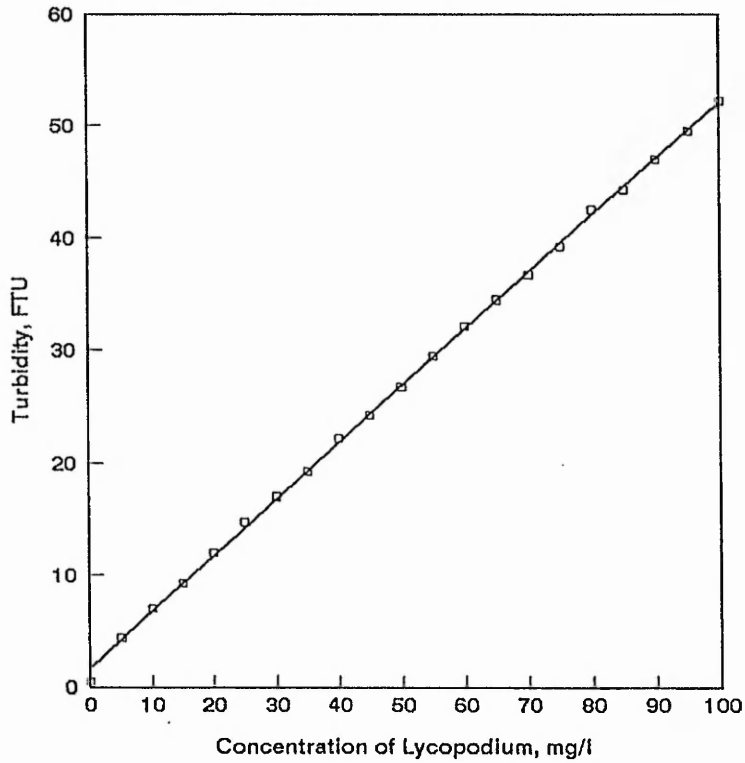

Figure (A-6) Calibration curve for lycopodium turbidity, 0 - 100 mg/l

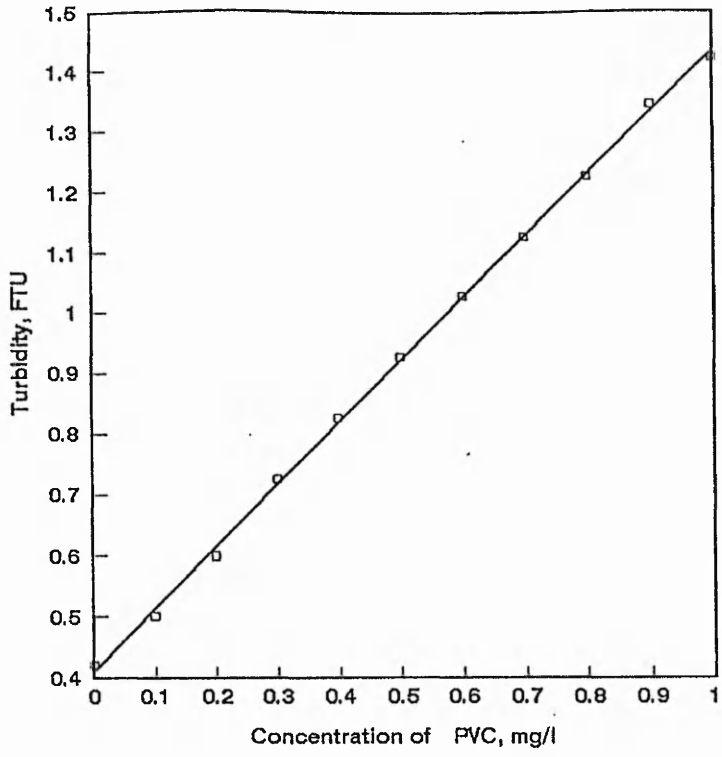

Figure (A-7) Calibration curve for PVC turbidity, 0 - 1.0 mg/l

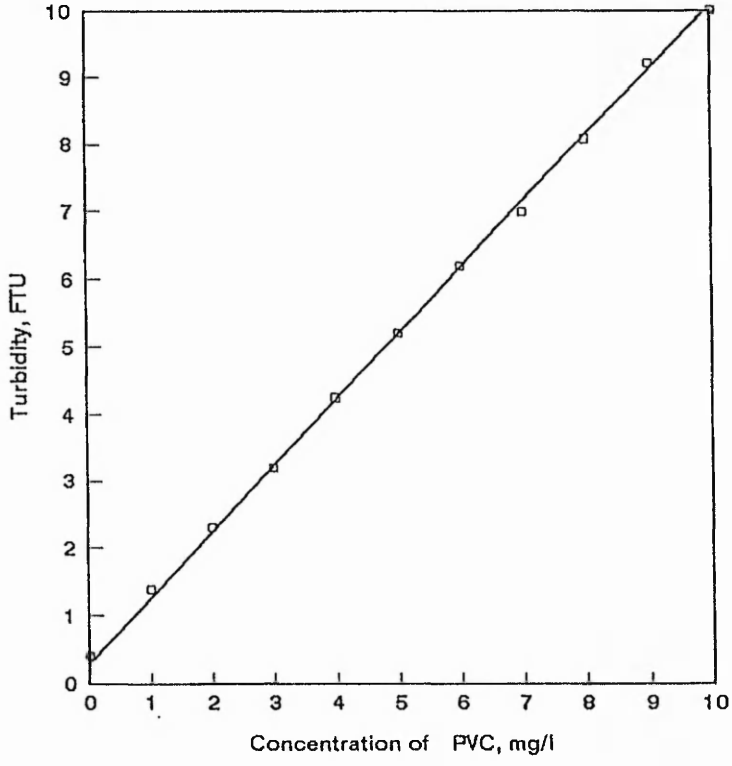

Figure (A-8) Calibration curve for PVC turbidity, 0 - 10 mg/l

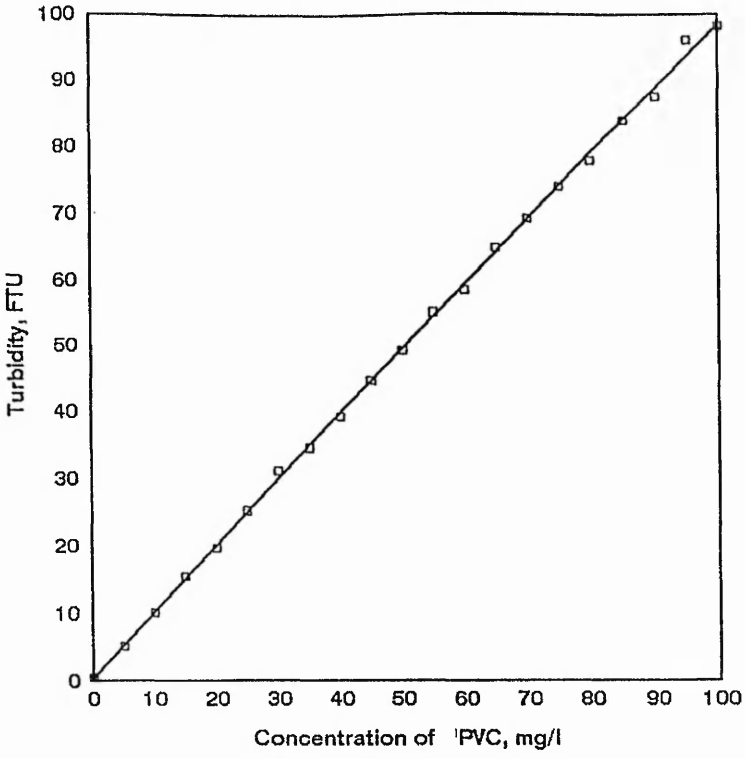

Figure (A-9) Calibration curve for PVC turbidity, 0 - 100 mg/l

Appendix 4 Coagulation-Flocculation Jar Test Results

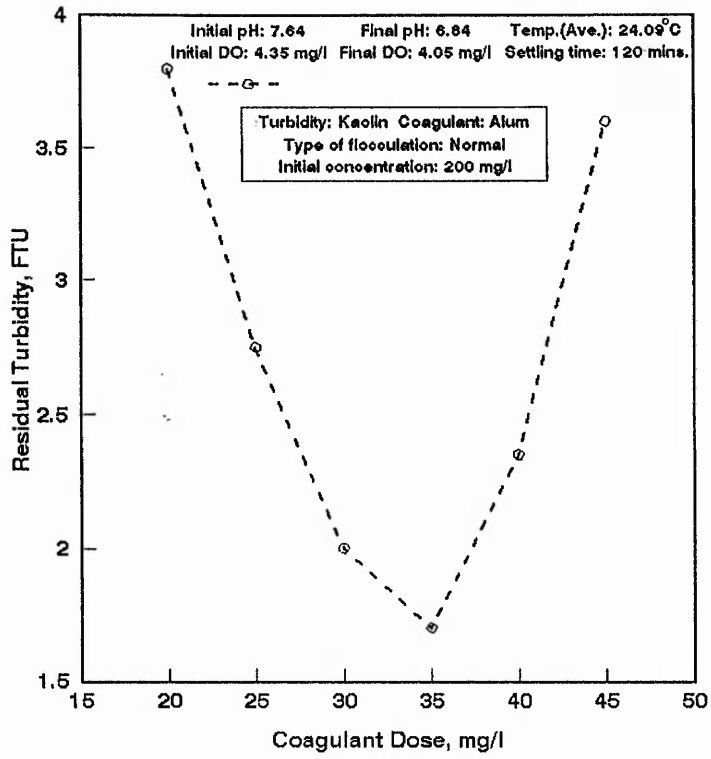

Figure (B-1) Coagulation and flocculation Jar Test curve

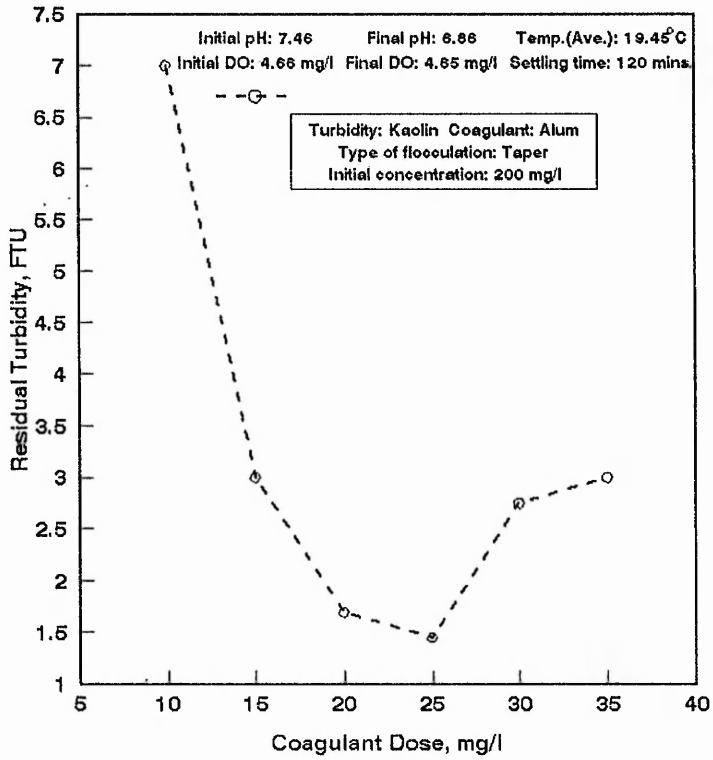

Figure (B-2) Coagulation and flocculation Jar Test curve

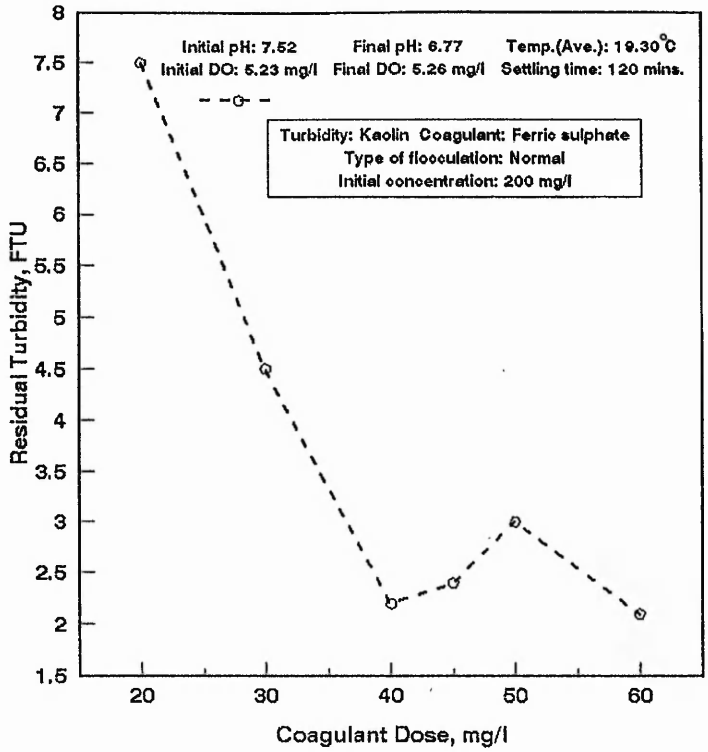

Figure (B-3) Coagulation and flocculation Jar Test curve

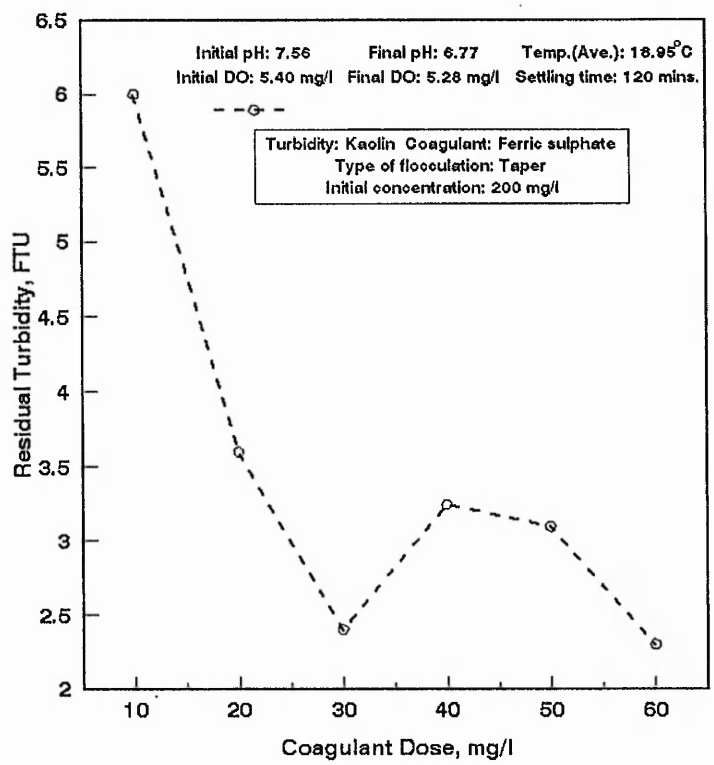

Figure (B-4) Coagulation and flocculation Jar Test curve

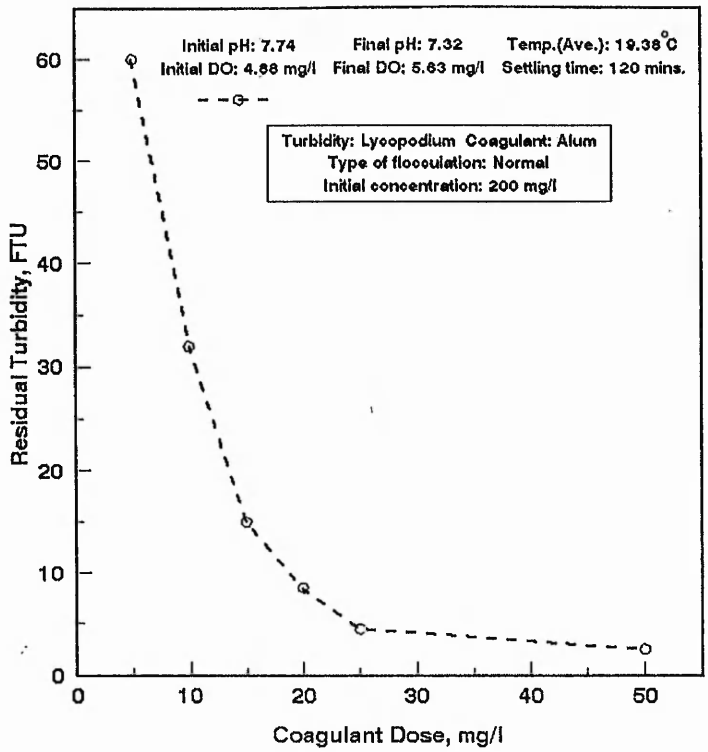

Figure (B-5) Coagulation and flocculation Jar Test curve

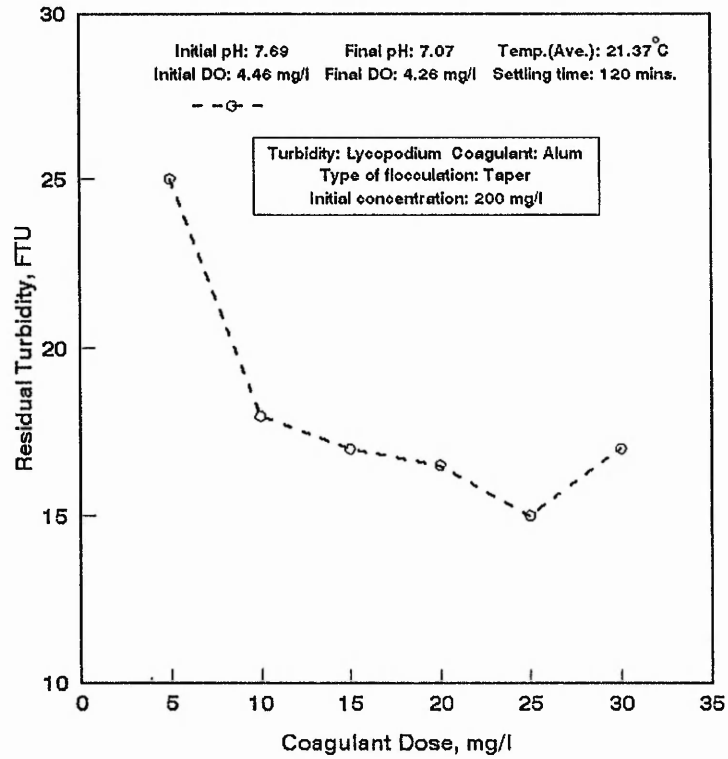

Figure (B-6) Coagulation and flocculation Jar Test curve

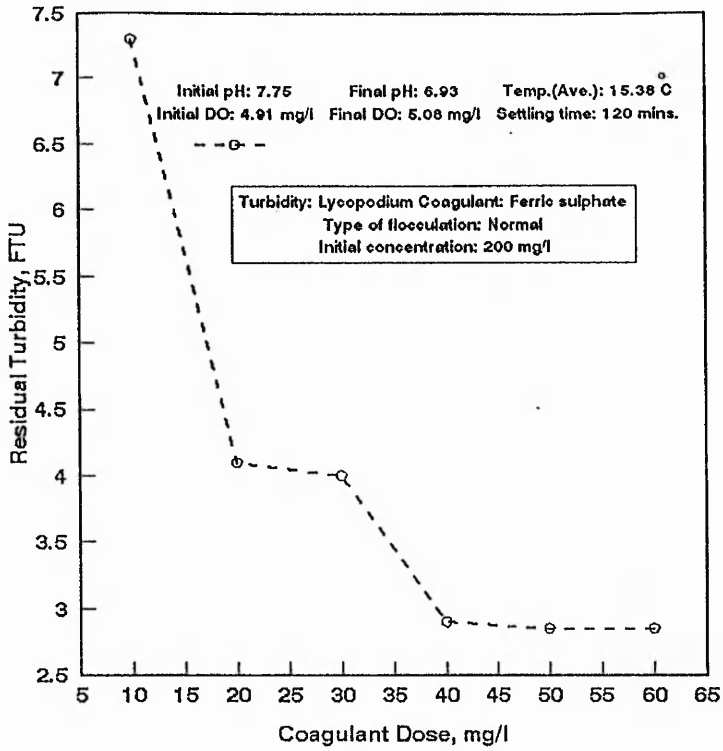

Figure (B-7) Coagulation and flocculation Jar Test curve

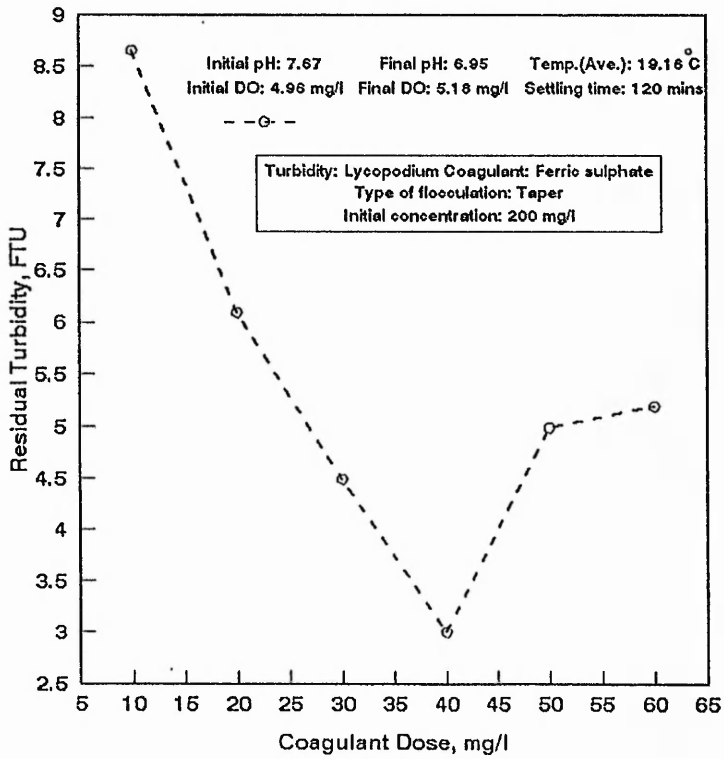

Figure (B-8) Coagulation and flocculation Jar Test curve

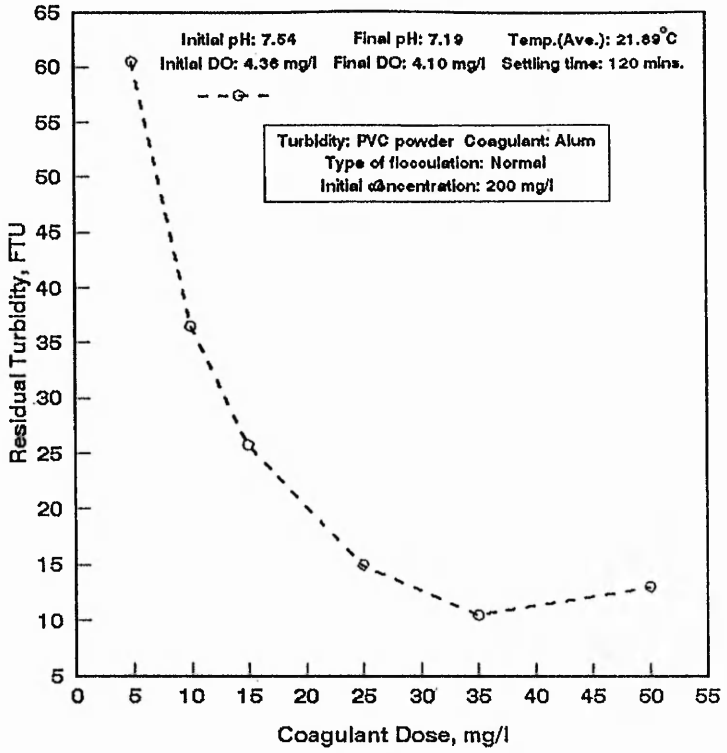

Figure (B-9) Coagulation and flocculation Jar Test curve

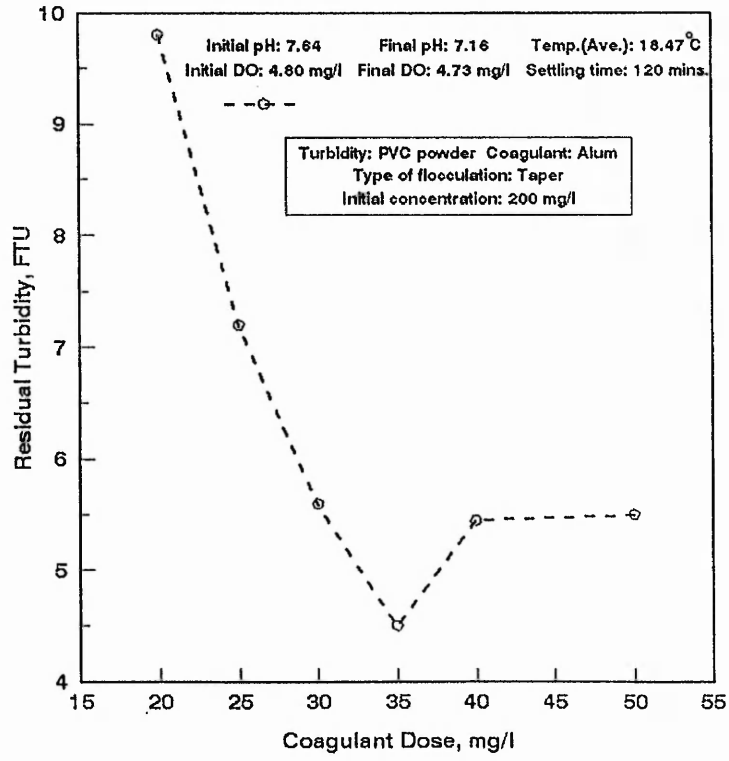

Figure (B-10) Coagulation and flocculation Jar Test curve

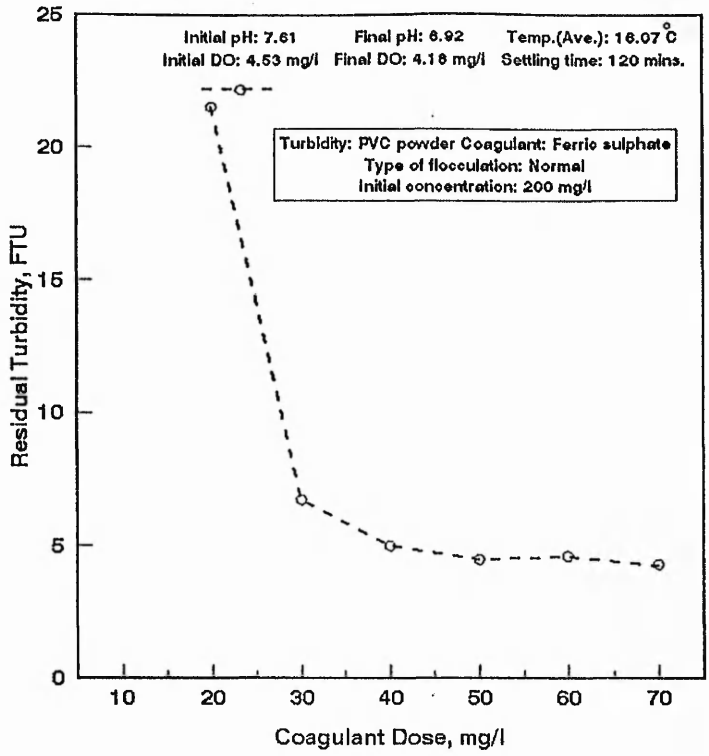

Figure (B-11) Coagulation and flocculation Jar Test curve

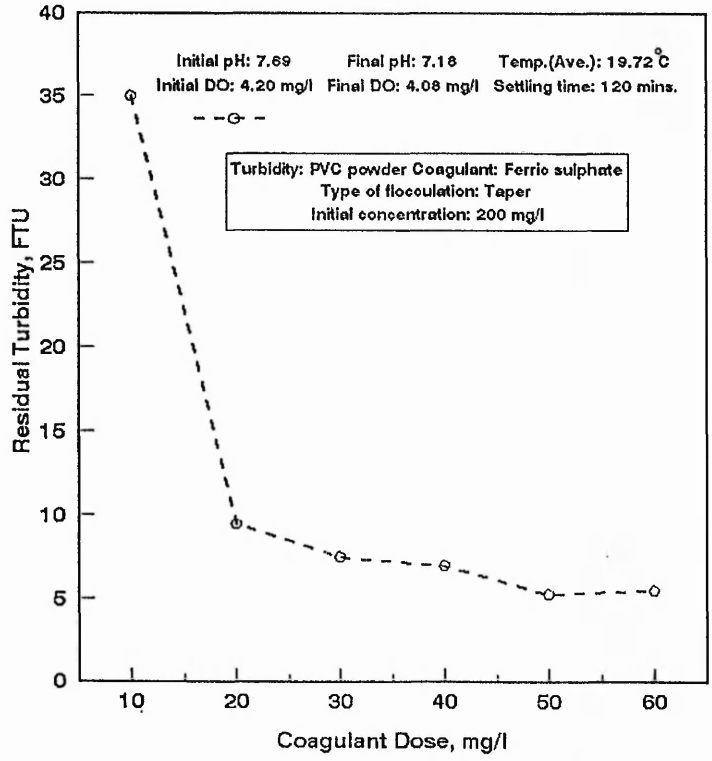

Figure (B-12) Coagulation and flocculation Jar Test curve

Appendix 5 Experimental Data

Table (C - 1). Details of Experimental Run

Date : 04 - 01 - 94	Run No : 02
Synthetic Turbidity : Kaolin	Size Range, micrometer : 2 - 53
Coagulant : Aluminium Sulphate	Coagulant Dose, mg/l : 35
Air Flow-rate, cm^3/min. : 100	Orifice Diameter, mm. : 1·0
Flocculation Type : Normal	Flocculation Time, min. : 20
Rapid Mixing Time, min. : 2·0	Ambient Temperature, °C : 15·50

Parameters	Initial Conditions (Before Flocculation)		Final Conditions (After Flocculation)	
Dissolved Oxygen, mg/l	4·80		5·20	
p^H	7·32		6·90	
Temperature, °C	10·20		12·70	
Nitrate_Nitrogen, N, mg/l	4·20 (TpW)	3·80 (TrW)	0·00 (Flocc)	0·00 (sed)
Iron, Fe, mg/l	0·01 (TpW)	0·11 (TrW)	0·16 (Flocc)	0·03 (sed)
Suspension Concentration, mg/l	200		194·25	

Initial Alkalinity, mg $CaCO_3$/l : 125	Final Alkalinity, mg $CaCO_3$/l : 100
Initial Aluminium Concentration, mg/l : 3·00	Final Aluminium Concentration, mg/l : 0·14

Contd....

Table (C - 1). Details of Experimental Runs

Run no: 02 Date: 04-01-94

Depth (m)	Residual Turbidity, FTU (T)			Suspension Concentration, mg/l (C)			Removal Efficiency, percentage (R)					
	Time, min.											
	30			60			90			120		
	T	C	R	T	C	R	T	C	R	T	C	R
0.20	60·00	66·66	66·67	36·00	40·00	80·00	27·00	30·00	85·00	21·50	23·88	88·06
0.40	72·00	80·00	60·00	40·00	44·44	77·78	27·50	30·55	84·72	24·50	27·22	86·39
0.60	75·00	83·25	58·37	42·00	46·62	76·69	29·00	32·19	83·90	25·00	27·77	86·11
0.80	77·00	85·47	57·26	43·00	47·77	76·11	30·00	33·33	83·33	26·00	28·86	85·57
1.00	79·00	87·77	56·11	44·00	48·84	75·58	31·00	34·44	82·78	27·00	30·00	85·00
1.20	80·00	88·88	55·58	45·00	49·95	75·02	32·00	35·55	82·22	27·50	30·55	84·72
1.40	91·00	101·11	49·44	45·50	50·50	74·75	34·00	37·77	81·11	28·00	31·11	84·44
1.60	96·50	107·22	46·39	46·00	51·06	74·47	35·50	39·44	80·28	28·50	31·63	84·18
1.80	100·00	111·11	44·44	44·00	48·84	75·58	33·00	36·63	81·68	29·00	32·19	83·90
2.00	105·00	116·66	41·67	43·50	48·28	75·85	33·50	37·22	81·39	28·50	31·66	84·17
2.20	110·00	122·22	38·89	46·00	51·11	74·44	35·00	38·88	80·56	29·00	32·22	83·89

Table (C - 2). Details of Experimental Run

Date : 19-04-94	Run No : 38
Synthetic Turbidity : Lycopodium	Size Range, micrometer : 35
Coagulant : Aluminium sulphate	Coagulant Dose, mg/l : 35
Air Flow-rate, cm^3/min. : 100	Orifice Diameter, mm. : 1·0
Flocculation Type : Normal	Flocculation Time, min. : 20
Rapid Mixing Time, min. : 2·0	Ambient Temperature, °C : 16·50

Parameters	Initial Conditions (Before Flocculation)	Final Conditions (After Flocculation)
Dissolved Oxygen, mg/l	4·90	5·30
p^H	7·56	6·40
Temperature, °C	14·11	15·10
Nitrate Nitrogen, N, mg/l	4·80 (Tp W) 3·90(Tr W)	2·60 (Flocc) 1·36 (Sed)
Iron, Fe, mg/l	0·03 (Tp W) 0·04 (Tr W)	0·04 (Flocc) 0·01 (Sed)
Suspension Concentration, mg/l	200	195·07

Initial Alkalinity, mg $CaCO_3$/l : 125	Final Alkalinity, mg $CaCO_3$/l : 115
Initial Aluminium Concentration, mg/l : 3·00	Final Aluminium Concentration, mg/l : 0·12

Contd....

Table (C - 2). Details of Experimental Runs

Run no: 38 Date: 19-04-94

Depth (m)	Residual Turbidity, FTU (T)			Suspension Concentration, mg/l (C)			Removal Efficiency, percentage (R)					
	Time, min.											
	60			120			180			240		
	T	C	R	T	C	R	T	C	R	T	C	R
0.20	81·00	150·31	24·84	33·50	61·73	69·13	25·50	46·81	76·59	16·00	29·09	85·45
0.40	85·00	157·77	21·11	37·00	68·25	65·87	27·00	49·60	75·20	17·00	30·95	84·52
0.60	78·00	142·85	28·57	32·00	58·93	70·53	28·00	51·47	74·26	18·00	32·82	83·59
0.80	76·00	140·99	29·50	31·00	57·06	71·47	25·50	46·81	76·59	18·50	33·75	83·12
1.00	75·00	139·12	30·44	30·50	56·13	71·93	21·50	39·35	80·32	18·50	33·75	83·12
1.20	70·00	129·80	35·10	30·50	56·13	71·93	20·50	37·48	81·26	17·00	30·95	84·52
1.40	64·00	118·61	40·69	30·50	56·13	71·93	19·00	34·68	82·66	16·50	30·02	84·99
1.60	57·50	106·49	46·75	30·00	55·20	72·40	18·00	32·82	83·59	15·00	27·22	86·39
1.80	55·00	101·82	49·09	29·50	54·27	72·86	17·00	30·95	84·52	13·00	23·49	88·25
2.00	50·00	92·50	53·75	29·00	53·33	73·33	16·00	29·09	85·45	12·00	21·63	89·18
2.20	49·00	90·63	54·68	26·00	47·74	76·13	15·50	28·16	85·92	11·50	20·70	89·65

Table (C - 3). Details of Experimental Run

Date : 09 - 05 - 94	Run No : 68
Synthetic Turbidity : PVC powder	Size Range, micrometer : 0·5 - 1·50
Coagulant : Aluminium Sulphate	Coagulant Dose, mg/l : 35
Air Flow-rate, cm^3/min. : 100	Orifice Diameter, mm. : 1·0
Flocculation Type : Normal	Flocculation Time, min. : 20
Rapid Mixing Time, min. : 2·0	Ambient Temperature, °C : 18·25

Parameters	Initial Conditions (Before Flocculation)	Final Conditions (After Flocculation)
Dissolved Oxygen, mg/l	5·36	5·67
p^H	7·49	7·09
Temperature, °C	15·76	16·55
Nitrate Nitrogen, N, mg/l	4·80 (TPW) 4·30(TmW)	3·10 (Flocc) 1·80 (Sed)
Iron, Fe, mg/l	0·05 (TP W) 0·06 (TPW)	0·12 (Flocc) 0·02 (Sed)
Suspension Concentration, mg/l	200	182·21

Initial Alkalinity, mg $CaCO_3$/l : 125	Final Alkalinity, mg $CaCO_3$/l : 120
Initial Aluminium Concentration, mg/l : 3·00	Final Aluminium Concentration, mg/l : 0·14

Contd....

Table (C - 3). Details of Experimental Runs

Run no: 68 Date: 09- 05- 94

Depth (m)	Residual Turbidity, FTU (T)			Suspension Concentration, mg/l (C)			Removal Efficiency, percentage (R)					
	Time, min.											
	30			60			90			120		
	T	C	R	T	C	R	T	C	R	T	C	R
0.20	37.50	38.06	80.97	14.00	13.95	93.02	12.50	12.41	93.79	5.50	5.23	97.38
0.40	72.00	73.46	63.27	28.00	28.31	85.84	15.50	15.49	92.25	12.00	11.90	94.05
0.60	88.50	90.39	54.80	36.00	36.52	81.73	18.00	18.05	90.97	15.00	14.97	92.51
0.80	91.50	93.46	53.27	40.00	40.62	79.68	20.50	20.62	89.69	17.00	17.03	91.48
1.00	100.00	102.18	48.91	45.00	45.75	77.12	29.00	29.34	85.33	18.00	18.05	90.97
1.20	105.00	107.31	46.34	50.00	50.88	74.56	33.00	33.44	83.28	19.00	19.08	90.46
1.40	110.00	112.44	43.78	61.00	62.17	68.91	32.00	32.42	83.79	22.00	22.16	88.92
1.60	120.00	122.70	38.65	46.50	47.29	76.35	35.00	35.49	82.25	25.00	25.23	87.38
1.80	175.00	179.13	10.43	62.00	63.20	68.39	35.50	36.01	81.99	30.50	30.88	84.56
2.00												
2.20												

Appendix 6 Isoconcentration lines for removal of Suspended Solids

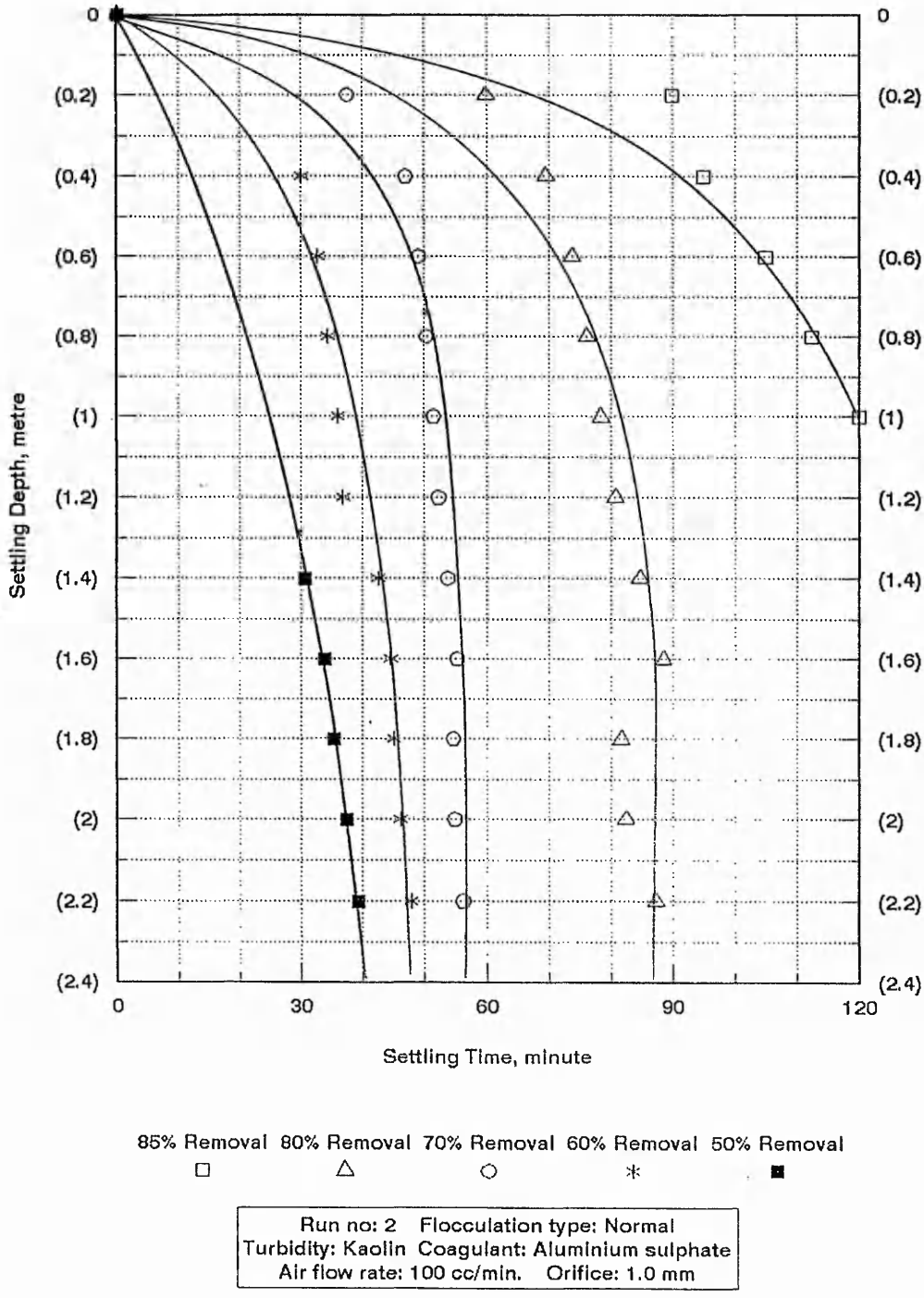

Figure (C-1) Isoconcentration lines for suspended solids removal (Development from a pneumatic flocculation)

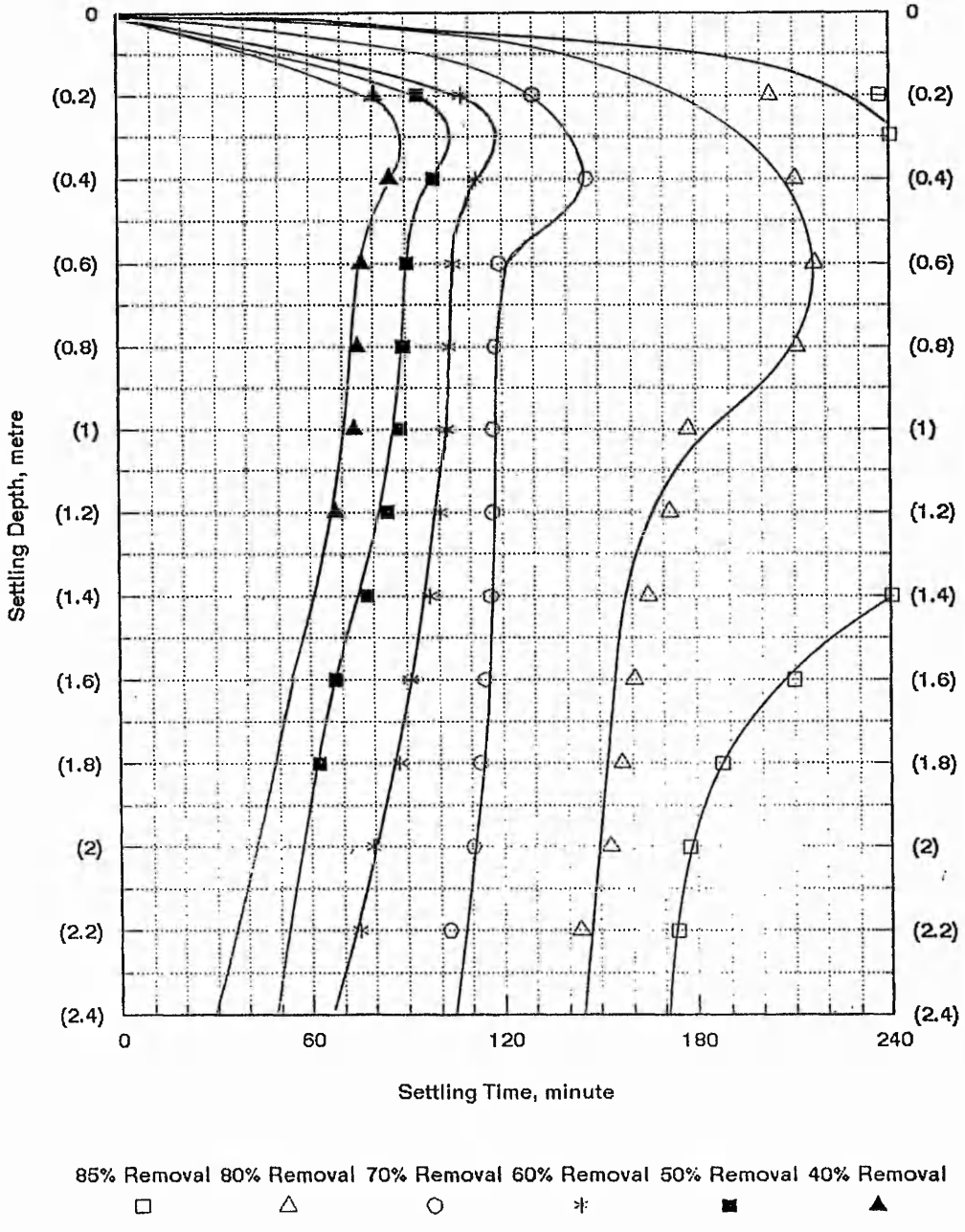

Figure (C-2) Isoconcentration lines for suspended solids removal (Development from a pneumatic flocculation)

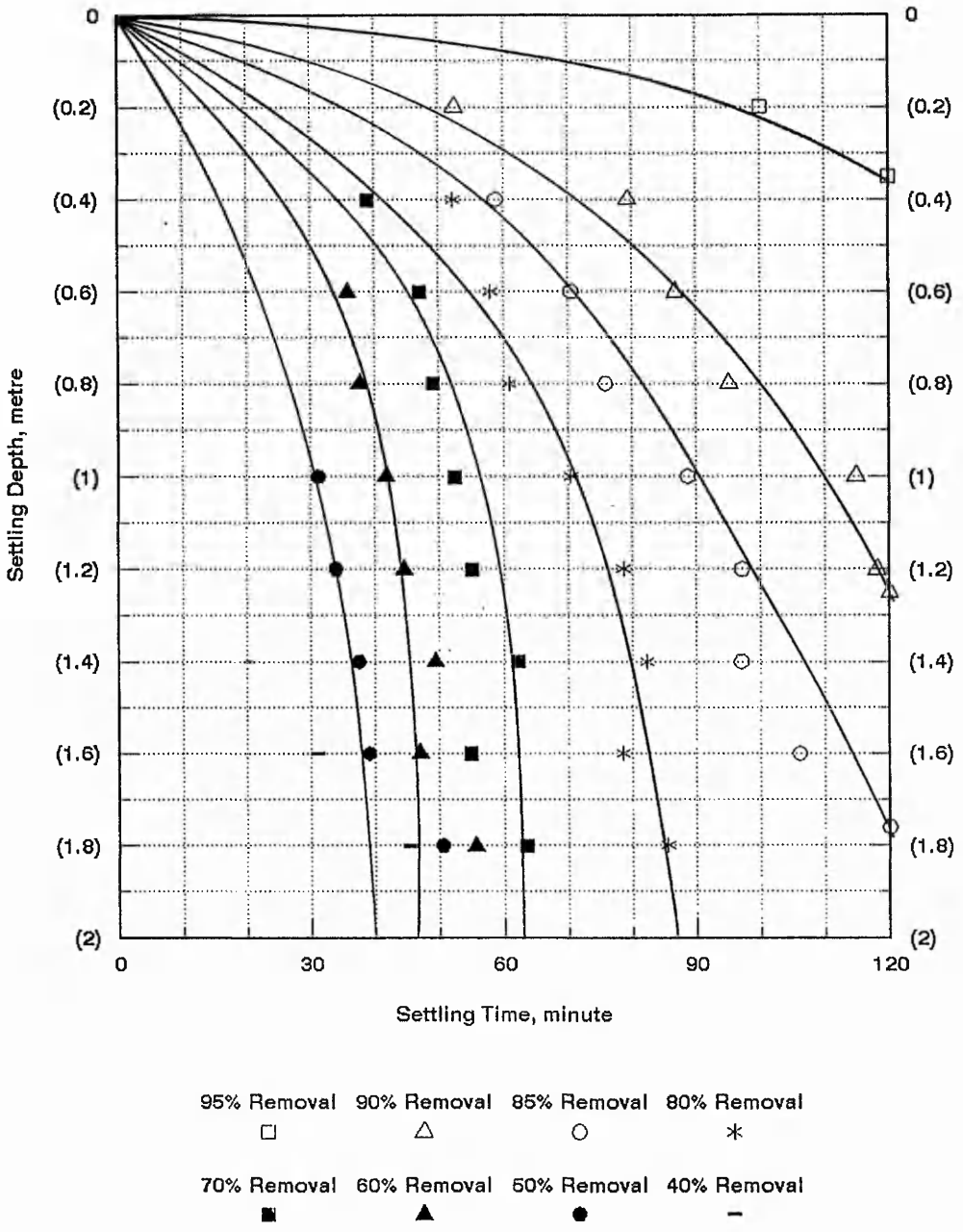

Figure (C-3) Isoconcentration lines for suspended solids removal (Development from a pneumatic flocculation)

Appendix 7 Removal Efficiency versus Air Flow Rate

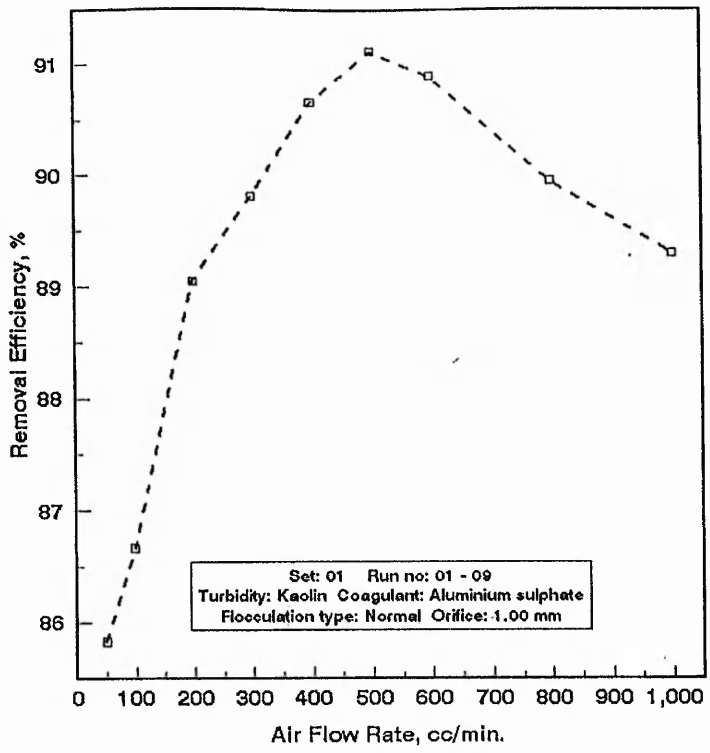

Figure (D-1) Removal Efficiency versus Air Flow Rate

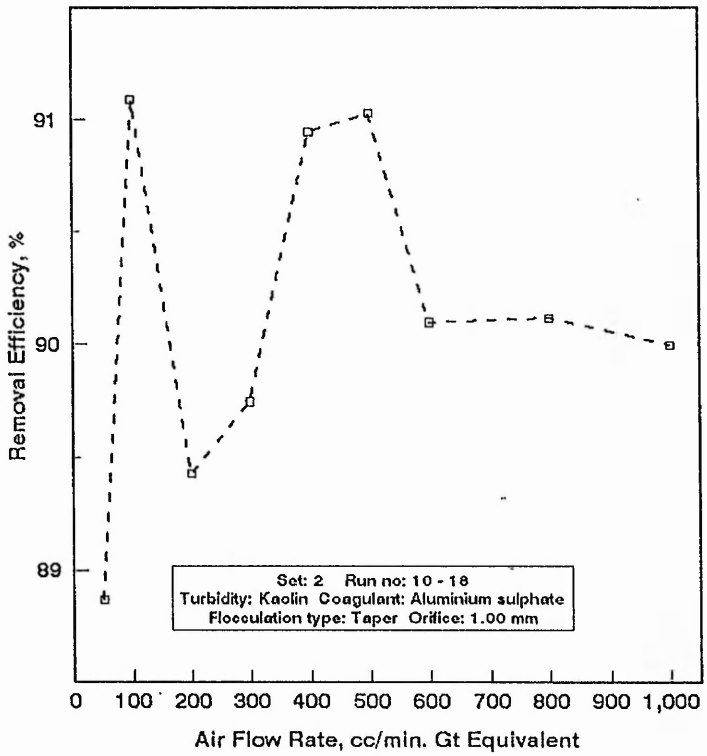

Figure (D-2) Removal Efficiency versus Air Flow Rate

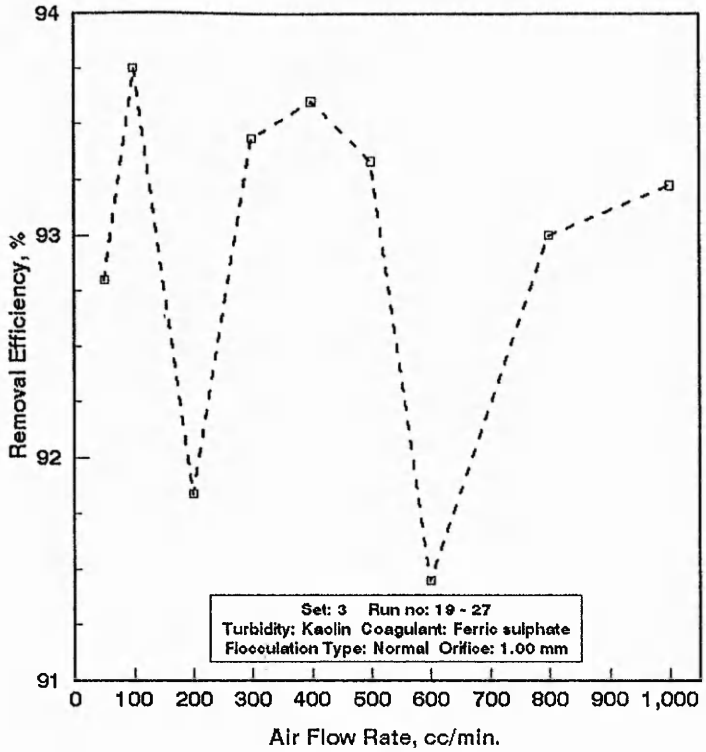

Figure (D-3) Removal Efficiency versus Air Flow Rate

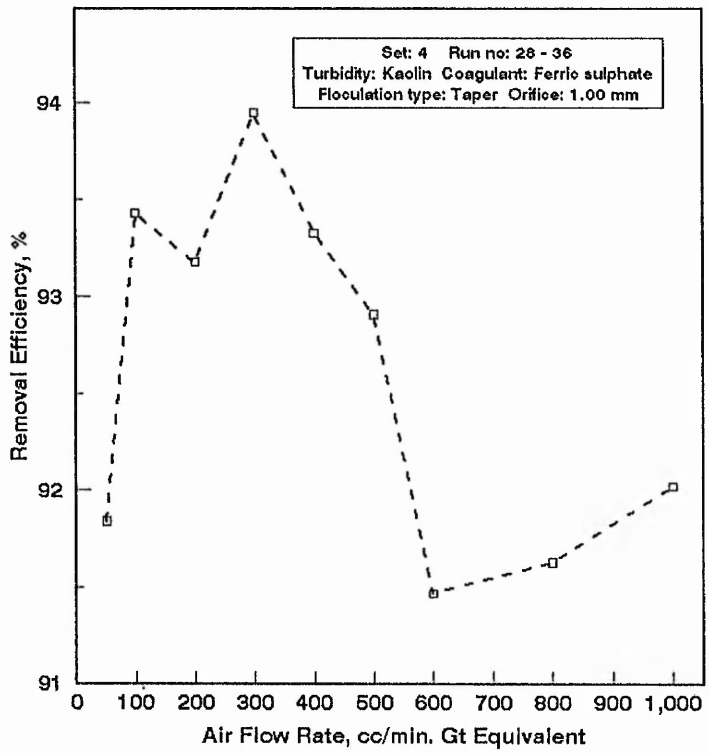

Figure (D-4) Removal Efficiency versus Air Flow Rate

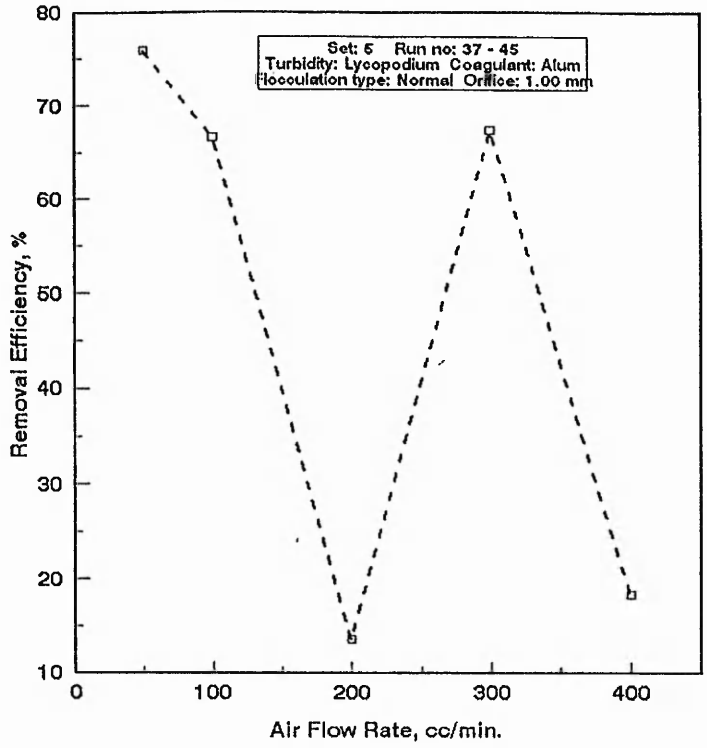

Figure (D-5) Removal Efficiency versus Air Flow Rate

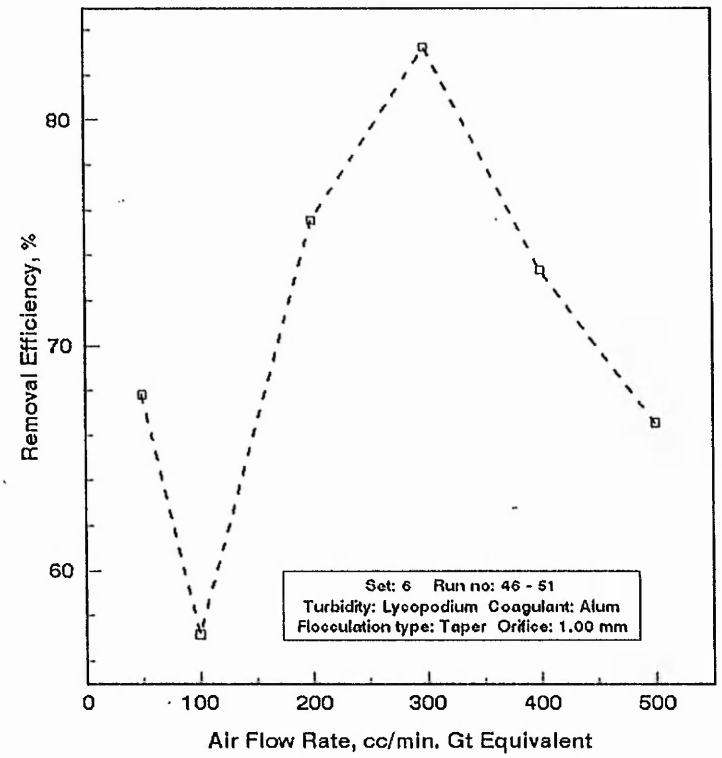

Figure (D-6) Removal Efficiency versus Air Flow Rate

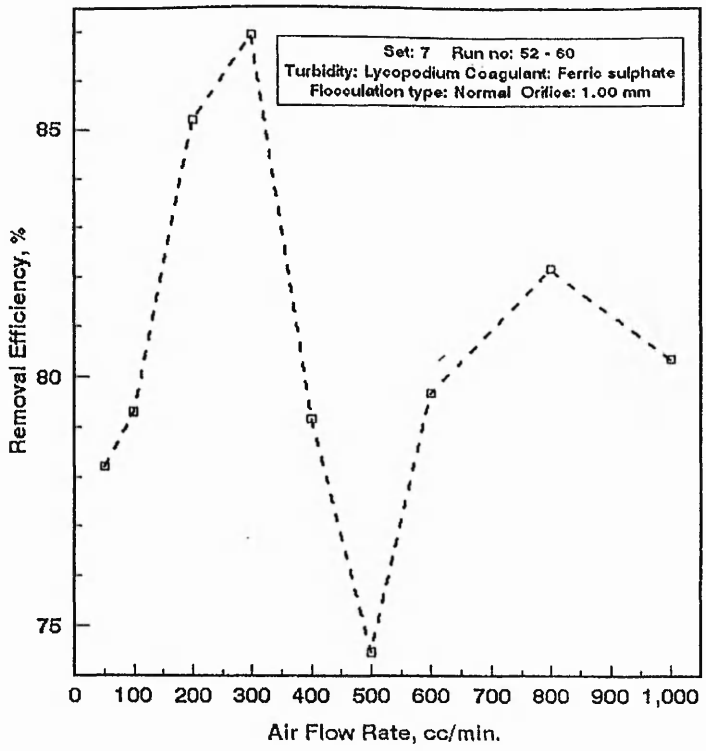

Figure (D-7) Removal Efficiency versus Air Flow Rate

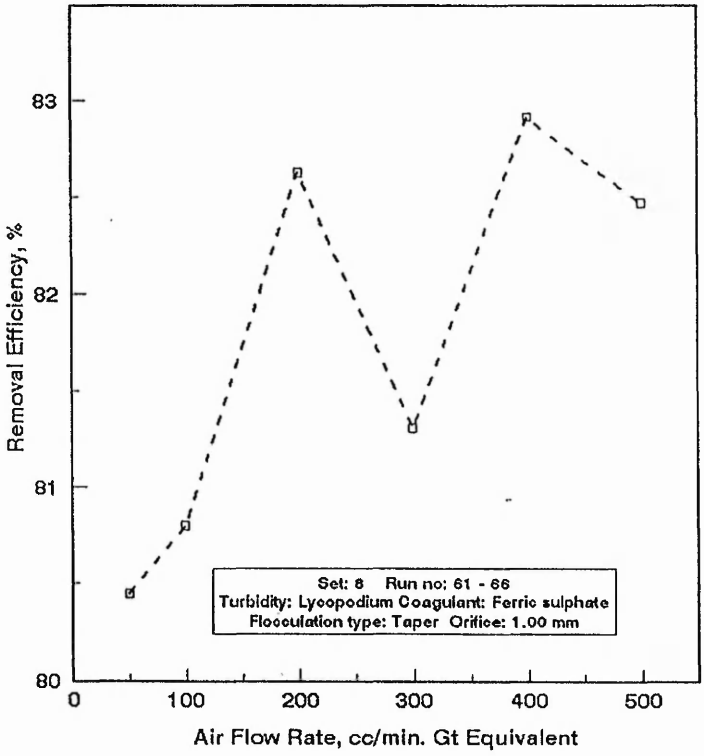

Figure (D-8) Removal Efficiency versus Air Flow Rate

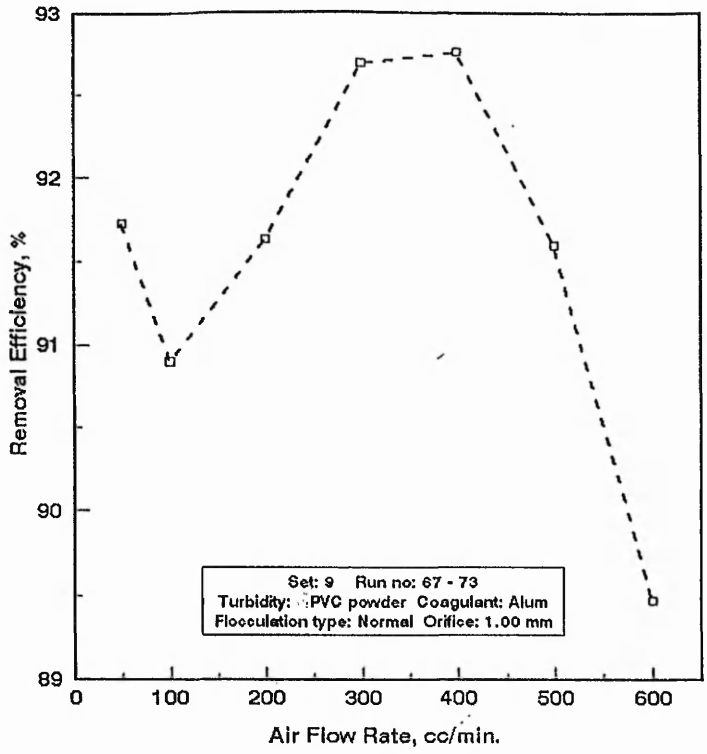

Figure (D-9) Removal Efficiency versus Air Flow Rate

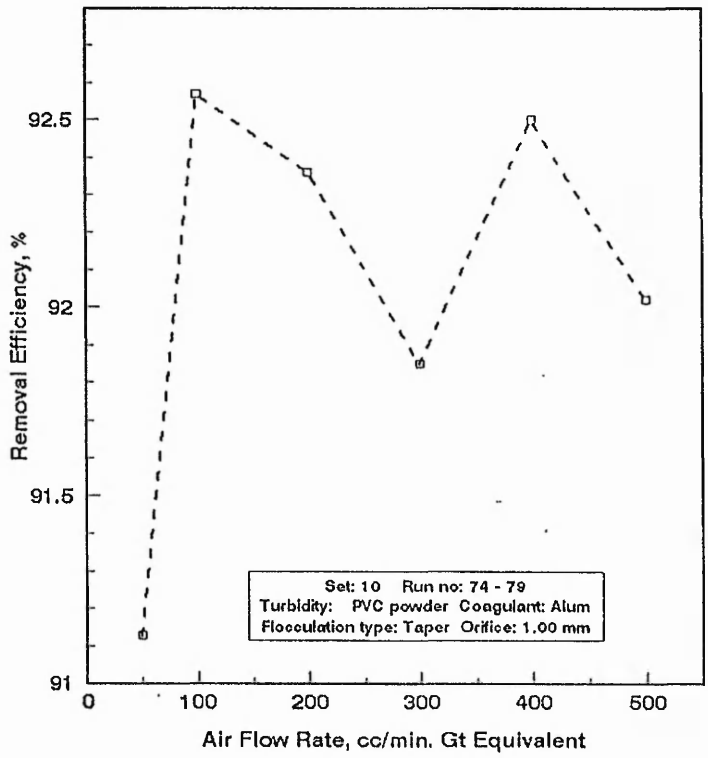

Figure (D-10) Removal Efficiency versus Air Flow Rate

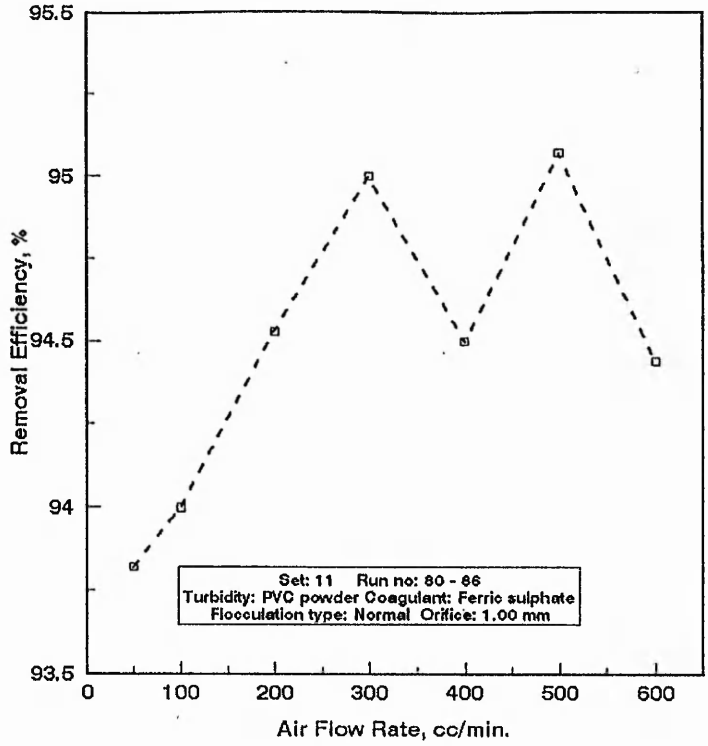

Figure (D-11) Removal Efficiency versus Air Flow Rate

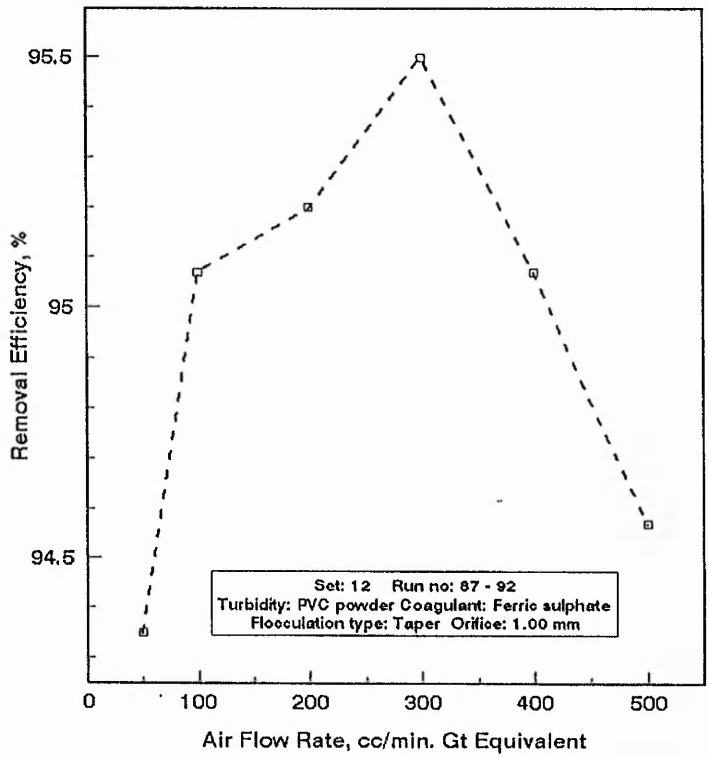

Figure (D-12) Removal Efficiency versus Air Flow Rate

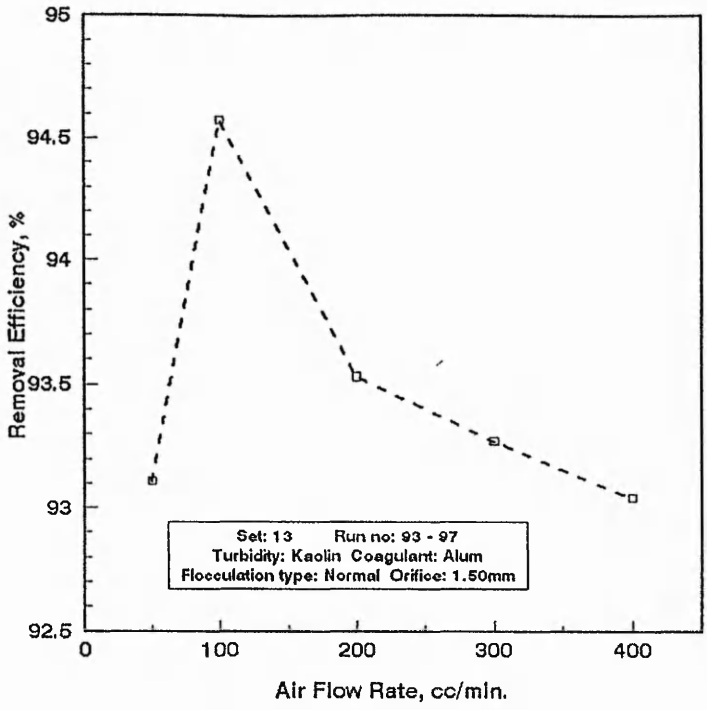

Figure (D-13) Removal Efficiency versus Air Flow Rate

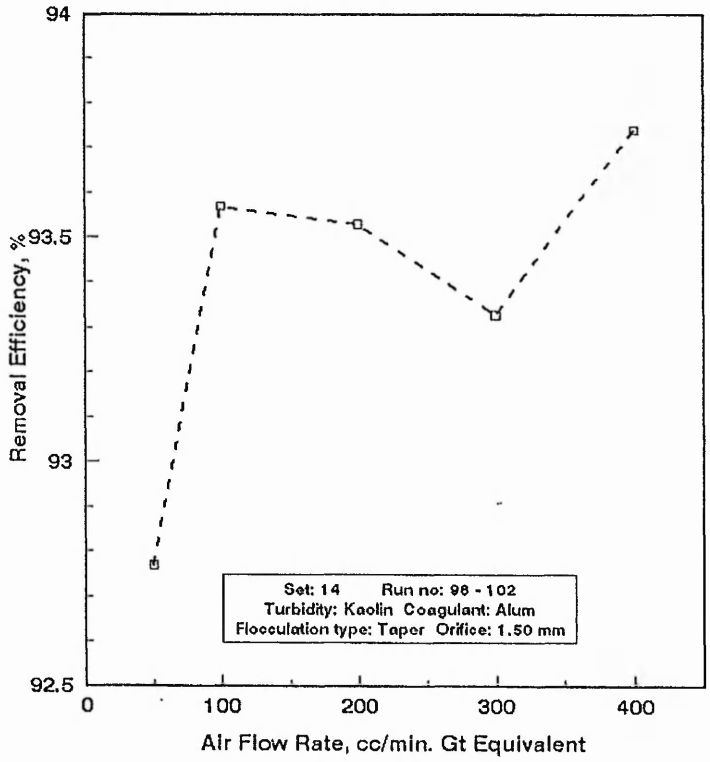

Figure (D-14) Removal Efficiency versus Air Flow Rate

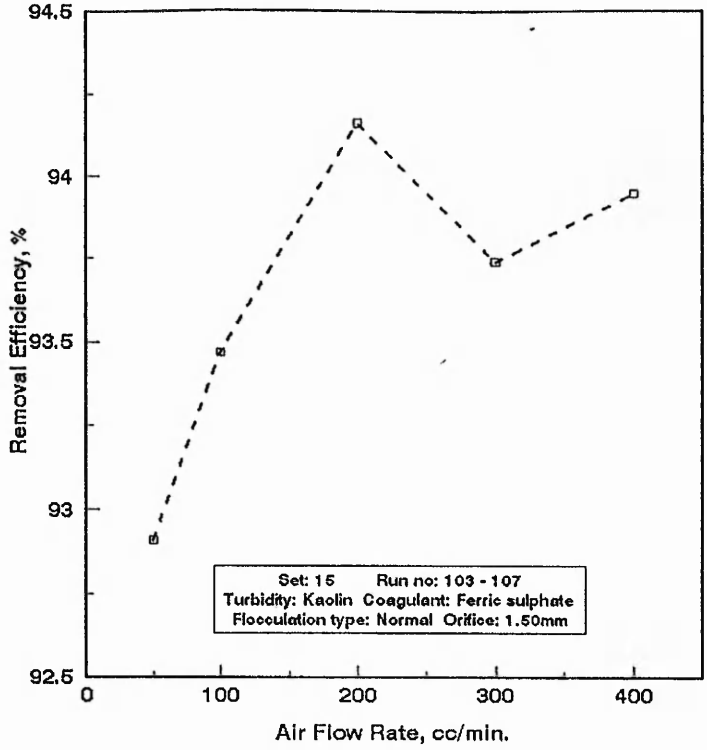

Figure (D-15) Removal Efficiency versus Air Flow Rate

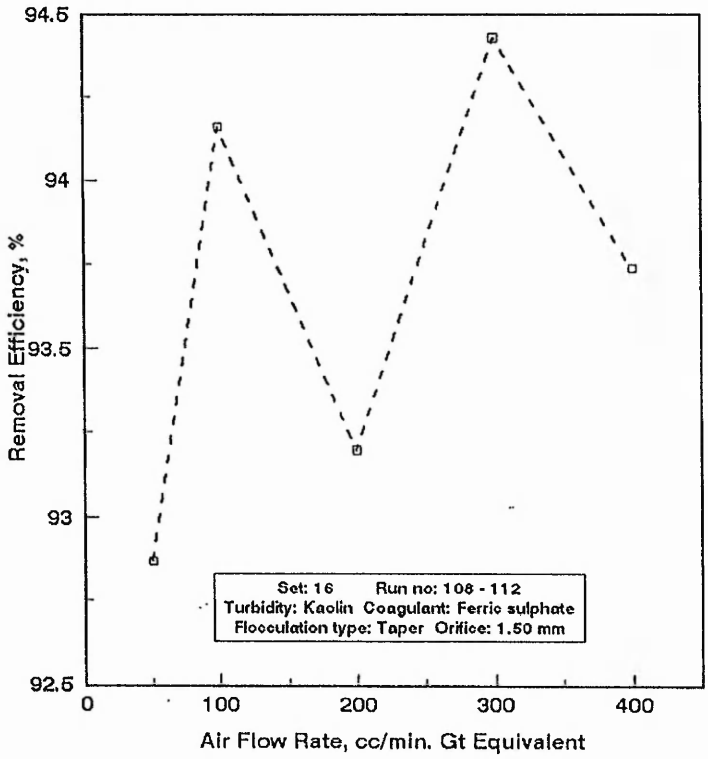

Figure (D-16) Removal Efficiency versus Air Flow Rate

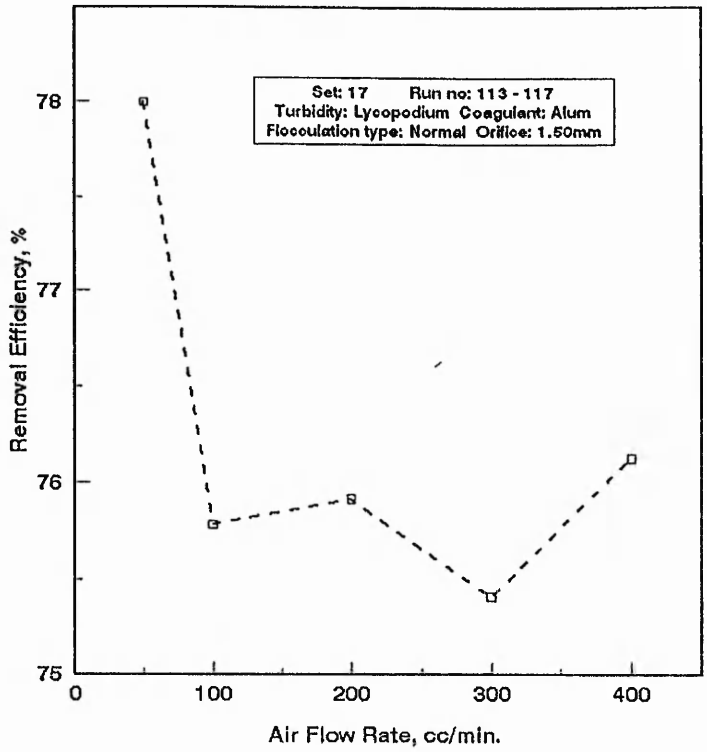

Figure (D-17) Removal Efficiency versus Air Flow Rate

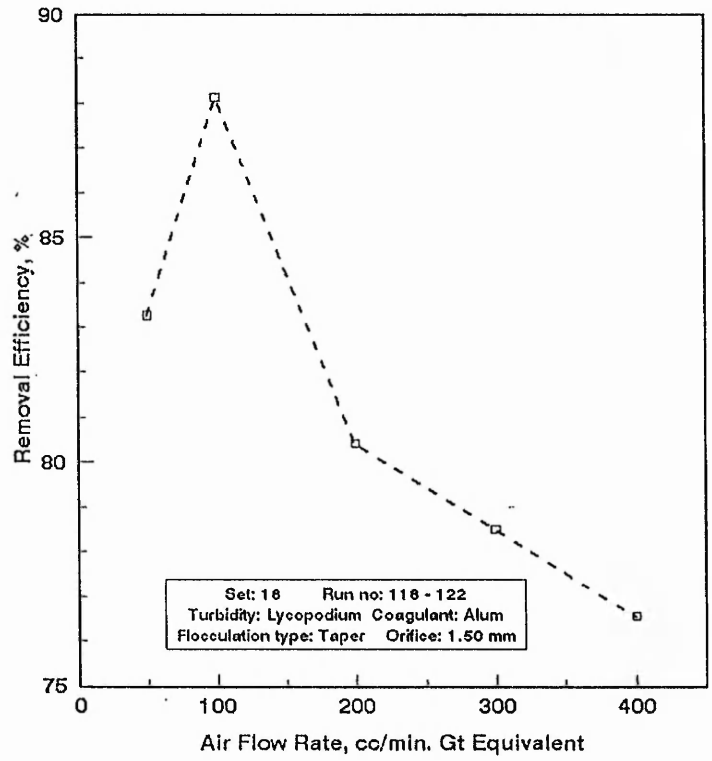

Figure (D-18) Removal Efficiency versus Air Flow Rate

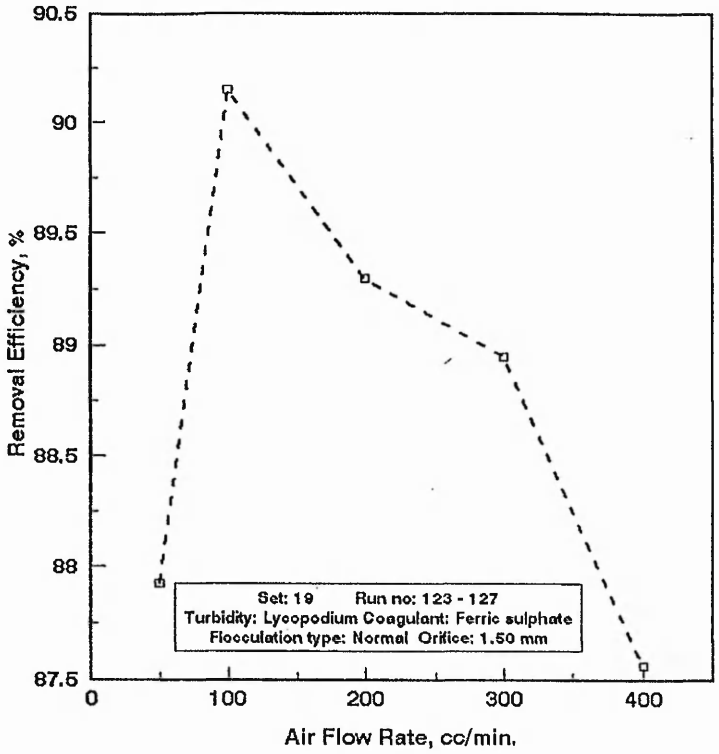

Figure (D-19) Removal Efficiency versus Air Flow Rate

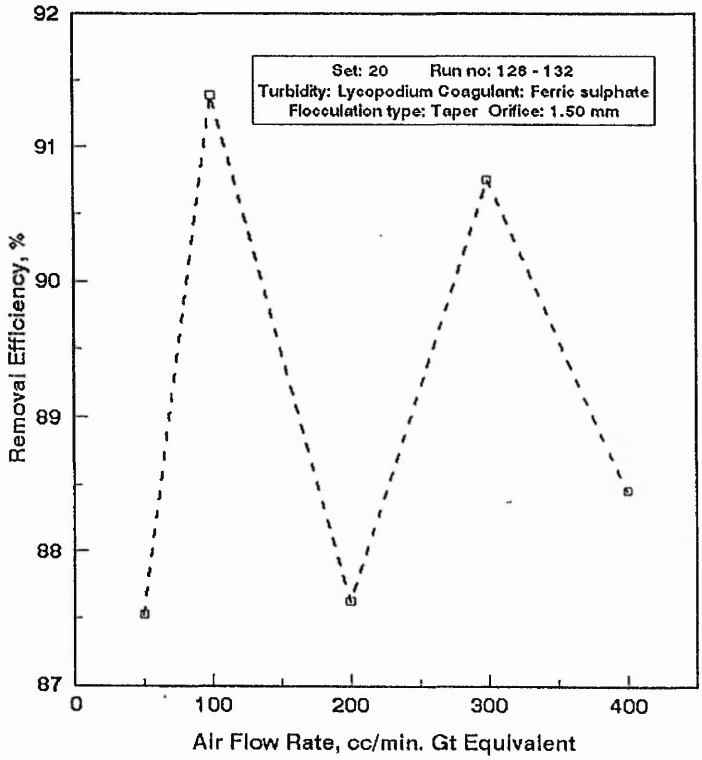

Figure (D-20) Removal Efficiency versus Air Flow Rate

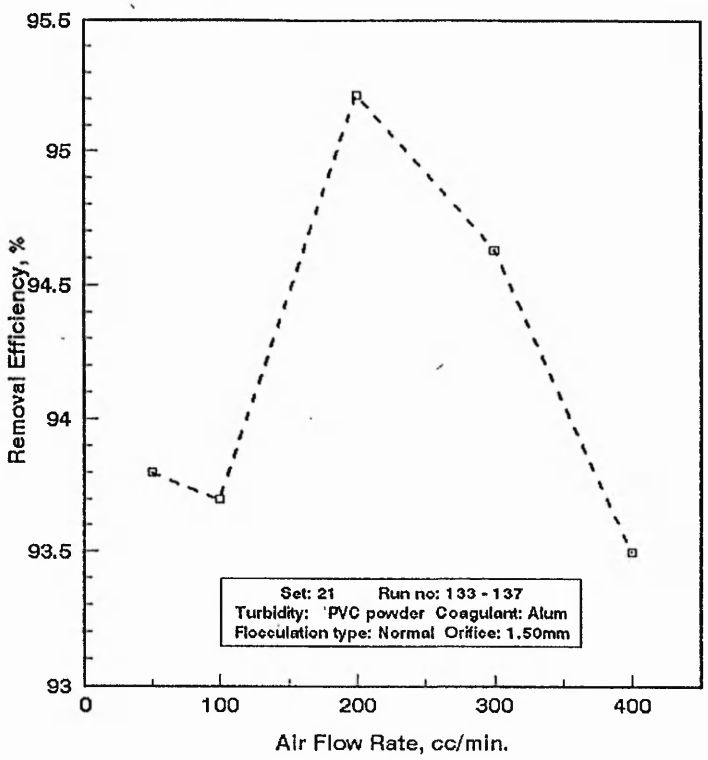

Figure (D-21) Removal Efficiency versus Air Flow Rate

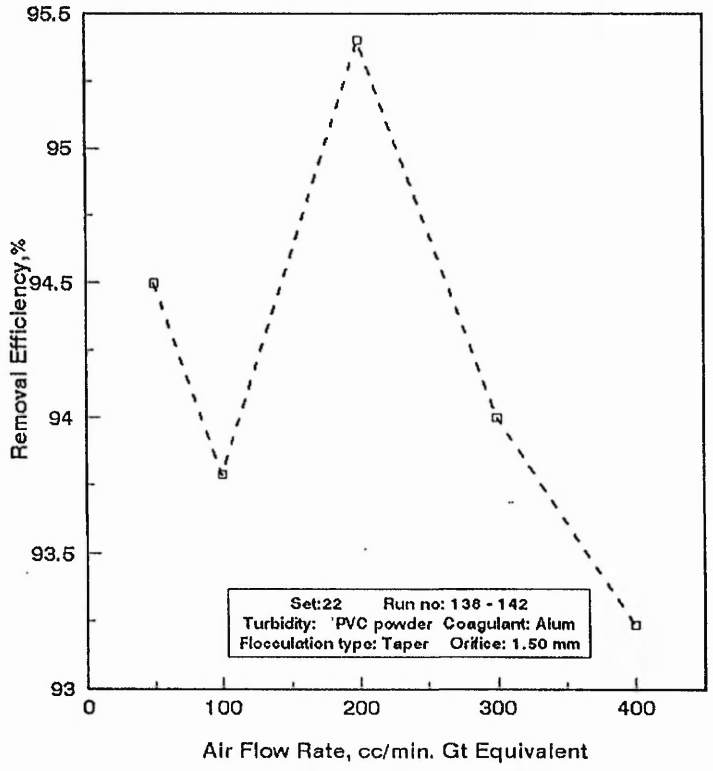

Figure (D-22) Removal Efficiency versus Air Flow Rate

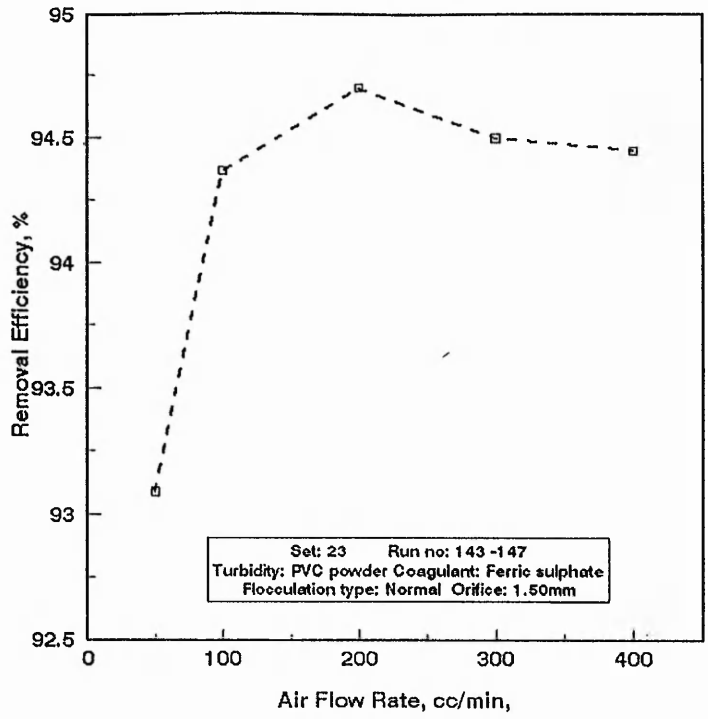

Figure (D-23) Removal Efficiency versus Air Flow Rate

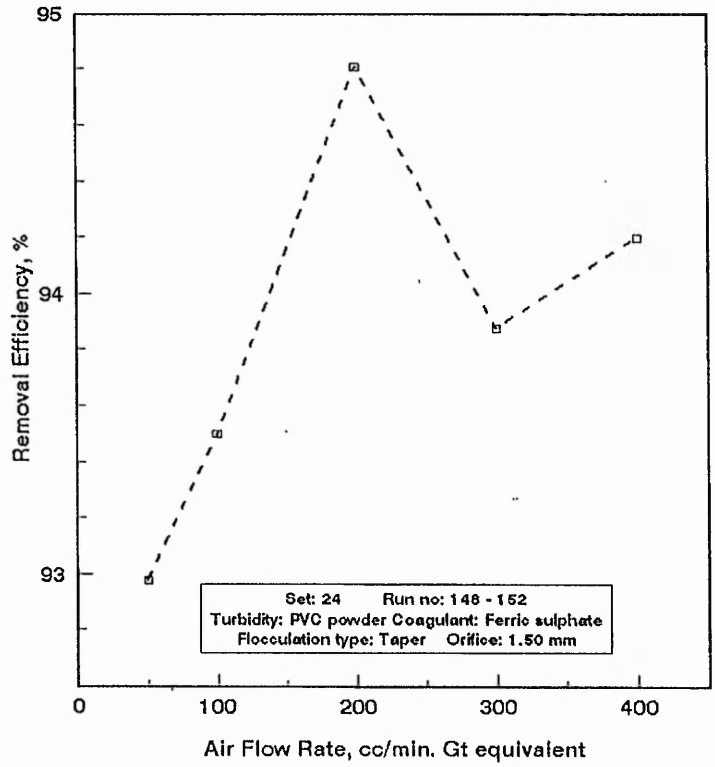

Figure (D-24) Removal Efficiency versus Air Flow Rate

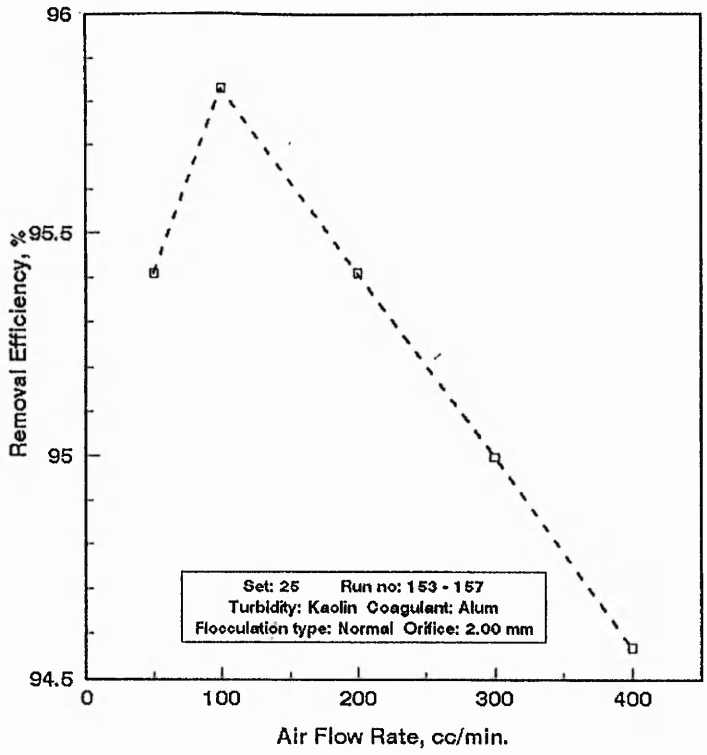

Figure (D-25) Removal Efficiency versus Air Flow Rate

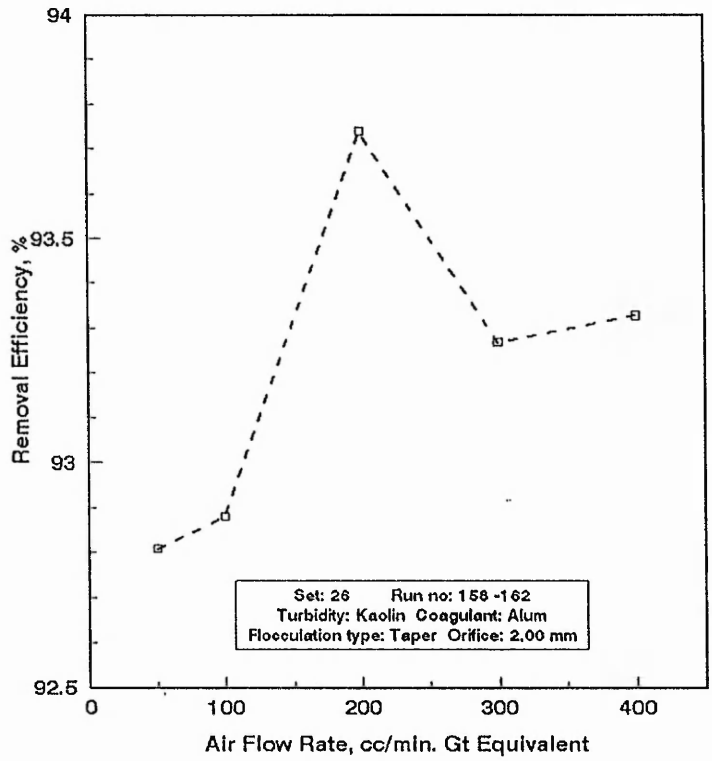

Figure (D-26) Removal Efficiency versus Air Flow Rate

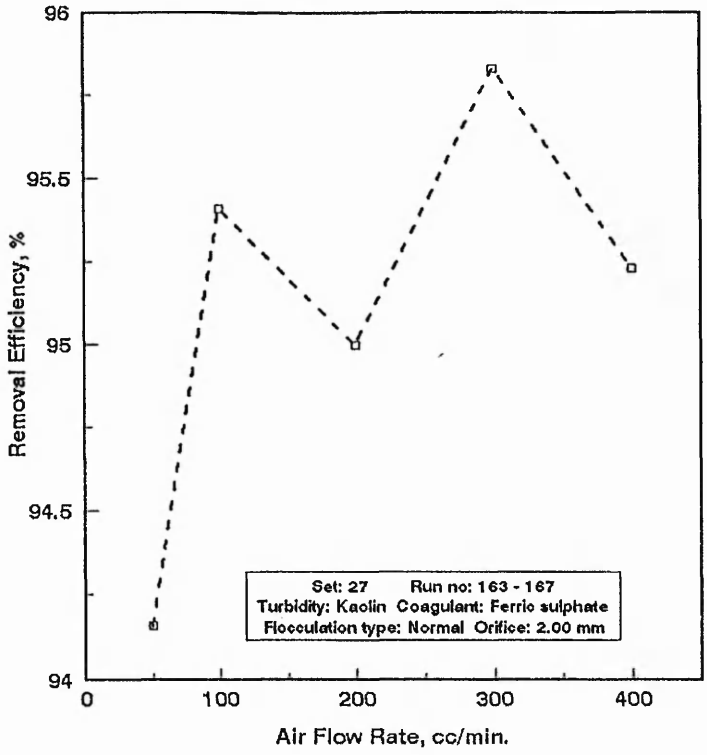

Figure (D-27) Removal Efficiency versus Air Flow Rate

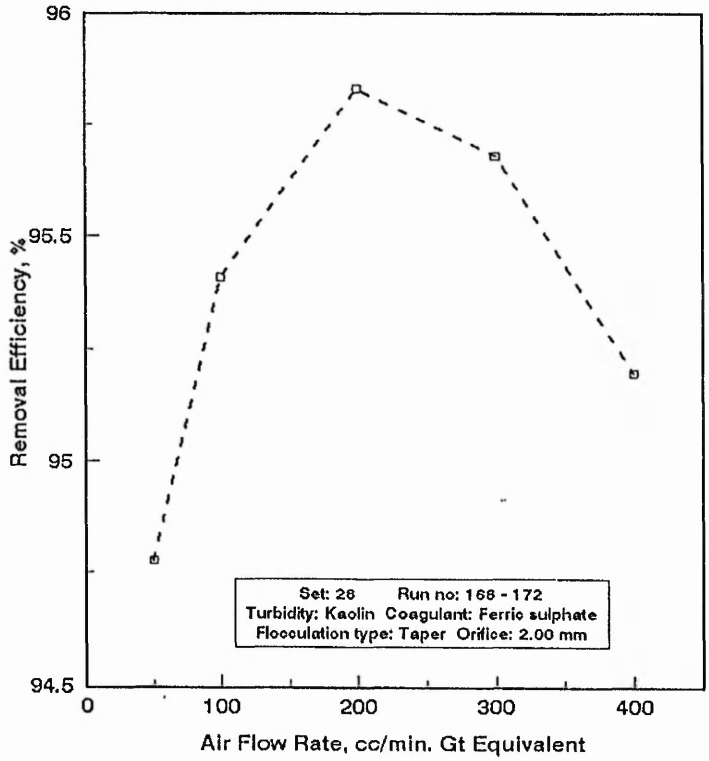

Figure (D-28) Removal Efficiency versus Air Flow Rate

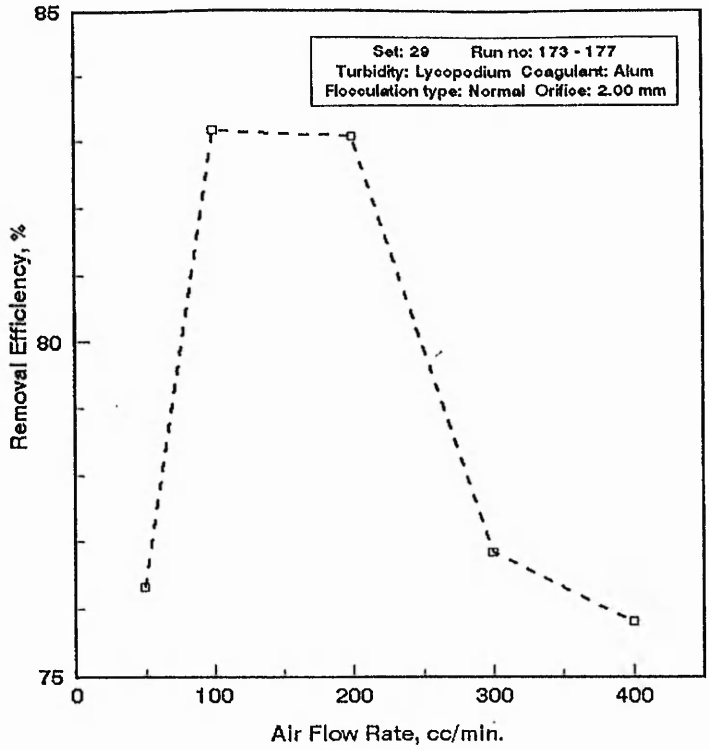

Figure (D-29) Removal Efficiency versus Air Flow Rate

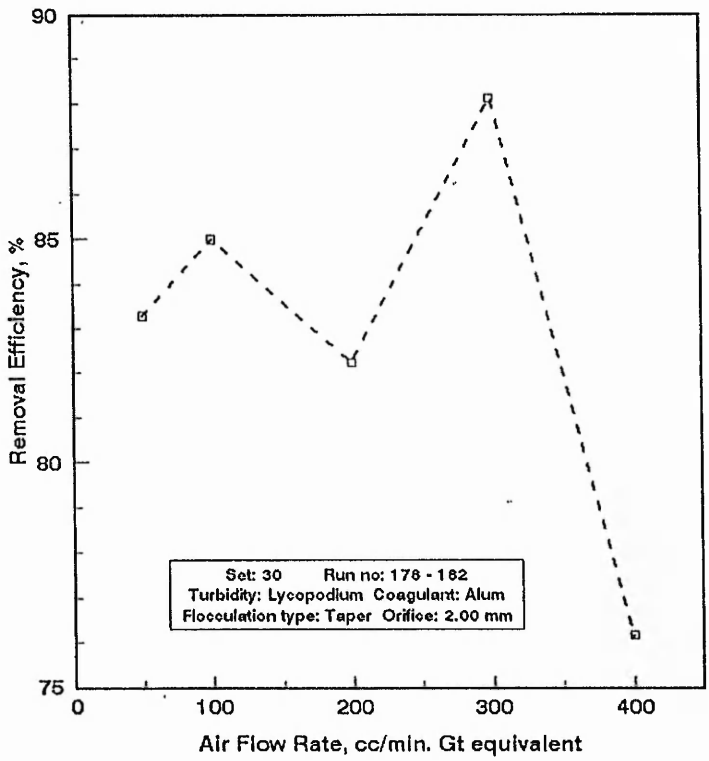

Figure (D-30) Removal Efficiency versus Air Flow Rate

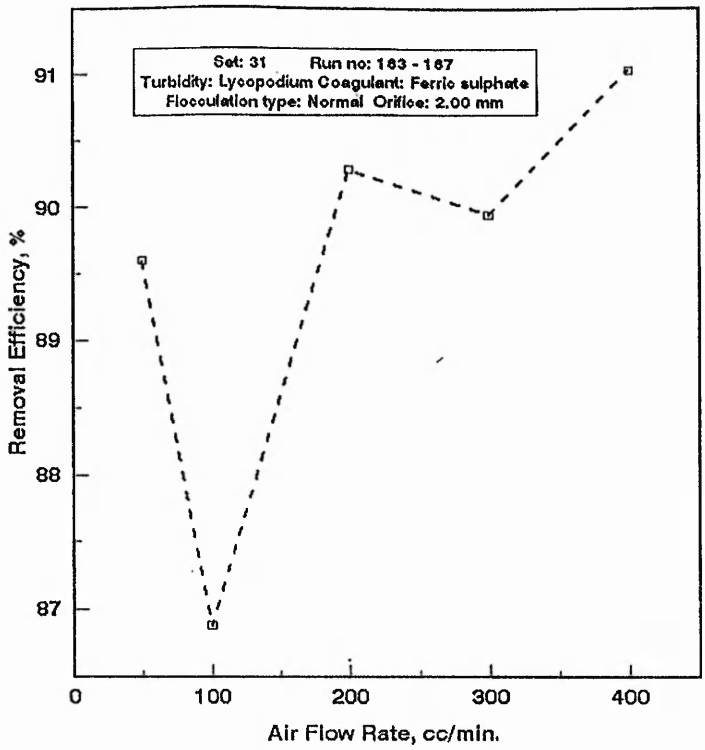

Figure (D-31) Removal Efficiency versus Air Flow Rate

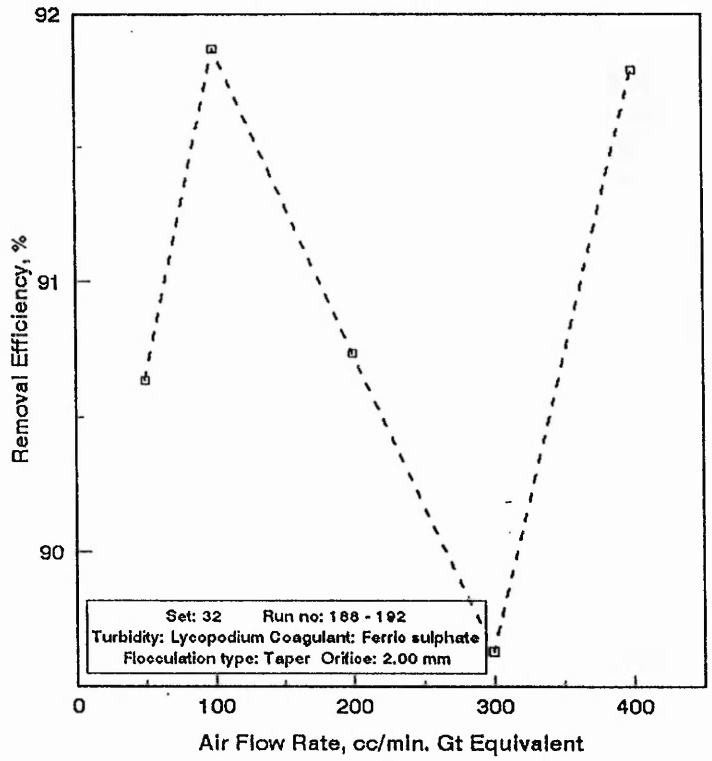

Figure (D-32) Removal Efficiency versus Air Flow Rate

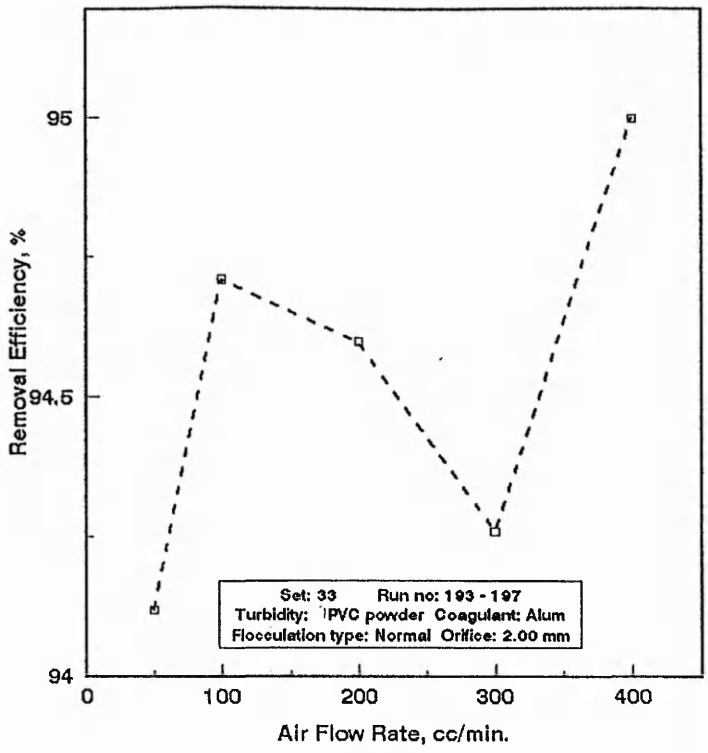

Figure (D-33) Removal Efficiency versus Air Flow Rate

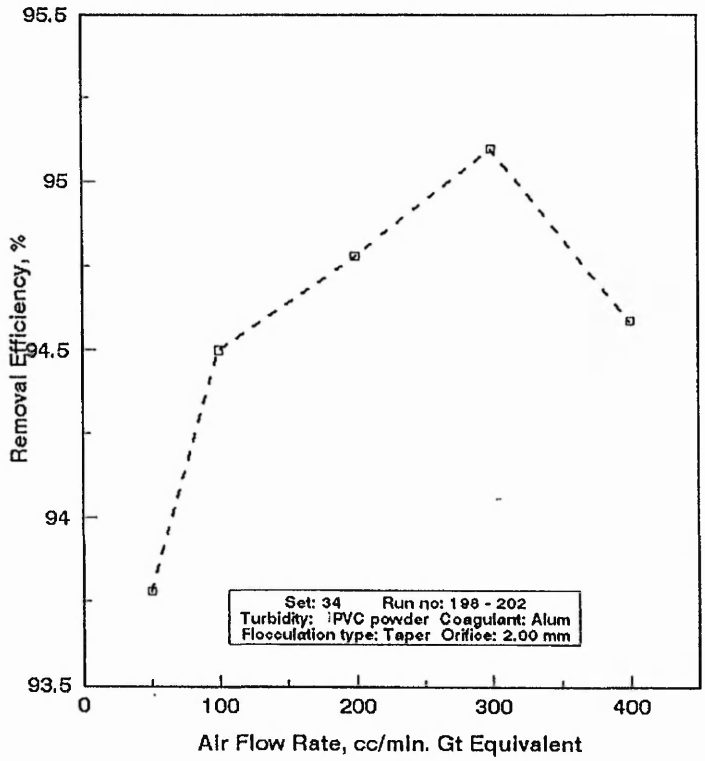

Figure (D-34) Removal Efficiency versus Air Flow Rate

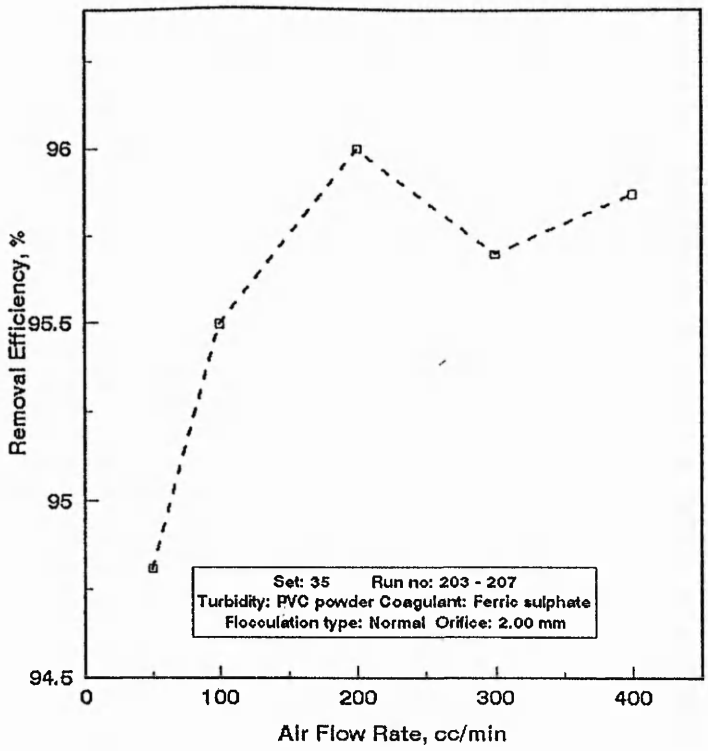

Figure (D-35) Removal Efficiency versus Air Flow Rate

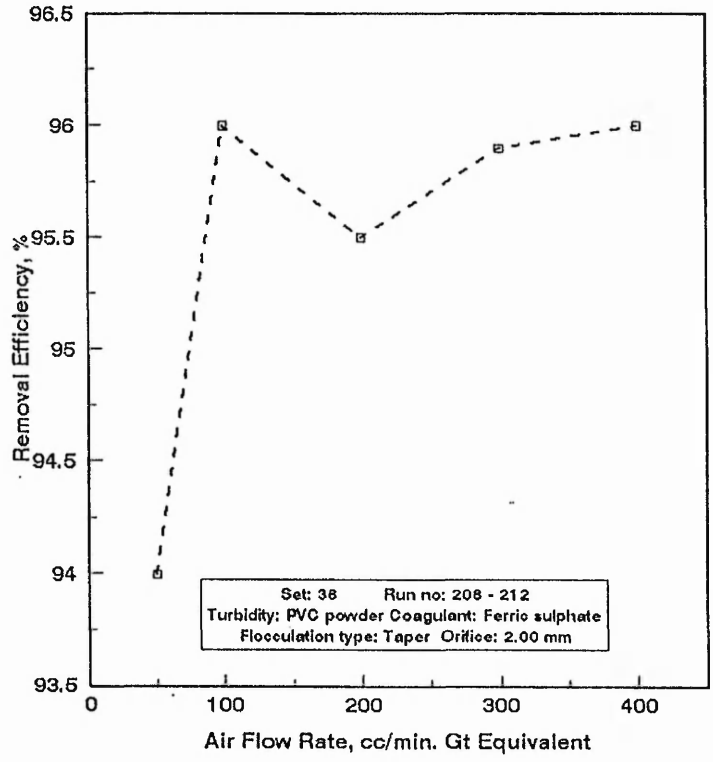

Figure (D-36) Removal Efficiency versus Air Flow Rate

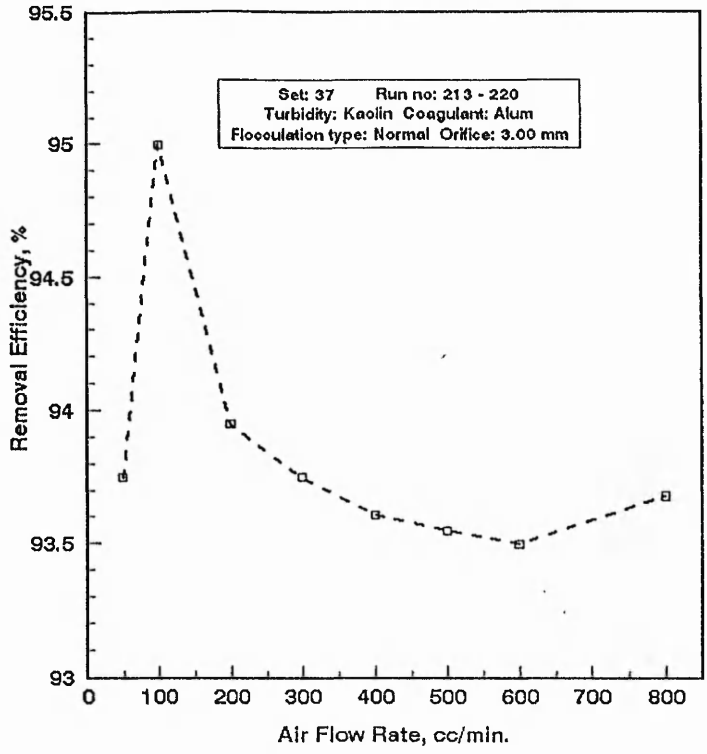

Figure (D-37) Removal Efficiency versus Air Flow Rate

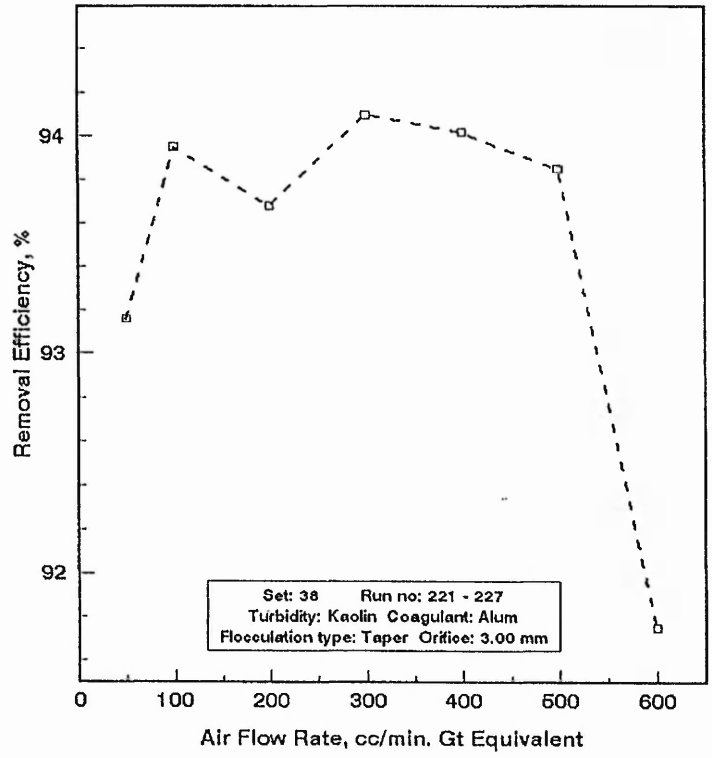

Figure (D-38) Removal Efficiency versus Air Flow Rate

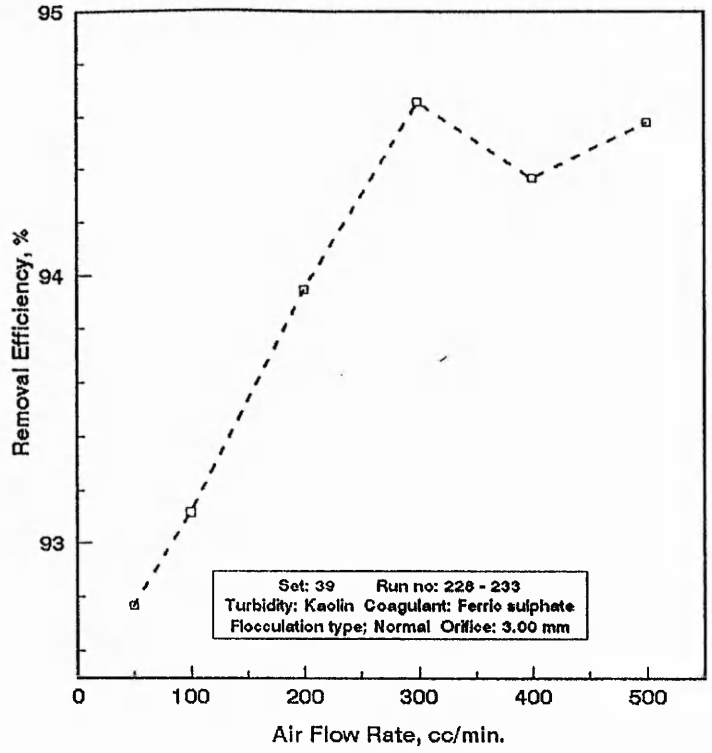

Figure (D-39) Removal Efficiency versus Air Flow Rate

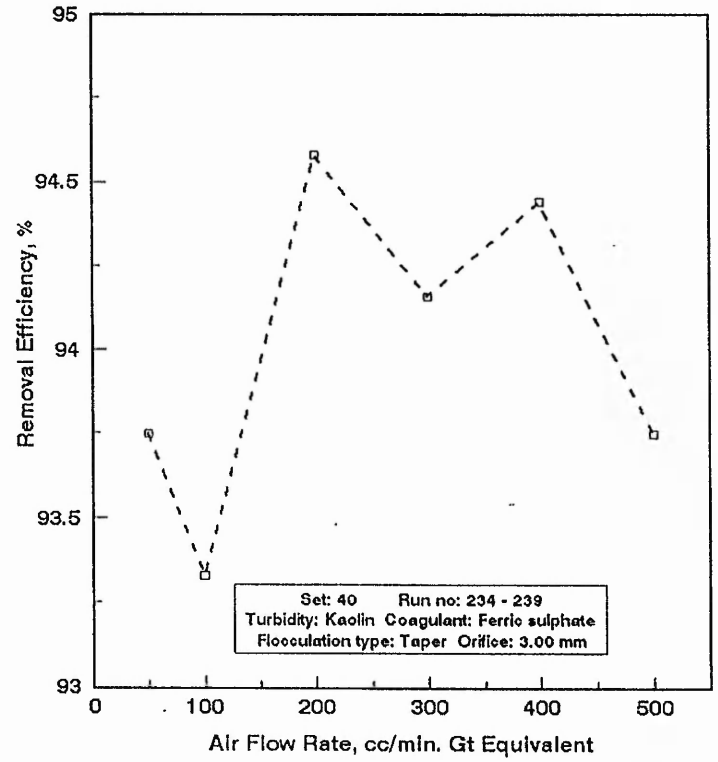

Figure (D-40) Removal Efficiency versus Air Flow Rate

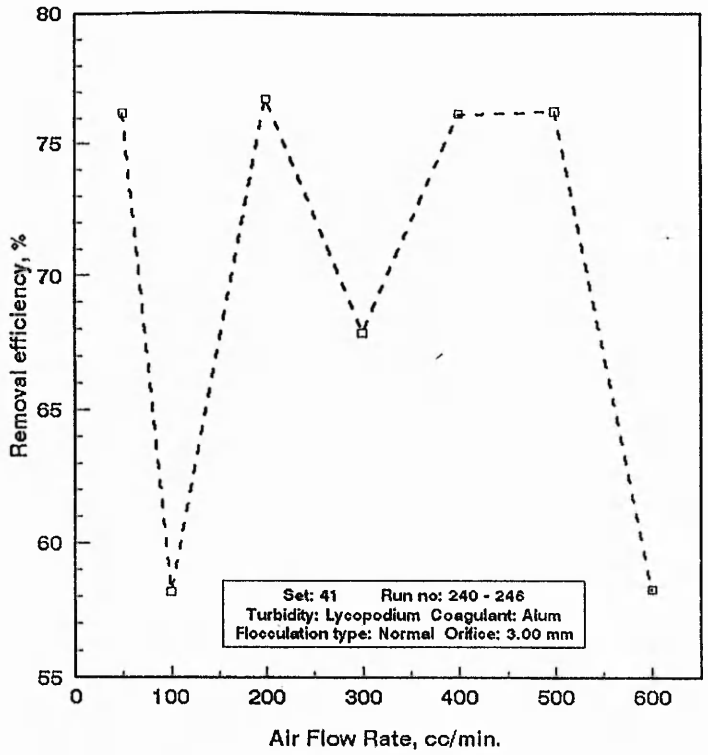

Figure (D-41) Removal Efficiency versus Air Flow Rate

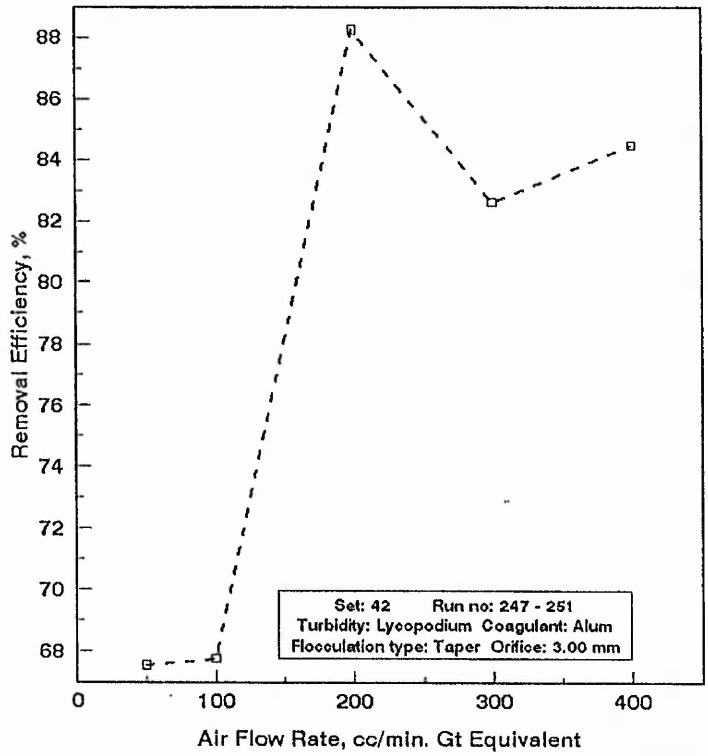

Figure (D-42) Removal Efficiency versus Air Flow Rate

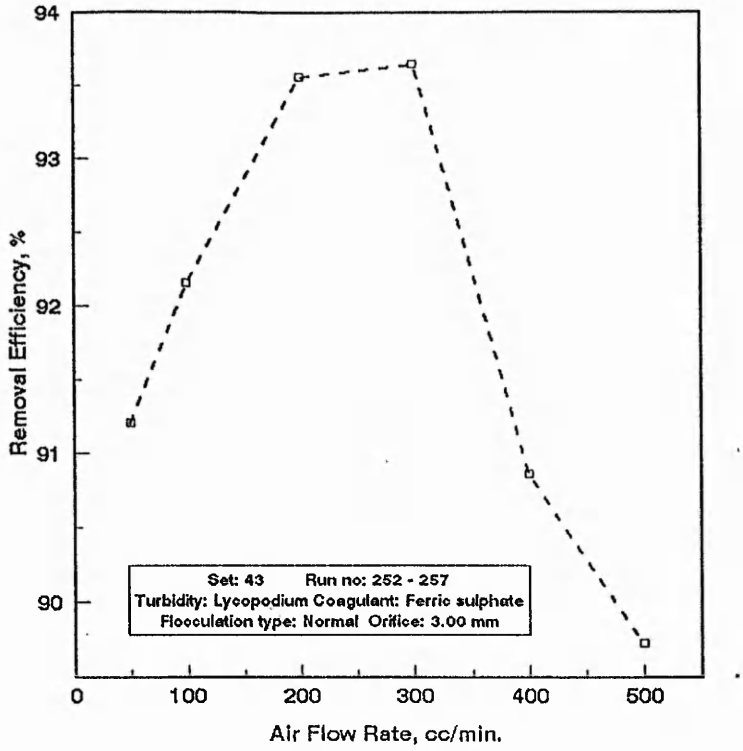

Figure (D-43) Removal Efficiency versus Air Flow Rate

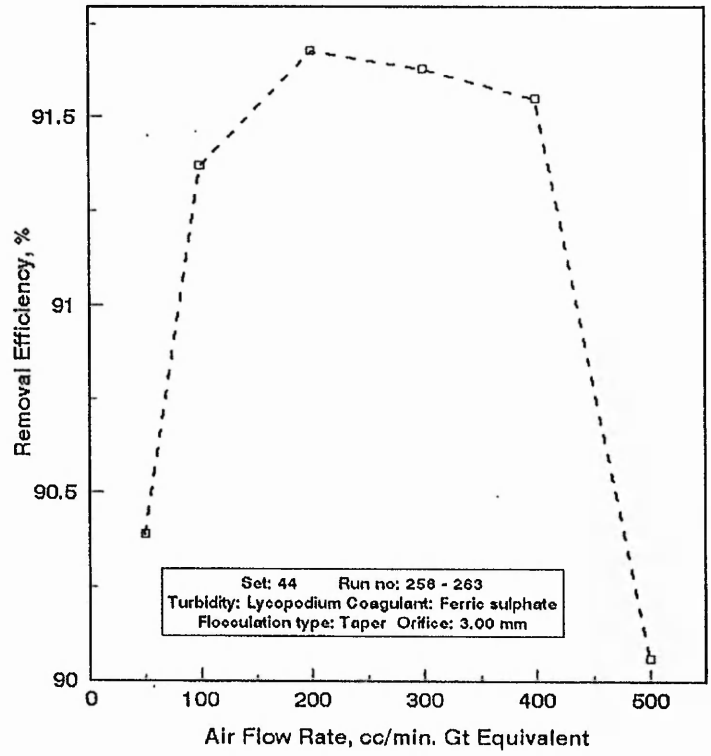

Figure (D-44) Removal Efficiency versus Air Flow Rate

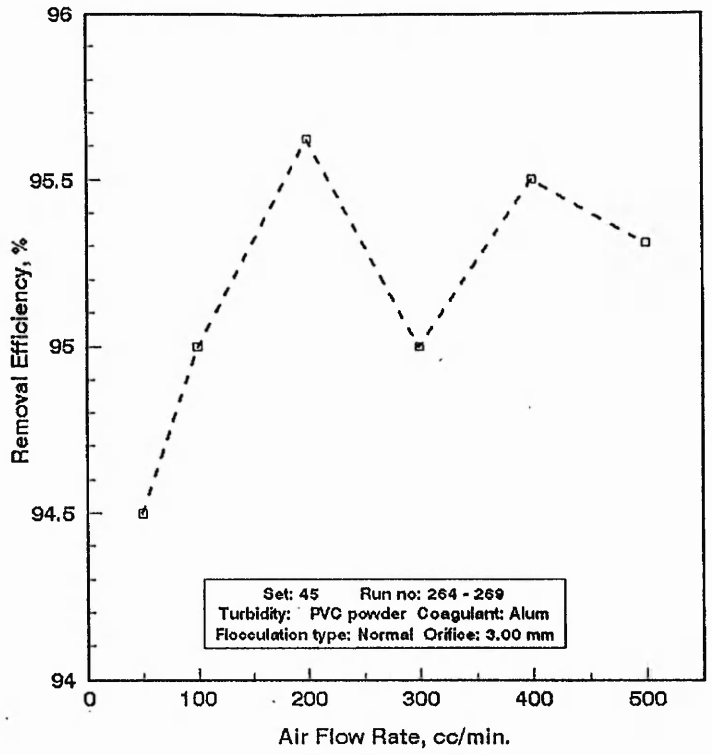

Figure (D-45) Removal Efficiency versus Air Flow Rate

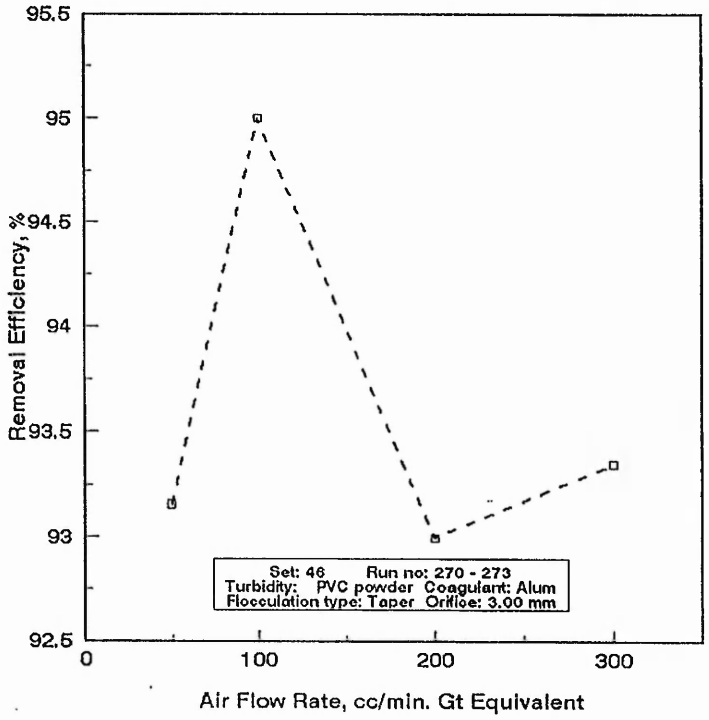

Figure (D-46) Removal Efficiency versus Air Flow Rate

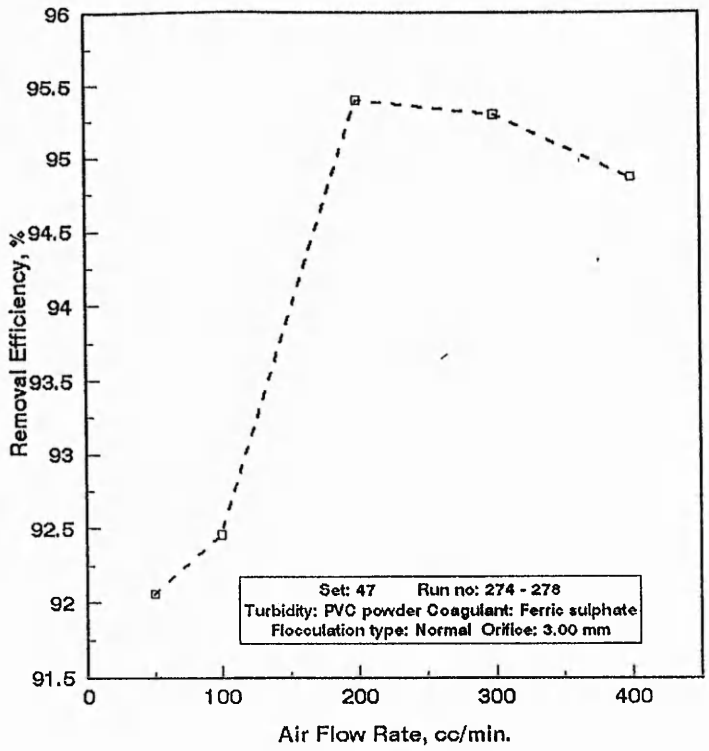

Figure (D-47) Removal Efficiency versus Air Flow Rate

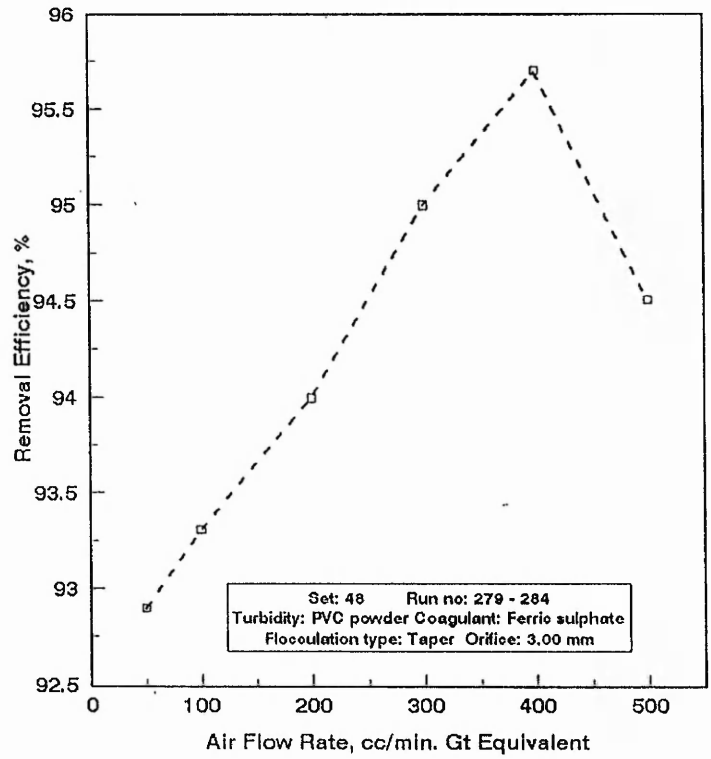

Figure (D-48) Removal Efficiency versus Air Flow Rate